

THE INPUT/OUTPUT MECHANISM OF CHAOS GENERATION

A THESIS SUBMITTED TO
THE GRADUATE SCHOOL OF NATURAL AND APPLIED SCIENCES
OF
MIDDLE EAST TECHNICAL UNIVERSITY

BY

MEHMET ONUR FEN

IN PARTIAL FULFILLMENT OF THE REQUIREMENTS
FOR
THE DEGREE OF DOCTOR OF PHILOSOPHY
IN
MATHEMATICS

SEPTEMBER 2013

Approval of the thesis:

THE INPUT/OUTPUT MECHANISM OF CHAOS GENERATION

submitted by **MEHMET ONUR FEN** in partial fulfillment of the requirements for the degree of **Doctor of Philosophy in Mathematics Department, Middle East Technical University** by,

Prof. Dr. Canan Özgen
Dean, Graduate School of **Natural and Applied Sciences**

Prof. Dr. Mustafa Korkmaz
Head of Department, **Mathematics**

Prof. Dr. Marat Akhmet
Supervisor, **Mathematics Department, METU**

Examining Committee Members:

Prof. Dr. Tanıl Ergenç
Mathematics Department, Atılım University

Prof. Dr. Marat Akhmet
Mathematics Department, METU

Prof. Dr. Hasan Taşeli
Mathematics Department, METU

Assist. Prof. Dr. Kostyantyn Zheltukhin
Mathematics Department, METU

Assist. Prof. Dr. Ahmet Beyaz
Mathematics Department, METU

Date:

I hereby declare that all information in this document has been obtained and presented in accordance with academic rules and ethical conduct. I also declare that, as required by these rules and conduct, I have fully cited and referenced all material and results that are not original to this work.

Name, Last Name: MEHMET ONUR FEN

Signature :

ABSTRACT

THE INPUT/OUTPUT MECHANISM OF CHAOS GENERATION

Fen, Mehmet Onur

Ph.D., Department of Mathematics

Supervisor : Prof. Dr. Marat Akhmet

September 2013, 134 pages

The main objective of this thesis is to develop a new method for chaos generation through the input/output mechanism on the basis of differential and discrete equations. In the thesis, this method is applied to various models in mechanics, electronics, meteorology and neural networks. Chaotic sets of continuous functions as well as the concepts of the generator and replicator of chaos are introduced. Inputs in the form of both continuous and piecewise continuous functions are applied to arbitrarily high dimensional systems with stable equilibrium points, and it is rigorously proven that the chaos type of the inputs is the same as for the outputs. Our theoretical results are based on the chaos in the sense of Devaney, Li-Yorke and the one obtained through period-doubling cascade. Besides, replication of Shil'nikov orbits, intermittency and the form of the bifurcation diagrams are investigated in the discussion form. It is shown that the usage of chaotic external inputs makes the dynamics of shunting inhibitory cellular neural networks exhibit chaotic motions. Moreover, the presence of chaos in the dynamics of the Duffing oscillator perturbed with a relay function is demonstrated. Models, in which the Lorenz system, shunting inhibitory cellular neural networks and Duffing oscillators are utilized as generators, are considered. Extension of chaos in open chains of Chua circuits and quasiperiodic motions as a possible skeleton of a chaotic attractor are also discussed. The controllability of the replicated chaos is theoretically proven and actualized by means of the OGY and Pyragas control methods.

Keywords: Replication of Chaos, Continuous Chaos, Chaotic Models in Mechanics and Electronics, Shunting Inhibitory Cellular Neural Networks, Control of the Replicated Chaos

ÖZ

KAOS ÜRETİMİNİN GİRDİ/ÇIKTI MEKANİZMASI

Fen, Mehmet Onur

Doktora, Matematik Bölümü

Tez Yöneticisi : Prof. Dr. Marat Akhmet

Eylül 2013, 134 sayfa

Bu tezin asıl amacı diferansiyel ve ayrık denklemler bazında girdi/çıkıtı mekanizması aracılığıyla kaos üretimi için yeni bir metodun geliştirilmesidir. Bu metot tezde, mekanik, elektronik, meteoroloji ve sinir ağlarında çeşitli modellere uygulanmıştır. Kaosun üreticisi ve çoğaltıcısı kavramlarının yanı sıra sürekli fonksiyonların kaotik kümeleri de tanıtılmıştır. Sürekli ve parçalı sürekli fonksiyon formatındaki girdiler, kararlı denge noktalarına sahip keyfi yükseklikte boyutu olan sistemlere uygulanmıştır ve girdilerin kaos tipinin çıktılarını ile aynı olduğu kesin olarak ispatlanmıştır. Teorik sonuçlarımız Devaney, Li-Yorke tipindeki ve periyot-çiftlenmesi çatallanması ile meydana gelen kaos tipine dayanmaktadır. Bunun yanı sıra, Shil'nikov yörüngelerinin, kesintili kaosun ve çatallanma diyagramlarının replikasyonları tartışma formatında incelenmiştir. Kaotik harici girdilerin kullanılmasının manevra engelleyici hücrel sinir ağlarının dinamiğinin kaotik hareketler meydana getirmesini sağladığı gösterilmiştir. Ayrıca, bir röle fonksiyonuyla etkilenmiş Duffing osilatörünün dinamiğinde kaosun varlığı ispat edilmiştir. Lorenz sistemlerinin, manevra engelleyici hücrel sinir ağlarının ve Duffing osilatörlerinin üretici olarak kullanıldığı modeller ele alınmıştır. Chua devrelerinin açık zincirlerinde kaos genişlemesi ve yarı-periyodik hareketlerin bir kaotik çekicinin muhtemel bir iskeleti olması ayrıca tartışılmıştır. Replike edilen kaosun kontrol edilebilirliği teorik olarak ispatlanmıştır ve OGY ve Pyragas kontrol metotları yardımıyla hayata geçirilmiştir.

Anahtar Kelimeler: Kaosun Replikasyonu, Sürekli Kaos, Mekanik ve Elektronikte Kaotik Modeller, Manevra Engelleyici Hücrel Sinir Ağları, Replike Olan Kaosun Kontrolü

To My Family

ACKNOWLEDGMENTS

First and foremost, I would like to express my deepest gratitude to my supervisor Prof. Dr. Marat Akhmet, for accepting me as his student and preparing me for the academic life. I also would like to thank to him not only for his valuable guidance and constant support throughout the preparation of this thesis, but also for everything that he taught me.

I offer my sincere thanks to the members of the examining committee for their valuable comments and suggestions. I extend my gratitude to all members of the Mathematics Department of Middle East Technical University for their continuous help during this long process.

Without the support of my parents Gülsen Fen and Turgay Fen, I would not have succeeded in my studies. My thanks go to my parents for their confidence and support during the whole of my education life.

I also express my sincere thanks to the Scientific and Technological Research Council of Turkey (TÜBİTAK) for the scholarship (2228) provided during my postgraduate education.

Last, but not the least, I would like to thank to my fiancée Fatma Tokmak for her presence and support during the preparation process of my thesis.

TABLE OF CONTENTS

ABSTRACT	v
ÖZ	vi
ACKNOWLEDGMENTS	viii
TABLE OF CONTENTS	ix
LIST OF TABLES	xii
LIST OF FIGURES	xiii
CHAPTERS	
1 INTRODUCTION	1
1.1 Chaotic Dynamical Systems	2
1.2 The Input/Output Mechanism of Chaos and Morphogenesis	4
1.3 Synchronization of Chaotic Systems	7
1.4 Control of Chaos	8
1.5 Neural Networks and Chaos	9
1.6 Organization of the Thesis	9
2 REPLICATION OF CHAOS	11
2.1 Introduction	11
2.2 Preliminaries	16
2.3 Description of Chaotic Sets of Functions	20
2.3.1 Chaotic set of functions in Devaney's sense	20
2.3.2 Chaotic set of functions in Li-Yorke sense	23
2.4 Hyperbolic Set of Functions	23
2.5 Replication of Devaney's Chaos	26
2.6 Replication of Li-Yorke Chaos	39
2.7 Morphogenesis of Chaos	45

2.8	Replication of Period-Doubling Cascade	51
2.9	Controlling Replication of Chaos	57
2.10	Discussion	61
2.10.1	Replication of intermittency	62
2.10.2	Replication of Shil'nikov orbits	63
2.10.3	Morphogenesis of the double-scroll Chua's attractor	66
2.10.4	Quasiperiodicity through chaos replication	68
2.10.5	Replicators with nonnegative eigenvalues	70
3	CHAOTIC PERIOD-DOUBLING AND OGY CONTROL FOR THE FORCED DUFFING EQUATION	73
3.1	Introduction and Preliminaries	73
3.2	The Chaos Emergence	76
3.2.1	The cascade: The analysis results	76
3.2.2	The Duffing equation's chaotic behavior	81
3.2.3	Lyapunov exponents	84
3.3	Controlling Results	85
3.3.1	The logistic map	85
3.3.2	The general system control	87
3.3.3	The Duffing equation control	90
3.4	Morphogenesis and the Logistic Map	93
3.5	Discussion	95
4	SICNNS WITH CHAOTIC EXTERNAL INPUTS	101
4.1	Introduction	101
4.2	Preliminaries	102
4.3	Chaotic Dynamics	105
4.4	Examples	110
4.5	Discussion	113
5	CONCLUSIONS	115
5.1	Synchronization versus Replication	117
	REFERENCES	119

CURRICULUM VITAE 133

LIST OF TABLES

TABLES

Table 3.1	Correlation between p and the period of $z_p(t)$	80
-----------	--	----

LIST OF FIGURES

FIGURES

Figure 1.1 The input-output mechanism.	5
Figure 2.1 The trajectory of system (2.6) with $x_3(0) = -2$ and $x_4(0) = 1$	13
Figure 2.2 The picture in (a) represents not only the projection of the whole attractor on the $x_1 - x_2$ plane but also the strange attractor of the generator. In a similar way, the picture shown in (b) represents the chaotic attractor of the replicator. The presented chaotic attractors of the generator and the replicator systems reveal that the chaos replication mechanism works consummately.	13
Figure 2.3 Replication of sensitivity in the result-system (2.20). The picture in (a) represents the 3-dimensional projection on the $x_1 - x_2 - x_3$ space, and the picture in (b) shows the 3-dimensional projection on the $x_4 - x_5 - x_6$ space. The sensitivity property is observable both in (a) and (b) such that the trajectories presented by blue and red colors move together in the first stage and then diverge. In other words, the sensitivity property of the generator system is mimicked by the replicator counterpart.	35
Figure 2.4 Morphogenesis of chaos through consecutive replications	46
Figure 2.5 Morphogenesis of chaos from a prior chaos as a core	46
Figure 2.6 In (a) and (b) projections of the result chaotic attractor on the $x_2 - x_4 - x_6$ and $x_3 - x_5 - x_7$ spaces are respectively presented. One can see in (a) and (b) the additional <i>foldings</i> which are not possible to observe in the 2-dimensional picture of the prior classical chaos shown in Figure 2.2, (a). In the same time, the shape of the original attractor is seen in the resulting chaos. The illustrations in (a) and (b) repeat the structure of the attractor of the generator and the similarity between these pictures is a manifestation of the morphogenesis of chaos.	47
Figure 2.7 The bifurcation diagrams of system (2.32) according to coordinates. The pictures in (a), (b), (c) and (d) represent the bifurcation diagrams corresponding to the x_2 , x_4 , x_6 and x_8 coordinates, respectively. It is observable that all replicators, likewise the generator, undergo period-doubling bifurcations at the same values of the parameter and all of them are chaotic for $\mu = \mu_\infty \equiv 40$	53
Figure 2.8 2-dimensional projections of the chaotic attractor of the result-system (2.32). The pictures in (a), (b), (c) and (d) represent the projections on the $x_1 - x_2$, $x_3 - x_4$, $x_5 - x_6$ and $x_7 - x_8$ planes, respectively. The picture in (a) shows the attractor of the prior chaos produced by the generator system (2.31), and in (b)-(d), the chaotic attractors of the remaining subsystems are observable. The illustrations in (b)-(d) repeat the structure of the attractor shown in (a), and these pictures are indicators of the chaos extension.	54

Figure 2.9 3–dimensional projections of the chaotic attractor of the result-system (2.32). (a) Projection on the $x_3 - x_5 - x_7$ space, (b) Projection on the $x_4 - x_6 - x_8$ space. The illustrations presented in (a) and (b) give information about the impressive chaotic attractor in the 8–dimensional space.	55
Figure 2.10 Pyragas control method applied to the result-system (2.41) with the aid of the corresponding control system (2.42). The pictures in (a), (b) and (c) show the graphs of the v_2 , v_5 and v_7 coordinates, respectively. The result of Pyragas control method applied to the generator system (2.39) is seen in (a). Through this method, the 2π –periodic solution of the generator and accordingly the 2π –periodic solutions of the first and the second replicator systems are stabilized. In other words, the chaos of the result-system (2.41) is controlled. The control starts at $t = 60$ and ends at $t = 200$, after which emergence of the chaos is observable again.	61
Figure 2.11 Intermittency in the Lorenz system (2.19), where $\sigma = 10$, $b = 8/3$ and $r = 166.25$. (a) The graph of the x_1 –coordinate, (b) The graph of the x_2 –coordinate, (c) The graph of the x_3 –coordinate.	62
Figure 2.12 Intermittency in the replicator system. The pictures in (a), (b) and (c) show the graphs of the x_4 , x_5 and x_6 coordinates, respectively. The analogy between the time-series of the generator and the replicator systems indicates the replication of intermittency.	63
Figure 2.13 Replication of a Shil’nikov type homoclinic orbit. In picture (a), one can see the projection on the $x_1 - x_2 - x_3$ space of the trajectory of system (2.46) corresponding to the initial data $x_1(0) = 1.57590$, $x_2(0) = 0$, $x_3(0) = 0$, $x_4(0) = -0.78795$, $x_5(0) = 0$ and $x_6(0) = 0$. The picture in (b) shows the projection on the $x_4 - x_5 - x_6$ space of the same trajectory. The parameter values $\alpha = 0.633625$, $\beta = 0.3375$ and $\mu = 2.16$ are used in the simulation. The picture in (a) represents a Shil’nikov type homoclinic orbit corresponding to the generator system (2.44), while the picture in (b) shows its replication through the system (2.46).	64
Figure 2.14 Projections of a complicated orbit of system (2.46) with the values $\alpha = 0.633625$, $\beta = 0.3375$ and $\mu = 0.83$. (a) Projection on the $x_1 - x_2 - x_3$ space, (b) Projection on the $x_4 - x_5 - x_6$ space. The initial data $x_1(0) = 1.57590$, $x_2(0) = 0$, $x_3(0) = 0$, $x_4(0) = -0.78795$, $x_5(0) = 0$, $x_6(0) = 0$ is used for the illustration. The picture in (a) represents the behavior of the trajectory corresponding to the generator (2.44), while the picture in (b) illustrates its replication.	65
Figure 2.15 3–dimensional projections of the chaotic attractor of the result-system (2.48). (a) Projection on the $x_1 - x_2 - x_3$ space, (b) Projection on the $x_4 - x_5 - x_6$ space. The picture in (a) shows the attractor of the original prior chaos of the generator system (2.47) and (b) represents the attractor of the first replicator. The resemblance between shapes of the attractors of the generator and the replicator systems makes the extension of chaos apparent.	67
Figure 2.16 3–dimensional projections of the chaotic attractor of the result-system (2.48). (a) Projection on the $x_7 - x_8 - x_9$ space, (b) Projection on the $x_{10} - x_{11} - x_{12}$ space. The pictures in (a) and (b) demonstrate the attractors generated by the second and the third replicator systems, respectively.	68

Figure 2.17 Pyragas control method applied to the result-system (2.53) by means of the corresponding control system (2.54). The pictures in (a),(b) and (c) represent the graphs of the v_2 , v_5 and v_8 coordinates, respectively. The simulation for the result-system (2.53) is provided such that in (a) and (b) periodic solutions with incommensurate periods 2 and 2π are controlled by the Pyragas method, and in (c), a quasiperiodic solution of the replicator system is pictured. The control starts at $t = 35$ and ends at $t = 120$. After switching off the control, chaos emerges again and irregular behavior reappears.	70
Figure 2.18 3–dimensional projections of the chaotic attractor of the result-system (2.55). (a) Projection on the $x_1 - x_2 - x_3$ space, (b) Projection on the $x_4 - x_5 - x_6$ space. In (a), the famous Lorenz attractor produced by the generator system (2.19) with coefficients $\sigma = 10$, $r = 28$ and $b = 8/3$ is shown. In (b), as in usual way, the projection of the chaotic attractor of the result-system (2.55), which can separately be considered as a chaotic attractor, is presented. Possibly one can call the attractor of the result-system as $6D$ Lorenz attractor.	71
Figure 2.19 3–dimensional projections of the chaotic attractor of the result-system (2.57). (a) Projection on the $x_1 - x_2 - x_3$ space, (b) Projection on the $x_4 - x_5 - x_6$ space. The picture in (a) indicates the famous Rössler attractor produced by the generator system (2.56).	72
Figure 3.1 Bifurcation diagrams of the Duffing equation perturbed with a pulse function $x'' + 0.18x' + 2x + 0.00004x^3 - 0.02\cos(2\pi t) = v(t, t_0, \mu)$, where $m_0 = 2$ and $m_1 = 1$. (a) The bifurcation diagram where the parameter μ varies between 2.6 and 4.0. (b) Magnification of (a) where μ is between 2.90 and 3.58. (c) Magnification of (b) where μ is between 3.400 and 3.572. (d) Magnification of (c) where μ changes from 3.460 to 3.571.	81
Figure 3.2 The periodic window which starts at $\mu = 3.8284$ in the bifurcation diagram of the Duffing equation perturbed with a pulse function $x'' + 0.18x' + 2x + 0.00004x^3 - 0.02\cos(2\pi t) = v(t, t_0, \mu)$, where $m_0 = 2$ and $m_1 = 1$. (a) The bifurcation diagram where μ is between 3.8250 and 3.8600. (b) Magnification of (a) where μ changes from 3.8350 to 3.8600.	83
Figure 3.3 Simulation results of the Duffing equation perturbed with a pulse function $x'' + 0.18x' + 2x + 0.00004x^3 - 0.02\cos(2\pi t) = v(t, t_0, \mu_\infty)$, where $m_0 = 2, m_1 = 1$ and $\mu_\infty = 3.8$. The pictures in (a) and (b) show the graphs of the x_1 and x_2 coordinates, respectively, while the picture in (c) represents the trajectory of the solution $(x_1(t), x_2(t))$	84
Figure 3.4 The OGY control method applied to the sequence $\{\kappa_i\}$, where $\kappa_{i+1} = 3.8\kappa_i(1 - \kappa_i)$, $\kappa_0 = 0.5$, around the fixed point $2.8/3.8$ of the logistic map with $\delta = 0.19$. The control is switched on at the iteration number $i = 25$ and switched off at $i = 60$	87
Figure 3.5 The OGY control method applied to the Duffing equation perturbed with a pulse function $x'' + 0.18x' + 2x + 0.00004x^3 - 0.02\cos(2\pi t) = v(t, t_0, \mu_\infty)$, where $m_0 = 2, m_1 = 1$ and $\mu_\infty = 3.8$. The control starts at time $t = \zeta_{25}$ and ends at $t = \zeta_{60}$. (a) The graph of the x_1 –coordinate. (b) The graph of the x_2 –coordinate. (c) The trajectory of the solution $(x_1(t), x_2(t))$	91
Figure 3.6 The trajectory of the solution $(x_1(t), x_2(t))$ for system (3.23).	92

Figure 3.7	The trajectory of the solution $(x_1(t), x_2(t))$ for the control system (3.25), where $m_0 = 2$ and $m_1 = 1$	93
Figure 3.8	2-dimensional projections of the chaotic attractor of the result-system (3.28). The pictures in (a), (b), (c) and (d) represent the projections on the $x_1 - x_2$, $x_3 - x_4$, $x_5 - x_6$ and $x_7 - x_8$ planes, respectively. The picture in (a) shows the attractor of the prior chaos produced by the generator (3.27), which is a relay-system, and in (b)-(d) the chaotic attractors of the replicator systems are observable. The illustrations in (b)-(d) repeated the structure of the attractor shown in (a), and the mimicry between these pictures is an indicator of the replication of chaos.	95
Figure 3.9	OGY control method applied to the result-relay-system (3.28). (a) The graph of the x_3 - coordinate, (b) The graph of the x_5 - coordinate, (c) The graph of the x_7 - coordinate.	96
Figure 3.10	The Pyragas control method applied to the Duffing equation perturbed with a pulse function $x'' + 0.18x' + 2x + 0.00004x^3 - 0.02 \cos(2\pi t) = v(t, t_0, \mu_\infty)$, where $m_0 = 2, m_1 = 1$ and $\mu_\infty = 3.8$. The control starts at time $t = \zeta_{30}$ and ends at $t = \zeta_{100}$. (a) The graph of the x_1 coordinate. (b) The graph of the x_2 coordinate. (c) The trajectory of the solution $(x_1(t), x_2(t))$	97
Figure 3.11	Simulation results of the perturbed Duffing equation $x'' + 0.18x' + 50x + 0.00004x^3 - 0.02 \cos(2\pi t) = v(t, t_0, \mu_\infty)$, where $m_0 = 2, m_1 = 1$ and $\mu_\infty = 3.8$. (a) The graph of the x_1 coordinate. (b) The graph of the x_2 coordinate. (c) The trajectory of the solution $(x_1(t), x_2(t))$	98
Figure 3.12	The OGY control method applied to the Duffing equation perturbed with a pulse function $x'' + 0.18x' + 50x + 0.00004x^3 - 0.02 \cos(2\pi t) = v(t, t_0, \mu_\infty)$, where $m_0 = 2, m_1 = 1$ and $\mu_\infty = 3.8$. The control starts at time $t = \zeta_{25}$ and ends at $t = \zeta_{60}$. (a) The graph of the x_1 coordinate. (b) The graph of the x_2 coordinate. (c) The trajectory of the solution $(x_1(t), x_2(t))$	99
Figure 4.1	The chaotic behavior of the <i>SICNN</i> (4.9).	111
Figure 4.2	The chaotic behavior of the <i>SICNN</i> (4.10).	112
Figure 4.3	The projection of the chaotic attractor of the network (4.10) on the $x_{22} - x_{31} - x_{33}$ space.	113

CHAPTER 1

INTRODUCTION

The main subject of this thesis is chaos. Since the literature on the subject is very rich, we are not original. In the same time, we consider in this thesis chaos as being an *input* for differential equations. Formally speaking, we insert chaos in the right-hand-side of the equations. This is what makes our studies a unique one among all others in the literature. One can remember that standardly, chaos is formed by solutions of discrete equations and differential equations. That is, chaos is an output with respect to these systems. One can consider, for example, the Lorenz system, the Duffing's oscillator and the Chua circuit. Another novelty of this thesis is that we describe expansion of chaos on the basis of the input-output mechanism by using the concept of *morphogenesis* to emphasize that the expansion keeps geometrical properties of chaos.

Let us describe the importance of the input-output mechanism in chaos analysis for both theory and applications:

1. In the theory of dynamical systems, a large number of results use in their formulation the input-output mechanism. For example, there are many theorems, which can be loosely formulated as follows: if the perturbation is periodic (bounded, almost periodic), then there is a unique periodic (bounded, almost periodic) solution. We propose to consider in our results the following implication to be considered: if the perturbation is chaotic, then there is a chaos in the set of solutions. Thus, one can say that our main proposal is to return investigation of chaos into the main stream of classical dynamical systems and, consequently, a huge number of rigorous mathematical methods, numerical instruments and applications, which rely on the mechanism, will now be involved for investigation of chaotic processes.
2. Despite the fact that many distinguished specialists in chaos theory and mathematics have been involved in the investigation, there are still many challenging problems related to origins of the chaotic theory: we do not have rigorously approved chaos in Lorenz systems, Duffing equations and other systems. Hopefully, the input-output mechanism will give new opportunities for the analysis of the basic models as well as help to revise the theory of chaos. We believe that exploration of the mechanism in considered models can give mathematical clarity there.

3. The mechanism can become a strong instrument in applications to real world problems through modeling the expansion of chaos. We hope that unpredictability of weather and irregularity as a global phenomena will be reflected in mathematical investigations more comprehensively. This is true not only for atmospheric processes, but also for any large systems in economic theory, biology, neural networks and computer sciences. Utilization of the input-output mechanism in cryptography and deciphering deals may give effective results, too. The input-output mechanism is very popular, for instance, in mechanics, chemistry, biology, cryptography, etc. Consequently, one can suppose that what we suggest has to be realized immediately for these real world problems.

The studies mentioned here are attractive, in the mathematical sense, since for the first time we have introduced what we understand as chaos for systems with continuous time. This may give a push for functional analysis of chaos to involve the operator theory results, etc. Hopefully, our approach will give a basis for a deeper comprehension and possibility to unite different appearances of chaos. In this framework, we also hope that the results can be developed for partial differential equations, integro-differential equations, functional differential equations, evolution systems, etc.

The content of this thesis is a good background for applications in mechanics, biology, molecular biology, physiology, pharmacology, secure communications, neural networks, and other real world problems involving complex behavior of models. Since chaos is present everywhere, we can say that our results are applicable in any field, where differential equations and difference equations are utilized as models.

1.1 Chaotic Dynamical Systems

The theory of dynamical systems starts with H. Poincaré, who studied nonlinear differential equations by introducing qualitative techniques to discuss the global properties of solutions [64]. His discovery of the homoclinic orbits figures prominently in the studies of chaotic dynamical systems. Poincaré first encountered the presence of homoclinic orbits in the three body problem of celestial mechanics [22]. A Poincaré homoclinic orbit is an orbit of intersection of the stable and unstable manifolds of a saddle periodic orbit. It is called structurally stable if the intersection is transverse, and structurally unstable or a homoclinic tangency if the invariant manifolds are tangent along the orbit [81]. In any neighborhood of a structurally stable Poincaré homoclinic orbit there exist nontrivial hyperbolic sets containing a countable number of saddle periodic orbits and continuum of non-periodic Poisson stable orbits [81, 204, 206]. For this reason, the presence of a structurally stable Poincaré homoclinic orbit can be considered as a criterion for the presence of complex dynamics [81].

The first mathematically rigorous definition of chaos is introduced by Li and Yorke [134] for one dimensional difference equations. According to [134], a continuous map $F : J \rightarrow J$, where $J \subset \mathbb{R}$ is an interval, exhibits chaos if: (i) For every natural number p , there exists

a p -periodic point of F in J ; (ii) There is an uncountable set $S \subset J$ containing no periodic points such that for every $s_1, s_2 \in S$ with $s_1 \neq s_2$ we have $\limsup_{k \rightarrow \infty} |F^k(s_1) - F^k(s_2)| > 0$ and $\liminf_{k \rightarrow \infty} |F^k(s_1) - F^k(s_2)| = 0$; (iii) For every $s \in S$ and periodic point $\bar{s} \in J$ we have $\limsup_{k \rightarrow \infty} |F^k(s) - F^k(\bar{s})| > 0$.

Generalizations of Li-Yorke chaos to high dimensional difference equations were provided in [20, 120, 133, 143]. According to results of [143], if a repelling fixed point of a differentiable map has an associated homoclinic orbit that is transversal in some sense, then the map must exhibit chaotic behavior. More precisely, if a multidimensional differentiable map has a snap-back repeller, then it is chaotic. Marotto's Theorem was used in [133] to prove rigorously the existence of Li-Yorke chaos in a spatiotemporal chaotic system. Furthermore, the notion of Li-Yorke sensitivity, which links the Li-Yorke chaos with the notion of sensitivity, was studied in [20], and generalizations of Li-Yorke chaos to mappings in Banach spaces and complete metric spaces were considered in [120].

Another mathematical definition of chaos for discrete-time dynamics was introduced by Devaney [64]. According to [64], a map $F : J \rightarrow J$, where $J \subset \mathbb{R}$ is an interval, has sensitive dependence on initial conditions if there exists $\delta > 0$ such that for any $x \in J$ and any neighborhood N of x there exists $y \in J$ and a positive integer k such that $|F^k(x) - F^k(y)| > \delta$. On the other hand, F is said to be topologically transitive if for any pair of open sets $U, V \subset J$ there exists a positive integer k such that $f^k(U) \cap V \neq \emptyset$. According to Devaney, a map $F : J \rightarrow J$ is chaotic on J if: (i) F has sensitive dependence on initial conditions; (ii) F is topologically transitive; (iii) Periodic points of F are dense in J . In other words, a chaotic map possesses three ingredients: unpredictability, indecomposability and an element of regularity.

Symbolic dynamics, whose earliest examples were constructed by Hadamard [90] and Morse [156], is one of the oldest techniques for the study of chaos. Symbolic dynamical systems are systems whose phase space consists of one-sided or two-sided infinite sequences of symbols chosen from a finite alphabet. Such dynamics arises in a variety of situations such as in horseshoe maps and the logistic map. The set of allowed sequences is invariant under the shift map, which is the most important ingredient in symbolic dynamics [64, 84, 92, 117, 232, 233]. Moreover, it is known that the symbolic dynamics admits the chaos in the sense of both Devaney and Li-Yorke [8, 10, 12, 64, 179].

The Smale Horseshoe map is first studied by Smale [207] and it is an example of a diffeomorphism which is structurally stable and possesses a chaotic invariant set [64, 117, 233]. The horseshoe arises whenever one has transverse homoclinic orbits, as in the case of the Duffing equation [85]. People used the symbolic dynamics to discover chaos, but we suppose that it can serve as an "embryo" for the morphogenesis of chaos.

From the mathematical point of view, chaotic systems are characterized by local instability and uniform boundedness of the trajectories. Since local instability of a linear system implies unboundedness of its solutions, chaotic system should be necessarily nonlinear [76]. Chaos in dynamical systems is commonly associated with the notion of a strange attractor, which is an

attractive limit set with a complicated structure of orbit behavior. This term was introduced by Ruelle and Takens [183] in the sense where the word strange means the limit set has a fractal structure [81]. The dynamics of chaotic systems are sensitive to small perturbations of initial conditions. This means that if we take two close but different points in the phase space and follow their evolution, then we see that the two phase trajectories starting from these points eventually diverge [64, 89]. The sensitive dependence on the initial condition is used both to stabilize the chaotic behavior in periodic orbits and to direct trajectories to a desired state [196].

It was Lorenz [137] who discovered that the dynamics of an infinite dimensional system being reduced to three dimensional equation can be next analyzed in its chaotic appearances by application of the simple unimodal one dimensional map. Smale [207] explained that the geometry of the horseshoe map is underneath of the Van der Pol equation's complex dynamics which was investigated by Cartwright and Littlewood [48] and later by Levinson [131]. Nowadays, the Smale horseshoes with its chaotic dynamics, is one of the basic instruments when one tries to recognize a chaos in a process. Guckenheimer and Williams [87] gave a geometric description of the flow of Lorenz attractor to show the structural stability of codimension 2. In addition to this, it was found out that the topology of the Lorenz attractor is considerably more complicated than the topology of the horseshoe [85]. Moreover, Levi [130] used a geometric approach for a simplified version of the Van der pol equation to show the existence of horseshoes embedded within the Van der Pol map and how the horseshoes fit in the phase plane.

1.2 The Input/Output Mechanism of Chaos and Morphogenesis

It is natural *to discover a chaos* [52, 96, 134, 137, 143, 145, 175, 180, 181, 183, 186, 189, 200, 215], and proceed by producing basic definitions and creating the theory. On the other hand, one can *shape* an irregular process by inserting chaotic elements in a system which has regular dynamics (let us say comprising an asymptotically stable equilibrium, a global attractor, etc). This approach to the problem also deserves consideration as it may allow for a more rigorous treatment of the phenomenon, and helps to develop new methods of investigation. Our results are of this type.

In this thesis, we use the idea that chaos can be used as input in systems of equations. To explain the input-output procedure which is realized in our study, let us give particular examples of systems used in the thesis. Consider the following system of differential equations,

$$\frac{dx}{dt} = B(x). \quad (1.1)$$

The system (1.1) is called *the base-system*. We assume that the system admits a regular property. For example, there is a globally asymptotically stable equilibrium of (1.1). Next, we apply to the system a perturbation, $I(t)$, which will be called an *input* and obtain the

following system,

$$\frac{dx}{dt} = B(x) + I(t), \quad (1.2)$$

which will be called as the *replicator* system.

Suppose that the input I admits a certain property, let us say, it is a bounded function. We assume then that there exists a unique solution, $x(t)$, of the last equation, the replicator, with the same property of boundedness. This solution is considered as an *output*. The process for obtaining the solution $x(t)$ of the replicator system by applying the perturbation $I(t)$ to the base-system (1.1) is called the *input-output mechanism*, and sometimes we shall call it the *machinery*. It is known that for certain base-systems, if the input is periodic, almost periodic, bounded, then there exists an output, which is also periodic, almost periodic, bounded. In this thesis, we consider inputs of the new nature: chaotic sets and chaotic functions. The motions which are in the chaotic attractor of the Lorenz system considered altogether provide us an example of a chaotic set of functions. Any element of this set is considered as a chaotic function. Both of these types of inputs will be used in our study effectively. To prove rigorously, by verification of all ingredients, that there exists a certain type of chaos generated by the input-output mechanism, we use the concept of the chaotic set. For simulations we shall use inputs in the form of chaotic functions. The diagram in Figure 1.1 illustrates the input-output mechanism schematically. We have to say that in the figure the input I can be a set of functions as well as a single function. The same is true for the output, $x(t)$.

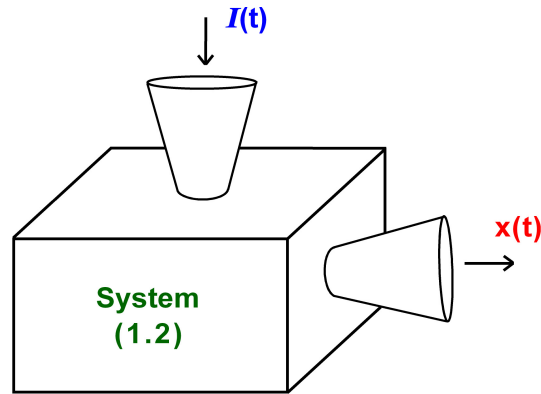


Figure 1.1: The input-output mechanism.

The main source of chaos in theory are difference and differential equations. For this reason we consider inputs, which are solutions of some systems of differential equations or discrete equations. These systems will be called *generators* in this thesis.

Thus, we can consider the following system of differential equations,

$$\frac{dz}{dt} = G(z), \quad (1.3)$$

and it is assumed that this system possesses chaos. We shall call this system a *generator*. If $z(t)$ is a solution of the system from the chaotic attractor, that is, it is a chaotic solution, then we notate $I(t) = z(t)$ and use the function $I(t)$ in the equation (1.2).

In this thesis, we have proved rigorously that the output is of the same type of chaos as the input if base-systems are with globally asymptotically stable equilibriums. We use the concept of morphogenesis for two reasons. First of all, morphogenesis is convenient to describe how the input-output mechanism works if chaos is an input. Secondly, it provides information about the structure of the chaos-output, if one knows the structure of the chaos-input. We give a full description of the chaos expansion as morphogenesis, if base-systems are linear and with constant matrices of coefficients.

The term morphogenesis is used issuing from the sense of the words *morph* meaning “form” and *genesis* meaning “creation”. This is similar to the idea such that morphogenesis is used in fields such as urban studies [58], architecture [182], mechanics [213], computer science [36], linguistics [91] and sociology [25, 45]. Morphogenesis in this thesis is understood in this weak sense, and mechanism of the replication is simple. In discussion form we consider inheritance of intermittency, the double-scroll Chua’s attractor and quasiperiodical motions as a possible skeleton of a chaotic attractor. We make comparison of the main concept of our study with Turing’s morphogenesis [223] and John von Neumann automata [160], considering that this may not be only a formal comparison, but will give ideas for the chaos development in the morphogenesis of Turing and for self-replicating machines.

We propose a rigorous identification method for replication of chaos from a prior one to systems with large dimensions. Extension of the formal properties and features of a complex motion can be observed such that ingredients of chaos united as known types of chaos, Devaney’s, Li-Yorke and others. This is true for other appearances of chaos: intermittency, structure of the chaotic attractor, its fractal dimension, form of the bifurcation diagram, the spectra of Lyapunov exponents, etc.

In our theoretical results of chaos extension, we use coupled systems in which the generator influences the replicator in a unidirectional way, that is, the generator affects the behavior of the replicator, but not the converse. The possibility of making use of more than one replicators and nonidentical systems in the machinery is an advantage of the procedure. On the other hand, contrary to the method that we present, in the synchronization of chaotic systems, one does not consider the type of the chaos that the master and slave systems admit. The problem that whether the synchronization of systems implies the same type of chaos for both master and slave has not been taken into account yet.

The concept of morphogenesis is considered carefully only in the second chapter of the thesis, for systems with stable equilibrium, since for systems with stable equilibriums all the known ingredients of chaos are proper.

1.3 Synchronization of Chaotic Systems

One of the usage areas of master-slave systems is the study of synchronization of chaotic systems [1, 3, 82, 100, 122, 168, 184]. In 1990, Pecora and Carroll [168] realized that two identical chaotic systems can be synchronized under appropriate unidirectional coupling schemes. Consider the system

$$x' = G(x), \quad (1.4)$$

as the master, where $x \in \mathbb{R}^d$, such that the steady evolution of the system occurs in a chaotic attractor. The dynamics of the slave system is governed by the equation

$$y' = H(x, y). \quad (1.5)$$

When the unidirectional drive is established, suppose that the right hand side of equation (1.5) satisfies that

$$H(x, y) = G(x), \quad (1.6)$$

for $y = x$, and the slave system takes the form

$$y' = G(y), \quad (1.7)$$

which is a copy of system (1.4), in the absence of driving. In unidirectional couplings, the signals of the master system acts on the slave system, but the converse is not true. Moreover, this action becomes null when the two systems follow identical trajectories [82]. The continuous control scheme [67, 113] and the method of replacement of variables [61, 169] can be used to obtain couplings in the form of the system (1.4) + (1.5). Synchronization of a slave system to a master system, under the condition (1.6), is known as identical synchronization, and it occurs when there are sets of initial data $\mathcal{B}_x \subset \mathbb{R}^d$ and $\mathcal{B}_y \subset \mathbb{R}^d$ for the master and slave systems, respectively, such that the equation $\lim_{t \rightarrow \infty} \|x(t) - y(t)\| = 0$ holds, where $(x(t), y(t))$ is a solution of system (1.4) + (1.5) with initial data $(x(0), y(0)) \in \mathcal{B}_x \times \mathcal{B}_y$.

In paper [4], Afraimovich et al. proposed the synchronization of chaotic systems that are different and not restricted in coupling. To realize this proposal, Rulkov et al. [184] considered the concept of generalized synchronization for unidirectionally coupled systems.

Consider the unidirectionally coupled system (1.4) + (1.5) such that the dimensions of the master and slave systems are d and r , respectively. Generalized synchronization [1, 3, 82, 100, 122, 184] is said to occur if there exist sets $\mathcal{B}_x \subset \mathbb{R}^d$, $\mathcal{B}_y \subset \mathbb{R}^r$ of initial conditions and a transformation ψ , defined on the chaotic attractor of (1.4), such that for all $x(0) \in \mathcal{B}_x$, $y(0) \in \mathcal{B}_y$ the relation

$$\lim_{t \rightarrow \infty} \|y(t) - \psi(x(t))\| = 0 \quad (1.8)$$

holds. In this case, a motion that starts on $\mathcal{B}_x \times \mathcal{B}_y$ collapses onto a manifold $M \subset \mathcal{B}_x \times \mathcal{B}_y$ of synchronized motions. The transformation ψ is not required to exist for the transient trajectories. Generalized synchronization includes the identical synchronization as a particular

case. That is, if ψ is the identity transformation, then identical synchronization takes place. The paper [100] deals with the case when the transformation ψ is differentiable.

According to Kocarev and Parlitz [122], generalized synchronization occurs in the dynamics of the coupled system (1.4) + (1.5) if and only if for all $x_0 \in \mathcal{B}_x, y_{10}, y_{20} \in \mathcal{B}_y$, the criterion

$$\lim_{t \rightarrow \infty} \|y(t, x_0, y_{10}) - y(t, x_0, y_{20})\| = 0 \quad (1.9)$$

holds, where $y(t, x_0, y_{10}), y(t, x_0, y_{20})$ denote the solutions of the slave system (1.5) with the initial data $y(0, x_0, y_{10}) = y_{10}, y(0, x_0, y_{20}) = y_{20}$ and the same $x(t), x(0) = x_0$.

As a consequence of generalized synchronization, the behavior of the slave system (1.5) can be predicted by the knowledge of the trajectories of the master system (1.4) and the transformation ψ . The master system is also predictable from the slave system, if ψ is invertible [122].

1.4 Control of Chaos

The idea of chaos control is based on the fact that chaotic attractors have a skeleton made of an infinite number of unstable periodic orbits [64, 82, 89, 114, 195]. Stability can be described as the ability of a system to keep itself working properly even when perturbations act on it, and this is the main goal to be achieved by the control strategy that is embedded in the system [195]. In other words, the aim of chaos control is to stabilize a previously chosen unstable periodic orbit by means of small perturbations applied to the system, so the chaotic dynamics is substituted by a periodic one chosen at will among the several available [82]. That is, when control is present, a chaotic trajectory transforms into a periodic one [76]. Experimental demonstrations of chaos control methods were presented in the papers [30, 32, 35, 68, 80, 94, 150, 194].

Small perturbations applied to control parameters can be used to stabilize chaos, keeping the parameters in the neighborhood of their nominal values, and this idea is first introduced by Ott, Grebogi and Yorke [163]. Experimental applications of the OGY control method requires a permanent computer analysis of the state of the system. The method deals with a Poincaré map and therefore, the parameter changes are discrete in time. Using this method, one can stabilize only those periodic orbits whose maximal Lyapunov exponent is small compared to the reciprocal of the time interval between parameter changes [177]. Another control method has been developed by Pyragas [177] to stabilize unstable periodic orbits applying small time continuous control to a parameter of a system while it evolves in continuous time, instead of a discrete control at the crossing of a surface [82]. Pyragas control method uses a delayed feedback employing a suitably amplified difference of an output measurement of the chaotic system and the respectively delayed measurement for control. The control signal vanishes in the post-transient behavior for the stabilized orbit. For this reason, the delay time has to be the exact value of the period of the unstable periodic orbit that will be stabilized [97]. Both of the OGY and Pyragas control methods will be utilized in the thesis.

1.5 Neural Networks and Chaos

The chaos phenomenon has been observed in the dynamics of neural networks [5, 6, 77, 86, 126, 158, 159, 176, 201, 205, 220, 231], and chaotic dynamics applying as external inputs are useful for separating image segments [201], information processing [158, 159] and synchronization of neural networks [136, 140, 240]. Aihara et. al. [6] proposed a model of a single neuron with chaotic dynamics by considering graded responses, relative refractoriness and spatio-temporal summation of inputs. Chaotic solutions of both the single chaotic neuron and the chaotic neural network composed of such neurons were demonstrated numerically in [6]. Focusing on the model proposed in [6], dynamical properties of a chaotic neural network in chaotic wandering state were studied concerning sensitivity to external inputs in [126]. On the other hand, in the paper [201], Aihara's chaotic neuron model is used as the fundamental model of elements in a network, and the synchronization characteristics in response to external inputs in a coupled lattice based on a Newman-Watts model are investigated. Besides, in the studies [158, 159], a network consisting of binary neurons which do not display chaotic behavior is considered, and by means of the reduction of synaptic connectivities it is shown that the state of the network in which cycle memories are embedded reveals chaotic wandering among memory attractor basins. Moreover, it is mentioned that chaotic wandering among memories is considerably intermittent. Chaotic solutions to the Hodgkin-Huxley equations with periodic forcing have been discovered in [5]. The paper [86] indicates the existence of chaotic solutions in the Hodgkin-Huxley model with its original parameters. An analytical proof for the existence of chaos through period-doubling cascade in a discrete-time neural network is given in [231], and the problem of creating a robust chaotic neural network is handled in [176].

1.6 Organization of the Thesis

The rest of the thesis is organized as follows.

In Chapter 2, we propose a rigorous method for replication of chaos from a prior one to systems with arbitrary large dimensions. Extension of the formal properties and features of a complex motion can be observed such that ingredients of chaos united as known types of chaos, Devaney's, Li-Yorke and obtained through period-doubling cascade. This is true for other appearances of chaos: intermittency, structure of the chaotic attractor, its fractal dimension, form of the bifurcation diagram, the spectra of Lyapunov exponents, etc. That is why we identify the extension of chaos through the replication as morphogenesis. To provide rigorous study of the subject, we introduce new definitions such as chaotic sets of functions, the generator and replicator of chaos, and precise description of ingredients for Devaney and Li-Yorke chaos in continuous dynamics. Appropriate simulations which illustrate the chaos replication phenomenon are provided. Moreover, in discussion form we consider inheritance of intermittency, replication of Shil'nikov orbits and quasiperiodical motions as a possible skeleton of a chaotic attractor. Chaos extension in an open chain of Chua circuits is also

demonstrated.

Chapter 3 deals with the Duffing equation forced with a pulse function, whose moments of discontinuity depend on the initial data. Existence of the chaos through period-doubling cascade is proved, and the OGY control method is used to stabilize the periodic solutions. Appropriate simulations of the chaos and stabilized periodic solutions are presented.

Taking advantage of external inputs, it is shown in Chapter 4 that shunting inhibitory cellular neural networks (SICNNs) behave chaotically. This is the first time that a theoretically approved chaos is obtained in SICNNs. The analysis is based on the Li-Yorke definition of chaos. We develop the concept of Li-Yorke chaos to continuous and multidimensional dynamics of SICNNs. Appropriate illustrations which support the theoretical results are depicted.

The last chapter of the thesis is devoted to conclusions and possible future studies. Moreover, a comparison of the synchronization theory of chaotic systems and replication of chaos is mentioned.

CHAPTER 2

REPLICATION OF CHAOS

2.1 Introduction

It is known that if one considers the evolution equation $u' = L[u] + I(t)$, where $L[u]$ is a linear operator with spectra placed in the left half of the complex plane, then a function $I(t)$ being considered as an *input* with a certain property (boundedness, periodicity, almost periodicity) produces through the equation the *output*, a solution with a similar property, boundedness/periodicity/almost periodicity [54, 75].

A reasonable question appears whether it is possible to use as input a chaotic motion and to obtain output also as a chaos of certain type. Our study is devoted to answer this question even if the input is inserted non-linearly. One must say that we consider as an input first of all a single function, a member of a chaotic set to obtain a solution, which is a member of another chaotic set. Beside that we consider the chaotic sets as the input and the output. We have been forced to consider sets of functions as inputs and outputs, since Devaney or Li-Yorke chaos are indicated through relation of motions (sensitivity, transitivity, proximality). Thus, we consider the input and the output not only as single functions, but also as collections of functions. The way of our investigation is arranged in the well accepted traditional mathematical fashion, but with a new and a more complex way of arrangement of the connections between the input and the output.

Since the concept of chaos is much more complex than just single periodic or almost periodic solutions, we have to use a special terminology for the chaos generation through the input-output mechanism, *replication of chaos*.

The technique of the replication used in this chapter is as follows. We need a source of chaotic inputs, but mostly chaos can be obtained through solving differential or difference equations. For this reason, we use special generator systems as the source of chaos or chaotic functions. Nevertheless, we emphasize that the generator is not necessarily the element of the replication procedure since it can be replaced by another source of a chaotic input, and in applications present result may be considered with, for example, chaotic inputs obtained from experimental activity. So, initially, we take into account a system of differential equations (the generator) which produces chaos, and we use this system to influence in a unidirectional way, another

system (the replicator) in such a manner that the replicator mimics the same ingredients of chaos provided to the generator. In the present chapter, we use such ingredients in the form of period-doubling cascade, Devaney and Li-Yorke chaos. For the study of the subject, we introduce new definitions such as chaotic sets of functions, the generator and replicator of chaos, and precise description of ingredients for Devaney and Li-Yorke chaos in continuous dynamics.

Throughout the chapter, the generator will be considered as a system of the form

$$x' = F(t, x), \quad (2.1)$$

where $F : \mathbb{R} \times \mathbb{R}^m \rightarrow \mathbb{R}^m$ is a continuous function in all its arguments, and the replicator is assumed to have the form

$$y' = Ay + g(x(t), y), \quad (2.2)$$

where $g : \mathbb{R}^m \times \mathbb{R}^n \rightarrow \mathbb{R}^n$ is a continuous function in all its arguments, the constant $n \times n$ real valued matrix A has real parts of eigenvalues all negative and the function $x(t)$ is a solution of system (2.1). The generator-replicator couple, (2.1) + (2.2), will be called in the remaining parts of the chapter as the *result-system*.

Now, to illustrate the replication mechanism discussed in our study, let us consider the following example. For our purposes, as the generator we shall take into account the Duffing's oscillator represented by the differential equation

$$x'' + 0.05x' + x^3 = 7.5 \cos t. \quad (2.3)$$

It is known that equation (2.3) possesses a chaotic attractor [218]. Defining the variables $x_1 = x$ and $x_2 = x'$, equation (2.3) can be reduced to the system

$$\begin{aligned} x_1' &= x_2 \\ x_2' &= -0.05x_2 - x_1^3 + 7.5 \cos t. \end{aligned} \quad (2.4)$$

Next, let us consider the following system

$$\begin{aligned} x_3' &= x_4 + x_1(t) \\ x_4' &= -3x_3 - 2x_4 - 0.008x_3^3 + x_2(t). \end{aligned} \quad (2.5)$$

In this form system (2.5) is a replicator. One has to emphasize that the linear part of the associated with (2.5) non-perturbed system

$$\begin{aligned} x_3' &= x_4 \\ x_4' &= -3x_3 - 2x_4 - 0.008x_3^3, \end{aligned} \quad (2.6)$$

has eigenvalues with negative real parts and does not admit chaos.

Figure 2.1 shows the trajectory of system (2.6) with $x_3(0) = -2$ and $x_4(0) = 1$. It is seen in the figure that the behavior of the solution is non-chaotic.

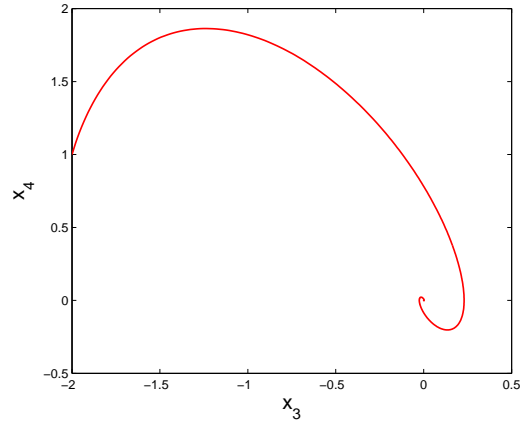


Figure 2.1: The trajectory of system (2.6) with $x_3(0) = -2$ and $x_4(0) = 1$.

To visualize the process of replication by the result-system, (2.4) + (2.5), let us consider the Poincaré sections of the both. By marking the trajectory of this system with the initial data $x_1(0) = 2, x_2(0) = 3, x_3(0) = -1, x_4(0) = 1$ stroboscopically at times that are integer multiples of 2π , we obtain the Poincaré section and in Figure 2.2, where the chaos replication is apparent, we illustrate its 2-dimensional projections. Figure 2.2, (a) represents the projection of the Poincaré section on the $x_1 - x_2$ plane, and we note that this projection is in fact the strange attractor of the generator system (2.4). On the other hand, the projection on the $x_3 - x_4$ plane presented in Figure 2.2, (b) is the attractor corresponding to the replicator system (2.5). One can see that the attractor indicated in Figure 2.2, (b) repeated the structure of the attractor shown in Figure 2.2, (a) and this result is a manifestation of the replication of chaos. One has to think about mathematical aspects of this phenomena and in our study we handle this problem.

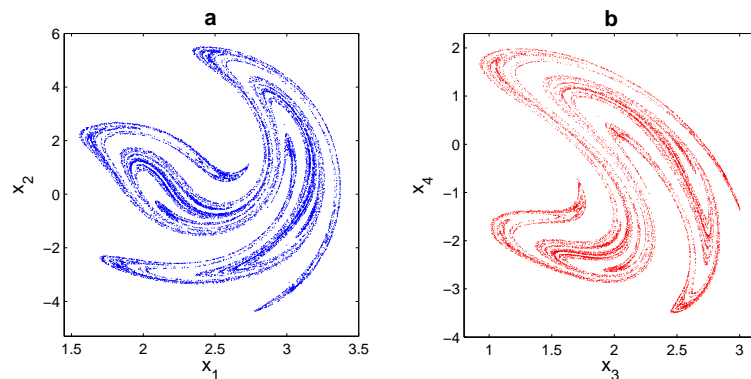


Figure 2.2: The picture in (a) represents not only the projection of the whole attractor on the $x_1 - x_2$ plane but also the strange attractor of the generator. In a similar way, the picture shown in (b) represents the chaotic attractor of the replicator. The presented chaotic attractors of the generator and the replicator systems reveal that the chaos replication mechanism works consummately.

In our theoretical results, we use coupled systems in which the generator influences the replicator in a unidirectional way. In other words, the generator affects the behavior of the replicator counterpart in such a way that the solutions of the generator are used as an input for the latter. The possibility of making use of more than one replicator systems with arbitrarily high dimensions in the extension mechanism is an advantage of our procedure. Moreover, we are describing a process involving the replication of chaos which does not occur in the course of time, but instead an **instantaneous** one. In other words, the prior chaos is mimicked in all existing replicators such that the generating mechanism works through arranging connections between systems not with the lapse of time.

Since we do not restrict ourselves in this chapter with a simple couple *the generator-the replicator*, but get them in different combinations and numbers, having the geometric features of chaos saved, we shall call the extension of chaos as *morphogenesis*.

In our study, we try to use the term morphogenesis issuing from the sense of the words *morph* meaning “form” and *genesis* meaning “creation” [62]. In other words, similar to the ideas of René Thom [217], we employ the word *morphogenesis* as its etymology indicates, to denote *processes creating forms*. One should understand *morphogenesis of chaos* as a form-generating mechanism emerging from a dynamical process which is based on replication of chaos. Here, we accept the form (morph) not only as a type of chaos, but also accompanying concepts as the structure of the chaotic attractor, its fractal dimension, form of the bifurcation diagram, the spectra of Lyapunov exponents, inheritance of intermittency, etc.

To understand the concept of our study better, let us consider morphogenesis of fractal structures [141, 142]. It is important to say that Mandelbrot fractal structures exhibit the appearance of fractal hierarchy looking **in**, that is, **a part is similar to the whole**. Examples for this are the Julia sets [42, 152] and the Sierpinski carpet [170]. In our morphogenesis both directions, **in** and **out**, are present. Indeed, the fractal structure of the prior chaos has hierarchy looking **in**, and the structure for the result-system is obtained considering hierarchy looking **out**, that is, when **the whole is similar to the part**.

In our results, we do not consider the chaos synchronization problem, but we say that the type of the chaos is kept *invariant* in the procedure. That is why the classes which can be considered with respect to this *invariance* is expectedly wider than those investigated for synchronization of chaos. Since we do not request strong relation and accordance between the solutions of the generator and the replicator in the asymptotic point of view, the terms *master* and *slave* as well as *drive* and *response* are not preferred to be used for the analyzed systems. On the other hand, contrary to the method that we present, in the synchronization of chaotic systems, one does not consider the type of the chaos that the master and slave systems admit. The problem that whether the synchronization of systems implies the same type of chaos for both master and slave has not been taken into account yet.

The phenomenon of the form recognition for chaotic processes has already begun in pioneering papers [48, 85, 87, 130, 131, 137, 207]. All these results say about chaos recognition, by

reducing complex behavior to the structure with recognizable chaos. In [7, 9, 10, 11, 12, 13, 16, 17], we provide a different and constructive way when a recognized chaos can be extended saving the form of chaos to a multidimensional system. In the present study, we generalize the idea to the morphogenesis of chaos.

Nowadays, one can consider the development of a multidimensional chaos from a low dimensional one in different ways. One of them is the chaotic itinerancy [102, 107, 108, 109, 110, 190, 220, 221]. The itinerant motion among varieties of ordered states through high dimensional chaotic motion can be observed and this behavior is named as chaotic itinerancy. In other words, chaotic itinerancy is a universal dynamics in high dimensional dynamical systems, showing itinerant motion among varieties of low-dimensional ordered states through high dimensional chaos. This phenomenon occurs in different real world processes: optical turbulence [102], globally coupled chaotic systems [107, 108], non-equilibrium neural networks [220, 221], analysis of brain activities [78] and ecological systems [119]. One can see that in its degenerated form chaotic itinerancy relates to intermittency [154, 175], since they both represent dynamical interchange of irregularity and regularity.

Likewise the itinerant chaos observed in brain activities, we have low dimensional chaos in the subsystems considered and high dimensional chaos is obtained when one considers all subsystems as a whole. The main difference compared to our technique is in the elapsed time for the occurrence of the process. In our discussions, no itinerant motion is observable and all resultant chaotic subsystems process simultaneously, whereas the low dimensional chaotic motions take place as time elapses in the case of chaotic itinerancy. Knowledge of the type of chaos is another difference between chaotic itinerancy and our procedure. Possibly the present way of replication of chaos will give a light to the solutions of problems about extension of irregular behavior (crises, collapses, etc.) in interrelated or multiple connected systems which can arise in problems of classical mechanics [154], electrical systems [51, 116], economic theory [138] and brain activity investigations [78].

In systems whose dimension is at least four, it is possible to observe chaotic attractors with at least two positive Lyapunov exponents and such systems are called hyperchaotic [211]. An example of a four dimensional hyperchaotic system is discovered by Rössler [181]. Combining two or more chaotic, not necessarily identical, systems is a way of achieving hyperchaos [112, 115, 116]. However, in the present chapter, we take into account exactly one chaotic system with a known type of chaos, and use this system as the generator to reproduce the same type of chaos in other systems. On the other hand, the crucial phenomenon in the hyperchaotic systems is the existence of two or more positive Lyapunov exponents and the type of chaos is not taken into account. In our way of morphogenesis, the critical situation is rather the replication of a known type of chaos.

The paper [223] was one of the first studies that consider mathematically the self-replicating forms using a set of reaction-diffusion equations [193]. Taking inspiration from the ideas of Turing, Smale [208] considers the problem of whether oscillations can be generated through coupling of identical systems which tend to an equilibrium. A similar question is also rea-

sonable for the achievement of chaos in such systems and it is found out that, without using a chaotic input, it is possible to obtain coupled systems which exhibit chaotic behavior. The existence of strange attractors in a family of vector fields consisting of two Brusselators linearly coupled by diffusion is proved analytically in the paper [71] and numerical examples of such a chaotic behavior are provided in [72]. Such couplings display several cases of Hopf-pitchfork singularities of codimensions 2, 3 and 4. In all these cases, the corresponding bifurcation diagrams provide regions of parameters such that the system exhibits synchronization, regions where synchronization depends on the initial state and regions where orbits show infinitely many transients of synchronization [73]. Another example of a linearly coupled system which exhibit chaotic behavior can be found in [241]. According to the results of paper [241], a sufficiently large coupling coefficient used in a network of linearly coupled identical systems, where each node is located in a non-chaotic region, leads to existence of a positive transversal Lyapunov exponent and makes the system behave chaotically. The Lorenz systems with stable equilibria can be used in the construction of such a network of linearly coupled systems. Distinctively, in our study, we make use of coupled systems such that exactly one of them is chaotic with a known type of chaos and prove theoretically that the same type of chaos is extended. Moreover, in the presented mechanism, we are not restricted to use linear couplings as well as identical systems.

In the next section we will present assumptions for systems (2.1) and (2.2) which are needed for the chaos replication, and introduce the chaotic attractors of these systems in the functional sense.

2.2 Preliminaries

In the chapter, \mathbb{R} and \mathbb{N} denote the sets of real numbers and natural numbers, respectively, and the uniform norm $\|\Gamma\| = \sup_{\|v\|=1} \|\Gamma v\|$ for matrices is used.

Since the matrix A , which is aforementioned in system (2.2), is supposed to admit eigenvalues all with negative real parts, it is easy to verify the existence of positive numbers N and ω such that $\|e^{At}\| \leq Ne^{-\omega t}$, $t \geq 0$. These numbers will be used in the last condition below.

The following assumptions on systems (2.1) and (2.2) are needed throughout the chapter:

(A1) There exists a positive number T such that the function $F(t, x)$ satisfies the periodicity condition

$$F(t + T, x) = F(t, x),$$

for all $t \in \mathbb{R}$, $x \in \mathbb{R}^m$;

(A2) There exists a positive number L_0 such that

$$\|F(t, x_1) - F(t, x_2)\| \leq L_0 \|x_1 - x_2\|,$$

for all $t \in \mathbb{R}$, $x_1, x_2 \in \mathbb{R}^m$;

(A3) There exists a positive number $H_0 < \infty$ such that

$$\sup_{t \in \mathbb{R}, x \in \mathbb{R}^m} \|F(t, x)\| \leq H_0;$$

(A4) There exists a positive number L_1 such that

$$\|g(x_1, y) - g(x_2, y)\| \geq L_1 \|x_1 - x_2\|,$$

for all $x_1, x_2 \in \mathbb{R}^m, y \in \mathbb{R}^n$;

(A5) There exist positive numbers L_2 and L_3 such that

$$\|g(x_1, y) - g(x_2, y)\| \leq L_2 \|x_1 - x_2\|,$$

for all $x_1, x_2 \in \mathbb{R}^m, y \in \mathbb{R}^n$, and

$$\|g(x, y_1) - g(x, y_2)\| \leq L_3 \|y_1 - y_2\|,$$

for all $x \in \mathbb{R}^m, y_1, y_2 \in \mathbb{R}^n$;

(A6) There exists a positive number M_0 such that

$$\sup_{x \in \mathbb{R}^m, y \in \mathbb{R}^n} \|g(x, y)\| \leq M_0;$$

(A7) $NL_3 - \omega < 0$.

Remark 2.2.1 *The results presented in the remaining parts are also true even if we replace the non-autonomous system (2.1) by the autonomous equation*

$$x' = \bar{F}(x), \tag{2.7}$$

where the function $\bar{F} : \mathbb{R}^m \rightarrow \mathbb{R}^m$ is continuous with conditions which are counterparts of (A2) and (A3).

At the present time, systems of differential equations which are known to exhibit chaotic behavior are either nonautonomous and periodic in time such as the Duffing and Van der Pol oscillators or autonomous such as the Lorenz, Chua and Rössler systems. In a similar way, in our investigations of chaos generation, we take advantage of periodic nonautonomous systems as well as autonomous ones as generators.

Using the theory of quasilinear equations [93], one can verify that for a given solution $x(t)$ of system (2.1), there exists a unique bounded on \mathbb{R} solution $y(t)$ of the system $y' = Ay + g(x(t), y)$, denoted by $y(t) = \phi_{x(t)}(t)$, which satisfies the integral equation

$$y(t) = \int_{-\infty}^t e^{A(t-s)} g(x(s), y(s)) ds. \tag{2.8}$$

Our main assumption is the existence of a nonempty set \mathcal{A}_x of all solutions of system (2.1), uniformly bounded on \mathbb{R} . That is, there exists a positive number H such that $\sup_{t \in \mathbb{R}} \|x(t)\| \leq H$, for all $x(t) \in \mathcal{A}_x$.

Let us introduce the sets of functions

$$\mathcal{A}_y = \{ \phi_{x(t)}(t) \mid x(t) \in \mathcal{A}_x \}, \quad (2.9)$$

and

$$\mathcal{A} = \{ (x(t), \phi_{x(t)}(t)) \mid x(t) \in \mathcal{A}_x \}. \quad (2.10)$$

We note that for all $y(t) \in \mathcal{A}_y$ one has $\sup_{t \in \mathbb{R}} \|y(t)\| \leq M$, where $M = \frac{NM_0}{\omega}$.

Next, we reveal that if the set \mathcal{A}_x is an attractor with basin \mathcal{U}_x , that is, for each $x(t) \in \mathcal{U}_x$ there exists $\bar{x}(t) \in \mathcal{A}_x$ such that $\|x(t) - \bar{x}(t)\| \rightarrow 0$ as $t \rightarrow \infty$, then the set \mathcal{A}_y is also an attractor in the same sense. Denote by \mathcal{U}_y the set consisting of all solutions of system $y' = Ay + g(x(t), y)$, where $x(t) \in \mathcal{U}_x$. In the next lemma we specify the basin of attraction of \mathcal{A}_y .

Lemma 2.2.1 \mathcal{U}_y is a basin of \mathcal{A}_y .

Proof. Fix an arbitrary positive number ε and let $y(t) \in \mathcal{U}_y$ be a given solution of the system $y' = Ay + g(x(t), y)$ for some $x(t) \in \mathcal{U}_x$. In this case, there exists $\bar{x}(t) \in \mathcal{A}_x$ such that $\|x(t) - \bar{x}(t)\| \rightarrow 0$ as $t \rightarrow \infty$. Let $\alpha = \frac{\omega - NL_3}{\omega - NL_3 + NL_2}$ and $\bar{y}(t) = \phi_{\bar{x}(t)}(t)$. Condition (A7) implies that the number α is positive. Under the circumstances, one can find $R_0 = R_0(\varepsilon) > 0$ such that if $t \geq R_0$, then $\|x(t) - \bar{x}(t)\| < \alpha\varepsilon$ and $N\|y(R_0) - \bar{y}(R_0)\| e^{(NL_3 - \omega)t} < \alpha\varepsilon$. The functions $y(t)$ and $\bar{y}(t)$ satisfy the relations

$$y(t) = e^{A(t-R_0)}y(R_0) + \int_{R_0}^t e^{A(t-s)}g(x(s), y(s))ds,$$

and

$$\bar{y}(t) = e^{A(t-R_0)}\bar{y}(R_0) + \int_{R_0}^t e^{A(t-s)}g(\bar{x}(s), \bar{y}(s))ds,$$

respectively. Making use of these relations, one can verify that

$$\begin{aligned} y(t) - \bar{y}(t) &= e^{A(t-R_0)}(y(R_0) - \bar{y}(R_0)) \\ &+ \int_{R_0}^t e^{A(t-s)} [g(x(s), y(s)) - g(x(s), \bar{y}(s))] ds \\ &+ \int_{R_0}^t e^{A(t-s)} [g(x(s), \bar{y}(s)) - g(\bar{x}(s), \bar{y}(s))] ds. \end{aligned}$$

Therefore, we have

$$\begin{aligned} \|y(t) - \bar{y}(t)\| &\leq Ne^{-\omega(t-R_0)} \|y(R_0) - \bar{y}(R_0)\| + \frac{NL_2\alpha\varepsilon}{\omega} e^{-\omega t} (e^{\omega t} - e^{\omega R_0}) \\ &+ NL_3 \int_{R_0}^t e^{-\omega(t-s)} \|y(s) - \bar{y}(s)\| ds. \end{aligned}$$

Let $u : [R_0, \infty) \rightarrow [0, \infty)$ be a function defined as $u(t) = e^{\omega t} \|y(t) - \bar{y}(t)\|$. By means of this definition, we reach the inequality

$$u(t) \leq Ne^{\omega R_0} \|y(R_0) - \bar{y}(R_0)\| + \frac{NL_2\alpha\varepsilon}{\omega} (e^{\omega t} - e^{\omega R_0}) + NL_3 \int_{R_0}^t u(s) ds.$$

Now, let $\psi(t) = \frac{NL_2\alpha\varepsilon}{\omega} e^{\omega t}$ and $\phi(t) = \psi(t) + c$, where

$$c = Ne^{\omega R_0} \|y(R_0) - \bar{y}(R_0)\| - \frac{NL_2\alpha\varepsilon}{\omega} e^{\omega R_0}.$$

Using these functions we get

$$u(t) \leq \phi(t) + NL_3 \int_{R_0}^t u(s) ds.$$

Applying Gronwall's Lemma [55] to the last inequality for $t \geq R_0$, we attain the inequality

$$u(t) \leq c + \psi(t) + NL_3 \int_{R_0}^t e^{NL_3(t-s)} c ds + NL_3 \int_{R_0}^t e^{NL_3(t-s)} \psi(s) ds$$

and hence,

$$\begin{aligned} u(t) &\leq c + \psi(t) + c \left(e^{NL_3(t-R_0)} - 1 \right) \\ &+ \frac{N^2 L_2 L_3 \alpha \varepsilon}{\omega(\omega - NL_3)} e^{\omega t} \left(1 - e^{(NL_3 - \omega)(t-R_0)} \right) \\ &= \frac{NL_2\alpha\varepsilon}{\omega} e^{\omega t} + N \|y(R_0) - \bar{y}(R_0)\| e^{\omega R_0} e^{NL_3(t-R_0)} \\ &- \frac{NL_2\alpha\varepsilon}{\omega} e^{\omega R_0} e^{NL_3(t-R_0)} + \frac{N^2 L_2 L_3 \alpha \varepsilon}{\omega(\omega - NL_3)} e^{\omega t} \left(1 - e^{(NL_3 - \omega)(t-R_0)} \right). \end{aligned}$$

Thus,

$$\begin{aligned} \|y(t) - \bar{y}(t)\| &\leq \frac{NL_2\alpha\varepsilon}{\omega} + N \|y(R_0) - \bar{y}(R_0)\| e^{(NL_3 - \omega)(t-R_0)} \\ &- \frac{NL_2\alpha\varepsilon}{\omega} e^{(NL_3 - \omega)(t-R_0)} + \frac{N^2 L_2 L_3 \alpha \varepsilon}{\omega(\omega - NL_3)} \left(1 - e^{(NL_3 - \omega)(t-R_0)} \right) \\ &< N \|y(R_0) - \bar{y}(R_0)\| e^{(NL_3 - \omega)(t-R_0)} + \frac{NL_2\alpha\varepsilon}{\omega - NL_3}. \end{aligned}$$

Consequently, for $t \geq 2R_0$, we have that

$$\|y(t) - \bar{y}(t)\| < \left(1 + \frac{NL_2}{\omega - NL_3} \right) \alpha \varepsilon = \varepsilon,$$

and hence $\|y(t) - \bar{y}(t)\| \rightarrow 0$ as $t \rightarrow \infty$.

The proof of the lemma is completed. \square

Now, let us define the set \mathcal{U} consisting the solutions $(x(t), y(t))$ of system (2.1)+(2.2), where $x(t) \in \mathcal{U}_x$. Next, we state the following corollary of Lemma 2.2.1.

Corollary 2.2.1 \mathcal{U} is a basin of \mathcal{A} .

Proof. Let $(x(t), y(t)) \in \mathcal{U}$ be a given solution of system (2.1) + (2.2). According to Lemma 2.2.1, one can find $(\bar{x}(t), \bar{y}(t)) \in \mathcal{A}$ such that $\|x(t) - \bar{x}(t)\| \rightarrow 0$ as $t \rightarrow \infty$ and $\|y(t) - \bar{y}(t)\| \rightarrow 0$ as $t \rightarrow \infty$. Consequently, $\|(x(t), y(t)) - (\bar{x}(t), \bar{y}(t))\| \rightarrow 0$ as $t \rightarrow \infty$. The proof is finalized. \square

2.3 Description of Chaotic Sets of Functions

In this section, the descriptions for the chaotic sets of continuous functions will be introduced and the definitions of the chaotic features will be presented, both in the Devaney's sense and in the sense of Li-Yorke.

Let us denote by

$$\mathcal{B} = \{\psi(t) \mid \psi : \mathbb{R} \rightarrow K \text{ is continuous}\} \quad (2.11)$$

a collection of functions, where $K \subset \mathbb{R}^q$, $q \in \mathbb{N}$, is a bounded region.

We start with the description of chaotic sets of functions in Devaney's sense and then continue with the Li-Yorke counterpart.

2.3.1 Chaotic set of functions in Devaney's sense

In this part, we shall elucidate the ingredients of the chaos in Devaney's sense for the set \mathcal{B} , which is introduced by (2.11), and the first definition is about the sensitivity of chaotic sets of functions.

Definition 2.3.1 \mathcal{B} is called sensitive if there exist positive numbers ε and Δ such that for every $\psi(t) \in \mathcal{B}$ and for arbitrary $\delta > 0$ there exist $\bar{\psi}(t) \in \mathcal{B}$, $t_0 \in \mathbb{R}$ and an interval $J \subset [t_0, \infty)$, with length not less than Δ , such that $\|\psi(t_0) - \bar{\psi}(t_0)\| < \delta$ and $\|\psi(t) - \bar{\psi}(t)\| > \varepsilon$, for all $t \in J$.

Definition 2.3.1 considers the inequality ($> \varepsilon$) over the interval J . In the Devaney's chaos definition for the map, the inequality is assumed for discrete moments. Let us reveal how one can extend the inequality from a discrete point to an interval by considering continuous flows.

In [64], it is indicated that a continuous map $\varphi : \Lambda \rightarrow \Lambda$, with an invariant domain $\Lambda \subset \mathbb{R}^k$, $k \in \mathbb{N}$, has sensitive dependence on initial conditions if there exists $\bar{\varepsilon} > 0$ such that for any $x \in \Lambda$ and any neighborhood \mathcal{U} of x , there exist $y \in \mathcal{U}$ and a natural number n such that $\|\varphi^n(x) - \varphi^n(y)\| > \bar{\varepsilon}$.

Suppose that the set \mathcal{A}_x satisfies the definition of sensitivity in the following sense. There exists $\bar{\varepsilon} > 0$ such that for every $x(t) \in \mathcal{A}_x$ and arbitrary $\delta > 0$, there exist $\bar{x}(t) \in \mathcal{A}_x$, $t_0 \in \mathbb{R}$ and a real number $\zeta \geq t_0$ such that $\|x(t_0) - \bar{x}(t_0)\| < \delta$ and $\|x(\zeta) - \bar{x}(\zeta)\| > \bar{\varepsilon}$.

In this case, for given $x(t) \in \mathcal{A}_x$ and $\delta > 0$, one can find $\bar{x}(t) \in \mathcal{A}_x$ and $\zeta \geq t_0$ such that $\|x(t_0) - \bar{x}(t_0)\| < \delta$ and $\|x(\zeta) - \bar{x}(\zeta)\| > \bar{\varepsilon}$. Let $\Delta = \frac{\bar{\varepsilon}}{8HL_0}$ and take a number Δ_1 such that $\Delta \leq \Delta_1 \leq \frac{\bar{\varepsilon}}{4HL_0}$. Using appropriate integral equations for $t \in [\zeta, \zeta + \Delta_1]$, it can be verified that

$$\begin{aligned} \|x(t) - \bar{x}(t)\| &\geq \|x(\zeta) - \bar{x}(\zeta)\| - \left\| \int_{\zeta}^t [F(s, x(s)) - F(s, \bar{x}(s))] ds \right\| \\ &> \bar{\varepsilon} - 2HL_0\Delta_1 \\ &\geq \frac{\bar{\varepsilon}}{2}. \end{aligned}$$

The last inequality confirms that \mathcal{A}_x satisfies Definition 2.3.1 with $\varepsilon = \bar{\varepsilon}/2$ and $J = [\zeta, \zeta + \Delta_1]$. So the definition is a natural one. It provides more information than discrete moments and for us it is important that the extension on the interval is useful to prove the property for chaos extension.

In the next two definitions, we continue with the existence of a dense function in the set of chaotic functions followed by the transitivity property.

Definition 2.3.2 \mathcal{B} possesses a dense function $\psi^*(t) \in \mathcal{B}$ if for every function $\psi(t) \in \mathcal{B}$, arbitrary small $\varepsilon > 0$ and arbitrary large $E > 0$, there exist a number $\xi > 0$ and an interval $J \subset \mathbb{R}$, with length E , such that $\|\psi(t) - \psi^*(t + \xi)\| < \varepsilon$, for all $t \in J$.

Definition 2.3.3 \mathcal{B} is called transitive if it possesses a dense function.

Now, let us recall the definition of transitivity for maps [64]. A continuous map φ with an invariant domain $\Lambda \subset \mathbb{R}^k, k \in \mathbb{N}$, possesses a dense orbit if there exists $c^* \in \Lambda$ such that for each $c \in \Lambda$ and arbitrary number $\varepsilon > 0$, there exist natural numbers k_0 and l_0 such that $\|\varphi^{l_0}(c) - \varphi^{l_0+k_0}(c^*)\| < \varepsilon$, and maps which have dense orbits are called transitive.

Suppose that \mathcal{A}_x satisfies the transitivity property in the following sense. There exists a function $x^*(t) \in \mathcal{A}_x$ such that for each $x(t) \in \mathcal{A}_x$ and arbitrary positive number ε , there exist a real number ζ_0 and a natural number m_0 such that $\|x(\zeta_0) - x^*(\zeta_0 + m_0T)\| < \varepsilon$.

Fix an arbitrary function $x(t) \in \mathcal{A}_x$, arbitrary small $\varepsilon > 0$ and arbitrary large $E > 0$. Under the circumstances, one can find $\zeta_0 \in \mathbb{R}$ and $m_0 \in \mathbb{N}$ such that $\|x(\zeta_0) - x^*(\zeta_0 + m_0T)\| < \varepsilon e^{-L_0E}$.

Using the condition (A2) together with the convenient integral equations that $x(t)$ and $x^*(t)$ satisfy, it is easy to obtain for $t \in [\zeta_0, \zeta_0 + E]$ that

$$\|x(t) - x^*(t + m_0T)\| \leq \|x(\zeta_0) - x^*(\zeta_0 + m_0T)\| + \int_{\zeta_0}^t L_0 \|x(s) - x^*(s + m_0T)\| ds,$$

and by the help of the Gronwall-Bellman inequality [56], we get

$$\|x(t) - x^*(t + m_0T)\| \leq \|x(\zeta_0) - x^*(\zeta_0 + m_0T)\| e^{L_0(t-\zeta_0)} < \varepsilon.$$

The last inequality shows that the set \mathcal{A}_x satisfies Definition 2.3.2 with $\xi = k_0T$ and is transitive in accordance with Definition 2.3.3.

The following definition describes the density of periodic functions inside \mathcal{B} .

Definition 2.3.4 \mathcal{B} admits a dense collection $\mathcal{G} \subset \mathcal{B}$ of periodic functions if for every function $\psi(t) \in \mathcal{B}$, arbitrary small $\varepsilon > 0$ and arbitrary large $E > 0$, there exist $\tilde{\psi}(t) \in \mathcal{G}$ and an interval $J \subset \mathbb{R}$, with length E , such that $\|\psi(t) - \tilde{\psi}(t)\| < \varepsilon$, for all $t \in J$.

Let us remind the definition of density of periodic orbits for maps [64]. The set of periodic orbits of a continuous map ϕ with an invariant domain $\Lambda \subset \mathbb{R}^k, k \in \mathbb{N}$, is called dense in Λ if for each $c \in \Lambda$, arbitrary positive number ε , there exist a natural number l_0 and a point $\tilde{c} \in \Lambda$ such that the sequence $\{\phi^i(\tilde{c})\}$ is periodic and $\|\phi^{l_0}(c) - \phi^{l_0}(\tilde{c})\| < \varepsilon$.

Let us denote by \mathcal{G}_x the set of all periodic functions inside \mathcal{A}_x . Suppose that \mathcal{A}_x satisfies density of periodic solutions as follows. For an arbitrary function $x(t) \in \mathcal{A}_x$ and arbitrary small $\varepsilon > 0$ there exist a periodic function $\tilde{x}(t) \in \mathcal{G}_x$ and a number $\zeta_0 \in \mathbb{R}$ such that $\|x(\zeta_0) - \tilde{x}(\zeta_0)\| < \varepsilon$.

Let us fix an arbitrary function $x(t) \in \mathcal{A}_x$, arbitrary small $\varepsilon > 0$ and arbitrary large $E > 0$. In that case, there exist a periodic function $\tilde{x}(t) \in \mathcal{G}_x$ and $\zeta_0 \in \mathbb{R}$ such that $\|x(\zeta_0) - \tilde{x}(\zeta_0)\| < \varepsilon e^{-L_0 E}$.

It can be easily verified for $t \in [\zeta_0, \zeta_0 + E]$ that the inequality

$$\|x(t) - \tilde{x}(t)\| \leq \|x(\zeta_0) - \tilde{x}(\zeta_0)\| + \int_{\zeta_0}^t L_0 \|x(s) - \tilde{x}(s)\| ds,$$

holds, and therefore for each t from the same interval of time we have

$$\|x(t) - \tilde{x}(t)\| \leq \|x(\zeta_0) - \tilde{x}(\zeta_0)\| e^{L_0(t-\zeta_0)} < \varepsilon.$$

Consequently, the set \mathcal{A}_x satisfies Definition 2.3.4 with $J = [\zeta_0, \zeta_0 + E]$.

Finally, we introduce in the next definition the chaotic set of functions in Devaney's sense.

Definition 2.3.5 The collection \mathcal{B} of functions is called a Devaney's chaotic set if

- (D1) \mathcal{B} is sensitive;
- (D2) \mathcal{B} is transitive;
- (D3) \mathcal{B} admits a dense collection of periodic functions.

In the next subsection, the chaotic properties of the set \mathcal{B} will be imposed in the sense of Li-Yorke.

2.3.2 Chaotic set of functions in Li-Yorke sense

The ingredients of Li-Yorke chaos for the collection of functions \mathcal{B} , which is defined by (2.11), will be described in this part. Making use of discussions similar to the ones made in the previous subsection, we extend, below, the definitions for the ingredients of Li-Yorke chaos from maps [20, 120, 134, 224] to continuous flows and we just omit these indications here.

Definition 2.3.6 *A couple of functions $(\psi(t), \bar{\psi}(t)) \in \mathcal{B} \times \mathcal{B}$ is called proximal if for arbitrary small $\varepsilon > 0$ and arbitrary large $E > 0$, there exist infinitely many disjoint intervals with length no less than E such that $\|\psi(t) - \bar{\psi}(t)\| < \varepsilon$, for each t from these intervals.*

Definition 2.3.7 *A couple of functions $(\psi(t), \bar{\psi}(t)) \in \mathcal{B} \times \mathcal{B}$ is frequently (ε_0, Δ) -separated if there exist positive numbers ε_0, Δ and infinitely many disjoint intervals of length no less than Δ , such that $\|\psi(t) - \bar{\psi}(t)\| > \varepsilon_0$, for each t from these intervals.*

Remark 2.3.1 *The numbers ε_0 and Δ taken into account in Definition 2.3.7 depend on the functions $\psi(t)$ and $\bar{\psi}(t)$.*

Definition 2.3.8 *A couple of functions $(\psi(t), \bar{\psi}(t)) \in \mathcal{B} \times \mathcal{B}$ is a Li-Yorke pair if it is proximal and frequently (ε_0, Δ) -separated for some positive numbers ε_0 and Δ .*

Definition 2.3.9 *An uncountable set $\mathcal{C} \subset \mathcal{B}$ is called a scrambled set if \mathcal{C} does not contain any periodic functions and each couple of different functions inside $\mathcal{C} \times \mathcal{C}$ is a Li-Yorke pair.*

Definition 2.3.10 *\mathcal{B} is called a Li-Yorke chaotic set if*

- (LY1) *There exists a positive number T_0 such that \mathcal{B} admits a periodic function of period kT_0 , for any $k \in \mathbb{N}$;*
- (LY2) *\mathcal{B} possesses a scrambled set \mathcal{C} ;*
- (LY3) *For any function $\psi(t) \in \mathcal{C}$ and any periodic function $\bar{\psi}(t) \in \mathcal{B}$, the couple $(\psi(t), \bar{\psi}(t))$ is frequently (ε_0, Δ) -separated for some positive numbers ε_0 and Δ .*

2.4 Hyperbolic Set of Functions

The definitions of stable and unstable sets of hyperbolic periodic orbits of autonomous systems are given in [166], and information about such sets of solutions of perturbed non-autonomous systems can be found in [129]. Moreover, homoclinic structures in almost periodic systems were studied in [151, 167, 192]. In this section, we give a definition for hyperbolic collection of uniformly bounded functions and before this, we start with the descriptions of stable and unstable sets of a function.

We define the stable set of a function $\psi(t) \in \mathcal{B}$, where the collection \mathcal{B} is defined by (2.11), as the set of functions

$$W^s(\psi(t)) = \{u(t) \in \mathcal{B} \mid \|u(t) - \psi(t)\| \rightarrow 0 \text{ as } t \rightarrow \infty\}, \quad (2.12)$$

and, similarly, we define the unstable set of a function $\psi(t) \in \mathcal{B}$ as the set of functions

$$W^u(\psi(t)) = \{v(t) \in \mathcal{B} \mid \|v(t) - \psi(t)\| \rightarrow 0 \text{ as } t \rightarrow -\infty\}. \quad (2.13)$$

Definition 2.4.1 *The set of functions \mathcal{B} is called hyperbolic if both the stable and unstable sets of each function $\psi(t) \in \mathcal{B}$ possess at least one element different from $\psi(t)$.*

Theorem 2.4.1 *If \mathcal{A}_x is hyperbolic, then the same is true for \mathcal{A}_y .*

Proof. Fix an arbitrary positive number ε and a function $y(t) = \phi_{x(t)}(t) \in \mathcal{A}_y$. Let $\alpha = \frac{\omega - NL_3}{\omega - NL_3 + NL_2}$ and $\beta = \frac{\omega - NL_3}{1 + NL_2}$. By condition (A7), one can verify that the numbers α and β are both positive.

Due to the hyperbolicity of \mathcal{A}_x , both the stable set $W^s(x(t))$ and the unstable set $W^u(x(t))$ of $x(t)$ contain at least one element different from $x(t)$.

Let us take an arbitrary function $u(t) \in W^s(x(t))$ such that $u(t) \neq x(t)$. Since $\|x(t) - u(t)\| \rightarrow 0$ as $t \rightarrow \infty$ and $NL_3 - \omega < 0$, there exists a positive number R_1 , which depends on ε , such that $\|x(t) - u(t)\| < \alpha\varepsilon$ and $e^{(NL_3 - \omega)t} < \frac{\omega\alpha\varepsilon}{2M_0N}$ for $t \geq R_1$. Let $\bar{y}(t) = \phi_{u(t)}(t)$. We note that $\bar{y}(t) \neq y(t)$. Otherwise, if $\bar{y}(t) = y(t)$, then the equality $g(x(t), y(t)) = g(u(t), y(t))$ holds, and this implies that $x(t) = u(t)$ by condition (A4), which is a contradiction. We shall prove that the function $\bar{y}(t)$ belongs to the stable set of $y(t)$.

The bounded on \mathbb{R} functions $y(t)$ and $\bar{y}(t)$ satisfy the relations

$$y(t) = \int_{-\infty}^t e^{A(t-s)} g(x(s), y(s)) ds,$$

and

$$\bar{y}(t) = \int_{-\infty}^t e^{A(t-s)} g(u(s), \bar{y}(s)) ds,$$

respectively, for $t \geq R_1$.

Therefore, one can easily reach up the equation

$$\begin{aligned} y(t) - \bar{y}(t) &= \int_{-\infty}^{R_1} e^{A(t-s)} [g(x(s), y(s)) - g(u(s), \bar{y}(s))] ds \\ &+ \int_{R_1}^t e^{A(t-s)} \{ [g(x(s), y(s)) - g(x(s), \bar{y}(s))] + [g(x(s), \bar{y}(s)) - g(u(s), \bar{y}(s))] \} ds, \end{aligned}$$

which implies that

$$\begin{aligned} \|y(t) - \bar{y}(t)\| &\leq \int_{-\infty}^{R_1} 2M_0N e^{-\omega(t-s)} ds \\ &+ \int_{R_1}^t e^{-\omega(t-s)} (NL_3 \|y(s) - \bar{y}(s)\| + NL_2 \|x(s) - u(s)\|) ds \\ &\leq \frac{2M_0N}{\omega} e^{-\omega(t-R_1)} + \int_{R_1}^t e^{-\omega(t-s)} (NL_3 \|y(s) - \bar{y}(s)\| + NL_2 \alpha \varepsilon) ds. \end{aligned}$$

Using the Gronwall type inequality indicated in [242], we obtain that

$$\|y(t) - \bar{y}(t)\| \leq \frac{2M_0N}{\omega} e^{(NL_3 - \omega)(t-R_1)} + \frac{NL_2 \alpha \varepsilon}{\omega - NL_3} [1 - e^{(NL_3 - \omega)(t-R_1)}], \quad t \geq R_1.$$

For this reason, for all $t \geq 2R_1$, one has

$$\|y(t) - \bar{y}(t)\| \leq \frac{2M_0N}{\omega} e^{(NL_3 - \omega)R_1} + \frac{NL_2 \alpha \varepsilon}{\omega - NL_3} < \left(1 + \frac{NL_2}{\omega - NL_3}\right) \alpha \varepsilon = \varepsilon.$$

According to the last inequality, we have that $\|y(t) - \bar{y}(t)\| \rightarrow 0$ as $t \rightarrow \infty$. Hence, the function $\bar{y}(t)$ belongs to the stable set $W^s(y(t))$ of $y(t)$.

On the other hand, let $v(t)$ be a function inside the unstable set $W^u(x(t))$ such that $v(t) \neq x(t)$. Since $\|x(t) - v(t)\|$ tends to 0 as $t \rightarrow -\infty$, there exists a negative number $R_2(\varepsilon)$ such that $\|x(t) - v(t)\| < \beta \varepsilon$ for $t \leq R_2$. Let $\tilde{y}(t) = \phi_{v(t)}(t)$. It is worth noting that $\tilde{y}(t) \neq y(t)$. Now, our purpose is to show that $\tilde{y}(t)$ belongs to the unstable set $W^u(y(t))$ of $y(t)$.

By the help of the integral equations

$$y(t) = \int_{-\infty}^t e^{A(t-s)} g(x(s), y(s)) ds,$$

and

$$\tilde{y}(t) = \int_{-\infty}^t e^{A(t-s)} g(v(s), \tilde{y}(s)) ds,$$

we obtain that

$$\begin{aligned} y(t) - \tilde{y}(t) &= \int_{-\infty}^t e^{A(t-s)} [g(x(s), y(s)) - g(v(s), y(s))] ds \\ &+ \int_{-\infty}^t e^{A(t-s)} [g(v(s), y(s)) - g(v(s), \tilde{y}(s))] ds. \end{aligned}$$

Therefore, for $t \leq R_2$, one has

$$\begin{aligned} \|y(t) - \tilde{y}(t)\| &\leq \int_{-\infty}^t NL_2 e^{-\omega(t-s)} \|x(t) - v(t)\| ds \\ &+ \int_{-\infty}^t e^{-\omega(t-s)} NL_3 \|y(s) - \tilde{y}(s)\| ds \\ &\leq \frac{NL_2 \beta \varepsilon}{\omega} + \frac{NL_3}{\omega} \sup_{t \leq R_2} \|y(t) - \tilde{y}(t)\|. \end{aligned}$$

Hence, we attain that $\sup_{t \leq R_2} \|y(t) - \tilde{y}(t)\| \leq \frac{NL_2\beta\varepsilon}{\omega} + \frac{NL_3}{\omega} \sup_{t \leq R_2} \|y(t) - \tilde{y}(t)\|$. Accordingly, one can verify that

$$\sup_{t \leq R_2} \|y(t) - \tilde{y}(t)\| \leq \frac{NL_2\beta\varepsilon}{\omega - NL_3} < \varepsilon.$$

The last inequality confirms that $\|y(t) - \tilde{y}(t)\| \rightarrow 0$ as $t \rightarrow -\infty$. Therefore $\tilde{y}(t) \in W^u(y(t))$.

Consequently, the set \mathcal{A}_y is hyperbolic since an arbitrary function $y(t) \in \mathcal{A}_y$ has stable and unstable sets which possess at least one element different from $y(t)$.

The theorem is proved. \square

Theorem 2.4.1 implies the following corollary.

Corollary 2.4.1 *If \mathcal{A}_x is hyperbolic, then the same is true for \mathcal{A} .*

Next, we continue with another corollary of Theorem (2.4.1), following the definitions of homoclinic and heteroclinic functions.

A function $\psi_1(t) \in \mathcal{B}$ is said to be homoclinic to the function $\psi_0(t) \in \mathcal{B}$, $\psi_0(t) \neq \psi_1(t)$, if $\psi_1(t) \in W^s(\psi_0(t)) \cap W^u(\psi_0(t))$.

On the other hand, a function $\psi_2(t) \in \mathcal{B}$ is called heteroclinic to the functions $\psi_0(t), \psi_1(t) \in \mathcal{B}$, $\psi_0(t) \neq \psi_2(t)$, $\psi_1(t) \neq \psi_2(t)$, if $\psi_2(t) \in W^s(\psi_0(t)) \cap W^u(\psi_1(t))$.

Corollary 2.4.2 *If $x_1(t) \in \mathcal{A}_x$ is homoclinic to the function $x_0(t) \in \mathcal{A}_x$, $x_0(t) \neq x_1(t)$, then $\phi_{x_1(t)}(t) \in \mathcal{A}_y$ is homoclinic to the function $\phi_{x_0(t)}(t) \in \mathcal{A}_y$.*

Similarly, if $x_2(t) \in \mathcal{A}_x$ is heteroclinic to the functions $x_0(t), x_1(t) \in \mathcal{A}_x$, $x_0(t) \neq x_2(t)$, $x_1(t) \neq x_2(t)$, then $\phi_{x_2(t)}(t)$ is heteroclinic to the functions $\phi_{x_0(t)}(t), \phi_{x_1(t)}(t) \in \mathcal{A}_y$.

In the next section, we theoretically prove that the set \mathcal{A}_y replicates the ingredients of Devaney's chaos provided to the set \mathcal{A}_x , and as a consequence the same is valid also for the set \mathcal{A} . The same problem for the chaos in the sense of Li-Yorke will be handled in Section 2.6.

2.5 Replication of Devaney's Chaos

In this part, we will prove theoretically that the ingredients of Devaney's chaos furnished to the set \mathcal{A}_x are all replicated by the set \mathcal{A}_y .

Suppose that the function $g(x, y)$ which is used in the right hand side of system (2.2) has

component functions $g_j(x, y)$, $j = 1, 2, \dots, n$. That is,

$$g(x, y) = \begin{pmatrix} g_1(x, y) \\ g_2(x, y) \\ \vdots \\ g_n(x, y) \end{pmatrix},$$

where each $g_j(x, y)$, $j = 1, 2, \dots, n$, is a real valued function.

We start with the following assertion, which will be needed in the proof of Lemma 2.5.2.

Lemma 2.5.1 *The set of functions*

$$\mathcal{F} = \{g_j(x(t), \phi_{x(t)}(t)) - g_j(\bar{x}(t), \phi_{\bar{x}(t)}(t)) \mid 1 \leq j \leq n, x(t) \in \mathcal{A}_x, \bar{x}(t) \in \mathcal{A}_x\}$$

is an equicontinuous family on \mathbb{R} .

Proof. Let us define a function $h : \mathbb{R}^m \times \mathbb{R}^m \times \mathbb{R}^n \rightarrow \mathbb{R}^n$ by the formula

$$h(x_1, x_2, x_3) = g(x_1, x_3) - g(x_2, x_3).$$

Being continuous on the compact region

$$\mathcal{D} = \{(x_1, x_2, x_3) \in \mathbb{R}^m \times \mathbb{R}^m \times \mathbb{R}^n \mid \|x_1\| \leq H, \|x_2\| \leq H, \|x_3\| \leq M\},$$

the function $h(x_1, x_2, x_3)$ is uniformly continuous on \mathcal{D} .

Fix an arbitrary $\varepsilon > 0$. Our aim is to determine a positive number $\delta = \delta(\varepsilon)$ such that for all $t_1, t_2 \in \mathbb{R}$ with $|t_1 - t_2| < \delta$ the inequality

$$\|h(x(t_1), \bar{x}(t_1), \phi_{x(t_1)}(t_1)) - h(x(t_2), \bar{x}(t_2), \phi_{x(t_2)}(t_2))\| < \varepsilon$$

holds for all $x(t), \bar{x}(t) \in \mathcal{A}_x$.

By uniform continuity of the function $h(x_1, x_2, x_3)$ on \mathcal{D} , one can find a number $\delta_1 = \delta_1(\varepsilon) > 0$ such that for all $(x_1^0, x_2^0, x_3^0), (x_1^1, x_2^1, x_3^1) \in \mathbb{R}^m \times \mathbb{R}^m \times \mathbb{R}^n$ with $\|(x_1^0, x_2^0, x_3^0) - (x_1^1, x_2^1, x_3^1)\| < \delta_1$, the inequality

$$\|h(x_1^0, x_2^0, x_3^0) - h(x_1^1, x_2^1, x_3^1)\| < \varepsilon$$

holds.

Since $\|x'(t)\| \leq H_0$ for each $x(t) \in \mathcal{A}_x$, the set \mathcal{A}_x is an equicontinuous family on \mathbb{R} . Therefore, there exists a number $\delta_2 = \delta_2(\delta_1) > 0$ such that for all $t_1, t_2 \in \mathbb{R}$ satisfying $|t_1 - t_2| < \delta_2$ we have $\|x(t_1) - x(t_2)\| < \delta_1/3$ for all $x(t) \in \mathcal{A}_x$.

Similarly, the set \mathcal{A}_y is also an equicontinuous family on \mathbb{R} , since $\|y'(t)\| \leq \|A\|M + M_0$ for each $y(t) \in \mathcal{A}_y$. Thus, one can find a number $\delta_3 = \delta_3(\delta_1) > 0$ such that for all $t_1, t_2 \in \mathbb{R}$ with $|t_1 - t_2| < \delta_3$, the inequality $\|y(t_1) - y(t_2)\| < \delta_1/3$ is valid for all $y(t) \in \mathcal{A}_y$.

In this case, for all $t_1, t_2 \in \mathbb{R}$ with $|t_1 - t_2| < \min\{\delta_2, \delta_3\}$, one has

$$\begin{aligned} & \left\| (x(t_1), \bar{x}(t_1), \phi_{x(t)}(t_1)) - (x(t_2), \bar{x}(t_2), \phi_{x(t)}(t_2)) \right\| \\ & \leq \|x(t_1) - x(t_2)\| + \|\bar{x}(t_1) - \bar{x}(t_2)\| + \|\phi_{x(t)}(t_1) - \phi_{x(t)}(t_2)\| \\ & < \delta_1, \end{aligned}$$

for all $x(t), \bar{x}(t) \in \mathcal{A}_x$.

Hence, taking $\delta(\varepsilon) = \min\{\delta_2, \delta_3\}$, one can see that for all $t_1, t_2 \in \mathbb{R}$ with $|t_1 - t_2| < \delta$, the inequality

$$\begin{aligned} & \left\| (g_j(x(t_1), \phi_{x(t)}(t_1)) - g_j(\bar{x}(t_1), \phi_{x(t)}(t_1))) \right. \\ & \quad \left. - (g_j(x(t_2), \phi_{x(t)}(t_2)) - g_j(\bar{x}(t_2), \phi_{x(t)}(t_2))) \right\| \\ & \leq \|h(x(t_1), \bar{x}(t_1), \phi_{x(t)}(t_1)) - h(x(t_2), \bar{x}(t_2), \phi_{x(t)}(t_2))\| \\ & < \varepsilon \end{aligned}$$

holds for all $1 \leq j \leq n$ and $x(t), \bar{x}(t) \in \mathcal{A}_x$. Consequently, the family \mathcal{F} is equicontinuous on \mathbb{R} .

The lemma is proved. \square

We continue with replication of sensitivity in the next lemma.

Lemma 2.5.2 *Sensitivity of the set \mathcal{A}_x implies the same feature for the set \mathcal{A}_y .*

Proof. Fix an arbitrary $\delta > 0$ and let $y(t) \in \mathcal{A}_y$ be a given solution of system (2.2). In this case, there exists $x(t) \in \mathcal{A}_x$ such that $y(t) = \phi_{x(t)}(t)$.

Let us choose a number $\bar{\varepsilon} = \bar{\varepsilon}(\delta) > 0$ small enough which satisfies the inequality

$$\left(1 + \frac{NL_2}{\omega - NL_3}\right) \bar{\varepsilon} < \delta.$$

Then take $R = R(\bar{\varepsilon}) < 0$ sufficiently large in absolute value such that

$$\frac{2M_0N}{\omega} e^{(\omega - NL_3)R} < \bar{\varepsilon},$$

and let $\delta_1 = \delta_1(\bar{\varepsilon}, R) = \bar{\varepsilon}e^{L_0R}$. Since the set of functions \mathcal{A}_x is sensitive, there exist positive numbers ε_0 and Δ such that the inequalities $\|x(t_0) - \bar{x}(t_0)\| < \delta_1$ and $\|x(t) - \bar{x}(t)\| > \varepsilon_0$, $t \in J$, hold for some solution $\bar{x}(t) \in \mathcal{A}_x$, a number $t_0 \in \mathbb{R}$ and an interval $J \subset [t_0, \infty)$ whose length is not less than Δ .

Using the couple of integral equations

$$x(t) = x(t_0) + \int_{t_0}^t F(s, x(s)) ds,$$

$$\bar{x}(t) = \bar{x}(t_0) + \int_{t_0}^t F(s, \bar{x}(s)) ds$$

together with condition (A2), one can see that the inequality

$$\|x(t) - \bar{x}(t)\| \leq \|x(t_0) - \bar{x}(t_0)\| + \left| \int_{t_0}^t L_0 \|x(s) - \bar{x}(s)\| ds \right|$$

holds for $t \in [t_0 + R, t_0]$. Applying the Gronwall-Bellman inequality [56], we obtain that

$$\|x(t) - \bar{x}(t)\| \leq \|x(t_0) - \bar{x}(t_0)\| e^{L_0|t-t_0|}$$

and therefore $\|x(t) - \bar{x}(t)\| < \bar{\varepsilon}$ for $t \in [t_0 + R, t_0]$.

Let us denote $\bar{y}(t) = \phi_{\bar{x}(t)}(t)$. First, we will show that $\|y(t_0) - \bar{y}(t_0)\| < \delta$.

The functions $y(t)$ and $\bar{y}(t)$ satisfy the relations

$$y(t) = \int_{-\infty}^t e^{A(t-s)} g(x(s), y(s)) ds$$

and

$$\bar{y}(t) = \int_{-\infty}^t e^{A(t-s)} g(\bar{x}(s), \bar{y}(s)) ds,$$

respectively. Therefore,

$$y(t) - \bar{y}(t) = \int_{-\infty}^t e^{A(t-s)} [g(x(s), y(s)) - g(\bar{x}(s), \bar{y}(s))] ds$$

and hence we obtain that

$$\begin{aligned} \|y(t) - \bar{y}(t)\| &\leq \int_{t_0+R}^t N e^{-\omega(t-s)} \|g(x(s), y(s)) - g(x(s), \bar{y}(s))\| ds \\ &+ \int_{t_0+R}^t N e^{-\omega(t-s)} \|g(x(s), \bar{y}(s)) - g(\bar{x}(s), \bar{y}(s))\| ds \\ &+ \int_{-\infty}^{t_0+R} N e^{-\omega(t-s)} \|g(x(s), y(s)) - g(\bar{x}(s), \bar{y}(s))\| ds. \end{aligned}$$

Since $\|x(t) - \bar{x}(t)\| < \bar{\varepsilon}$ for $t \in [t_0 + R, t_0]$, one has

$$\begin{aligned} \|y(t) - \bar{y}(t)\| &\leq NL_3 \int_{t_0+R}^t e^{-\omega(t-s)} \|y(s) - \bar{y}(s)\| ds \\ &+ \frac{NL_2 \bar{\varepsilon}}{\omega} e^{-\omega t} (e^{\omega t} - e^{\omega(t_0+R)}) + \frac{2M_0 N}{\omega} e^{-\omega(t-t_0-R)}. \end{aligned}$$

Now, let us introduce the functions $u(t) = e^{\omega t} \|y(t) - \bar{y}(t)\|$, $k(t) = \frac{NL_2 \bar{\varepsilon}}{\omega} e^{\omega t}$ and $h(t) = c + k(t)$, where $c = \left(\frac{2M_0 N}{\omega} - \frac{NL_2 \bar{\varepsilon}}{\omega} \right) e^{\omega(t_0+R)}$.

These definitions give us the inequality

$$u(t) \leq h(t) + \int_{t_0+R}^t NL_3 u(s) ds.$$

Applying Lemma 2.2 [34] to the last inequality, we achieve that

$$u(t) \leq h(t) + NL_3 \int_{t_0+R}^t e^{NL_3(t-s)} h(s) ds.$$

Therefore, on the time interval $[t_0 + R, t_0]$, the inequality

$$\begin{aligned} u(t) &\leq c + k(t) + c \left(e^{NL_3(t-t_0-R)} - 1 \right) \\ &+ \frac{N^2 L_2 L_3 \bar{\varepsilon}}{\omega} e^{NL_3 t} \int_{t_0+R}^t e^{(\omega - NL_3)s} ds \\ &= \frac{NL_2 \bar{\varepsilon}}{\omega} e^{\omega t} + \left(\frac{2M_0 N}{\omega} - \frac{NL_2 \bar{\varepsilon}}{\omega} \right) e^{\omega R} e^{NL_3(t-t_0-R)} \\ &+ \frac{N^2 L_2 L_3 \bar{\varepsilon}}{\omega(\omega - NL_3)} e^{\omega t} \left[1 - e^{(NL_3 - \omega)(t-t_0-R)} \right] \end{aligned}$$

holds.

The last inequality leads to

$$\|y(t) - \bar{y}(t)\| \leq \frac{NL_2 \bar{\varepsilon}}{\omega - NL_3} + \frac{2M_0 N}{\omega} e^{(NL_3 - \omega)(t-t_0-R)},$$

and consequently, we obtain that

$$\begin{aligned} \|y(t_0) - \bar{y}(t_0)\| &\leq \frac{NL_2 \bar{\varepsilon}}{\omega - NL_3} + \frac{2M_0 N}{\omega} e^{(\omega - NL_3)R} \\ &< \left(1 + \frac{NL_2}{\omega - NL_3} \right) \bar{\varepsilon} \\ &< \delta. \end{aligned}$$

In the remaining part of the proof, we will show the existence of a positive number ε_1 and an interval $J^1 \subset J$, with a fixed length which is independent of $y(t), \bar{y}(t) \in \mathcal{A}_y$, such that the inequality $\|y(t) - \bar{y}(t)\| > \varepsilon_1$ holds for all $t \in J^1$.

According to Lemma 2.5.1, there exists a positive number $\tau < \Delta$, independent of the functions $x(t), \bar{x}(t) \in \mathcal{A}_x, y(t), \bar{y}(t) \in \mathcal{A}_y$, such that for any $t_1, t_2 \in \mathbb{R}$ with $|t_1 - t_2| < \tau$ the inequality

$$\begin{aligned} &\left| (g_j(x(t_1), y(t_1)) - g_j(\bar{x}(t_1), y(t_1))) \right. \\ &\quad \left. - (g_j(x(t_2), y(t_2)) - g_j(\bar{x}(t_2), y(t_2))) \right| \\ &< \frac{L_1 \varepsilon_0}{2n} \end{aligned} \tag{2.14}$$

holds, for all $1 \leq j \leq n$.

Condition (A4) implies that, for all $t \in J$, the inequality

$$\|g(x(t), y(t)) - g(\bar{x}(t), y(t))\| \geq L_1 \|x(t) - \bar{x}(t)\|$$

is satisfied. Therefore, for each $t \in J$, there exists an integer $j_0 = j_0(t)$, $1 \leq j_0 \leq n$, such that

$$\left| g_{j_0}(x(t), y(t)) - g_{j_0}(\bar{x}(t), y(t)) \right| \geq \frac{L_1}{n} \|x(t) - \bar{x}(t)\|.$$

Otherwise, if there exists $s \in J$ such that for all $1 \leq j \leq n$, the inequality

$$|g_j(x(s), y(s)) - g_j(\bar{x}(s), y(s))| < \frac{L_1}{n} \|x(s) - \bar{x}(s)\|$$

holds, then one encounters with a contradiction since

$$\begin{aligned} \|g(x(s), y(s)) - g(\bar{x}(s), y(s))\| &\leq \sum_{j=1}^n |g_j(x(s), y(s)) - g_j(\bar{x}(s), y(s))| \\ &< L_1 \|x(s) - \bar{x}(s)\|. \end{aligned}$$

Now, let s_0 be the midpoint of the interval J and $\theta = s_0 - \tau/2$. One can find an integer $j_0 = j_0(s_0)$, $1 \leq j_0 \leq n$, such that

$$|g_{j_0}(x(s_0), y(s_0)) - g_{j_0}(\bar{x}(s_0), y(s_0))| \geq \frac{L_1}{n} \|x(s_0) - \bar{x}(s_0)\| > \frac{L_1 \varepsilon_0}{n}. \quad (2.15)$$

On the other hand, making use of inequality (2.14), for all $t \in [\theta, \theta + \tau]$ we have

$$\begin{aligned} &|g_{j_0}(x(s_0), y(s_0)) - g_{j_0}(\bar{x}(s_0), y(s_0))| - |g_{j_0}(x(t), y(t)) - g_{j_0}(\bar{x}(t), y(t))| \\ &\leq |(g_{j_0}(x(t), y(t)) - g_{j_0}(\bar{x}(t), y(t))) - (g_{j_0}(x(s_0), y(s_0)) - g_{j_0}(\bar{x}(s_0), y(s_0)))| \\ &< \frac{L_1 \varepsilon_0}{2n}. \end{aligned}$$

Therefore, by means of (2.15), we obtain that the inequality

$$\begin{aligned} &|g_{j_0}(x(t), y(t)) - g_{j_0}(\bar{x}(t), y(t))| \\ &> |g_{j_0}(x(s_0), y(s_0)) - g_{j_0}(\bar{x}(s_0), y(s_0))| - \frac{L_1 \varepsilon_0}{2n} \\ &> \frac{L_1 \varepsilon_0}{2n} \end{aligned} \quad (2.16)$$

holds for all $t \in [\theta, \theta + \tau]$.

By applying the mean value theorem for integrals, one can find $s_1, s_2, \dots, s_n \in [\theta, \theta + \tau]$ such that

$$\int_{\theta}^{\theta+\tau} [g(x(s), y(s)) - g(\bar{x}(s), y(s))] ds = \begin{pmatrix} \tau [g_1(x(s_1), y(s_1)) - g_1(\bar{x}(s_1), y(s_1))] \\ \tau [g_2(x(s_2), y(s_2)) - g_2(\bar{x}(s_2), y(s_2))] \\ \vdots \\ \tau [g_n(x(s_n), y(s_n)) - g_n(\bar{x}(s_n), y(s_n))] \end{pmatrix}.$$

Thus, using (2.16), one can verify that

$$\begin{aligned} &\left\| \int_{\theta}^{\theta+\tau} [g(x(s), y(s)) - g(\bar{x}(s), y(s))] ds \right\| \\ &\geq \tau |g_{j_0}(x(s_{j_0}), y(s_{j_0})) - g_{j_0}(\bar{x}(s_{j_0}), y(s_{j_0}))| \\ &> \frac{\tau L_1 \varepsilon_0}{2n}. \end{aligned} \quad (2.17)$$

It is clear that, for $t \in [\theta, \theta + \tau]$, the solutions $y(t)$ and $\bar{y}(t)$ satisfy the integral equations

$$y(t) = y(\theta) + \int_{\theta}^t Ay(s)ds + \int_{\theta}^t g(x(s), y(s))ds,$$

and

$$\bar{y}(t) = \bar{y}(\theta) + \int_{\theta}^t A\bar{y}(s)ds + \int_{\theta}^t g(\bar{x}(s), \bar{y}(s))ds,$$

respectively, and herewith the equation

$$\begin{aligned} y(t) - \bar{y}(t) &= (y(\theta) - \bar{y}(\theta)) + \int_{\theta}^t A(y(s) - \bar{y}(s))ds \\ &+ \int_{\theta}^t [g(x(s), y(s)) - g(\bar{x}(s), y(s))]ds \\ &+ \int_{\theta}^t [g(\bar{x}(s), y(s)) - g(\bar{x}(s), \bar{y}(s))]ds \end{aligned}$$

holds. Hence, we have the inequality

$$\begin{aligned} \|y(\theta + \tau) - \bar{y}(\theta + \tau)\| &\geq \left\| \int_{\theta}^{\theta + \tau} [g(x(s), y(s)) - g(\bar{x}(s), y(s))]ds \right\| \\ &- \|y(\theta) - \bar{y}(\theta)\| - \int_{\theta}^{\theta + \tau} \|A\| \|y(s) - \bar{y}(s)\| ds \\ &- \int_{\theta}^{\theta + \tau} L_3 \|y(s) - \bar{y}(s)\| ds. \end{aligned} \quad (2.18)$$

Now, assume that $\max_{t \in [\theta, \theta + \tau]} \|y(t) - \bar{y}(t)\| \leq \frac{\tau L_1 \varepsilon_0}{2n[2 + \tau(L_3 + \|A\|)]}$. In the present case, one encounters with a contradiction since, by means of the inequalities (2.17) and (2.18), we have

$$\begin{aligned} \max_{t \in [\theta, \theta + \tau]} \|y(t) - \bar{y}(t)\| &\geq \|y(\theta + \tau) - \bar{y}(\theta + \tau)\| \\ &> \frac{\tau L_1 \varepsilon_0}{2n} - [1 + \tau(L_3 + \|A\|)] \max_{t \in [\theta, \theta + \tau]} \|y(t) - \bar{y}(t)\| \\ &\geq \frac{\tau L_1 \varepsilon_0}{2n[2 + \tau(L_3 + \|A\|)]}. \end{aligned}$$

Therefore, one can see that the inequality

$$\max_{t \in [\theta, \theta + \tau]} \|y(t) - \bar{y}(t)\| > \frac{\tau L_1 \varepsilon_0}{2n[2 + \tau(L_3 + \|A\|)]}$$

is valid.

Suppose that at a point $\eta \in [\theta, \theta + \tau]$, the real valued function $\|y(t) - \bar{y}(t)\|$ takes its maximum on the interval $[\theta, \theta + \tau]$. That is,

$$\max_{t \in [\theta, \theta + \tau]} \|y(t) - \bar{y}(t)\| = \|y(\eta) - \bar{y}(\eta)\|.$$

For $t \in [\theta, \theta + \tau]$, by virtue of the integral equations

$$y(t) = y(\eta) + \int_{\eta}^t Ay(s)ds + \int_{\eta}^t g(x(s), y(s))ds,$$

and

$$\bar{y}(t) = \bar{y}(\eta) + \int_{\eta}^t A\bar{y}(s)ds + \int_{\eta}^t g(\bar{x}(s), \bar{y}(s))ds,$$

we obtain

$$\begin{aligned} y(t) - \bar{y}(t) &= (y(\eta) - \bar{y}(\eta)) + \int_{\eta}^t A(y(s) - \bar{y}(s))ds \\ &+ \int_{\eta}^t [g(x(s), y(s)) - g(\bar{x}(s), \bar{y}(s))]ds. \end{aligned}$$

Define

$$\tau^1 = \min \left\{ \frac{\tau}{2}, \frac{\tau L_1 \varepsilon_0}{8n(M\|A\| + M_0)[2 + \tau(L_3 + \|A\|)]} \right\}$$

and let

$$\theta^1 = \begin{cases} \eta, & \text{if } \eta \leq \theta + \tau/2 \\ \eta - \tau^1, & \text{if } \eta > \theta + \tau/2 \end{cases}.$$

We note that the interval $J^1 = [\theta^1, \theta^1 + \tau^1]$ is a subset of $[\theta, \theta + \tau]$ and hence of J .

For $t \in J^1$, we have that

$$\begin{aligned} \|y(t) - \bar{y}(t)\| &\geq \|y(\eta) - \bar{y}(\eta)\| - \left| \int_{\eta}^t \|A\| \|y(s) - \bar{y}(s)\| ds \right| \\ &- \left| \int_{\eta}^t \|g(x(s), y(s)) - g(\bar{x}(s), \bar{y}(s))\| ds \right| \\ &> \frac{\tau L_1 \varepsilon_0}{2n[2 + \tau(L_3 + \|A\|)]} - 2\tau^1(M\|A\| + M_0) \\ &\geq \frac{\tau L_1 \varepsilon_0}{4n[2 + \tau(L_3 + \|A\|)]}. \end{aligned}$$

Consequently, the inequality $\|y(t) - \bar{y}(t)\| > \varepsilon_1$ holds for $t \in J^1$, where

$$\varepsilon_1 = \frac{\tau L_1 \varepsilon_0}{4n[2 + \tau(L_3 + \|A\|)]},$$

and the length of the interval J^1 does not depend on the functions $x(t), \bar{x}(t) \in \mathcal{A}_x$.

The proof of the lemma is finalized. \square

Through Lemma 2.5.2, we mention the replication of sensitivity feature from the set of functions \mathcal{A}_x to \mathcal{A}_y , that is, from the generator system to the replicator counterpart. In a similar way, it is reasonable to analyze the sensitivity of the set of functions \mathcal{A} , which is defined through equation (2.10). In the present case, we shall say that the set \mathcal{A} is sensitive provided that \mathcal{A}_y is sensitive. This description is a natural one since, otherwise, the inequality $\|x(t) - \bar{x}(t)\| > \varepsilon_0$ implies that

$$\|(x(t), \phi_{x(t)}(t)) - (\bar{x}(t), \phi_{\bar{x}(t)}(t))\| > \varepsilon_0$$

in the same interval of time, which already signifies sensitivity of \mathcal{A} . But in replication of chaos, the crucial idea is the extension of sensitivity not only by the result-system, but also by

the replicator, and one should understand sensitivity of the result-system as a property which is equivalent to the sensitivity of the replicator. According to this explanation, we note that if \mathcal{A}_x is sensitive, then Lemma 2.5.2 implies the same feature for the set \mathcal{A}_y , and hence for the set \mathcal{A} .

Now, let us illustrate the replication of sensitivity through an example. It is known that the Lorenz system

$$\begin{aligned}x'_1 &= \sigma(-x_1 + x_2) \\x'_2 &= -x_2 + rx_1 - x_1x_3 \\x'_3 &= -bx_3 + x_1x_2,\end{aligned}\tag{2.19}$$

with the coefficients $\sigma = 10, b = 8/3, r = 28$ admits sensitivity [137]. We use system (2.19) with the specified coefficients as the generator and constitute the 6-dimensional result-system

$$\begin{aligned}x'_1 &= 10(-x_1 + x_2) \\x'_2 &= -x_2 + 28x_1 - x_1x_3 \\x'_3 &= -\frac{8}{3}x_3 + x_1x_2 \\x'_4 &= -5x_4 + x_3 \\x'_5 &= -2x_5 + 0.0002(x_2 - x_5)^3 + 4x_2 \\x'_6 &= -3x_6 - 3x_1.\end{aligned}\tag{2.20}$$

When system (2.20) is considered in the form of system (2.1) + (2.2), one can see that the diagonal matrix A whose entries on the diagonal are $-5, -2, -3$ satisfies the inequality $\|e^{At}\| \leq Ne^{-\omega t}$ with the coefficients $N = 1$ and $\omega = 2$. We note that the function $g : \mathbb{R}^3 \times \mathbb{R}^3 \rightarrow \mathbb{R}^3$ defined as

$$g(x_1, x_2, x_3, x_4, x_5, x_6) = (x_3, 0.0002(x_2 - x_5)^3 + 4x_2, -3x_1)$$

provides the conditions (A4) and (A5) with constants $L_1 = 1/\sqrt{3}, L_2 = 11\sqrt{3}/2$ and $L_3 = 3/2$ since the chaotic attractor of system (2.20) is inside a compact region such that $|x_2| \leq 30$ and $|x_5| \leq 50$. Consequently, system (2.20) satisfies the condition (A7).

In Figure 2.3, one can see the 3-dimensional projections in the $x_1 - x_2 - x_3$ and $x_4 - x_5 - x_6$ spaces of two different trajectories of the result-system (2.20) with adjacent initial conditions, such that one of them is in blue color and the other in red color. For the trajectory with blue color, we make use of the initial data $x_1(0) = -8.57, x_2(0) = -2.39, x_3(0) = 33.08, x_4(0) = 5.32, x_5(0) = 10.87, x_6(0) = -6.37$ and for the one with red color, we use the initial data $x_1(0) = -8.53, x_2(0) = -2.47, x_3(0) = 33.05, x_4(0) = 5.33, x_5(0) = 10.86, x_6(0) = -6.36$. In the simulation, the trajectories move on the time interval $[0, 3]$. The results seen in Figure 2.3 supports our theoretical results indicated in Lemma 2.5.2 such that the replicator system, likewise the generator counterpart, admits the sensitivity feature. That is, the solutions of both the generator and the replicator given by blue and red colors diverge, even though they start and move close to each other in the first stage.

In the next assertion we continue with the replication of transitivity.

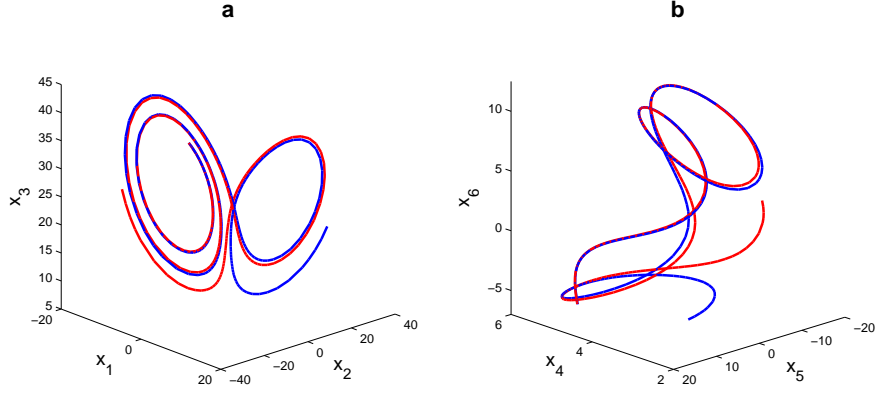


Figure 2.3: Replication of sensitivity in the result-system (2.20). The picture in (a) represents the 3–dimensional projection on the $x_1 - x_2 - x_3$ space, and the picture in (b) shows the 3–dimensional projection on the $x_4 - x_5 - x_6$ space. The sensitivity property is observable both in (a) and (b) such that the trajectories presented by blue and red colors move together in the first stage and then diverge. In other words, the sensitivity property of the generator system is mimicked by the replicator counterpart.

Lemma 2.5.3 *Transitivity of \mathcal{A}_x implies the same feature for \mathcal{A}_y .*

Proof. Fix an arbitrary small $\varepsilon > 0$, an arbitrary large $E > 0$ and let $y(t) \in \mathcal{A}_y$ be a given function. Arising from the description (2.9) of the set \mathcal{A}_y , there exists a function $x(t) \in \mathcal{A}_x$ such that $y(t) = \phi_{x(t)}(t)$. Let $\gamma = \frac{\omega(\omega - NL_3)}{2M_0N(\omega - NL_3) + NL_2\omega}$. Condition (A7) guarantees that γ is positive. Since there exists a dense solution $x^*(t) \in \mathcal{A}_x$, one can find $\xi > 0$ and an interval $J \subset \mathbb{R}$ with length E such that $\|x(t) - x^*(t + \xi)\| < \gamma\varepsilon$ for all $t \in J$. Without loss of generality, assume that J is a closed interval, that is, $J = [a, a + E]$ for some real number a .

Let $y^*(t) = \phi_{x^*(t)}(t)$. For $t \in J$, the bounded on \mathbb{R} solutions $y(t)$ and $y^*(t)$ satisfy the relations

$$y(t) = \int_{-\infty}^t e^{A(t-s)} g(x(s), y(s)) ds,$$

and

$$y^*(t) = \int_{-\infty}^t e^{A(t-s)} g(x^*(s), y^*(s)) ds,$$

respectively. The second equation above implies that

$$y^*(t + \xi) = \int_{-\infty}^{t+\xi} e^{A(t+\xi-s)} g(x^*(s), y^*(s)) ds.$$

Using the transformation $\bar{s} = s - \xi$, and replacing \bar{s} by s again, it is easy to verify that

$$y^*(t + \xi) = \int_{-\infty}^t e^{A(t-s)} g(x^*(s + \xi), y^*(s + \xi)) ds.$$

Therefore, for $t \in J$, we have that

$$\begin{aligned} y(t) - y^*(t + \xi) &= \int_{-\infty}^a e^{A(t-s)} [g(x(s), y(s)) - g(x^*(s + \xi), y^*(s + \xi))] ds \\ &+ \int_a^t e^{A(t-s)} [g(x(s), y(s)) - g(x(s), y^*(s + \xi))] ds \\ &+ \int_a^t e^{A(t-s)} [g(x(s), y^*(s)) - g(x^*(s + \xi), y^*(s + \xi))] ds, \end{aligned}$$

which implies the inequality

$$\begin{aligned} \|y(t) - y^*(t + \xi)\| &\leq \int_{-\infty}^a 2M_0 N e^{-\omega(t-s)} ds \\ &+ \int_a^t NL_3 e^{-\omega(t-s)} \|y(s) - y^*(s + \xi)\| ds \\ &+ \int_a^t NL_2 e^{-\omega(t-s)} \|x(s) - x^*(s + \xi)\| ds \\ &\leq \frac{2M_0 N}{\omega} e^{-\omega(t-a)} + \frac{NL_2 \gamma \mathcal{E}}{\omega} e^{-\omega t} (e^{\omega t} - e^{\omega a}) \\ &+ \int_a^t NL_3 e^{-\omega(t-s)} \|y(s) - y^*(s + \xi)\| ds. \end{aligned}$$

Hence, we get

$$\begin{aligned} e^{\omega t} \|y(t) - y^*(t + \xi)\| &\leq \frac{2M_0 N}{\omega} e^{\omega a} + \frac{NL_2 \gamma \mathcal{E}}{\omega} (e^{\omega t} - e^{\omega a}) \\ &+ \int_a^t NL_3 e^{\omega s} \|y(s) - y^*(s + \xi)\| ds. \end{aligned}$$

Through the implementation of Lemma 2.2 [34] to the last inequality, we obtain

$$\begin{aligned} e^{\omega t} \|y(t) - y^*(t + \xi)\| &\leq \frac{2M_0 N}{\omega} e^{\omega a} + \frac{NL_2 \gamma \mathcal{E}}{\omega} (e^{\omega t} - e^{\omega a}) \\ &+ \int_a^t NL_3 \left[\frac{2M_0 N}{\omega} e^{\omega a} + \frac{NL_2 \gamma \mathcal{E}}{\omega} (e^{\omega s} - e^{\omega a}) \right] e^{NL_3(t-s)} ds \\ &= \frac{NL_2 \gamma \mathcal{E}}{\omega} e^{\omega t} + \left(\frac{2M_0 N}{\omega} - \frac{NL_2 \gamma \mathcal{E}}{\omega} \right) e^{\omega a} e^{NL_3(t-a)} \\ &+ \frac{N^2 L_2 L_3 \gamma \mathcal{E}}{\omega(\omega - NL_3)} e^{NL_3 t} \left(e^{(\omega - NL_3)t} - e^{(\omega - NL_3)a} \right). \end{aligned}$$

Multiplying both sides by $e^{-\omega t}$, one can attain that

$$\begin{aligned} \|y(t) - y^*(t)\| &\leq \frac{2M_0 N}{\omega} e^{(NL_3 - \omega)(t-a)} \\ &+ \left(\frac{NL_2 \gamma \mathcal{E}}{\omega} + \frac{N^2 L_2 L_3 \gamma \mathcal{E}}{\omega(\omega - NL_3)} \right) \left(1 - e^{(NL_3 - \omega)(t-a)} \right) \\ &= \frac{2M_0 N}{\omega} e^{(NL_3 - \omega)(t-a)} + \frac{NL_2 \gamma \mathcal{E}}{\omega - NL_3} \left(1 - e^{(NL_3 - \omega)(t-a)} \right). \end{aligned}$$

Now, suppose that the number E is sufficiently large such that

$$E > \frac{2}{\omega - NL_3} \ln \left(\frac{1}{\gamma \mathcal{E}} \right).$$

If $t \in [a + E/2, a + E]$, then it is true that

$$e^{(NL_3 - \omega)(t-a)} \leq e^{(NL_3 - \omega)\frac{E}{2}} < \gamma\varepsilon.$$

As a result, we have

$$\|y(t) - y^*(t + \xi)\| < \left[\frac{2M_0N}{\omega} + \frac{NL_2}{\omega - NL_3} \right] \gamma\varepsilon = \varepsilon,$$

for $t \in J_1 = [a_1, a_1 + E_1]$, where $a_1 = a + E/2$ and $E_1 = E/2$. Consequently, the set \mathcal{A}_y is transitive in compliance with Definition 2.3.3.

The lemma is proved. \square

The extension of the last ingredient of chaos in the sense of Devaney is presented in the following lemma.

Lemma 2.5.4 *If \mathcal{A}_x admits a dense collection of periodic functions, then the same is true for \mathcal{A}_y .*

Proof. Fix a function $y(t) = \phi_{x(t)}(t) \in \mathcal{A}_y$, an arbitrary small number $\varepsilon > 0$ and an arbitrary large number $E > 0$. Let $\gamma = \frac{\omega(\omega - NL_3)}{2M_0N(\omega - NL_3) + NL_2\omega}$, which is a positive number by condition (A7). Suppose that \mathcal{G}_x is a dense collection of periodic functions inside \mathcal{A}_x . In this case, there exist $\tilde{x}(t) \in \mathcal{G}_x$ and an interval $J \subset \mathbb{R}$ with length E such that $\|x(t) - \tilde{x}(t)\| < \gamma\varepsilon$, for all $t \in J$. Without loss of generality, assume that J is a closed interval, that is, $J = [a, a + E]$ for some $a \in \mathbb{R}$.

We note that by condition (A4) there is a one-to-one correspondence between the sets \mathcal{G}_x and

$$\mathcal{G}_y = \{ \phi_{x(t)}(t) \mid x(t) \in \mathcal{G}_x \}, \quad (2.21)$$

such that if $x(t) \in \mathcal{G}_x$ is periodic then $\phi_{x(t)}(t) \in \mathcal{G}_y$ is also periodic with the same period, and vice versa. Therefore, $\mathcal{G}_y \subset \mathcal{A}_y$ is a collection of periodic functions and in the proof our aim is to verify that the set \mathcal{G}_y is dense in \mathcal{A}_y .

Let $\tilde{y}(t) = \phi_{\tilde{x}(t)}(t)$, which clearly belongs to the set \mathcal{G}_y . Making use of the relations

$$y(t) = \int_{-\infty}^t e^{A(t-s)} g(x(s), y(s)) ds,$$

and

$$\tilde{y}(t) = \int_{-\infty}^t e^{A(t-s)} g(\tilde{x}(s), \tilde{y}(s)) ds,$$

for $t \in J$, we attain that

$$\begin{aligned} y(t) - \tilde{y}(t) &= \int_{-\infty}^a e^{A(t-s)} [g(x(s), y(s)) - g(\tilde{x}(s), \tilde{y}(s))] ds \\ &+ \int_a^t e^{A(t-s)} [g(x(s), y(s)) - g(x(s), \tilde{y}(s))] ds \\ &+ \int_a^t e^{A(t-s)} [g(x(s), \tilde{y}(s)) - g(\tilde{x}(s), \tilde{y}(s))] ds. \end{aligned}$$

The last equation implies that

$$\begin{aligned}
\|y(t) - \tilde{y}(t)\| &\leq \int_{-\infty}^a 2M_0 N e^{-\omega(t-s)} ds \\
&+ \int_a^t NL_3 e^{-\omega(t-s)} \|y(s) - \tilde{y}(s)\| ds \\
&+ \int_a^t NL_2 e^{-\omega(t-s)} \|x(s) - \tilde{x}(s)\| ds \\
&\leq \frac{2M_0 N}{\omega} e^{-\omega(t-a)} + \frac{NL_2 \gamma \mathcal{E}}{\omega} e^{-\omega t} (e^{\omega t} - e^{\omega a}) \\
&+ \int_a^t NL_3 e^{-\omega(t-s)} \|y(s) - \tilde{y}(s)\| ds.
\end{aligned}$$

Hence, we have

$$\begin{aligned}
e^{\omega t} \|y(t) - \tilde{y}(t)\| &\leq \frac{2M_0 N}{\omega} e^{\omega a} + \frac{NL_2 \gamma \mathcal{E}}{\omega} (e^{\omega t} - e^{\omega a}) \\
&+ \int_a^t NL_3 e^{\omega s} \|y(s) - \tilde{y}(s)\| ds.
\end{aligned}$$

Application of Lemma 2.2 [34] to the last inequality yields

$$\begin{aligned}
e^{\omega t} \|y(t) - \tilde{y}(t)\| &\leq \frac{2M_0 N}{\omega} e^{\omega a} + \frac{NL_2 \gamma \mathcal{E}}{\omega} (e^{\omega t} - e^{\omega a}) \\
&+ \int_a^t NL_3 \left[\frac{2M_0 N}{\omega} e^{\omega a} + \frac{NL_2 \gamma \mathcal{E}}{\omega} (e^{\omega s} - e^{\omega a}) \right] e^{NL_3(t-s)} ds \\
&= \frac{NL_2 \gamma \mathcal{E}}{\omega} e^{\omega t} + \left(\frac{2M_0 N}{\omega} - \frac{NL_2 \gamma \mathcal{E}}{\omega} \right) e^{\omega a} e^{NL_3(t-a)} \\
&+ \frac{N^2 L_2 L_3 \gamma \mathcal{E}}{\omega(\omega - NL_3)} e^{NL_3 t} \left(e^{(\omega - NL_3)t} - e^{(\omega - NL_3)a} \right).
\end{aligned}$$

Multiplying both sides by $e^{-\omega t}$, we obtain that

$$\begin{aligned}
\|y(t) - \tilde{y}(t)\| &\leq \frac{2M_0 N}{\omega} e^{(NL_3 - \omega)(t-a)} \\
&+ \left(\frac{NL_2 \gamma \mathcal{E}}{\omega} + \frac{N^2 L_2 L_3 \gamma \mathcal{E}}{\omega(\omega - NL_3)} \right) \left(1 - e^{(NL_3 - \omega)(t-a)} \right) \\
&= \frac{2M_0 N}{\omega} e^{(NL_3 - \omega)(t-a)} + \frac{NL_2 \gamma \mathcal{E}}{\omega - NL_3} \left(1 - e^{(NL_3 - \omega)(t-a)} \right).
\end{aligned}$$

Suppose that the number E is sufficiently large such that $E > \frac{2}{\omega - NL_3} \ln \left(\frac{1}{\gamma \mathcal{E}} \right)$. If $a + \frac{E}{2} \leq t \leq a + E$, then one has $e^{(NL_3 - \omega)(t-a)} \leq e^{(NL_3 - \omega)E/2} < \gamma \mathcal{E}$. Consequently, the inequality

$$\|y(t) - \tilde{y}(t)\| < \left(\frac{2M_0 N}{\omega} + \frac{NL_2}{\omega - NL_3} \right) \gamma \mathcal{E} = \varepsilon,$$

holds for $t \in J_1 = [a_1, a_1 + E_1]$, where $a_1 = a + E/2$ and $E_1 = E/2$.

The proof of the lemma is accomplished. \square

We end up the present part by stating the following theorem and its immediate corollary, which can be verified as consequences of Lemma 2.5.2, Lemma 2.5.3 and Lemma 2.5.4.

Theorem 2.5.1 *If the set \mathcal{A}_x is Devaney's chaotic, then the same is true for the set \mathcal{A}_y .*

Corollary 2.5.1 *If the set \mathcal{A}_x is Devaney's chaotic, then \mathcal{A} is chaotic in the same way.*

In the next part, the replication of chaos in the Li–Yorke sense is taken into account.

2.6 Replication of Li-Yorke Chaos

Our aim in this section is to prove that if \mathcal{A}_x is chaotic in the sense of Li-Yorke, then the same is valid for the set \mathcal{A}_y , and consequently for the set \mathcal{A} .

We start by indicating the following assertion, which presents the replication of proximity feature in accordance with Definition 2.3.6.

Lemma 2.6.1 *If a couple of functions $(x(t), \bar{x}(t)) \in \mathcal{A}_x \times \mathcal{A}_x$ is proximal, then the same is true for the couple $(\phi_{x(t)}(t), \phi_{\bar{x}(t)}(t)) \in \mathcal{A}_y \times \mathcal{A}_y$.*

Proof. Fix an arbitrary small positive number ε and an arbitrary large positive number E . Define $\gamma = \frac{\omega(\omega - NL_3)}{2M_0N(\omega - NL_3) + NL_2\omega}$. Condition (A7) implies that γ is positive. Because a given couple of functions $(x(t), \bar{x}(t)) \in \mathcal{A}_x \times \mathcal{A}_x$ is proximal, one can find a sequence of real numbers $\{E_i\}$ satisfying $E_i \geq E$ for each $i \in \mathbb{N}$, and a sequence $\{a_i\}$, $a_i \rightarrow \infty$ as $i \rightarrow \infty$, such that we have $\|x(t) - \bar{x}(t)\| < \gamma\varepsilon$, for each t from the intervals $J_i = [a_i, a_i + E_i]$, $i \in \mathbb{N}$, and $J_i \cap J_j = \emptyset$ whenever $i \neq j$.

Let us fix an arbitrary natural number i . Since the functions $y(t) = \phi_{x(t)}(t) \in \mathcal{A}_y$ and $\bar{y}(t) = \phi_{\bar{x}(t)}(t) \in \mathcal{A}_y$ satisfy the relations

$$y(t) = \int_{-\infty}^t e^{A(t-s)} g(x(s), y(s)) ds,$$

and

$$\bar{y}(t) = \int_{-\infty}^t e^{A(t-s)} g(\bar{x}(s), \bar{y}(s)) ds,$$

respectively, for $t \in J_i$, we have that

$$\begin{aligned} y(t) - \bar{y}(t) &= \int_{-\infty}^{a_i} e^{A(t-s)} [g(x(s), y(s)) - g(\bar{x}(s), \bar{y}(s))] ds \\ &+ \int_{a_i}^t e^{A(t-s)} [g(x(s), y(s)) - g(x(s), \bar{y}(s))] ds \\ &+ \int_{a_i}^t e^{A(t-s)} [g(x(s), \bar{y}(s)) - g(\bar{x}(s), \bar{y}(s))] ds. \end{aligned}$$

This implies that the inequality

$$\begin{aligned}
\|y(t) - \bar{y}(t)\| &\leq \int_{-\infty}^{a_i} 2M_0N e^{-\omega(t-s)} ds \\
&+ \int_{a_i}^t NL_3 e^{-\omega(t-s)} \|y(s) - \bar{y}(s)\| ds \\
&+ \int_{a_i}^t NL_2 e^{-\omega(t-s)} \|x(s) - \bar{x}(s)\| ds \\
&\leq \frac{2M_0N}{\omega} e^{-\omega(t-a)} + \frac{NL_2\gamma\mathcal{E}}{\omega} e^{-\omega t} (e^{\omega t} - e^{\omega a}) \\
&+ \int_{a_i}^t NL_3 e^{-\omega(t-s)} \|y(s) - \bar{y}(s)\| ds
\end{aligned}$$

is valid. Hence, we attain that

$$\begin{aligned}
e^{\omega t} \|y(t) - \bar{y}(t)\| &\leq \frac{2M_0N}{\omega} e^{\omega a_i} + \frac{NL_2\gamma\mathcal{E}}{\omega} (e^{\omega t} - e^{\omega a_i}) \\
&+ \int_{a_i}^t NL_3 e^{\omega s} \|y(s) - \bar{y}(s)\| ds.
\end{aligned}$$

Implementing Lemma 2.2 [34] to the last inequality, we obtain

$$\begin{aligned}
e^{\omega t} \|y(t) - \bar{y}(t)\| &\leq \frac{2M_0N}{\omega} e^{\omega a_i} + \frac{NL_2\gamma\mathcal{E}}{\omega} (e^{\omega t} - e^{\omega a_i}) \\
&+ \int_a^t NL_3 \left[\frac{2M_0N}{\omega} e^{\omega a_i} + \frac{NL_2\gamma\mathcal{E}}{\omega} (e^{\omega s} - e^{\omega a_i}) \right] e^{NL_3(t-s)} ds \\
&= \frac{NL_2\gamma\mathcal{E}}{\omega} e^{\omega t} + \left(\frac{2M_0N}{\omega} - \frac{NL_2\gamma\mathcal{E}}{\omega} \right) e^{\omega a_i} e^{NL_3(t-a_i)} \\
&+ \frac{N^2L_2L_3\gamma\mathcal{E}}{\omega(\omega - NL_3)} e^{NL_3t} \left(e^{(\omega - NL_3)t} - e^{(\omega - NL_3)a_i} \right).
\end{aligned}$$

Multiplying both sides by the term $e^{-\omega t}$, one can verify that

$$\begin{aligned}
\|y(t) - \bar{y}(t)\| &\leq \frac{2M_0N}{\omega} e^{(NL_3 - \omega)(t-a_i)} \\
&+ \left(\frac{NL_2\gamma\mathcal{E}}{\omega} + \frac{N^2L_2L_3\gamma\mathcal{E}}{\omega(\omega - NL_3)} \right) \left(1 - e^{(NL_3 - \omega)(t-a_i)} \right) \\
&= \frac{2M_0N}{\omega} e^{(NL_3 - \omega)(t-a_i)} + \frac{NL_2\gamma\mathcal{E}}{\omega - NL_3} \left(1 - e^{(NL_3 - \omega)(t-a_i)} \right).
\end{aligned}$$

If E is sufficiently large such that $E > \frac{2}{\omega - NL_3} \ln \left(\frac{1}{\gamma\mathcal{E}} \right)$, then one has

$$e^{(NL_3 - \omega)(t-a_i)} < e^{(NL_3 - \omega)E_i/2} \leq e^{(NL_3 - \omega)E/2} < \gamma\mathcal{E},$$

for $t \in [a_i + E_i/2, a_i + E_i]$.

Since the natural number i was arbitrarily chosen, for each $i \in \mathbb{N}$, we have that

$$\|y(t) - \bar{y}(t)\| < \left(\frac{2M_0N}{\omega} + \frac{NL_2}{\omega - NL_3} \right) \gamma\mathcal{E} = \varepsilon,$$

for each $t \in \tilde{J}_i = [\tilde{a}_i, \tilde{a}_i + \tilde{E}_i]$, where $\tilde{a}_i = a_i + E_i/2$ and $\tilde{E}_i = E_i/2$. Note that for each i the interval $\tilde{J}_i \subset \mathbb{R}$ has a length no less than $\tilde{E} = E/2$. As a consequence, the couple of functions $(\phi_{x(t)}(t), \phi_{\bar{x}(t)}(t)) \in \mathcal{A}_y \times \mathcal{A}_y$ is proximal according to Definition 2.3.6.

The proof is completed. \square

The following lemma indicates the replication of the next characteristic feature of Li-Yorke chaos.

Lemma 2.6.2 *If a pair $(x(t), \bar{x}(t)) \in \mathcal{A}_x \times \mathcal{A}_x$ is frequently (ε_0, Δ) -separated for some positive numbers ε_0 and Δ , then the pair $(\phi_{x(t)}(t), \phi_{\bar{x}(t)}(t)) \in \mathcal{A}_y \times \mathcal{A}_y$ is frequently $(\varepsilon_1, \bar{\Delta})$ -separated for some positive numbers ε_1 and $\bar{\Delta}$.*

Proof. Since a given couple of functions $(x(t), \bar{x}(t)) \in \mathcal{A}_x \times \mathcal{A}_x$ is frequently (ε_0, Δ) -separated for some $\varepsilon_0 > 0$ and $\Delta > 0$, there exist infinitely many disjoint intervals, each with a length no less than Δ , such that $\|x(t) - \bar{x}(t)\| > \varepsilon_0$ for each t from these intervals. Without loss of generality, assume that these intervals are all closed subsets of \mathbb{R} . In that case, one can find a sequence $\{\Delta_i\}$ satisfying $\Delta_i \geq \Delta$, $i \in \mathbb{N}$, and a sequence $\{d_i\}$, $d_i \rightarrow \infty$ as $i \rightarrow \infty$, such that for each $i \in \mathbb{N}$ the inequality $\|x(t) - \bar{x}(t)\| > \varepsilon_0$ holds for $t \in J_i = [d_i, d_i + \Delta_i]$, and $J_i \cap J_j = \emptyset$ whenever $i \neq j$. Throughout the proof, let us denote $y(t) = \phi_{x(t)}(t) \in \mathcal{A}_y$ and $\bar{y}(t) = \phi_{\bar{x}(t)}(t) \in \mathcal{A}_y$.

Our aim is to show the existence of positive numbers $\varepsilon_1, \bar{\Delta}$ and infinitely many disjoint intervals $\bar{J}_i \subset J_i, i \in \mathbb{N}$, each with length $\bar{\Delta}$, such that the inequality $\|y(t) - \bar{y}(t)\| > \varepsilon_1$ holds for each t from the intervals $\bar{J}_i, i \in \mathbb{N}$.

As in Section 2.5, we again suppose that $g(x, y) = \begin{pmatrix} g_1(x, y) \\ g_2(x, y) \\ \vdots \\ g_n(x, y) \end{pmatrix}$, where each $g_j(x, y)$, $1 \leq$

$j \leq n$, is a real valued function. Using the equicontinuity on \mathbb{R} of the family \mathcal{F} , which is mentioned in Lemma 2.5.1, one can find a positive number $\tau < \Delta$, independent of the functions $x(t), \bar{x}(t) \in \mathcal{A}_x$, $y(t), \bar{y}(t) \in \mathcal{A}_y$, such that for any $t_1, t_2 \in \mathbb{R}$ with $|t_1 - t_2| < \tau$ the inequality

$$\begin{aligned} & \left| (g_j(x(t_1), y(t_1)) - g_j(\bar{x}(t_1), y(t_1))) \right. \\ & \quad \left. - (g_j(x(t_2), y(t_2)) - g_j(\bar{x}(t_2), y(t_2))) \right| \\ & < \frac{L_1 \varepsilon_0}{2n} \end{aligned} \tag{2.22}$$

holds for all $1 \leq j \leq n$.

Suppose that the sequence $\{s_i\}$ denotes the midpoints of the intervals J_i , that is, $s_i = d_i + \Delta_i/2$ for each $i \in \mathbb{N}$. Let us define a sequence $\{\theta_i\}$ through the equation $\theta_i = s_i - \tau/2$.

Let us fix an arbitrary natural number i . In a similar way to the method specified in the proof of Lemma 2.5.2, one can show the existence of an integer $j_i = j_i(s_i)$, $1 \leq j_i \leq n$, such that

$$|g_{j_i}(x(s_i), y(s_i)) - g_{j_i}(\bar{x}(s_i), y(s_i))| \geq \frac{L_1}{n} \|x(s_i) - \bar{x}(s_i)\| > \frac{L_1 \varepsilon_0}{n}. \quad (2.23)$$

On the other hand, making use of the inequality (2.22), it is easy to verify that

$$\begin{aligned} & |g_{j_i}(x(s_i), y(s_i)) - g_{j_i}(\bar{x}(s_i), y(s_i))| - |g_{j_i}(x(t), y(t)) - g_{j_i}(\bar{x}(t), y(t))| \\ & \leq |(g_{j_i}(x(t), y(t)) - g_{j_i}(\bar{x}(t), y(t))) - (g_{j_i}(x(s_i), y(s_i)) - g_{j_i}(\bar{x}(s_i), y(s_i))))| \\ & < \frac{L_1 \varepsilon_0}{2n}, \end{aligned}$$

for all $t \in [\theta_i, \theta_i + \tau]$. Therefore, by favour of (2.23), we obtain that the inequality

$$\begin{aligned} & |g_{j_i}(x(t), y(t)) - g_{j_i}(\bar{x}(t), y(t))| \\ & > |g_{j_i}(x(s_i), y(s_i)) - g_{j_i}(\bar{x}(s_i), y(s_i))| - \frac{L_1 \varepsilon_0}{2n} \\ & > \frac{L_1 \varepsilon_0}{2n} \end{aligned} \quad (2.24)$$

is valid on the same interval.

Using the mean value theorem for integrals, it is possible to find numbers $s_1^i, s_2^i, \dots, s_n^i$ that belong to the interval $[\theta_i, \theta_i + \tau]$ such that

$$\begin{aligned} & \left\| \int_{\theta_i}^{\theta_i + \tau} [g(x(s), y(s)) - g(\bar{x}(s), y(s))] ds \right\| \\ & = \left\| \begin{pmatrix} \int_{\theta_i}^{\theta_i + \tau} [g_1(x(s), y(s)) - g_1(\bar{x}(s), y(s))] ds \\ \int_{\theta_i}^{\theta_i + \tau} [g_2(x(s), y(s)) - g_2(\bar{x}(s), y(s))] ds \\ \vdots \\ \int_{\theta_i}^{\theta_i + \tau} [g_n(x(s), y(s)) - g_n(\bar{x}(s), y(s))] ds \end{pmatrix} \right\| \\ & = \left\| \begin{pmatrix} \tau [g_1(x(s_1^i), y(s_1^i)) - g_1(\bar{x}(s_1^i), y(s_1^i))] \\ \tau [g_2(x(s_2^i), y(s_2^i)) - g_2(\bar{x}(s_2^i), y(s_2^i))] \\ \vdots \\ \tau [g_n(x(s_n^i), y(s_n^i)) - g_n(\bar{x}(s_n^i), y(s_n^i))] \end{pmatrix} \right\|. \end{aligned}$$

Hence, the inequality (2.24) yields that

$$\begin{aligned} & \left\| \int_{\theta_i}^{\theta_i + \tau} [g(x(s), y(s)) - g(\bar{x}(s), y(s))] ds \right\| \\ & \geq \tau |g_{j_i}(x(s_{j_i}^i), y(s_{j_i}^i)) - g_{j_i}(\bar{x}(s_{j_i}^i), y(s_{j_i}^i))| \\ & > \frac{\tau L_1 \varepsilon_0}{2n}. \end{aligned}$$

For $t \in [\theta_i, \theta_i + \tau]$, the functions $y(t) \in \mathcal{A}_y$ and $\bar{y}(t) \in \mathcal{A}_y$ satisfy the relations

$$y(t) = y(\theta_i) + \int_{\theta_i}^t Ay(s) ds + \int_{\theta_i}^t g(x(s), y(s)) ds,$$

and

$$\bar{y}(t) = \bar{y}(\theta_i) + \int_{\theta_i}^t A\bar{y}(s)ds + \int_{\theta_i}^t g(\bar{x}(s), \bar{y}(s))ds,$$

respectively, and herewith the equation

$$\begin{aligned} y(t) - \bar{y}(t) &= (y(\theta_i) - \bar{y}(\theta_i)) + \int_{\theta_i}^t A(y(s) - \bar{y}(s))ds \\ &+ \int_{\theta_i}^t [g(x(s), y(s)) - g(\bar{x}(s), y(s))]ds \\ &+ \int_{\theta_i}^t [g(\bar{x}(s), y(s)) - g(\bar{x}(s), \bar{y}(s))]ds \end{aligned}$$

is achieved. Taking $t = \theta_i + \tau$ in the last equation, we attain the inequality

$$\begin{aligned} \|y(\theta_i + \tau) - \bar{y}(\theta_i + \tau)\| &\geq \left\| \int_{\theta_i}^{\theta_i + \tau} [g(x(s), y(s)) - g(\bar{x}(s), y(s))]ds \right\| \\ &- \|y(\theta_i) - \bar{y}(\theta_i)\| - \int_{\theta_i}^{\theta_i + \tau} (\|A\| + L_3) \|y(s) - \bar{y}(s)\| ds \end{aligned} \quad (2.25)$$

Now, assume that $\max_{t \in [\theta_i, \theta_i + \tau]} \|y(t) - \bar{y}(t)\| \leq \frac{\tau L_1 \varepsilon_0}{2n[2 + \tau(L_3 + \|A\|)]}$. In this case, one arrives at a contradiction since, by means of the inequalities (2.24) and (2.25), we have

$$\begin{aligned} \max_{t \in [\theta_i, \theta_i + \tau]} \|y(t) - \bar{y}(t)\| &\geq \|y(\theta_i + \tau) - \bar{y}(\theta_i + \tau)\| \\ &> \frac{\tau L_1 \varepsilon_0}{2n} - [1 + \tau(L_3 + \|A\|)] \max_{t \in [\theta_i, \theta_i + \tau]} \|y(t) - \bar{y}(t)\| \\ &\geq \frac{\tau L_1 \varepsilon_0}{2n} - [1 + \tau(L_3 + \|A\|)] \frac{\tau L_1 \varepsilon_0}{2n[2 + \tau(L_3 + \|A\|)]} \\ &= \frac{\tau L_1 \varepsilon_0}{2n} \left(1 - \frac{1 + \tau(L_3 + \|A\|)}{2 + \tau(L_3 + \|A\|)} \right) \\ &= \frac{\tau L_1 \varepsilon_0}{2n[2 + \tau(L_3 + \|A\|)]}. \end{aligned}$$

Therefore, it is true that $\max_{t \in [\theta_i, \theta_i + \tau]} \|y(t) - \bar{y}(t)\| > \frac{\tau L_1 \varepsilon_0}{2n[2 + \tau(L_3 + \|A\|)]}$.

Suppose that the real valued function $\|y(t) - \bar{y}(t)\|$ takes its maximum value for $t \in [\theta_i, \theta_i + \tau]$ at a point η_i . In other words, for some $\eta_i \in [\theta_i, \theta_i + \tau]$, we have that

$$\max_{t \in [\theta_i, \theta_i + \tau]} \|y(t) - \bar{y}(t)\| = \|y(\eta_i) - \bar{y}(\eta_i)\|.$$

Making use of the integral equations

$$y(t) = y(\eta_i) + \int_{\eta_i}^t Ay(s)ds + \int_{\eta_i}^t g(x(s), y(s))ds,$$

and

$$\bar{y}(t) = \bar{y}(\eta_i) + \int_{\eta_i}^t A\bar{y}(s)ds + \int_{\eta_i}^t g(\bar{x}(s), \bar{y}(s))ds,$$

on the time interval $[\theta_i, \theta_i + \tau]$, one can obtain that

$$\begin{aligned} y(t) - \bar{y}(t) &= (y(\eta_i) - \bar{y}(\eta_i)) + \int_{\eta_i}^t A(y(s) - \bar{y}(s)) ds \\ &+ \int_{\eta_i}^t [g(x(s), y(s)) - g(\bar{x}(s), \bar{y}(s))] ds. \end{aligned}$$

Define the numbers

$$\bar{\Delta} = \min \left\{ \frac{\tau}{2}, \frac{\tau L_1 \varepsilon_0}{8n(M \|A\| + M_0)[2 + \tau(L_3 + \|A\|)]} \right\}$$

and

$$\theta_i^1 = \begin{cases} \eta_i, & \text{if } \eta_i \leq \theta_i + \tau/2 \\ \eta_i - \tau^1, & \text{if } \eta_i > \theta_i + \tau/2 \end{cases}.$$

For each $t \in [\theta_i^1, \theta_i^1 + \bar{\Delta}]$, we have that

$$\begin{aligned} \|y(t) - \bar{y}(t)\| &\geq \|y(\eta_i) - \bar{y}(\eta_i)\| - \left| \int_{\eta_i}^t \|A\| \|y(s) - \bar{y}(s)\| ds \right| \\ &- \left| \int_{\eta_i}^t \|g(x(s), y(s)) - g(\bar{x}(s), \bar{y}(s))\| ds \right| \\ &> \frac{\tau L_1 \varepsilon_0}{2n[2 + \tau(L_3 + \|A\|)]} - 2M \|A\| \tau^1 - 2M_0 \tau^1 \\ &= \frac{\tau L_1 \varepsilon_0}{2n[2 + \tau(L_3 + \|A\|)]} - 2\tau^1(M \|A\| + M_0) \\ &\geq \frac{\tau L_1 \varepsilon_0}{4n[2 + \tau(L_3 + \|A\|)]}. \end{aligned}$$

The information mentioned above is true for an arbitrarily chosen natural number i . Therefore, for each $i \in \mathbb{N}$, the interval $\bar{J}_i = [\theta_i^1, \theta_i^1 + \bar{\Delta}]$ is a subset of $[\theta_i, \theta_i + \tau]$, and hence of J_i .

Moreover, for any $i \in \mathbb{N}$, we have $\|y(t) - \bar{y}(t)\| > \varepsilon_1$, $t \in \bar{J}_i$, where $\varepsilon_1 = \frac{\tau L_1 \varepsilon_0}{4n[2 + \tau(L_3 + \|A\|)]}$.

Consequently, according to Definition 2.3.7, the pair $(\phi_{x(t)}(t), \phi_{\bar{x}(t)}(t)) \in \mathcal{A}_x \times \mathcal{A}_y$ is frequently $(\varepsilon_1, \bar{\Delta})$ -separated.

The proof of the lemma is finalized. \square

Now, we state and prove the main theorem of the present section. In the proof, we suppose that $\mathcal{G}_x \subset \mathcal{A}_x$ denotes the set of periodic functions inside \mathcal{A}_x and the set $\mathcal{G}_y \subset \mathcal{A}_y$, defined through equation (2.21), denotes the set of periodic functions inside \mathcal{A}_y .

Theorem 2.6.1 *If the set \mathcal{A}_x is Li-Yorke chaotic, then the same is true for the set \mathcal{A}_y .*

Proof. It can be easily verified that for any natural number k , $x(t) \in \mathcal{G}_x$ is a kT -periodic function if and only if $\phi_{x(t)}(t) \in \mathcal{G}_y$ is kT -periodic, where \mathcal{G}_x and \mathcal{G}_y denote the sets of all periodic functions inside \mathcal{A}_x and \mathcal{A}_y , respectively. Therefore, the set \mathcal{A}_y admits a kT -periodic function for any $k \in \mathbb{N}$.

Next, suppose that the set \mathcal{C}_x is a scrambled set inside \mathcal{A}_x and define the set

$$\mathcal{C}_y = \{ \phi_{x(t)}(t) \mid x(t) \in \mathcal{C}_x \}. \quad (2.26)$$

Condition (A4) implies that there is a one-to-one correspondence between the sets \mathcal{C}_x and \mathcal{C}_y . Since the scrambled set \mathcal{C}_x is uncountable, it is clear that the set \mathcal{C}_y is also uncountable. Moreover, using the same condition one can show that no periodic functions exist inside \mathcal{C}_y , since no such functions take place inside the set \mathcal{C}_x . That is, $\mathcal{C}_y \cap \mathcal{G}_y = \emptyset$.

Since each couple of functions inside $\mathcal{C}_x \times \mathcal{C}_x$ is proximal, Lemma 2.6.1 implies the same feature for each couple of functions inside $\mathcal{C}_y \times \mathcal{C}_y$.

Similarly, Lemma 2.6.2 implies that if each couple of functions $(x(t), \bar{x}(t)) \in \mathcal{C}_x \times \mathcal{C}_x$ ($\mathcal{C}_x \times \mathcal{G}_x$) is frequently (ε_0, Δ) -separated for some positive numbers ε_0 and Δ , then each couple of functions $(y(t), \bar{y}(t)) \in \mathcal{C}_y \times \mathcal{C}_y$ ($\mathcal{C}_y \times \mathcal{G}_y$) is frequently $(\varepsilon_1, \bar{\Delta})$ -separated for some positive numbers ε_1 and $\bar{\Delta}$. Consequently, the set \mathcal{C}_y is a scrambled set inside \mathcal{A}_x , and according to Definition 2.3.10, \mathcal{A}_y is Li-Yorke chaotic.

The proof of the theorem is accomplished. \square

An immediate corollary of Theorem 2.6.1 is the following.

Corollary 2.6.1 *If the set \mathcal{A}_x is Li-Yorke chaotic, then the set \mathcal{A} is chaotic in the same way.*

2.7 Morphogenesis of Chaos

Two different mechanisms of chaos extension (morphogenesis) through applying replication are considered in this study. The first one is illustrated schematically in Figure 2.4. The figure represents consecutively connected systems as boxes and the blue arrows symbolize unidirectional couplings between two systems. In the first coupling, we take into account a generator system, the leftmost box in the figure, which is connected with a second system considered as a replicator in the couple. In the next coupling, the second system is considered as a generator with respect to the third one. That is, it changes its role in the extension process. In the third coupling, the third system is considered as a generator and the fourth one as a replicator. In summary, the mechanism proceeds as follows. We take into account consecutive unidirectionally coupled systems such that the initial one is a generator and at each next coupling the role of the previously chaotic replicator changes and we start to use it as a generator. As a result of the mechanism all individual subsystems are chaotic as well as the system which consists of all subsystems. Moreover, the type of the chaos is saved under this procedure.

In Figure 2.5 we show another mechanism of chaos extension. Here, the generator is surrounded by three replicators and the blue arrows symbolize, again, unidirectional couplings between two systems. Distinctively from the former mechanism, the replicators do not change

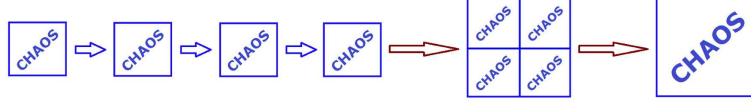


Figure 2.4: Morphogenesis of chaos through consecutive replications

their role with respect to each other according to the special topology of connection. The generator is coupled with all other replicators such that it is rather a core than a beginning element. The result of the mechanism is similar to the former such that all replicators as well as the system consisting of all subsystems become chaotic, saving the chaos type of the generator.

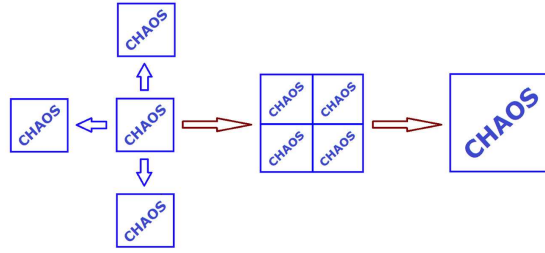


Figure 2.5: Morphogenesis of chaos from a prior chaos as a core

We call the two ways as *the chain* and *the core* mechanisms, respectively, and the system which unites the generator and several replicators, of type (2.2), in either extension mechanism as *the result-system*. Theoretically, we do not discuss constraints on the dimension of the result-system, but under certain conditions it seems that the dimension is not restricted for both mechanisms. However, this is definitely true for the core mechanism even with infinite dimensions. We will discuss and simulate the chain mechanism in the chapter, mainly, since the core mechanism can be discussed very similarly. One can invent other mechanisms, for example, by considering “composition” of the two mechanisms proposed presently.

Next, to exemplify the chaos extension procedure of our study, according to the chain mechanism shown in Figure 2.4 we set up the following 8–dimensional result-system

$$\begin{aligned}
 x_1' &= x_2 \\
 x_2' &= -0.05x_2 - x_1^3 + 7.5 \cos t \\
 x_3' &= x_4 + x_1 \\
 x_4' &= -3x_3 - 2x_4 - 0.008x_3^3 + x_2 \\
 x_5' &= x_6 + x_3 \\
 x_6' &= -3x_5 - 2.1x_6 - 0.007x_5^3 + x_4 \\
 x_7' &= x_8 + x_5 \\
 x_8' &= -3.1x_7 - 2.2x_8 - 0.006x_7^3 + x_6.
 \end{aligned} \tag{2.27}$$

We note that system (2.27) consists of four subsystems with coordinates (x_1, x_2) , (x_3, x_4) ,

(x_5, x_6) and (x_7, x_8) such that the subsystem (x_1, x_2) is exactly the generator used in system (2.4) + (2.5), while the subsystem (x_3, x_4) is the replicator of (2.4) + (2.5).

According to the theoretical results of the present chapter, system (2.27) possesses a chaotic attractor in the 8–dimensional phase space. By marking the trajectory of this system with the initial data $x_1(0) = 2, x_2(0) = 3, x_3(0) = x_5(0) = x_7(0) = -1, x_4(0) = x_6(0) = x_8(0) = 1$ stroboscopically at times that are integer multiples of 2π , we obtain the Poincaré section inside the 8–dimensional space. In Figure 2.6, which informs us about morphogenesis, the 3–dimensional projections of the whole Poincaré section on the $x_2 - x_4 - x_6$ and $x_3 - x_5 - x_7$ spaces are shown. One can see in Figure 2.6, (a) and in Figure 2.6, (b) the additional *foldings* which are not possible to observe in the classical strange attractor shown in Figure 2.2, (a).

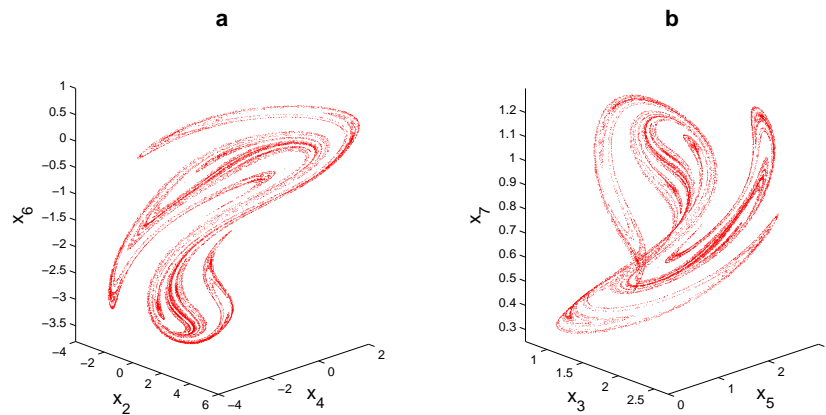


Figure 2.6: In (a) and (b) projections of the result chaotic attractor on the $x_2 - x_4 - x_6$ and $x_3 - x_5 - x_7$ spaces are respectively presented. One can see in (a) and (b) the additional *foldings* which are not possible to observe in the 2–dimensional picture of the prior classical chaos shown in Figure 2.2, (a). In the same time, the shape of the original attractor is seen in the resulting chaos. The illustrations in (a) and (b) repeat the structure of the attractor of the generator and the similarity between these pictures is a manifestation of the morphogenesis of chaos.

Despite we are restricted to make illustrations at most in 3–dimensional spaces, taking inspiration from Figure 2.2 and Figure 2.6, one can imagine that the structure of the original Poincaré section in the 8–dimensional space will be similar through its fractal structure, but more beautiful and impressive than its projections. From this point of view, we are not surprised since these facts have been proved theoretically.

Next, we shall handle the problem that whether the chaos extension procedure works for all existing systems in the mechanisms presented above, from the theoretical point of view. Since the core mechanism does not need any additional theoretical discussions, we will consider the chain mechanism.

In addition to the system (2.1) + (2.2), we take into account the system

$$z' = Bz + h(y(t), z), \quad (2.28)$$

where $h : \mathbb{R}^n \times \mathbb{R}^l \rightarrow \mathbb{R}^l$ is a continuous function in all of its arguments, the constant $l \times l$ real valued matrix B has real parts of eigenvalues all negative and $y(t)$ is a solution system (2.2).

It is easy to verify the existence of positive numbers \tilde{N} and $\tilde{\omega}$ such that $\|e^{Bt}\| \leq \tilde{N}e^{-\tilde{\omega}t}$, for all $t \geq 0$.

In our next theoretical discussions, the system (2.28) will serve as the third system in the chain mechanism presented by Figure 2.4, and we need the following assumptions which are counterparts of the conditions (A4) – (A7) presented in Section 2.2.

(A8) There exists a positive number \tilde{L}_1 such that

$$\|h(y_1, z) - h(y_2, z)\| \geq \tilde{L}_1 \|y_1 - y_2\|,$$

for all $y_1, y_2 \in \mathbb{R}^n, z \in \mathbb{R}^l$;

(A9) There exist positive numbers \tilde{L}_2 and \tilde{L}_3 such that

$$\|h(y_1, z) - h(y_2, z)\| \leq \tilde{L}_2 \|y_1 - y_2\|,$$

for all $y_1, y_2 \in \mathbb{R}^n, z \in \mathbb{R}^l$, and

$$\|h(y, z_1) - h(y, z_2)\| \leq \tilde{L}_3 \|z_1 - z_2\|,$$

for all $y \in \mathbb{R}^n, z_1, z_2 \in \mathbb{R}^l$;

(A10) There exists a positive number K_0 such that

$$\sup_{y \in \mathbb{R}^n, z \in \mathbb{R}^l} \|h(y, z)\| \leq K_0;$$

(A11) $\tilde{N}\tilde{L}_3 - \tilde{\omega} < 0$.

Likewise the definition for the set of functions \mathcal{A}_y , given by (2.9), let us denote by \mathcal{A}_z the set of all bounded on \mathbb{R} solutions of system $z' = Bz + h(y(t), z)$, for any $y(t) \in \mathcal{A}_y$.

In a similar way to the Lemma 2.2.1, one can show that the set

$$\mathcal{U}_z = \{z(t) \mid z(t) \text{ is a solution of the system } z' = Az + g(y(t), z) \text{ for some } y(t) \in \mathcal{U}_y\}$$

is a basin of \mathcal{A}_z . Furthermore, a similar result of Theorem 2.4.1 introduced in Section 2.4, hold also for the set \mathcal{A}_z .

We state in the next theorem that similar results of the Theorems 2.5.1 and 2.6.1 presented in Sections 2.5 and 2.6, respectively, hold also for the set \mathcal{A}_z .

We note that, in the case of the presence of arbitrary finite number of systems, which obey conditions that are counterparts of (A4) – (A7), one can prove that a similar result of the next theorem holds for the chain mechanism.

Theorem 2.7.1 *If the set \mathcal{A}_x is Devaney chaotic or Li-Yorke chaotic, then the set \mathcal{A}_z is chaotic in the same way as both \mathcal{A}_x and \mathcal{A}_y .*

Proof. In the proof, we will show that for each $z(t) \in \mathcal{A}_z$ and arbitrary $\delta > 0$, there exist $\bar{z}(t) \in \mathcal{A}_z$ and $t_0 \in \mathbb{R}$ such that $\|z(t_0) - \bar{z}(t_0)\| < \delta$, which is needed to show sensitivity of \mathcal{A}_z . The remaining parts of the proof can be performed in a similar way to the proofs presented in Sections 2.5 and 2.6, and therefore are omitted.

Suppose that the set \mathcal{A}_x is sensitive. Fix an arbitrary $\delta > 0$ and let $z(t) \in \mathcal{A}_z$ be a given solution of system (2.28). In this case, there exists $y(t) = \phi_{x(t)}(t) \in \mathcal{A}_y$, where $x(t) \in \mathcal{A}_x$, such that $z(t)$ is the unique bounded on \mathbb{R} solution of the system $z' = Bz + h(y(t), z)$.

Let us choose a number $\bar{\varepsilon} = \bar{\varepsilon}(\delta) > 0$ small enough which satisfies the inequality

$$\left(1 + \frac{\tilde{N}\tilde{L}_2}{\tilde{\omega} - \tilde{N}\tilde{L}_3}\right) \left(1 + \frac{NL_2}{\omega - NL_3}\right) \bar{\varepsilon} < \delta$$

and denote $\varepsilon_1 = \left(1 + \frac{NL_2}{\omega - NL_3}\right) \bar{\varepsilon}$. Now, take $R = R(\bar{\varepsilon}) < 0$ sufficiently large in absolute value such that both of the inequalities $\frac{2M_0N}{\omega} e^{-(NL_3 - \omega)R/2} \leq \bar{\varepsilon}$ and $\frac{2\tilde{M}_0\tilde{N}}{\tilde{\omega}} e^{-(\tilde{N}\tilde{L}_3 - \tilde{\omega})R/2} \leq \varepsilon_1$ are valid, and let $\delta_1 = \delta_1(\bar{\varepsilon}, R) = \bar{\varepsilon}e^{L_0R}$. Since the set \mathcal{A}_x is sensitive, one can find $\bar{x}(t) \in \mathcal{A}_x$ and $t_0 \in \mathbb{R}$ such that the inequality $\|x(t_0) - \bar{x}(t_0)\| < \delta_1$ holds.

As in the case of the proof of Lemma 2.5.2, for $t \in [t_0 + R, t_0]$, one can verify that

$$\|x(t) - \bar{x}(t)\| < \bar{\varepsilon}$$

and

$$\|y(t) - \bar{y}(t)\| \leq \frac{NL_2\bar{\varepsilon}}{\omega - NL_3} + \frac{2M_0N}{\omega} e^{(NL_3 - \omega)(t - t_0 - R)}.$$

According to the last inequality, we have $\|y(t) - \bar{y}(t)\| \leq \varepsilon_1$, for $t \in [t_0 + R/2, t_0]$.

Suppose that $\bar{z}(t)$ is the unique bounded on \mathbb{R} solution of the system $z' = Bz + h(\bar{y}(t), z)$. One can see that the relations

$$z(t) = \int_{-\infty}^t e^{B(t-s)} h(y(s), z(s)) ds$$

and

$$\bar{z}(t) = \int_{-\infty}^t e^{B(t-s)} h(\bar{y}(s), \bar{z}(s)) ds,$$

are valid. Using these equations, it can be verified that

$$\begin{aligned} \|z(t) - \bar{z}(t)\| &\leq \int_{t_0 + \frac{R}{2}}^t \tilde{N} e^{-\tilde{\omega}(t-s)} \|h(y(s), z(s)) - h(y(s), \bar{z}(s))\| ds \\ &+ \int_{t_0 + \frac{R}{2}}^t \tilde{N} e^{-\tilde{\omega}(t-s)} \|h(y(s), \bar{z}(s)) - h(\bar{y}(s), \bar{z}(s))\| ds \\ &+ \int_{-\infty}^{t_0 + \frac{R}{2}} \tilde{N} e^{-\tilde{\omega}(t-s)} \|h(y(s), z(s)) - h(\bar{y}(s), \bar{z}(s))\| ds. \end{aligned}$$

Since $\|y(t) - \bar{y}(t)\| < \varepsilon_1$ for $t \in [t_0 + R/2, t_0]$, one has

$$\begin{aligned} \|z(t) - \bar{z}(t)\| &\leq \tilde{N}\tilde{L}_3 \int_{t_0 + \frac{R}{2}}^t e^{-\tilde{\omega}(t-s)} \|z(s) - \bar{z}(s)\| ds \\ &+ \tilde{N}\tilde{L}_2 \varepsilon_1 \int_{t_0 + \frac{R}{2}}^t e^{-\tilde{\omega}(t-s)} ds + 2\tilde{M}_0\tilde{N} \int_{-\infty}^{t_0 + \frac{R}{2}} e^{-\tilde{\omega}(t-s)} ds \\ &\leq \tilde{N}\tilde{L}_3 \int_{t_0 + \frac{R}{2}}^t e^{-\tilde{\omega}(t-s)} \|z(s) - \bar{z}(s)\| ds \\ &+ \frac{\tilde{N}\tilde{L}_2 \varepsilon_1}{\tilde{\omega}} e^{-\tilde{\omega}t} (e^{\tilde{\omega}t} - e^{\tilde{\omega}(t_0 + R/2)}) + \frac{2\tilde{M}_0\tilde{N}}{\tilde{\omega}} e^{-\tilde{\omega}(t-t_0-R/2)}. \end{aligned}$$

Now, let us introduce the functions $u(t) = e^{\tilde{\omega}t} \|z(t) - \bar{z}(t)\|$, $k(t) = \frac{\tilde{N}\tilde{L}_2 \varepsilon_1}{\tilde{\omega}} e^{\tilde{\omega}t}$, and $v(t) = c + k(t)$ where $c = \left(\frac{2\tilde{M}_0\tilde{N}}{\tilde{\omega}} - \frac{\tilde{N}\tilde{L}_2 \varepsilon_1}{\tilde{\omega}} \right) e^{\tilde{\omega}(t_0 + R/2)}$.

These definitions imply that $u(t) \leq v(t) + \int_{t_0 + \frac{R}{2}}^t \tilde{N}\tilde{L}_3 u(s) ds$ and applying Lemma 2.2 [34] leads to

$$u(t) \leq v(t) + \tilde{N}\tilde{L}_3 \int_{t_0 + \frac{R}{2}}^t e^{\tilde{N}\tilde{L}_3(t-s)} h(s) ds.$$

Therefore, for $t \in [t_0 + R/2, t_0]$ we have

$$\begin{aligned} u(t) &\leq c + k(t) + c \left(e^{\tilde{N}\tilde{L}_3(t-t_0-R/2)} - 1 \right) + \frac{N^2 \tilde{L}_2 \tilde{L}_3 \varepsilon_1}{\tilde{\omega}} e^{\tilde{N}\tilde{L}_3 t} \int_{t_0 + \frac{R}{2}}^t e^{(\tilde{\omega} - \tilde{N}\tilde{L}_3)s} ds \\ &= \frac{\tilde{N}\tilde{L}_2 \varepsilon_1}{\tilde{\omega}} e^{\tilde{\omega}t} + \left(\frac{2\tilde{M}_0\tilde{N}}{\tilde{\omega}} - \frac{\tilde{N}\tilde{L}_2 \varepsilon_1}{\tilde{\omega}} \right) e^{\tilde{\omega}t} e^{\tilde{N}\tilde{L}_3(t-t_0-R/2)} \\ &+ \frac{\tilde{N}^2 \tilde{L}_2 \tilde{L}_3 \varepsilon_1}{\tilde{\omega}(\tilde{\omega} - \tilde{N}\tilde{L}_3)} e^{\tilde{\omega}t} \left[1 - e^{(\tilde{N}\tilde{L}_3 - \tilde{\omega})(t-t_0-R/2)} \right], \end{aligned}$$

and hence

$$\|z(t) - \bar{z}(t)\| \leq \frac{\tilde{N}\tilde{L}_2 \varepsilon_1}{\tilde{\omega} - \tilde{N}\tilde{L}_3} \left[1 - e^{(\tilde{N}\tilde{L}_3 - \tilde{\omega})(t-t_0-R/2)} \right] + \frac{2\tilde{M}_0\tilde{N}}{\tilde{\omega}} e^{(\tilde{N}\tilde{L}_3 - \tilde{\omega})(t-t_0-R/2)}.$$

Consequently, the inequality

$$\begin{aligned} \|z(t_0) - \bar{z}(t_0)\| &\leq \frac{\tilde{N}\tilde{L}_2 \varepsilon_1}{\tilde{\omega} - \tilde{N}\tilde{L}_3} + \frac{2\tilde{M}_0\tilde{N}}{\tilde{\omega}} e^{(\tilde{\omega} - \tilde{N}\tilde{L}_3)R/2} \\ &< \left(1 + \frac{\tilde{N}\tilde{L}_2}{\tilde{\omega} - \tilde{N}\tilde{L}_3} \right) \varepsilon_1 \\ &< \delta \end{aligned}$$

is valid.

The theorem is proved. \square

2.8 Replication of Period-Doubling Cascade

We start this section by describing the chaos through period-doubling cascade [21, 92, 187] for the set of functions \mathcal{A}_x , and deal with its replication by the set of functions \mathcal{A}_y , which is defined by equation (2.9).

Suppose that there exists a function $G : \mathbb{R} \times \mathbb{R}^m \times \mathbb{R} \rightarrow \mathbb{R}^m$ which is continuous in all of its arguments such that $F(t, x) = G(t, x, \mu_\infty)$ for some finite number μ_∞ , which will be explained below.

To discuss chaos through period-doubling cascade, let us consider the system

$$x' = G(t, x, \mu), \quad (2.29)$$

where μ is a parameter.

We say that the set \mathcal{A}_x is chaotic through period-doubling cascade if there exist a natural number k and a sequence of period-doubling bifurcation values $\{\mu_m\}$, $\mu_m \rightarrow \mu_\infty$ as $m \rightarrow \infty$, such that for each $m \in \mathbb{N}$ as the parameter μ increases (or decreases) through μ_m , system (2.29) undergoes a period-doubling bifurcation and a periodic solution with period $k2^m T$ appears. As a consequence, at $\mu = \mu_\infty$, there exist infinitely many unstable periodic solutions of system (2.29), and hence of system (2.1), all lying in a bounded region. In this case, the set \mathcal{A}_x admits periodic functions of periods $kT, 2kT, 4kT, 8kT, \dots$.

Now, making use of the equation (2.8), one can show that for any natural number p , if $x(t) \in \mathcal{A}_x$ is a pT -periodic function then $\phi_{x(t)}(t) \in \mathcal{A}_y$ is also pT -periodic. Moreover, condition (A4) implies that the converse is also true. Consequently, if the set \mathcal{A}_x admits periodic functions of periods $kT, 2kT, 4kT, 8kT, \dots$, then the same is valid for \mathcal{A}_y , with no additional periodic functions of any other period. Furthermore, the technique indicated in the proof of Lemma 2.5.2 can be used to show that these periodic solutions are all unstable and this provides us an opportunity to state the following theorem.

Theorem 2.8.1 *If the set \mathcal{A}_x is chaotic through period-doubling cascade, then the same is true for \mathcal{A}_y .*

The following corollary of Theorem 2.8.1 states that the result-system (2.1) + (2.2) is chaotic through the period-doubling cascade, provided the system (2.1) is.

Corollary 2.8.1 *If the set \mathcal{A}_x is chaotic through period-doubling cascade, then the same is true for \mathcal{A} .*

Our theoretical results show that the replicator system (2.2), likewise the generator counterpart, undergoes period-doubling bifurcations as the parameter μ increases or decreases

through the values $\mu_m, m \in \mathbb{N}$. That is, the sequence $\{\mu_m\}$ of bifurcation parameters is exactly the same for both generator and replicator systems. In this case, if the generator system obeys the Feigenbaum universality [74, 198, 218, 243] then one can conclude that the same is true also for the replicator. In other words, when $\lim_{m \rightarrow \infty} \frac{\mu_m - \mu_{m+1}}{\mu_{m+1} - \mu_{m+2}}$ is evaluated, the universal constant known as the Feigenbaum number 4.6692016... is achieved and this universal number is the same for both generator and replicator.

It is worth saying that the results about replication of period-doubling cascade as well as the Feigenbaum's universal behavior, which can be perceived as another aspect of morphogenesis of chaos, are true also for chaos extension mechanisms shown in Figure 2.4 and Figure 2.5. In our next example, using the chain mechanism, we will illustrate through simulations the morphogenesis of period-doubling cascade.

In paper [189], it is indicated that the Duffing's equation

$$x'' + 0.3x' + x^3 = \mu \cos t \quad (2.30)$$

admits the chaos through period-doubling cascade at the parameter value $\mu = \mu_\infty \equiv 40$. Defining the new variables $x_1 = x$ and $x_2 = x'$, equation (2.30) can be rewritten as a system in the following form

$$\begin{aligned} x_1' &= x_2 \\ x_2' &= -0.3x_2 - x_1^3 + \mu \cos t. \end{aligned} \quad (2.31)$$

Making use of system (2.31) as the generator, let us constitute the 8-dimensional result-system

$$\begin{aligned} x_1' &= x_2 \\ x_2' &= -0.3x_2 - x_1^3 + \mu \cos t \\ x_3' &= 2x_3 - x_4 + 0.4 \tan((x_1 + x_3)/10) \\ x_4' &= 17x_3 - 6x_4 + x_2 \\ x_5' &= -2x_5 + 0.5 \sin x_6 - 4x_4 \\ x_6' &= -x_5 - 4x_6 - \tan(x_3/2) \\ x_7' &= 2x_7 + 5x_8 - 0.0003(x_7 - x_8)^3 - 1.5x_6 \\ x_8' &= -5x_7 - 8x_8 + 4x_5. \end{aligned} \quad (2.32)$$

System (2.32) is designed according to the chain mechanism indicated in Figure 2.4. In the coupling between the subsystems with coordinates (x_1, x_2) and (x_3, x_4) the former is the generator and the latter is the replicator. In the second coupling between the subsystems with coordinates (x_3, x_4) and (x_5, x_6) , this time the former is used as the generator although it was the replicator in the previous coupling. The final coupling between the subsystems with coordinates (x_5, x_6) and (x_7, x_8) is constructed in a similar way. In this exemplification we will refer to subsystems with coordinates (x_1, x_2) , (x_3, x_4) , (x_5, x_6) and (x_7, x_8) as the first, second, third and the fourth subsystems, respectively.

According to our theoretical discussions, the result-system (2.32) with the parameter value $\mu = \mu_\infty \equiv 40$ admits a chaotic attractor in the 8-dimensional phase space, which is obtained

through period-doubling cascade. For the parameter value μ between 30 and 40, the bifurcation diagrams corresponding to the x_2 , x_4 , x_6 and x_8 coordinates of system (2.32) are illustrated in Figure 2.7. The picture shown in Figure 2.7, (a) is the bifurcation diagram of the system (2.31), while the pictures presented in Figure 2.7, (b), (c) and (d) correspond to the second, third and the fourth subsystems, respectively. For the parameter values where stable periodic solutions exist, the one-to-one correspondence between the periodic solutions of the subsystems is observable in the figure. Moreover, it is seen in Figure 2.7, (b), (c) and (d) that, likewise the first subsystem, all other subsystems undergo period-doubling bifurcations at the same parameter values such that for $\mu = \mu_\infty$ all of them are chaotic. One should recognize that the similarities between the presented bifurcation diagrams indicate morphogenesis of period-doubling cascade.

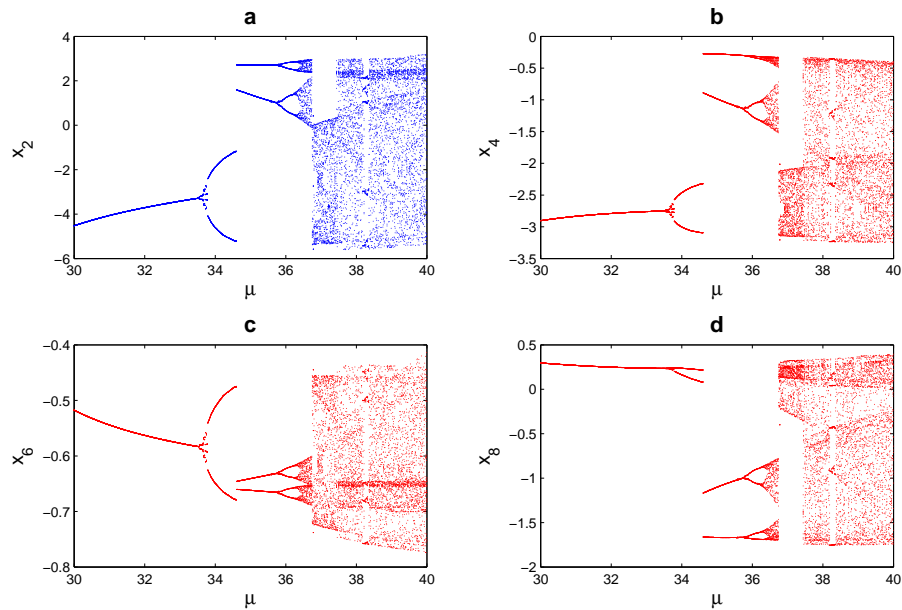


Figure 2.7: The bifurcation diagrams of system (2.32) according to coordinates. The pictures in (a), (b), (c) and (d) represent the bifurcation diagrams corresponding to the x_2 , x_4 , x_6 and x_8 coordinates, respectively. It is observable that all replicators, likewise the generator, undergo period-doubling bifurcations at the same values of the parameter and all of them are chaotic for $\mu = \mu_\infty \equiv 40$.

In Figure 2.8, (a)-(d), we depict the 2-dimensional projections of the trajectory of system (2.32), with the initial data $x_1(0) = 2.16$, $x_2(0) = -9.28$, $x_3(0) = -0.21$, $x_4(0) = -2.03$, $x_5(0) = 3.36$, $x_6(0) = -0.52$, $x_7(0) = 3.07$, $x_8(0) = -0.32$, on the planes $x_1 - x_2$, $x_3 - x_4$, $x_5 - x_6$, and $x_7 - x_8$, respectively. The picture in Figure 2.8, (a), shows in fact the attractor of the prior chaos produced by the generator system (2.31) and similarly the illustrations in Figure 2.8, (b) – (d) correspond to the chaotic attractors of the second, third and the fourth subsystems, respectively. The resemblance between the shapes of the attractors of the subsystems reflect the morphogenesis of chaos in the result-system (2.32).

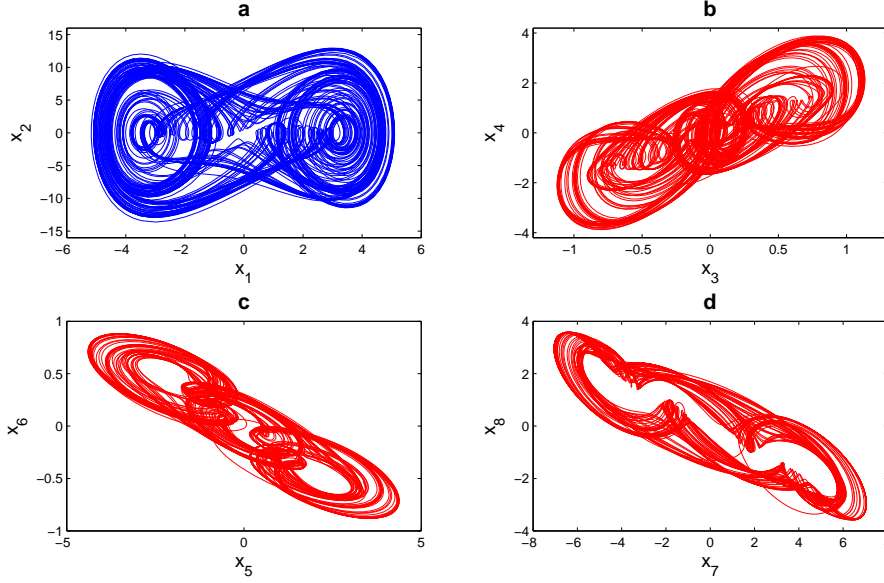


Figure 2.8: 2–dimensional projections of the chaotic attractor of the result-system (2.32). The pictures in (a), (b), (c) and (d) represent the projections on the $x_1 - x_2$, $x_3 - x_4$, $x_5 - x_6$ and $x_7 - x_8$ planes, respectively. The picture in (a) shows the attractor of the prior chaos produced by the generator system (2.31), and in (b)-(d), the chaotic attractors of the remaining subsystems are observable. The illustrations in (b)-(d) repeat the structure of the attractor shown in (a), and these pictures are indicators of the chaos extension.

To obtain a better impression about the chaotic attractor of system (2.32), in Figure 2.9 we demonstrate the 3–dimensional projections of the trajectory with the same initial data as above, on the $x_3 - x_5 - x_7$ and $x_4 - x_6 - x_8$ spaces. Although we are restricted to make illustrations at most in 3–dimensional spaces and not able to provide a picture of the whole chaotic attractor, the results shown both in Figure 2.8 and Figure 2.9 give us an idea about the spectacular chaotic attractor of system (2.32).

We note that system (2.32) exhibits a symmetry under the transformation

$$\mathcal{H} : (x_1, x_2, x_3, x_4, x_5, x_6, x_7, x_8, t) \rightarrow (-x_1, -x_2, -x_3, -x_4, -x_5, -x_6, -x_7, -x_8, t + \pi)$$

and the presented attractors are symmetric around the origin due to the symmetry of the result-system (2.32) under this transformation.

Now, let us show that the first replicator system which is included inside (2.32) satisfies the condition (A7).

In the calculations below, we will denote by $\|\cdot\|$ the matrix norm which is induced by the usual Euclidean norm in \mathbb{R}^l . That is,

$$\|\Gamma\| = \max \{ \sqrt{\zeta} : \zeta \text{ is an eigenvalue of } \Gamma^T \Gamma \} \quad (2.33)$$

for any $l \times l$ matrix Γ with real entries, and Γ^T denotes the transpose of the matrix Γ [98].

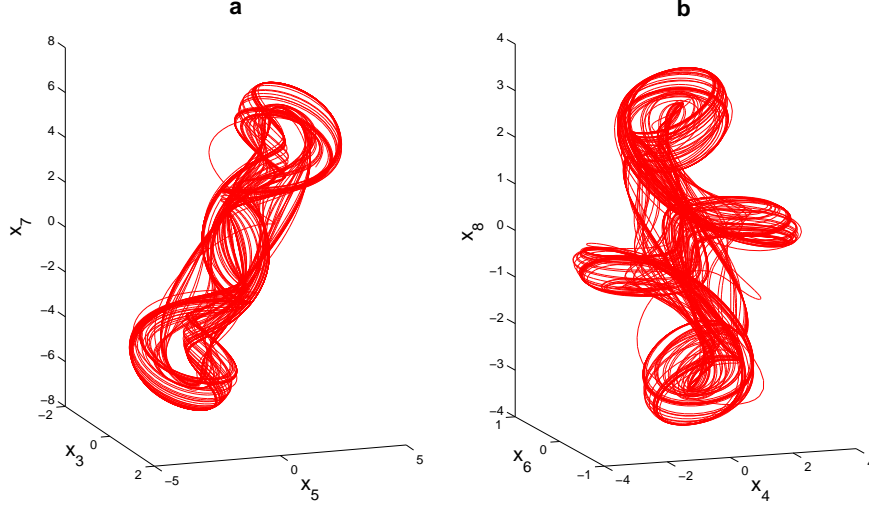


Figure 2.9: 3–dimensional projections of the chaotic attractor of the result-system (2.32). (a) Projection on the $x_3 - x_5 - x_7$ space, (b) Projection on the $x_4 - x_6 - x_8$ space. The illustrations presented in (a) and (b) give information about the impressive chaotic attractor in the 8–dimensional space.

When the system

$$\begin{aligned} x_3' &= 2x_3 - x_4 + 0.4 \tan((x_1 + x_3)/10) \\ x_4' &= 17x_3 - 6x_4 + x_2 \end{aligned} \quad (2.34)$$

is considered in the form of system (2.2), one can see that the matrix A can be written as $A = \begin{pmatrix} 2 & -1 \\ 17 & -6 \end{pmatrix}$, which admits the complex conjugate eigenvalues $-2 \mp i$.

The real Jordan form of the matrix A is given by $J = \begin{pmatrix} -2 & -1 \\ 1 & -2 \end{pmatrix}$ and the identity $P^{-1}AP = J$ is satisfied where $P = \begin{pmatrix} 0 & 1 \\ -1 & 4 \end{pmatrix}$. Evaluating the exponential matrix e^{At} we obtain that

$$e^{At} = e^{-2t} P \begin{pmatrix} \cos t & -\sin t \\ \sin t & \cos t \end{pmatrix} P^{-1}. \quad (2.35)$$

Taking $N = \|P\| \|P^{-1}\| < 18$ and $\omega = 2$, one can see that the inequality $\|e^{At}\| \leq Ne^{-\omega t}$ holds for all $t \geq 0$. The function $g : \mathbb{R}^2 \times \mathbb{R}^2 \rightarrow \mathbb{R}^2$ defined as

$$g(x_1, x_2, x_3, x_4) = \left(0.4 \tan \left(\frac{x_1 + x_3}{10} \right), x_2 \right)$$

satisfies the conditions (A4) and (A5) with constants $L_1 = \sqrt{2}/50$, $L_2 = \sqrt{2}$ and $L_3 = 0.08$ since the chaotic attractor of system (2.32) satisfies the inequalities $|x_1| \leq 6$, $|x_3| \leq 3/2$, and consequently $|\frac{x_1 + x_3}{10}| \leq 3/4$. Therefore, the condition (A7) is satisfied.

In a similar way, for the second replicator system, making use of $|x_3| \leq 3/2$ once again, one can show that the function $h : \mathbb{R}^2 \times \mathbb{R}^2 \rightarrow \mathbb{R}^2$ defined as

$$h(x_3, x_4, x_5, x_6) = \left(0.5 \sin x_6 - 4x_4, -\tan\left(\frac{x_3}{2}\right) \right)$$

satisfies the counterparts of the conditions (A4) and (A5) with constants $L_1 = \sqrt{2}/4$, $L_2 = 4\sqrt{2}$ and $L_3 = 1/2$.

Now, we shall focus on the third replicator system

$$\begin{aligned} x_7' &= 2x_7 + 5x_8 - 0.00004(x_7 - x_8)^3 - \frac{3}{2}x_6 \\ x_8' &= -5x_7 - 8x_8 + 4x_5. \end{aligned} \quad (2.36)$$

The matrix of coefficients of the system (2.36) with the assumed coefficients is

$$A = \begin{pmatrix} 2 & 5 \\ -5 & -8 \end{pmatrix}.$$

It can be easily seen that -3 is an eigenvalue of the matrix A with multiplicity 2. The real Jordan form of the matrix A is $J = \begin{pmatrix} -3 & 1 \\ 0 & -3 \end{pmatrix}$ and the identity $J = P^{-1}AP$ is satisfied

where $P = \begin{pmatrix} 1 & 0 \\ -1 & 1/5 \end{pmatrix}$. Evaluating the exponential matrix e^{At} we have

$$e^{At} = e^{-3t} P \begin{pmatrix} 1 & t \\ 0 & 1 \end{pmatrix} P^{-1}. \quad (2.37)$$

If we denote by I the 2×2 identity matrix, then using equation (2.37), one can conclude for $t \geq 0$ that

$$\begin{aligned} \|e^{At}\| &\leq e^{-3t} \|P\| \|P^{-1}\| \left\| I + \begin{pmatrix} 0 & t \\ 0 & 0 \end{pmatrix} \right\| \\ &\leq e^{-3t} \|P\| \|P^{-1}\| (1+t) \\ &= e^{-2t} \|P\| \|P^{-1}\| \frac{1+t}{e^t} \\ &\leq e^{-2t} \|P\| \|P^{-1}\| \end{aligned}$$

since $1+t \leq e^t$ for all $t \geq 0$.

Thus, taking $N = \|P\| \|P^{-1}\| < 10.2$ and $\omega = 2$, one can see that the inequality $\|e^{At}\| \leq Ne^{-\omega t}$ holds for all $t \geq 0$. Furthermore, the function $k : \mathbb{R}^2 \times \mathbb{R}^2 \rightarrow \mathbb{R}^2$ defined by the formula

$$k(x_5, x_6, x_7, x_8) = \left(0.0003(x_7 - x_8)^3 - \frac{3}{2}x_6, 4x_5 \right)$$

satisfies the conditions (A4) and (A5) with constants $L_1 = 3\sqrt{2}/4$, $L_2 = 4\sqrt{2}$ and $L_3 = 0.19$, since the chaotic attractor of system (2.36) satisfies the inequalities $|x_7| \leq 8$, $|x_8| \leq 4$. Therefore, $NL_3 - \omega < 0$ and condition (A7) is satisfied.

Remark 2.8.1 *We have proved that the replicator system (2.2) exhibits chaos in the sense of Devaney, Li-Yorke and the one obtained through period-doubling cascade, provided that the generator system (2.1) or (2.7) exhibits the same types of chaos. Since Lemma 2.2.1 implies the presence of the criterion (1.9) for the unidirectionally coupled system (2.7) + (2.2), in which an autonomous generator is used, we can say that generalized synchronization takes place in the dynamics of system (2.7) + (2.2).*

The next section is devoted to the results about controlling the replicated chaos.

2.9 Controlling Replication of Chaos

In the previous sections, we have theoretically proved replication of chaos for specific types and controlling the extended chaos is another interesting problem. The next theorem and its corollary indicate a method to control the chaos of the replicator system (2.2) and the result-system (2.1) + (2.2), respectively, and reveal that controlling the chaos of system (2.1) is sufficient for this.

Theorem 2.9.1 *Assume that for arbitrary $\varepsilon > 0$, a periodic solution $x_p(t) \in \mathcal{A}_x$ is stabilized such that for any solution $x(t)$ of system (2.1) there exist real numbers a and $E > 0$ such that the inequality $\|x(t) - x_p(t)\| < \varepsilon$ holds for $t \in [a, a + E]$.*

Then, the periodic solution $\phi_{x_p(t)}(t) \in \mathcal{A}_y$ is stabilized such that for any solution $y(t)$ of system (2.2) there exists a number $b \geq a$ such that the inequality $\|y(t) - \phi_{x_p(t)}(t)\| < \left(1 + \frac{NL_2}{\omega - NL_3}\right) \varepsilon$ holds for $t \in [b, a + E]$, provided that the number E is sufficiently large.

Proof. Fix an arbitrary solution $y(t)$ of system $y' = Ay + g(x(t), y)$ for some solution $x(t)$ of system (2.1). According to our assumption, there exist numbers a and $E > 0$ such that the inequality $\|x(t) - x_p(t)\| < \varepsilon$ holds for $t \in [a, a + E]$. Let us denote $y_p(t) = \phi_{x_p(t)}(t) \in \mathcal{A}_y$. It is clear that the function $y_p(t)$ is periodic with the same period as $x_p(t)$. Since $y(t)$ and $y_p(t)$ satisfy the integral equations

$$y(t) = e^{A(t-a)}y(a) + \int_a^t e^{A(t-s)}g(x(s), y(s))ds,$$

and

$$y_p(t) = e^{A(t-a)}y_p(a) + \int_a^t e^{A(t-s)}g(x_p(s), y_p(s))ds,$$

respectively, one has

$$\begin{aligned} y(t) - y_p(t) &= e^{A(t-a)}(y(a) - y_p(a)) \\ &+ \int_a^t e^{A(t-s)} [g(x(s), y(s)) - g(x(s), y_p(s))] ds \\ &+ \int_a^t e^{A(t-s)} [g(x(s), y_p(s)) - g(x_p(s), y_p(s))] ds. \end{aligned}$$

By the help of the last equation, we have

$$\begin{aligned} \|y(t) - y_p(t)\| &\leq N e^{-\omega(t-a)} \|y(a) - y_p(a)\| + \frac{NL_2 \varepsilon}{\omega} e^{-\omega t} (e^{\omega t} - e^{\omega a}) \\ &+ NL_3 \int_a^t e^{-\omega(t-s)} \|y(s) - y_p(s)\| ds. \end{aligned}$$

Let $u : [a, a + E] \rightarrow [0, \infty)$ be a function defined as $u(t) = e^{\omega t} \|y(t) - y_p(t)\|$. In this case, we reach the inequality

$$u(t) \leq N e^{\omega a} \|y(a) - y_p(a)\| + \frac{NL_2 \varepsilon}{\omega} (e^{\omega t} - e^{\omega a}) + NL_3 \int_a^t u(s) ds.$$

Implementation of Lemma 2.2 [34] to the last inequality, where $t \in [a, a + E]$, provides us

$$\begin{aligned} u(t) &\leq \frac{NL_2 \varepsilon}{\omega} e^{\omega t} + N \|y(a) - y_p(a)\| e^{\omega a} e^{NL_3(t-a)} \\ &- \frac{NL_2 \varepsilon}{\omega} e^{\omega a} e^{NL_3(t-a)} + \frac{N^2 L_2 L_3 \varepsilon}{\omega(\omega - NL_3)} e^{\omega t} \left(1 - e^{(NL_3 - \omega)(t-a)}\right), \end{aligned}$$

and consequently,

$$\begin{aligned} \|y(t) - y_p(t)\| &\leq \frac{NL_2 \varepsilon}{\omega} + N \|y(a) - y_p(a)\| e^{(NL_3 - \omega)(t-a)} \\ &- \frac{NL_2 \varepsilon}{\omega} e^{(NL_3 - \omega)(t-a)} + \frac{N^2 L_2 L_3 \varepsilon}{\omega(\omega - NL_3)} \left(1 - e^{(NL_3 - \omega)(t-a)}\right) \\ &< N \|y(a) - y_p(a)\| e^{(NL_3 - \omega)(t-a)} + \frac{NL_2 \varepsilon}{\omega - NL_3}. \end{aligned}$$

If $y(a) = y_p(a)$, then clearly $\|y_p(t) - y(t)\| < \left(1 + \frac{NL_2}{\omega - NL_3}\right) \varepsilon$, $t \in [a, a + E]$. Suppose that $y(a) \neq y_p(a)$. For $t \geq a + \frac{1}{NL_3 - \omega} \ln \left(\frac{\varepsilon}{N \|y(a) - y_p(a)\|}\right)$, the inequality $e^{(NL_3 - \omega)(t-a)} \leq \frac{\varepsilon}{N \|y(a) - y_p(a)\|}$ is satisfied. Assume that the number E is sufficiently large so that $E > \frac{1}{NL_3 - \omega} \ln \left(\frac{\varepsilon}{N \|y(a) - y_p(a)\|}\right)$. Thus, taking

$$b = \max \left\{ a, a + \frac{1}{NL_3 - \omega} \ln \left(\frac{\varepsilon}{N \|y(a) - y_p(a)\|}\right) \right\}$$

and

$$\tilde{E} = \min \left\{ E, E - \frac{1}{NL_3 - \omega} \ln \left(\frac{\varepsilon}{N \|y(a) - y_p(a)\|}\right) \right\}$$

one attains $\|y(t) - y_p(t)\| < \left(\frac{\omega - NL_3 + NL_2}{\omega - NL_3}\right) \varepsilon$, for $t \in [b, b + \tilde{E}]$. Here the number \tilde{E} stands for the duration of control for system (2.2). We note that $b \geq a$, $0 < \tilde{E} \leq E$ and $b + \tilde{E} = a + E$.

Hence $\|y(t) - y_p(t)\| < \left(1 + \frac{NL_2}{\omega - NL_3}\right) \varepsilon$, for $t \in [b, a + E]$.

The proof of the theorem is finalized. \square

An immediate corollary of Theorem 2.9.1 is the following.

Corollary 2.9.1 *Assume that the conditions of Theorem 2.9.1 hold. In this case, the periodic solution $z_p(t) = (x_p(t), \phi_{x_p(t)}(t)) \in \mathcal{A}$ is stabilized such that for any solution $z(t)$ of system (2.1) + (2.2) there exists a number $b \geq a$ such that the inequality $\|z_p(t) - z(t)\| < \left(2 + \frac{NL_2}{\omega - NL_3}\right) \varepsilon$ holds for $t \in [b, a + E]$, provided that the number E is sufficiently large.*

Proof. Making use of the inequality

$$\|z(t) - z_p(t)\| \leq \|x(t) - x_p(t)\| + \|y(t) - \phi_{x_p(t)}(t)\|,$$

and the conclusion of Theorem 2.9.1, one can show that the inequality

$$\|z_p(t) - z(t)\| < \left(2 + \frac{NL_2}{\omega - NL_3}\right) \varepsilon$$

holds for $t \in [b, a + E]$ and for some $b \geq a$. The proof is completed. \square

Remark 2.9.1 *As a conclusion of Theorem 2.9.1, the transient time for control to take effect may increase and the duration of control may decrease as the number of consecutive replicator systems increase.*

In the remaining part of this section, our aim is to present an illustration which confirms the results of Theorem 2.9.1, and for our purposes, we will make use of the Pyragas control method [177]. Therefore, primarily, we continue with a brief explanation of this method.

A delayed feedback control method for the stabilization of unstable periodic orbits of a chaotic system was proposed by Pyragas [177]. In this method, one considers a system of the form

$$x' = H(x, q), \tag{2.38}$$

where $q = q(t)$ is an externally controllable parameter and for $q = 0$ it is assumed that the system (2.38) is in the chaotic state of interest, whose periodic orbits are to be stabilized [76, 82, 177, 243]. According to Pyragas method, an unstable ξ -periodic solution of the system (2.38) with $q = 0$, can be stabilized by the control law $q(t) = C[s(t - \xi) - s(t)]$, where the parameter C represents the strength of the perturbation and $s(t) = \sigma[x(t)]$ is a scalar signal given by some function of the state of the system.

It is indicated in [82] that in order to apply the Pyragas control method to the chaotic Duffing oscillator given by the system

$$\begin{aligned} x_1' &= x_2 \\ x_2' &= -0.10x_2 + 0.5x_1(1 - x_1^2) + 0.24 \sin t, \end{aligned} \tag{2.39}$$

one can construct the corresponding control system

$$\begin{aligned} v_1' &= v_2 \\ v_2' &= -0.10v_2 + 0.5v_1(1 - v_1^2) + 0.24\sin(v_3) + C[v_2(t - 2\pi) - v_2(t)] \\ v_3' &= 1, \end{aligned} \quad (2.40)$$

where $q(t) = C[v_2(t - 2\pi) - v_2(t)]$ is the control law and an unstable 2π -periodic solution can be stabilized by choosing an appropriate value for the parameter C .

Now, let us combine system (2.39) with two consecutive replicator systems and set up the following 6-dimensional result-system

$$\begin{aligned} x_1' &= x_2 \\ x_2' &= -0.10x_2 + 0.5x_1(1 - x_1^2) + 0.24\sin t \\ x_3' &= x_4 - 0.1x_1 \\ x_4' &= -3x_3 - 2x_4 - 0.008x_3^3 + 1.6x_2 \\ x_5' &= x_6 + 0.6x_3 \\ x_6' &= -3.1x_5 - 2.1x_6 - 0.007x_5^3 + 2.5x_4. \end{aligned} \quad (2.41)$$

In system (2.41) the subsystems with coordinates (x_3, x_4) and (x_5, x_6) correspond to the first and the second replicator systems, respectively. Since our procedure of morphogenesis is valid for specific types of chaos such as in Devaney's and Li-Yorke sense and through period-doubling cascade, we expect that our procedure is also applicable to any other chaotic system with an unspecified type of chaos. Accordingly, system (2.41) is chaotic since the generator system (2.39) is chaotic.

Theorem 2.9.1 specifies that in order to control the chaos of system (2.41) one should control the chaos of the generator system, which is the subsystem of (2.41) with coordinates (x_1, x_2) . In accordance with this purpose, we will use the Pyragas control method by means of the system

$$\begin{aligned} v_1' &= v_2 \\ v_2' &= -0.10v_2 + 0.5v_1(1 - v_1^2) + 0.24\sin(v_3) + C[v_2(t - 2\pi) - v_2(t)] \\ v_3' &= 1 \\ v_4' &= v_5 - 0.1v_1 \\ v_5' &= -3v_4 - 2v_5 - 0.008v_4^3 + 1.6v_2 \\ v_6' &= v_7 + 0.6v_4 \\ v_7' &= -3.1v_6 - 2.1v_7 - 0.007v_6^3 + 2.5v_5, \end{aligned} \quad (2.42)$$

which is the control system corresponding to (2.41).

Let us consider a solution of system (2.42) with the initial data $v_1(0) = 0.2$, $v_2(0) = 0.2$, $v_3(0) = 0$, $v_4(0) = -0.5$, $v_5(0) = 0.1$, $v_6 = -0.2$ and $v_7(0) = 0.1$. We let the system evolve freely taking $C = 0$ until $t = 60$, and at that moment we switch on the control by taking $C = 0.84$. At $t = 200$, we switch off the control and start to use the value of the parameter $C = 0$ again. In Figure 2.10 one can see the graphs of the v_2, v_5, v_7 coordinates of the solution. Supporting the result of Theorem 2.9.1, it is observable in Figure 2.10 that stabilizing

a 2π -periodic solution of the generator system provides the stabilization of the corresponding 2π -periodic solutions of the replicator systems. After switching off the control, the 2π -periodic solutions of the generator and replicators lose their stability and chaos emerges again. For the coordinates v_1, v_4 and v_6 we have similar results which are not just pictured here.

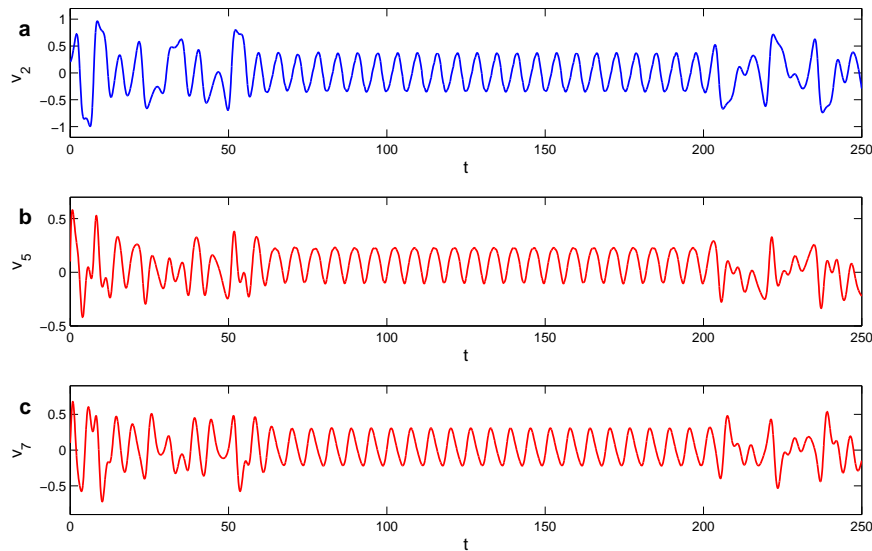


Figure 2.10: Pyragas control method applied to the result-system (2.41) with the aid of the corresponding control system (2.42). The pictures in (a), (b) and (c) show the graphs of the v_2 , v_5 and v_7 coordinates, respectively. The result of Pyragas control method applied to the generator system (2.39) is seen in (a). Through this method, the 2π -periodic solution of the generator and accordingly the 2π -periodic solutions of the first and the second replicator systems are stabilized. In other words, the chaos of the result-system (2.41) is controlled. The control starts at $t = 60$ and ends at $t = 200$, after which emergence of the chaos is observable again.

2.10 Discussion

In this part of the chapter, we intend to consider not rigorously proved, but interesting phenomena which can be considered in the framework of our results. So, we shall give some additional light on the results obtained above and say about the possibility for the replication of intermittency, Shil'nikov orbits and relay systems. We also demonstrate the possibility of quasiperiodic motions as an infinite basis of chaos.

We start our discussions with replication of intermittency.

2.10.1 Replication of intermittency

In the previous sections, we have rigorously proved replication of specific types of chaos such as period-doubling cascade, Devaney's and Li-Yorke chaos. Consequently, one can expect that the same procedure also works for the intermittency route.

Pomeau and Manneville [175] observed chaos through intermittency in the Lorenz system (2.19), with the coefficients $\sigma = 10$, $b = 8/3$ and values of r slightly larger than the critical value $r_c \approx 166.06$. To observe intermittent behavior in the Lorenz system, let us consider a solution of system (2.19) together with the coefficients $\sigma = 10$, $b = 8/3$, $r = 166.25$ using the initial data $x_1(0) = -23.3$, $x_2(0) = 38.3$ and $x_3(0) = 193.4$. The time-series for the x_1 , x_2 and x_3 coordinates of the solution are indicated in Figure 2.11, where one can see that regular oscillations are interrupted by irregular ones.

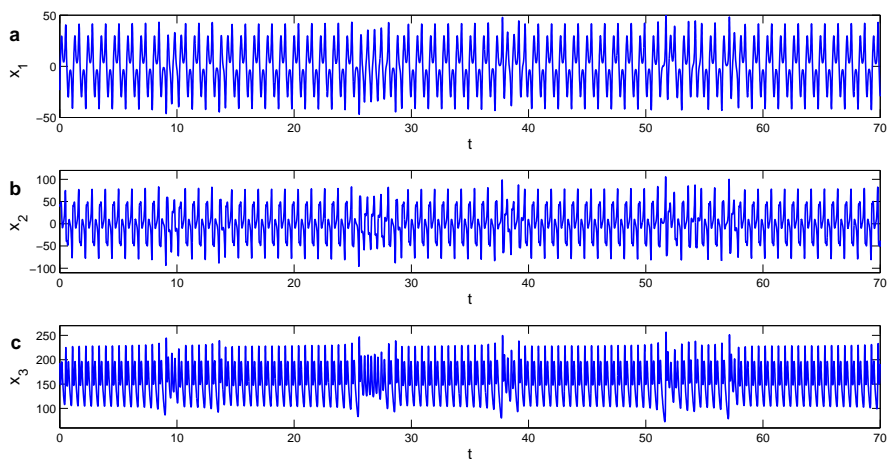


Figure 2.11: Intermittency in the Lorenz system (2.19), where $\sigma = 10$, $b = 8/3$ and $r = 166.25$. (a) The graph of the x_1 -coordinate, (b) The graph of the x_2 -coordinate, (c) The graph of the x_3 -coordinate.

To perform replication of intermittency, let us consider the Lorenz system (2.19) as a generator and set up the 6-dimensional result-system

$$\begin{aligned}
 x_1' &= \sigma(-x_1 + x_2) \\
 x_2' &= -x_2 + rx_1 - x_1x_3 \\
 x_3' &= -bx_3 + x_1x_2 \\
 x_4' &= -x_4 + 4x_1 \\
 x_5' &= x_6 + 2x_2 \\
 x_6' &= -3x_5 - 2x_6 - 0.00005x_5^3 + 0.5x_4,
 \end{aligned} \tag{2.43}$$

again with the coefficients $\sigma = 10$, $b = 8/3$ and $r = 166.25$. It can be easily verified that condition (A7) is valid for system (2.43). We consider the trajectory of system (2.43) corresponding to the initial data $x_1(0) = -23.3$, $x_2(0) = 38.3$, $x_3(0) = 193.4$, $x_4(0) = -17.7$,

$x_5(0) = 11.4$, and $x_6(0) = 2.5$, and represent the graphs for the x_4, x_5 and x_6 coordinates in Figure 2.12 such that the intermittent behavior in the replicator system is observable. The similarity between the graphs of the coordinates corresponding to the generator and the replicator counterpart reveals the replication of intermittency.

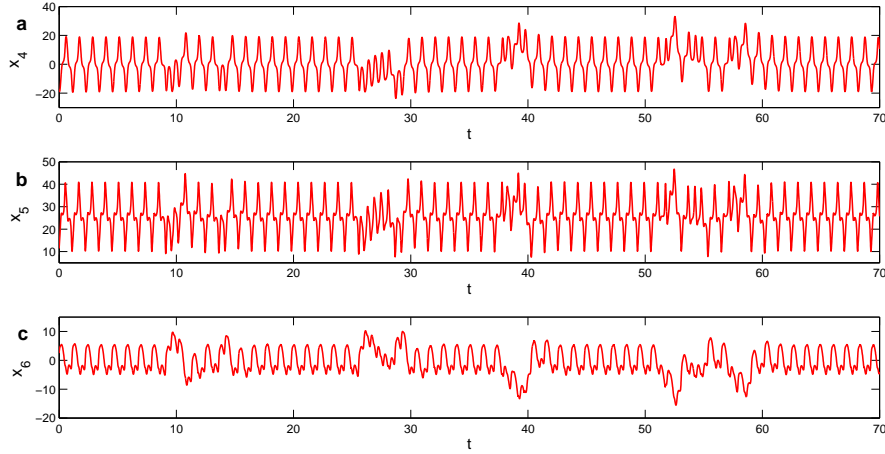


Figure 2.12: Intermittency in the replicator system. The pictures in (a), (b) and (c) show the graphs of the x_4, x_5 and x_6 coordinates, respectively. The analogy between the time-series of the generator and the replicator systems indicates the replication of intermittency.

2.10.2 Replication of Shil'nikov orbits

To illustrate that by our method it may also be possible to replicate strange attractors [71, 85, 232], let us provide simulations of homoclinic and complicated Shil'nikov orbits (Figure 2.13 and Figure 2.14 correspondingly).

As a model for Shilnikov's orbits, the paper [26] considers the system

$$\begin{aligned} x_1' &= x_2 \\ x_2' &= x_3 \\ x_3' &= -x_2 - \beta x_3 + f_\mu(x_1), \end{aligned} \tag{2.44}$$

where

$$f_\mu(x) = \begin{cases} 1 - \mu x, & \text{if } x > 0 \\ 1 + \alpha x, & \text{if } x \leq 0. \end{cases} \tag{2.45}$$

The values $\alpha = 0.633625$, $\beta = 0.3375$ and the parameter μ used in system (2.44) are taken from [92]. There exists an equilibrium point $e_0 = (-1/\alpha, 0, 0)$ of system (2.44) and the eigenvalues of the matrix of linearization at e_0 are $0.4625, -0.4 \pm 1.1i$ such that the condition of the Shil'nikov's theorem about eigenvalues [203] is satisfied. For values of the parameter

μ near 2.16 system (2.44) possesses a special type homoclinic orbit—*Shil'nikov orbit*, and its presence implies chaotic dynamics [92]. In this case, Shil'nikov's theorem asserts that every neighborhood of the homoclinic orbit contains a countably infinite number of unstable periodic orbits [26, 203].

To demonstrate numerically the replication of a Shil'nikov orbit, let us consider the following system

$$\begin{aligned}
 x_1' &= x_2 \\
 x_2' &= x_3 \\
 x_3' &= -x_2 - \beta x_3 + f_\mu(x_1) \\
 x_4' &= -2x_4 + x_1 \\
 x_5' &= -0.6x_5 + 2x_2 + 0.1x_2^3 \\
 x_6' &= -1.2x_6 + 0.001 \sin(x_6) + x_3,
 \end{aligned} \tag{2.46}$$

where, again, the function $f_\mu(x)$ is given by formula (2.45).

System (2.44) is used as a generator in system (2.45), where the last three coordinates are of a replicator. Let us consider system (2.46) with the values $\alpha = 0.633625$, $\beta = 0.3375$ and $\mu = 2.16$ once again. In Figure 2.13 we show the trajectory of this system with initial data $x_1(0) = -1.5759$, $x_2(0) = 0$, $x_3(0) = 0$, $x_4(0) = -0.78795$, $x_5(0) = 0$ and $x_6(0) = 0$. The picture in Figure 2.13, (a), where we illustrate the projection of the trajectory on the $x_1 - x_2 - x_3$ space represents, in fact, the Shil'nikov orbit corresponding to the generator system (2.44). On the other hand, the picture in Figure 2.13, (b), shows the projection of the trajectory on the $x_4 - x_5 - x_6$ space and in this picture the replication of the Shil'nikov orbit is observable.

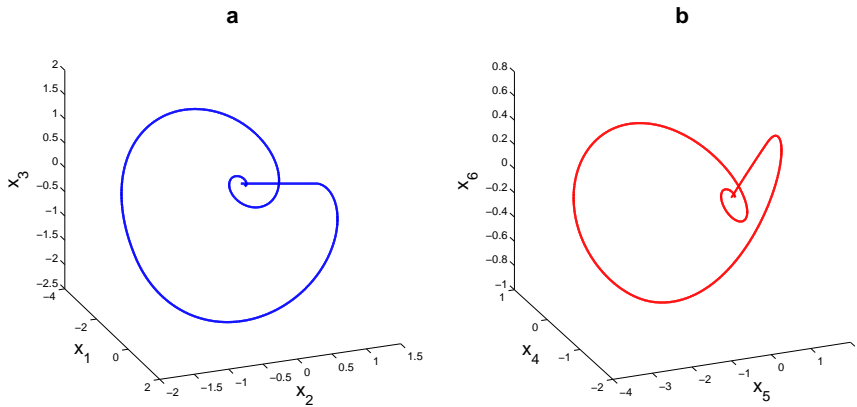


Figure 2.13: Replication of a Shil'nikov type homoclinic orbit. In picture (a), one can see the projection on the $x_1 - x_2 - x_3$ space of the trajectory of system (2.46) corresponding to the initial data $x_1(0) = -1.57590$, $x_2(0) = 0$, $x_3(0) = 0$, $x_4(0) = -0.78795$, $x_5(0) = 0$ and $x_6(0) = 0$. The picture in (b) shows the projection on the $x_4 - x_5 - x_6$ space of the same trajectory. The parameter values $\alpha = 0.633625$, $\beta = 0.3375$ and $\mu = 2.16$ are used in the simulation. The picture in (a) represents a Shil'nikov type homoclinic orbit corresponding to the generator system (2.44), while the picture in (b) shows its replication through the system (2.46).

Next, we consider system (2.46) with the values $\alpha = 0.633625$, $\beta = 0.3375$, $\mu = 0.83$ and take the trajectory of this system with the same initial data as above. In Figure 2.14, (a) and (b), we represent the projections of this trajectory on the $x_1 - x_2 - x_3$ and $x_4 - x_5 - x_6$ spaces, respectively. The picture in (a) represents the complicated behavior of the generator system (2.44) and one can see in picture (b) the replication of this behavior.

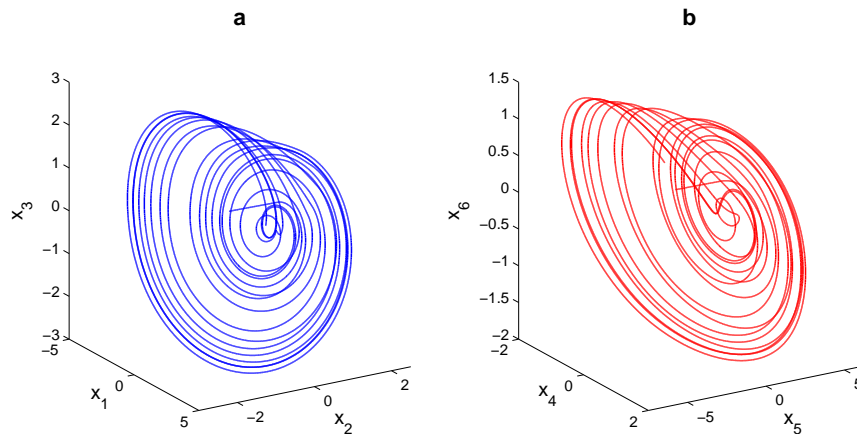


Figure 2.14: Projections of a complicated orbit of system (2.46) with the values $\alpha = 0.633625$, $\beta = 0.3375$ and $\mu = 0.83$. (a) Projection on the $x_1 - x_2 - x_3$ space, (b) Projection on the $x_4 - x_5 - x_6$ space. The initial data $x_1(0) = 1.57590$, $x_2(0) = 0$, $x_3(0) = 0$, $x_4(0) = -0.78795$, $x_5(0) = 0$, $x_6(0) = 0$ is used for the illustration. The picture in (a) represents the behavior of the trajectory corresponding to the generator (2.44), while the picture in (b) illustrates its replication.

We suppose that theoretical affirmation of our simulation results can be done if one considers interpretation of Shil'nikov's theorem [203] for the multidimensional replicator. That is, we are still questioning whether our approach can be somehow combined with methods indicating chaos through Shil'nikov type strange attractors [71, 232]. At least, it is easy to see that a homoclinic trajectory exists for a replicator as well as a denumerable set of unstable periodic solutions.

In next our discussion, we will emphasize by means of simulations the morphogenesis of the double-scroll Chua's attractor in a unidirectionally coupled open chain of Chua circuits. Approaches for the generation of hyperchaotic systems have already been discussed making use of Chua circuits which are all chaotic [24, 115]. It deserves to remark that to create hyperchaotic attractors in previous papers, others consider both involved interacting systems chaotic, but in our case only the first link of the chain is chaotic and other consecutive Chua systems are all non-chaotic.

2.10.3 Morphogenesis of the double-scroll Chua's attractor

There is a well known result of the chaoticity based on the double-scroll Chua's attractor [145]. It was proven first in the paper [52] rigorously, and the proof is based on the Shil'nikov's theorem [203]. Since the Chua circuit and its chaotic behavior is of extreme importance from the theoretical point of view and its usage area in electrical circuits by radio physicists and nonlinear scientists from other disciplines, one can suppose that morphogenesis of the chaos will also be of a practical and a theoretical interest.

In this part, we just take into account a simulation result which supports that morphogenesis idea can be developed also from this point of view.

Let us consider the dimensionless form of the Chua's oscillator given by the system

$$\begin{aligned}
 x'_1 &= k\alpha[x_2 - x_1 - f(x_1)] \\
 x'_2 &= k(x_1 - x_2 + x_3) \\
 x'_3 &= k(-\beta x_2 - \gamma x_3) \\
 f(x) &= bx + 0.5(a - b)(|x + 1| + |x - 1|),
 \end{aligned} \tag{2.47}$$

where $\alpha, \beta, \gamma, a, b$ and k are constants.

In paper [53], it is indicated that system (2.47) with the coefficients $\alpha = 21.32/5.75$, $\beta = 7.8351$, $\gamma = 1.38166392/12$, $a = -1.8459$, $b = -0.86604$ and $k = 1$ admits a stable equilibrium.

In what follows, as the generator, we make use of system (2.47) together with the coefficients $\alpha = 15.6$, $\beta = 25.58$, $\gamma = 0$, $a = -8/7$, $b = -5/7$ and $k = 1$ such that a double-scroll Chua's attractor takes place [21].

Consider the following 12-dimensional result-system

$$\begin{aligned}
 x'_1 &= 15.6[x_2 - (2/7)x_1 + (3/14)(|x_1 + 1| + |x_1 - 1|)] \\
 x'_2 &= x_1 - x_2 + x_3 \\
 x'_3 &= -25.58x_2 \\
 x'_4 &= (21.32/5.75)[x_5 - 0.13396x_4 + 0.48993(|x_4 + 1| + |x_4 - 1|)] + 2x_1 \\
 x'_5 &= x_4 - x_5 + x_6 + 5x_2 \\
 x'_6 &= -7.8351x_5 - (1.38166392/12)x_6 + 2x_3 \\
 x'_7 &= (21.32/5.75)[x_8 - 0.13396x_7 + 0.48993(|x_7 + 1| + |x_7 - 1|)] + 2x_4 \\
 x'_8 &= x_7 - x_8 + x_9 + 3x_5 \\
 x'_9 &= -7.8351x_8 - (1.38166392/12)x_9 - 0.001x_6 \\
 x'_{10} &= (21.32/5.75)[x_{11} - 0.13396x_{10} + 0.48993(|x_{10} + 1| + |x_{10} - 1|)] + 4x_7 \\
 x'_{11} &= x_{10} - x_{11} + x_{12} - 0.1x_8 \\
 x'_{12} &= -7.8351x_{11} - (1.38166392/12)x_{12} + 2x_9.
 \end{aligned} \tag{2.48}$$

System (2.48) consists of four unidirectionally coupled Chua circuits such that the subsystems with coordinates (x_1, x_2, x_3) , (x_4, x_5, x_6) , (x_7, x_8, x_9) and (x_{10}, x_{11}, x_{12}) correspond to the first, second, third and the fourth links of the open chain of circuits.

In Figure 2.15, we simulate the 3–dimensional projections on the $x_1 - x_2 - x_3$ and $x_4 - x_5 - x_6$ spaces of the trajectory of the result-system (2.48) with the initial data $x_1(0) = 0.634$, $x_2(0) = -0.093$, $x_3(0) = -0.921$, $x_4(0) = -8.013$, $x_5(0) = 0.221$, $x_6(0) = 6.239$, $x_7(0) = -50.044$, $x_8(0) = -0.984$, $x_9(0) = 48.513$, $x_{10}(0) = -256.325$, $x_{11}(0) = 7.837$, $x_{12}(0) = 264.331$. The projection on the $x_1 - x_2 - x_3$ space shows the double-scroll Chua’s attractor produced by the generator system (2.47), and projection on the $x_4 - x_5 - x_6$ space represents the chaotic attractor of the first replicator.

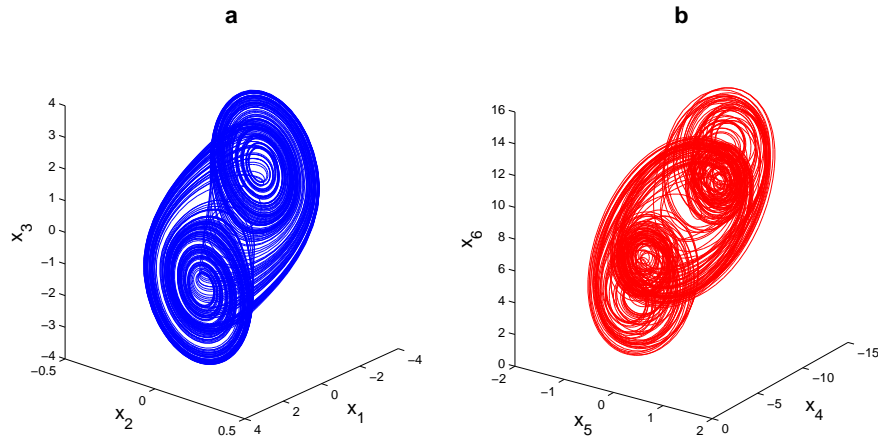


Figure 2.15: 3–dimensional projections of the chaotic attractor of the result-system (2.48). (a) Projection on the $x_1 - x_2 - x_3$ space, (b) Projection on the $x_4 - x_5 - x_6$ space. The picture in (a) shows the attractor of the original prior chaos of the generator system (2.47) and (b) represents the attractor of the first replicator. The resemblance between shapes of the attractors of the generator and the replicator systems makes the extension of chaos apparent.

In a similar way, we display the projections of the same trajectory on the $x_7 - x_8 - x_9$ and $x_{10} - x_{11} - x_{12}$ spaces, which correspond to the attractors of the second and the third replicator systems, in Figure 2.16. The illustrations shown in Figure 2.15 and Figure 2.16 indicate the extension of chaos in system (2.48). Possibly the result-system (2.48) produces a double-scroll Chua’s attractor with hyperchaos, where the number of positive Lyapunov exponents are more than one and even four.

The type of chaos for the double-scroll Chua circuit is proposed in paper [52]. It is an interesting problem to prove that this type of chaos can be replicated through the method discussed in our study. Nevertheless, we show by simulations that the regular behavior in Chua circuits placed in the extension mechanism can also be seen. This means that next special investigation has to be done. Moreover, this shows how one can use morphogenesis not only for chaos, but also for Chua circuits by uniting them in complexes in electrical (physical) sense, and observing the same properties as a unique separated Chua circuit admits. This is an interesting problem which can give a light for the complex behavior of huge electrical circuits.

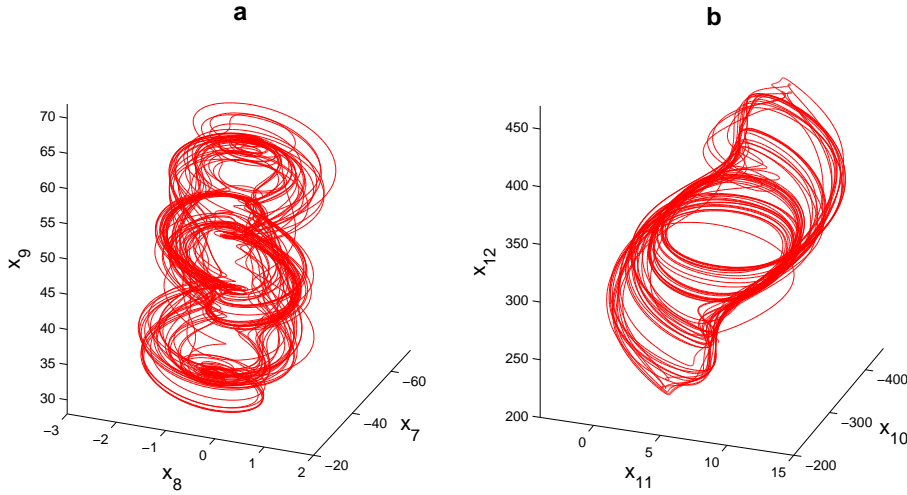


Figure 2.16: 3–dimensional projections of the chaotic attractor of the result-system (2.48). (a) Projection on the $x_7 - x_8 - x_9$ space, (b) Projection on the $x_{10} - x_{11} - x_{12}$ space. The pictures in (a) and (b) demonstrate the attractors generated by the second and the third replicator systems, respectively.

2.10.4 Quasiperiodicity through chaos replication

Now, let us indicate that if there are more than one generator system then the chaos extension mechanism will lead to some new forms such as periodicity gives birth to quasiperiodicity.

In paper [69], it is mentioned that the Duffing equation

$$x'' + 0.168x' - 0.5x(1 - x^2) = \mu \sin t, \quad (2.49)$$

where μ is a parameter, admits the chaos through period-doubling cascade at the parameter value $\mu = \mu_\infty \equiv 0.21$. That is, at the parameter value $\mu = \mu_\infty$, for each natural number k the equation (2.49) admits infinitely many periodic solutions with periods $2k\pi$. Using the change of variables $t = 2\pi s$ and $x(t) = y(s)$, and relabeling s as t , one attains the following equation

$$y'' + 0.168\pi y' - 0.5\pi^2 y(1 - y^2) = \pi^2 \mu \sin(\pi t). \quad (2.50)$$

Likewise equation (2.49), it is clear that equation (2.50), when considered with $\mu = \mu_\infty$, also admits the chaos through period-doubling cascade and has infinitely many periodic solutions with periods $2, 4, 8, \dots$

Using the new variables $x_1 = x$, $x_2 = x'$ and $x_3 = y$, $x_4 = y'$, one can convert the equations (2.49) and (2.50) to the systems

$$\begin{aligned} x_1' &= x_2 \\ x_2' &= -0.168x_2 + 0.5x_1(1 - x_1^2) + \mu \sin t \end{aligned} \quad (2.51)$$

and

$$\begin{aligned}x_3' &= x_4 \\x_4' &= -0.168\pi x_4 + 0.5\pi^2 x_3(1 - x_3^2) + \pi^2 \mu \sin(\pi t),\end{aligned}\tag{2.52}$$

respectively. Now, we shall make use both of the systems (2.51) and (2.52), with $\mu = \mu_\infty$, as generators to obtain a chaotic system with infinitely many quasiperiodic solutions. We mean that the two systems admit incommensurate periods and consequently their influence on the replicator will be quasiperiodic. In this case, one can expect that replicator will expose infinitely many quasiperiodic solutions. For that purpose, let us consider the 6–dimensional result-system

$$\begin{aligned}x_1' &= x_2 \\x_2' &= -0.168x_2 + 0.5x_1(1 - x_1^2) + 0.21 \sin t \\x_3' &= x_4 \\x_4' &= -0.168\pi x_4 + 0.5\pi^2 x_3(1 - x_3^2) + 0.21\pi^2 \sin(\pi t) \\x_5' &= x_6 + x_1 + x_3 \\x_6' &= -3x_5 - 2x_6 - 0.008x_5^3 + x_2 + x_4,\end{aligned}\tag{2.53}$$

where the last two equations are of a replicator.

To reveal existence of quasiperiodic solutions embedded in the chaotic attractor of system (2.53) we control the chaos of system (2.53) by the Pyragas method through the following control system

$$\begin{aligned}v_1' &= v_2 \\v_2' &= -0.168v_2 + 0.5v_1(1 - v_1^2) + 0.21 \sin v_3 + C_1(v_2(t - 2\pi) - v_2(t)) \\v_3' &= 1 \\v_4' &= v_5 \\v_5' &= -0.168\pi v_5 + 0.5\pi^2 v_4(1 - v_4^2) + 0.21\pi^2 \sin(\pi v_6) + C_2(v_5(t - 2) - v_5(t)) \\v_6' &= 1 \\v_7' &= v_8 + v_1 + v_4 \\v_8' &= -3v_7 - 2v_8 - 0.008v_7^3 + v_2 + v_5.\end{aligned}\tag{2.54}$$

We take into account the solution of the result-system (2.53) with the initial data $v_1(0) = 0.4$, $v_2(0) = -0.1$, $v_3(0) = 0$, $v_4(0) = -0.2$, $v_5(0) = 0.5$, $v_6(0) = 0$, $v_7(0) = 1.1$ and $v_8(0) = 2.5$. The simulation results are shown in Figure 2.17. The control mechanism starts at $t = 35$ and ends at $t = 120$. The chaos not only in the generator systems, but also in the replicator counterpart is observable before the control is switched on. During the control, we make use of the values of $C_1 = 0.62$ and $C_2 = 2.58$ to stabilize the periodic solutions corresponding to the generator systems (2.51) and (2.52) with periods 2π and 2, respectively. Up to $t = 35$ and after $t = 120$ the values $C_1 = C_2 = 0$ are used. Between $t = 35$ and $t = 120$, the quasiperiodic solution of the replicator is stabilized and after $t = 120$ chaos in the system (2.53) develops again.

Possibly the obtained simulation result and previous theoretical discussions can give a support to the idea of *quasiperiodical cascade* for the appearance of chaos which can be considered as a development of the popular period-doubling route to chaos.

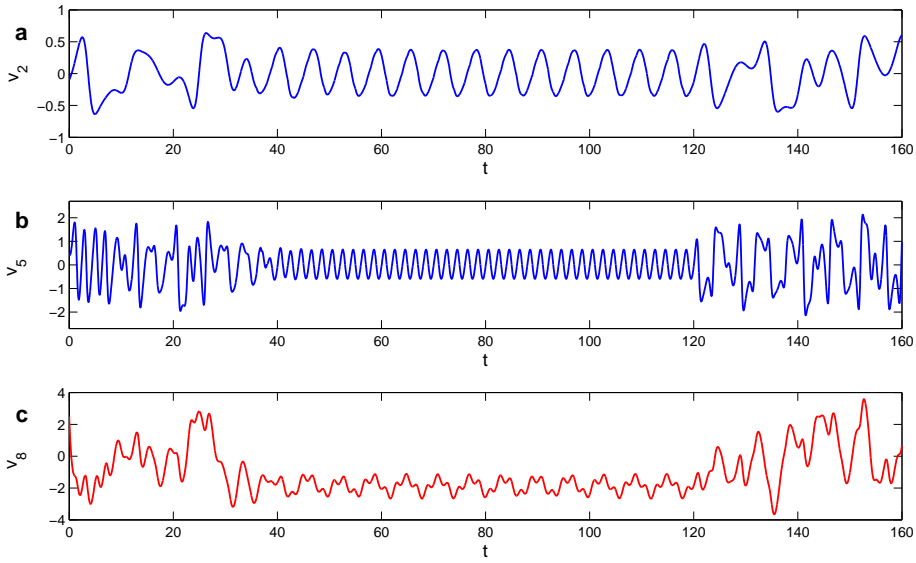


Figure 2.17: Pyragas control method applied to the result-system (2.53) by means of the corresponding control system (2.54). The pictures in (a),(b) and (c) represent the graphs of the v_2 , v_5 and v_8 coordinates, respectively. The simulation for the result-system (2.53) is provided such that in (a) and (b) periodic solutions with incommensurate periods 2 and 2π are controlled by the Pyragas method, and in (c), a quasiperiodic solution of the replicator system is pictured. The control starts at $t = 35$ and ends at $t = 120$. After switching off the control, chaos emerges again and irregular behavior reappears.

In paper [202], it has been mentioned that, in general, in the place of countable set of periodic solutions to form chaos, one can take an uncountable collection of Poisson stable motions which are dense in a quasi-minimal set. This can be also observed in Horseshoe attractor [207]. These emphasize that our simulation of quasiperiodic solutions can be considered as another evidence for the theoretical results.

2.10.5 Replicators with nonnegative eigenvalues

We recall that in our theoretical discussions, all eigenvalues of the real valued constant matrix A , used in system (2.2), are assumed to have negative real parts. Now, as open problems from the theoretical point of view, we shall discuss through simulations the problem of chaos replication in the case when the matrix A possesses an eigenvalue with positive or zero real part.

First, we are going to concentrate on the case of the existence of an eigenvalue with positive real part. Let us make use of the Lorenz system (2.19) together with the coefficients $\sigma = 10$, $r = 28$ and $b = 8/3$ as the generator, which is known to be chaotic [137, 211], and set up the

6–dimensional result-system

$$\begin{aligned}
 x_1' &= -10x_1 + 10x_2 \\
 x_2' &= -x_2 + 28x_1 - x_1x_3 \\
 x_3' &= -(8/3)x_3 + x_1x_2 \\
 x_4' &= -2x_4 + x_1 \\
 x_5' &= -3x_5 + x_2 \\
 x_6' &= 4x_6 - x_6^3 + x_3.
 \end{aligned} \tag{2.55}$$

It is crucial to note that system (2.55) is of the form (2.1) + (2.2), where the matrix A admits the eigenvalues -2 , -3 and 4 , such that one of them is positive. We take into account the solution of system (2.55) with the initial data $x_1(0) = -12.7$, $x_2(0) = -8.5$, $x_3(0) = 36.5$, $x_4(0) = -3.4$, $x_5(0) = -3.2$, $x_6(0) = 3.7$ and visualize in Figure 2.18 the projections of the corresponding trajectory on the $x_1 - x_2 - x_3$ and $x_4 - x_5 - x_6$ spaces. It is seen that the replicator system admits the chaos and the input-output mechanism works for system (2.55).

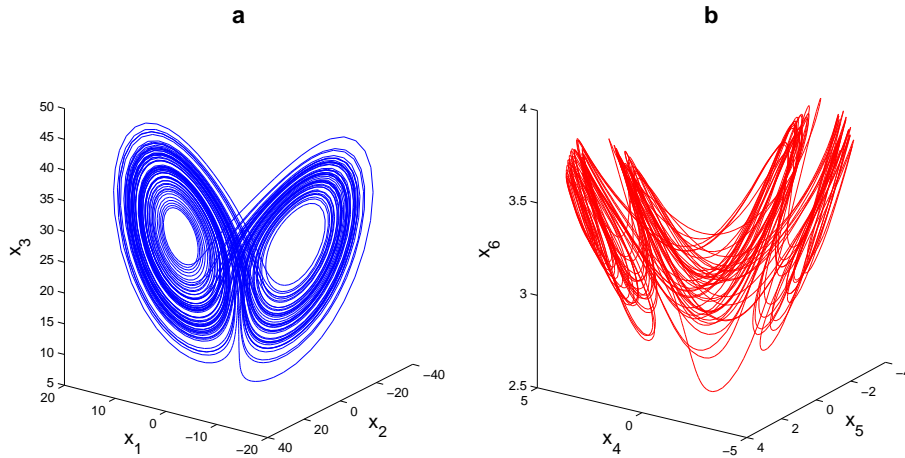


Figure 2.18: 3–dimensional projections of the chaotic attractor of the result-system (2.55). (a) Projection on the $x_1 - x_2 - x_3$ space, (b) Projection on the $x_4 - x_5 - x_6$ space. In (a), the famous Lorenz attractor produced by the generator system (2.19) with coefficients $\sigma = 10$, $r = 28$ and $b = 8/3$ is shown. In (b), as in usual way, the projection of the chaotic attractor of the result-system (2.55), which can separately be considered as a chaotic attractor, is presented. Possibly one can call the attractor of the result-system as $6D$ Lorenz attractor.

Next, we continue to our discussion with the case of the existence of an eigenvalue with a zero real part. This time we consider the chaotic Rössler system [180, 211] described by

$$\begin{aligned}
 x_1' &= -(x_2 + x_3) \\
 x_2' &= x_1 + 0.2x_2 \\
 x_3' &= 0.2 + x_3(x_1 - 5.7)
 \end{aligned} \tag{2.56}$$

as the generator, and constitute the result-system

$$\begin{aligned}
 x_1' &= -(x_2 + x_3) \\
 x_2' &= x_1 + 0.2x_2 \\
 x_3' &= 0.2 + x_3(x_1 - 5.7) \\
 x_4' &= -4x_4 + x_1 \\
 x_5' &= -x_5 + x_2 \\
 x_6' &= -0.2x_6^3 + x_3.
 \end{aligned}
 \tag{2.57}$$

In this case, one can consider system (2.57) as in the form of (2.1) + (2.2) where the matrix A is a diagonal matrix with entries $-4, -1, 0$ on the diagonal and admits the number 0 as an eigenvalue. We simulate the solution of system (2.57) with the initial data $x_1(0) = 4.6, x_2(0) = -3.3, x_3(0) = 0, x_4(0) = 1, x_5(0) = -3.7$ and $x_6(0) = 0.8$. The projections of the trajectory on the $x_1 - x_2 - x_3$ and $x_4 - x_5 - x_6$ spaces are seen in Figure 2.19.

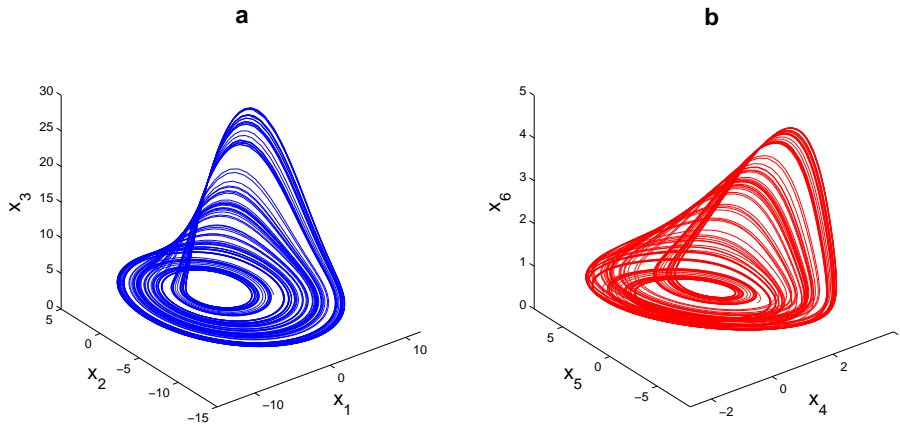


Figure 2.19: 3-dimensional projections of the chaotic attractor of the result-system (2.57). (a) Projection on the $x_1 - x_2 - x_3$ space, (b) Projection on the $x_4 - x_5 - x_6$ space. The picture in (a) indicates the famous Rössler attractor produced by the generator system (2.56).

Figure 2.19 confirms that the replicator mimics the complex behavior of the generator system even if the number 0 is an eigenvalue. The results of the simulations request more detailed investigation, which concern not only the theoretical existence of chaos, but also its resistance and stability. The attractor of the result-system (2.57) can possibly be called as $6D$ Rössler attractor. The similarity between the illustrations (a) and (b) supports the morphogenesis of chaos.

CHAPTER 3

CHAOTIC PERIOD-DOUBLING AND OGY CONTROL FOR THE FORCED DUFFING EQUATION

3.1 Introduction and Preliminaries

The Duffing equation is a second order differential equation of the type

$$x'' + c_1x' + c_2x + c_3x^3 = B\cos(\omega_0t), \quad (3.1)$$

where x is a function of t and $B, c_1, c_2, c_3, \omega_0$ are fixed real numbers [82].

Ueda examined chaos in an electrical circuit with a nonlinear inductor [225, 227] using the Duffing equation, and gave description for the parameters of these type of equations [226]. Moreover, in [27, 44, 83, 153, 155], the Duffing equations have been used to model physical systems. Further, Thompson and Stewart [218] provided many more details on the equation (3.1).

In the last decades, the effect of non-smoothness and discontinuity for the chaos phenomena was widely investigated and realized [7, 8, 9, 10, 11, 12, 13, 28, 29, 124, 230]. Non-smooth nonlinear characteristics are often encountered within the system components while considering real world problems and commonly used in control systems, such as mechanical, hydraulic, magnetic, biomedical, and physical systems [214, 245]. Moreover, these nonlinearities limit the system performance and it is known that they vary with time [245]. For systems with non-smooth characteristics, the control problem is very complicated and becomes even more difficult to handle in the case of unknown time-varying parameters [214, 245]. There have been developed control techniques to diminish the effects of unknown non-smooth nonlinearities [50, 125].

One of the important applications of nonlinear oscillators subjected to non-smooth perturbations is the vibro-impact oscillators which has a wide spectrum of studies among scientists and engineers. In the presence or absence of friction, the motion of vibro-impact systems is usually described by non-smooth nonlinear differential equations [31, 43, 65, 85, 101, 121, 157, 161, 162, 172, 185, 228, 234, 246]. Such systems have a complex dynamic structure that comprises chaotic motions, subharmonic oscillations, and coexistence of different attractors for the same excitation and system parameters under different initial data

[29, 50, 101, 125, 214, 228, 245]. In general, these systems involve multiple impact interactions in the form of jumps in the state space. On the other hand, vibro-impact dynamics has applications on lumped systems such as bouncing ball on a vibrating platform, mass-spring-dashpot systems, and on continuous systems such as strings and beams, which differ from lumped systems [101]. In papers [127, 128], feedback based control of impact oscillators under asymmetric double-sided barriers is proposed and it was shown that chaotic impact oscillators can be controlled and kept in a desired position using a synchronization scheme. The OGY control method is applied to impact oscillators and stabilized their chaotic attractor on period-1 and period-2 orbits using small time-dependent perturbations of the driving frequency [106]. Moreover, some results pertaining to chaotic motions in a periodically forced impacting system, which is analogous to the version of Duffing equations with negative linear stiffness have been presented in [200].

Our investigation demonstrates that processes comprising discontinuity phenomena is convenient to generate rigorously approved chaotic motions from the theoretical point of view. This is not surprising since the same we have already for discrete equations such as the logistic map and the Hénon map [105, 186]. But in our case we have proved assertively the presence of the chaos for continuous dynamics. We want to emphasize that despite the most popular and well known examples of chaos are the Lorenz systems and the Van der Pol equations, there are not definitely proved results of the chaos for them. Most advanced result of the Lorenz systems is given by J. Guckenheimer [87], where he considers not the system itself but the geometric approach. Similarly, the proof for the Van der Pol equations has been made by Levi [130] for the simplified version of the equation. On the other hand, for the Duffing equations, the occurrence of chaotic period-doubling is discussed by making simulations of bifurcation diagrams, but not proved mathematically [84, 188, 230]. Consequently, the problem of discovering chaos rigorously with precise indication which kind of chaos is admitted continuous to be very actual for the nonlinear science. For modified systems, in our papers [7, 8, 9, 10, 11, 12, 13], we provide the method which allows to analyze the problems rigorously. Of course we do not pretend that our results even are begin of the solution for the already discussed equation. But we hope this constructive approach may give a light on solutions of the problems in future.

Formation of chaos in systems with arbitrary large dimension is one of the significant consequences of our paper. More precisely, our results show that the chaos of one dimensional maps can be extended to multidimensional systems. In addition to this, extension of chaos control techniques for low dimensional maps to multidimensional systems is another result. Therefore, the present chapter leads for the applications of theoretical results for one dimensional maps to high dimensional systems. In this sense, it is a continuation of our investigations which we start in [7, 8, 9, 10, 11, 12, 13, 14, 16].

In the paper [215], besides the familiar period-doubling scenario to chaos, intermittent and quasiperiodic routes to chaos as well as period-adding sequences and Farey sequences are introduced in a nonlinear non-autonomous circuit, and verified experimentally and through simulations. On the other hand, a control method without feedback is developed for control-

ling a Duffing equation which admits chaos through the period-doubling cascade [111, 114]. Two different modifications of the OGY control method [70], which can lead to a better performance of the control and the method presented by Pyragas [177] are applied to the classical Duffing oscillator [70, 82], but in these cases the nature of chaos is not precise. Oppositely, in our results, we prove the type of the existing chaos theoretically and use the OGY method not for the classical Duffing equation but for the one which involves a pulse function, such that we emphasize it to be considered as a primary object of analysis.

Switching systems have important applications in high dimensional systems and hybrid systems [8, 191, 229], and the system taken into account in this chapter can be considered as one example. Moreover, the systems with impacts are convenient for simulations. The method and solutions that we present can be applied to hybrid systems in the future, for instance to impulsive systems [7, 185]. In this chapter, we construct chaos with prescribed properties such that chaos developed by using the logistic map with slightly deviated characteristics. Consequently, it can be effectively used for the security of communications and information using our chaos to mask and unmask [114, 118, 123, 238]. Since we have the chaos with known properties, it can also be used in master-slave systems and correspondingly to control these type of systems [168, 219]. Moreover, the research in the artificial neural networks emphasize that the deterministic chaos is a powerful mechanism for the storage and retrieval of information in the dynamics of artificial neural networks [59, 60, 139, 222]. Therefore, our results are also applicable to neuroscience.

The main object of the present investigation is the following modified Duffing equation

$$x'' + d_1x' + d_2x + d_3x^3 = D \cos(k\pi t) + v(t, t_0, \mu), \quad (3.2)$$

where d_1, d_2, d_3, D are real numbers and k is a natural number, the scalar pulse function $v(t, t_0, \mu)$ is defined below.

Using the new variables $x_1 = x$ and $x_2 = x'$, one can reduce the differential equation (3.2) to the system

$$\begin{aligned} x_1' &= x_2 \\ x_2' &= -d_1x_2 - d_2x_1 - d_3x_1^3 + D \cos(k\pi t) + v(t, t_0, \mu). \end{aligned} \quad (3.3)$$

Let \mathbb{R} and \mathbb{N} denote the sets of real numbers and natural numbers respectively, and I the unit interval $[0, 1]$.

In this study, we will investigate also the system,

$$\begin{aligned} z'(t) &= Az(t) + f(t, z) + v(t, t_0, \mu) \\ z(t_0) &= z_0, \quad (t_0, z_0) \in I \times \mathbb{R}^n, \end{aligned} \quad (3.4)$$

which is the general form of the system (3.3).

In system (3.4), $z \in \mathbb{R}^n, t \in \mathbb{R}_+ = [0, \infty)$, the $n \times n$ constant real valued matrix A has real parts of eigenvalues all negative. The function $f(t, z)$ satisfies the periodicity condition $f(t+2, z) = f(t, z)$, $t \in \mathbb{R}_+$, and is Lipschitzian with respect to z with the Lipschitz constant L .

Let us now, introduce the function $v(t, t_0, \mu)$ as follows

$$v(t, t_0, \mu) = \begin{cases} m_0, & \text{if } \zeta_{2i}(t_0, \mu) < t \leq \zeta_{2i+1}(t_0, \mu) \\ m_1, & \text{if } \zeta_{2i+1}(t_0, \mu) < t \leq \zeta_{2i+2}(t_0, \mu), \end{cases} \quad (3.5)$$

where i is a nonnegative integer and $m_0, m_1 \in \mathbb{R}^n$, such that $m_0 \neq m_1$. The sequence $\zeta(t_0, \mu) = \{\zeta_i(t_0, \mu)\}$, $i \geq 0$, is defined through the equation $\zeta_i(t_0, \mu) = i + \kappa_i(t_0, \mu)$, with $\kappa_{i+1}(t_0, \mu) = h(\kappa_i(t_0, \mu), \mu)$, $\kappa_0(t_0, \mu) = t_0$, and $h(s, \mu) = \mu s(1 - s)$ is the logistic map, the central auxiliary instrument in the present chapter.

We shall need those values of the parameter μ , which are between 3.57 and 4, such that the period-doubling cascade accumulates there to provide the chaotic structure [64, 179] for the logistic map, $h(s, \mu)$. In paper [103], it was proved that the measure of such μ is positive. In the sequel, we fix one of them, and notate it as μ_∞ . Moreover, we will not indicate the dependence on the parameter μ , if there is no need to specify it. Thus, for every $t_0 \in I$, the sequence $\kappa(t_0)$ of real numbers κ_i , $i \geq 0$, $\kappa(t_0) \subset I$ is defined. The sequence $\zeta(t_0)$ has the periodicity property if there exists a natural number p such that $\zeta_{i+p} = \zeta_i + p$, for all $i \geq 0$. In other words, if $\kappa_{i+p} = \kappa_i$, $i \geq 0$. The main object of the present chapter is to stabilize the periodic solutions of the chaotic structure generated by the differential equation (3.2).

We should point out that the adjoint linear equation of the non-perturbed Duffing equation

$$x'' + d_1 x' + d_2 x + d_3 x^3 = D \cos(k\pi t) \quad (3.6)$$

has eigenvalues both with negative real parts. The logistic map, which has the positive Lyapunov exponent [89, 198], gives rise to the emergence of chaos in the main equation (3.2) and generates the switching moments. That is, the chaotic scenario in our model is developing “along” the time axis.

We suppose that the main reason of dealing an equation of the type of equation (3.2) is that the generated chaos can give the way of analysis of systems with discontinuous perturbations, which is unfortunately far of to be complete [84].

The chapter is organized as follows. In the next section, the existence of the chaotic attractor is proved, through the period-doubling cascade. The third section contains results of the OGY control of the chaos.

3.2 The Chaos Emergence

3.2.1 The cascade: The analysis results

Let us start with the analysis of system (3.4). In what follows we assume that

$$\sup_{z \in \mathbb{R}^n, t \in \mathbb{R}_+} \|f(t, z)\| = M_0 < \infty$$

and we denote the maximum of the real parts of the eigenvalues of matrix A by σ . Note that σ is negative.

There exist a positive number N and a negative number $\alpha \geq \sigma$ such that $\|e^{At}\| \leq Ne^{\alpha t}$, for $t \geq 0$. Therefore, we can find a natural number p_0 such that $\|e^{Ap_0}\| \leq Ne^{\alpha p_0} < 1$. For $p \geq p_0$, we have

$$\|(I - e^{Ap})^{-1}\| \leq \frac{1}{1 - Ne^{\alpha p}} \leq \frac{1}{1 - Ne^{\alpha p_0}}.$$

Let us denote

$$K = \max \left\{ \max_{1 \leq i \leq p_0-1} \|(I - e^{Ai})^{-1}\|, \frac{1}{1 - Ne^{\alpha p_0}} \right\}, \quad (3.7)$$

and in the sequel we assume also that

$$\frac{-KNL}{\alpha} < 1. \quad (3.8)$$

A function $z(t)$, $z(t_0) = z_0$ is a solution of (3.4) on $[t_0, \infty)$, $t_0 \in I$ if: (i) $z(t)$ is continuous on $[t_0, \infty)$, (ii) the derivative $z'(t)$ exists at each point $t \in [t_0, \infty)$ with the possible exception of the points $\zeta_i(t_0)$, $i \geq 0$, where left sided derivatives exist, (iii) equation (3.4) is satisfied on each interval $(\zeta_i(t_0), \zeta_{i+1}(t_0)]$, $i \geq 0$ [10].

In [7, 9, 10, 11, 12, 13] we develop the approach, when a system of differential equations inserted with a chaotic element, the generator of switching moments, produces a chaotic attractor. It is proved that the attractor presents Li-Yorke [9, 12] and Devaney [10] chaos, as well as a quasi-minimal set [11]. In the same time, it is known that both Li-Yorke and Devaney scenario of chaos emergence are difficult in the simulation with the logistic map. Moreover, speaking generally, period-doubling cascade route to the chaos is most celebrated in simulations. That is why, in the present article we consider the route to identify a chaotic structure for the equation. One must say, also that, it is a difficult task to observe chaos in multidimensional systems, exceptionally with clear theoretically supported properties. The next result is suitable for systems with arbitrary finite dimension.

Consider the sequence of period-doubling bifurcation values $\{\mu_m\}$, $\mu_m \rightarrow \mu_\infty$ as $m \rightarrow \infty$ for the logistic map $h(s, \mu) = \mu s(1 - s)$ [197].

We shall say that the system (3.4) has a chaos through the period-doubling cascade at $\mu = \mu_\infty$, if for each p -periodic sequence $\{\kappa_i(t_0, \mu)\}$, $p \in \mathbb{N}$, where $t_0 \in I$, and μ is equal either to μ_m , $m \in \mathbb{N}$ or μ_∞ , there exists a unique periodic solution, $z_p(t)$, of the system (3.4) with the same μ . Moreover, all trajectories of these solutions lie in a bounded domain. This definition is natural since periodic solutions, which correspond to different sequences κ , do not coincide, and consequently, the equation (3.4) with $\mu = \mu_\infty$ has infinitely many periodic solutions.

The principal result of this section is the following theorem.

Theorem 3.2.1 *System (3.4) admits the chaos through period-doubling cascade at μ_∞ .*

Proof. Fix μ and $t_0 \in I$ such that the sequence $\{\kappa_i(t_0, \mu)\}$ is p -periodic, $p \in \mathbb{N}$. It is easily seen that to verify the theorem, one needs to prove that the system (3.4) with the same μ admits a periodic solution, $z_p(t)$, and the norms of all these periodic solutions with all the possible μ , are bounded with one and the same positive number.

Set $\rho_0 = \max\{\|m_0\|, \|m_1\|\}$, and pick a number $H = \frac{-KN}{\alpha}(M_0 + \rho_0)$, where the number K is defined by the formula (3.7). One can see that H does not depend on p .

We shall consider the cases in which p is even and odd. Let us start with p is even. Using the standard technique [93], one can verify that the solution $z_p(t)$, if exists, satisfies the integral equation

$$z_p(t) = \int_0^p (I - e^{Ap})^{-1} e^{A(p-s)} [f(t+s, z_p(t+s)) + v(t+s, t_0, \mu)] ds.$$

Introduce the set \mathcal{B}_1 of continuous functions $\varphi : [t_0, \infty) \rightarrow \mathbb{R}^n$ such that $\varphi(t+p) = \varphi(t)$, $t \geq t_0$ and $\|\varphi\|_1 \leq H$, where $\|\varphi\|_1 = \sup_{t \geq t_0} \|\varphi(t)\|$.

Define an operator S on the set \mathcal{B}_1 through the equation

$$S(\varphi)(t) = \int_0^p (I - e^{Ap})^{-1} e^{A(p-s)} [f(t+s, \varphi(t+s)) + v(t+s, t_0, \mu)] ds.$$

First of all, we shall check that $S(\mathcal{B}_1) \subseteq \mathcal{B}_1$.

Since p is even, we have for $\varphi \in \mathcal{B}_1$ that $f(t+p+s, \varphi(t+p+s)) = f(t+s, \varphi(t+s))$ and $v(t+p+s, t_0, \mu) = v(t+s, t_0, \mu)$ for each $t \geq t_0$ and $s \in [0, p]$. Therefore, $S(\varphi)(t+p) = S(\varphi)(t)$ for all $t \geq t_0$.

Let us define $\bar{M} = \max_{s \in [0, p]} \|(I - e^{Ap})^{-1} e^{A(p-s)}\|$. Take $\varphi \in \mathcal{B}_1$, and fix $\bar{t} \in [t_0, \infty)$ and an arbitrary $\varepsilon > 0$. Because the functions $f(t, z)$ and $\varphi(t)$ are continuous in all their arguments, the function $f(t, \varphi(t))$ is also continuous. Therefore, there exists a number $\delta_1 > 0$ such that for any $s \in [0, p]$ the inequality

$$\|f(t+s, \varphi(t+s)) - f(\bar{t}+s, \varphi(\bar{t}+s))\| < \frac{\varepsilon}{2p\bar{M}}$$

holds, provided that $|t - \bar{t}| < \delta_1$.

Set $\delta = \min\left\{\delta_1, \frac{\varepsilon}{2p\bar{M}\|m_0 - m_1\|}\right\}$. In the case that $|t - \bar{t}| < \delta$, one can verify that

$$\int_0^p \|v(t+s, t_0, \mu) - v(\bar{t}+s, t_0, \mu)\| ds < p\delta \|m_0 - m_1\|,$$

since there are at most p subintervals of $[0, p]$, each with a length less than δ , such that in each of these subintervals the functions $v(t+s, t_0, \mu)$ and $v(\bar{t}+s, t_0, \mu)$, $s \in [0, p]$, are different from each other.

Thus, if $|t - \bar{t}| < \delta$, then we obtain that

$$\|S(\varphi)(t) - S(\varphi)(\bar{t})\| = \left\| \int_0^p (I - e^{Ap})^{-1} e^{A(p-s)} [f(t+s, \varphi(t+s)) \right.$$

$$\begin{aligned}
& +v(t+s, t_0, \mu) - f(\bar{t}+s, \varphi(\bar{t}+s)) - v(\bar{t}+s, t_0, \mu) \Big] ds \Big\| \\
& \leq \bar{M} \int_0^p \|f(t+s, \varphi(t+s)) - f(\bar{t}+s, \varphi(\bar{t}+s))\| ds \\
& + \bar{M} \int_0^p \|v(t+s, t_0, \mu) - v(\bar{t}+s, t_0, \mu)\| ds \\
& < \frac{\varepsilon}{2} + p\delta\bar{M} \|m_0 - m_1\| \\
& \leq \varepsilon.
\end{aligned}$$

Hence, $S(\varphi)(t)$ is continuous on the interval $[t_0, \infty)$. On the other hand, for $\varphi \in \mathcal{B}_1$, one can attain for all $t \geq t_0$ that

$$\begin{aligned}
\|S(\varphi)(t)\| & \leq \int_0^p \left\| (I - e^{Ap})^{-1} \right\| \left\| e^{A(p-s)} \right\| \|f(t+s, \varphi(t+s)) + v(t+s, t_0, \mu)\| ds \\
& \leq KN(M_0 + \rho_0) \int_0^p e^{\alpha(p-s)} ds \\
& = \frac{-KN}{\alpha} (M_0 + \rho_0) (1 - e^{\alpha p}) \\
& \leq H.
\end{aligned}$$

The last inequality implies that $\|S(\varphi)\|_1 \leq H$. Consequently, $S(\mathcal{B}_1) \subseteq \mathcal{B}_1$.

Next, we shall show that the operator S is a contraction. For $\varphi_1, \varphi_2 \in \mathcal{B}_1$, we have that

$$\begin{aligned}
& S(\varphi_1)(t) - S(\varphi_2)(t) \\
& = \int_0^p (I - e^{Ap})^{-1} e^{A(p-s)} [f(t+s, \varphi_1(t+s)) - f(t+s, \varphi_2(t+s))] ds.
\end{aligned}$$

Therefore,

$$\begin{aligned}
& \|S(\varphi_1)(t) - S(\varphi_2)(t)\| \\
& \leq \int_0^p \left\| (I - e^{Ap})^{-1} \right\| \left\| e^{A(p-s)} \right\| \|f(t+s, \varphi_1(t+s)) - f(t+s, \varphi_2(t+s))\| ds \\
& \leq K \int_0^p NLe^{\alpha(p-s)} \|\varphi_1(t+s) - \varphi_2(t+s)\| ds \\
& \leq \frac{-KNL}{\alpha} (1 - e^{\alpha p}) \|\varphi_1 - \varphi_2\|_1 \\
& \leq \frac{-KNL}{\alpha} \|\varphi_1 - \varphi_2\|_1,
\end{aligned}$$

and hence $\|S(\varphi_1) - S(\varphi_2)\|_1 \leq \frac{-KNL}{\alpha} \|\varphi_1 - \varphi_2\|_1$.

Since $\frac{-KNL}{\alpha} < 1$, the operator S is a contraction. Thus, there exists a unique fixed point of S , and for each p -periodic $\{\kappa_i(t_0, \mu)\}$, there exists a unique solution of the system (3.4) with the same period, provided that p is even.

In the case that p is an odd natural number, due to its definition, the relay function $v(t, t_0, \mu)$ is $2p$ -periodic. Therefore, if $z_p(t)$ exists, it satisfies the integral equation

$$z_p(t) = \int_0^{2p} (I - e^{2Ap})^{-1} e^{A(2p-s)} [f(t+s, z_p(t+s)) + v(t+s, t_0)] ds.$$

Introduce the set \mathcal{B}_2 of continuous functions $\varphi : [t_0, \infty) \rightarrow \mathbb{R}^n$ such that $\varphi(t + 2p) = \varphi(t)$, $t \geq t_0$ and $\|\varphi\|_1 \leq H$, and define an operator $\bar{S} : \mathcal{B}_2 \rightarrow \mathcal{B}_2$ by means of the equation

$$\bar{S}(\varphi)(t) = \int_0^{2p} (I - e^{2Ap})^{-1} e^{A(2p-s)} [f(t+s, \varphi(t+s)) + v(t+s, t_0, \mu)] ds.$$

Similar to the case of even p , it can be proved that \bar{S} is a contraction. Therefore, for each p -periodic sequence $\{\kappa_i(t_0, \mu)\}$, where p is odd, there exists a unique $2p$ -periodic solution $z_p(t)$ of the system (3.4) such that $\|z_p(t)\| \leq H$ for all $t \geq t_0$. Consequently, system (3.4) admits the chaos through period-doubling cascade at μ_∞ . \square

As a result of the proof of Theorem 3.2.1 and making use of various parameter values of period-doubling bifurcations for the logistic map $h(s, \mu) = \mu s(1 - s)$ [21, 146], Table 3.1 is constructed. The table indicates the periodicity dependence between a p -periodic $\{\kappa_i(t_0, \mu)\}$ and the unique periodic solution $z_p(t)$ of system (3.4) with the same μ . In the table, we also specify the values of the parameter μ for which the p -periodic $\{\kappa_i(t_0, \mu)\}$ is stable, likewise the periodic solution $z_p(t)$ of system (3.4).

Table 3.1: Correlation between p and the period of $z_p(t)$

Range of μ	p	Period of $z_p(t)$
$1 < \mu < 3$	1	2
$3 < \mu < 3.4494$	2	2
$3.4494 < \mu < 3.5440$	4	4
$3.5440 < \mu < 3.5644$	8	8
$3.5644 < \mu < 3.5687$	16	16
$3.5687 < \mu < 3.5696$	32	32
...
$3.6265 < \mu < 3.6304$	6	6
...
$3.7382 < \mu < 3.7411$	5	10
...
$3.8284 < \mu < 3.8415$	3	6
...

If system (3.4) is compared with the system

$$\begin{aligned} z'(t) &= Az(t) + v(t, t_0, \mu) \\ z(t_0) &= z_0, (t_0, z_0) \in I \times \mathbb{R}^n, \end{aligned} \tag{3.9}$$

one can see that the difference is the presence of the function $f(t, z)$, and the old theorems from [10] can be repeated almost identically for system (3.4) considering the Lipschitz condition on the function $f(t, z)$.

3.2.2 The Duffing equation's chaotic behavior

In this part of the chapter, we consider both the Duffing equation (3.2) and the corresponding system (3.3) with the coefficients $d_1 = 0.18, d_2 = 2, d_3 = 0.00004, D = 0.02, k = 2$, and $m_0 = 2, m_1 = 1$.

The bifurcation diagram of equation (3.2) with the specified coefficients is shown in Figure 3.1. In the range of μ values greater than 3.57, correlatively to the behavior of the logistic map [21, 65], successive intervals of chaos and intervals of stable periodic solutions, called the periodic windows, appear in the diagram.

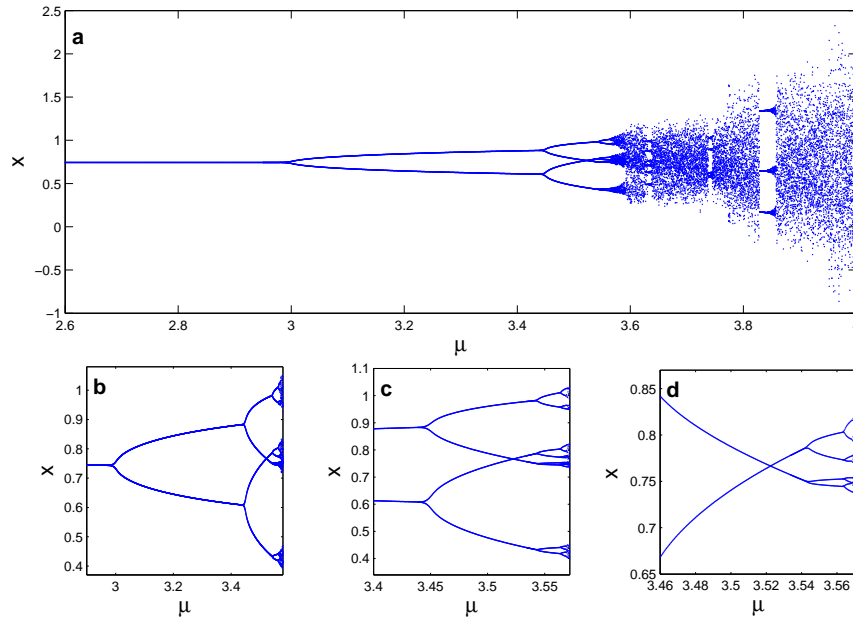


Figure 3.1: Bifurcation diagrams of the Duffing equation perturbed with a pulse function $x'' + 0.18x' + 2x + 0.00004x^3 - 0.02 \cos(2\pi t) = v(t, t_0, \mu)$, where $m_0 = 2$ and $m_1 = 1$. (a) The bifurcation diagram where the parameter μ varies between 2.6 and 4.0. (b) Magnification of (a) where μ is between 2.90 and 3.58. (c) Magnification of (b) where μ is between 3.400 and 3.55. (d) Magnification of (c) where μ changes from 3.460 to 3.571.

At $\mu = 3$, for which the period-doubling bifurcation for the logistic map occurs for the first time [146, 197], splitting occurs in the bifurcation diagram of equation (3.2) with the appointed coefficients, but period-doubling does not occur at this parameter value. That is, up to the second bifurcation value $\mu = 3.4494$, all periodic solutions of the Duffing equation have period 2. This is a prospective behavior, since the periodicity of the periodic solution of the Duffing equation corresponding to a p -periodic sequence $\{\kappa_i(t_0, \mu)\}$ is $2p$ in the case of p is an odd integer.

If we denote by $\{r_m\}$ the sequence of the values of the parameter μ at which the period-doubling bifurcations for the Duffing equation (3.2) with the given coefficients occur, it is

numerically observed that this sequence coincides with the sequence $\{\mu_m\}$, which has been defined above for the cascade of the logistic map, except the first term. That is, $r_m = \mu_{m+1}$, $m \geq 1$. Consequently, when $\lim_{m \rightarrow \infty} \frac{r_m - r_{m+1}}{r_{m+1} - r_{m+2}}$ is evaluated, the universal constant known as the Feigenbaum number 4.6692016... is achieved [198, 218, 243].

In the regions where stable periodic solutions exist, for a fixed value of the parameter μ , the bifurcation diagram represents the values of the stable periodic solutions of equation (3.2) at time $t = \zeta_0 \in I$, where ζ_0 is the initial term of the periodic sequence $\{\zeta_i\}$ corresponding to the same value of μ . We note that, for $\mu_m < \mu < \mu_{m+1}$, there are 2^m different choices for the periodic sequence $\{\zeta_i\}$ with periodicity 2^m , and this is the reason for the observation of 2^m different stable periodic solutions for these values of the parameter.

A stable periodic solution in turn becomes unstable and is replaced by a new couple of stable solutions as the parameter μ increases through the bifurcation values. A stable solution is replaced by a couple of stable periodic solutions of twice its period, except at the parameter values corresponding to a p -periodic $\{\kappa_i\}$ with p odd and the process continues in this way. For such values of μ , the periodicity does not change, by the same reasoning explained as above. In the intervals of chaos, all existing periodic solutions are unstable.

In Figure 3.2, one can see the larger image of the periodic window which starts at $\mu = 3.8284$, and its magnification for the parameter values between 3.8350 and 3.8600. It is observed that a similar copy of the whole bifurcation diagram reappears in this region.

Now, let us check that the conditions of the last theorem are true for the system (3.3). The matrix of coefficients of the system (3.3) with the assumed coefficients is $A = \begin{pmatrix} 0 & 1 \\ -2 & -0.18 \end{pmatrix}$.

The eigenvalues of the matrix A are $a \mp ib$, where $a = -0.09$ and $b = \sqrt{2 - 0.09^2}$. The real Jordan form of the matrix A is given by $J = \begin{pmatrix} a & -b \\ b & a \end{pmatrix}$ and the identity $P^{-1}AP = J$ is satisfied where $P = \begin{pmatrix} 0 & 1 \\ b & a \end{pmatrix}$ and $P^{-1} = \frac{1}{b} \begin{pmatrix} -a & 1 \\ b & 0 \end{pmatrix}$. Evaluating the exponential matrix e^{At} we have

$$e^{At} = e^{at} P \begin{pmatrix} \cos(bt) & -\sin(bt) \\ \sin(bt) & \cos(bt) \end{pmatrix} P^{-1}. \quad (3.10)$$

Denote by $\|\cdot\|$ the matrix norm which is induced by the usual Euclidean norm in \mathbb{R}^n . That is,

$$\|\Gamma\| = \max \left\{ \sqrt{\lambda} : \lambda \text{ is an eigenvalue of } \Gamma^T \Gamma \right\}$$

for any $n \times n$ matrix Γ with real entries, and Γ^T denotes the transpose of the matrix Γ [98].

One can see that

$$\|P\| = \left(\frac{3}{2} + \frac{\sqrt{1 + 0.18^2}}{2} \right)^{1/2},$$

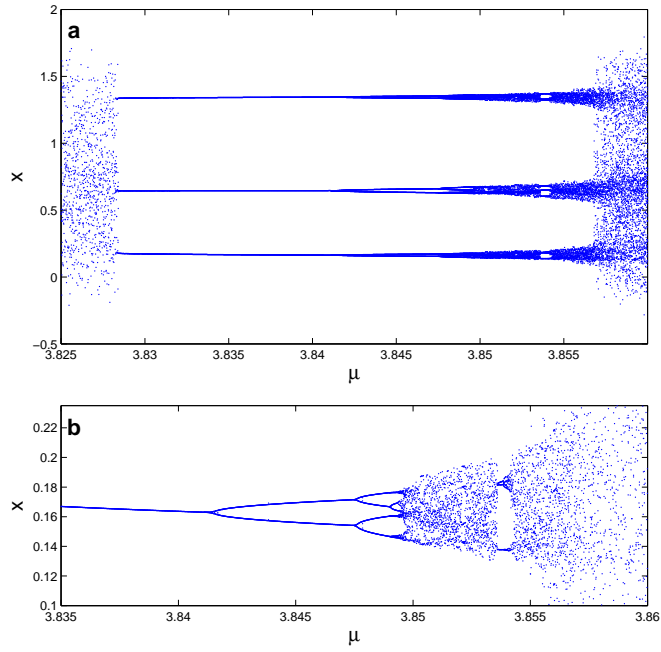


Figure 3.2: The periodic window which starts at $\mu = 3.8284$ in the bifurcation diagram of the Duffing equation perturbed with a pulse function $x'' + 0.18x' + 2x + 0.00004x^3 - 0.02\cos(2\pi t) = v(t, t_0, \mu)$, where $m_0 = 2$ and $m_1 = 1$. (a) The bifurcation diagram where μ is between 3.8250 and 3.8600. (b) Magnification of (a) where μ changes from 3.8350 to 3.8600.

and

$$\|P^{-1}\| = \frac{1}{\sqrt{2-0.09^2}} \left(\frac{3}{2} + \frac{\sqrt{1+0.18^2}}{2} \right)^{1/2}.$$

Therefore, using (3.10), we obtain $\|e^{At}\| \leq Ne^{\alpha t}$ where $N = \frac{3 + \sqrt{1+0.18^2}}{\sqrt{8-0.18^2}}$ and $\alpha = -0.09$.

In what follows, we use approximation with accuracy of 7 digits in the decimal part.

For $p_0 = 4$, $Ne^{\alpha p_0} = \left(\frac{3 + \sqrt{1+0.18^2}}{\sqrt{8-0.18^2}} \right) e^{-0.36} \cong 0.9926395 < 1$. One can easily evaluate that,

$$\max_{1 \leq i \leq 3} \left\{ \|(I - e^{J_i})^{-1}\| \right\} = \|(I - e^{J_1})^{-1}\| \cong 0.8045044.$$

Then, using the matrix identity $(I - e^{At})^{-1} = P(I - e^{Jt})^{-1}P^{-1}$, the inequality

$$\max_{1 \leq i \leq 3} \left\{ \|(I - e^{A_i})^{-1}\| \right\} \leq \|P\| \|P^{-1}\| \max_{1 \leq i \leq 3} \left\{ \|(I - e^{J_i})^{-1}\| \right\} \cong 1.1446324$$

is obtained. On the basis of above evaluations, one can find that

$$K = \max \left\{ \max_{1 \leq i \leq 3} \|(I - e^{A_i})^{-1}\|, \frac{1}{1 - Ne^{4\alpha}} \right\} \cong 135.8619956.$$

System (3.3) with the prescribed coefficients has the nonlinear term

$$f(t, x_1, x_2) = [0 \quad -0.00004x_1^3]^T.$$

The Lipschitz constant L for this function can be taken as 0.0003468 since the x_1 values of the chaotic attractor satisfies the condition $|x_1| \leq 1.7$. Thus $\frac{-KNL}{\alpha} \cong 0.7448557$ and the condition (3.8) is also satisfied.

We end up this part, by simulating a solution (x_1, x_2) of system (3.3) with initial data $x_1(0.5) = 0.01$, $x_2(0.5) = 0.025$ and $\mu_\infty = 3.8$. In Figure 3.3, the chaotic behavior of the solution is revealed.

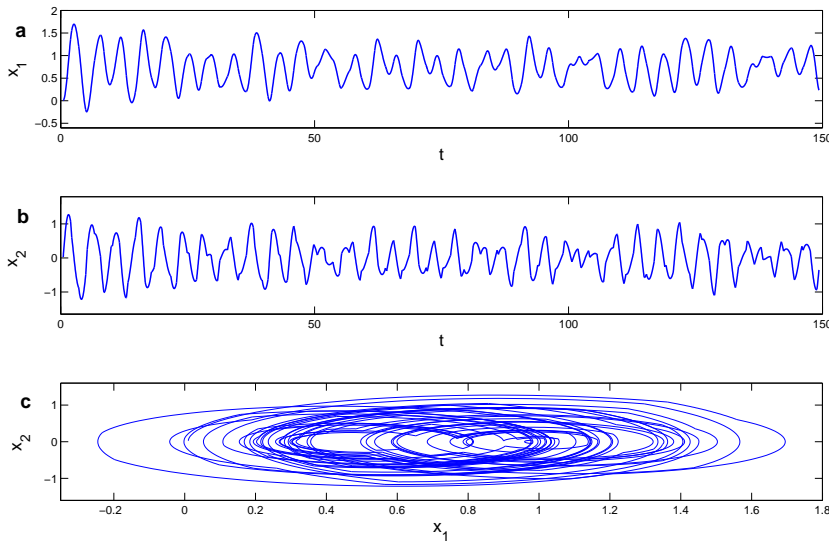


Figure 3.3: Simulation results of the Duffing equation perturbed with a pulse function $x'' + 0.18x' + 2x + 0.00004x^3 - 0.02\cos(2\pi t) = v(t, t_0, \mu_\infty)$, where $m_0 = 2, m_1 = 1$ and $\mu_\infty = 3.8$. The pictures in (a) and (b) show the graphs of the x_1 and x_2 coordinates, respectively, while the picture in (c) represents the trajectory of the solution $(x_1(t), x_2(t))$.

3.2.3 Lyapunov exponents

The Lyapunov exponent is a measure of divergence of state trajectories, and is one of the most important features of deterministic chaos [243]. There are well developed results for Lyapunov exponents of maps, and it is technically difficult for continuous dynamics [82, 164, 197, 198]. Evaluation procedures of Lyapunov exponents for continuous dynamics are, in general, provided for low dimensional systems [178, 210]. Our system, despite there is discontinuity property, evolves along continuous time. Therefore, to work with Lyapunov exponents, we should consider mainly the results for continuous dynamics. More exactly, our systems involve continuous and discrete dynamics such that the space variables change

continuously while the switching moments of time satisfy discrete equations, that is, they belong to the class of hybrid systems [8, 191, 229]. Consequently, we have to evaluate the divergence of solutions by continuous as well as discrete Lyapunov exponents. Moreover, our systems are essentially non-autonomous. That is why one has to consider the method of Lyapunov exponents for non-autonomous systems [210]. For chaos development the positive Lyapunov exponent is appropriate. So, one can conclude that the positiveness of one of the Lyapunov exponents is an indicator of chaos if the system is considered in a bounded region. That is why for the general case of our analysis in this chapter, it is sufficient to find that the Lyapunov exponent is positive for the logistic map, the generator of the switching moments.

To illustrate the general discussions, let us consider the following example.

Example. Let the equation

$$x' = -2x + v(t, t_0, \mu_\infty) \quad (3.11)$$

be given with $\mu_\infty = 3.8$.

If we consider two solutions of equation (3.11) with the same t_0 , they are both bounded and approach to each other with exponent -2 , that is, -2 is an eigenvalue. Since the equation is non-autonomous then it needs a special treatment [210]. When the time variable is considered as a spatial one, one can transform equation (3.11) to a system as

$$\begin{aligned} \frac{dx}{d\tau} &= -2x + v(\tau, t_0, \mu_\infty) \\ \frac{d\tau}{dt} &= 1 \\ \zeta_{i+1} &= i + 1 + h(\zeta_i - i, \mu_\infty). \end{aligned} \quad (3.12)$$

The second equation in (3.12) provides us the zero Lyapunov exponent [210]. Since our system involves the discrete equation, the logistic map with $\mu_\infty = 3.8$, it admits the third Lyapunov exponent which is approximately 0.432 [23]. This Lyapunov exponent describes the divergence of solutions with different initial moments along the time axis. Finally, we have obtained that the divergence of solutions of equation (3.11) is described through three Lyapunov exponents $\lambda_1 = 0.432$, $\lambda_2 = 0$, $\lambda_3 = -2$.

3.3 Controlling Results

3.3.1 The logistic map

We stabilize the periodic solutions by control of the switching moments of the pulse function, which are defined through the logistic map. Therefore, one will need the description of the OGY method for the map [196].

Suppose that the parameter μ , in the map, can be finely tuned in a small range around the value $\mu_\infty = 3.8$, that is, μ is allowed to vary in the range $[\mu_\infty - \delta, \mu_\infty + \delta]$, where δ is small. Denote

the target period- p orbit to be controlled as $\kappa^{(i)}(t_0, \mu_\infty)$, $i = 1, 2, \dots, p$ where t_0 belongs to the unit interval $I = [0, 1]$, $\kappa^{(i+1)}(t_0, \mu_\infty) = h(\kappa^{(i)}(t_0, \mu_\infty), \mu_\infty)$ and $\kappa^{(p+1)}(t_0, \mu_\infty) = \kappa^{(1)}(t_0, \mu_\infty)$. The logistic map, $h(s, \mu) = \mu s(1 - s)$, in the neighborhood of a periodic orbit can be approximated by a linear equation expanded around the periodic orbit. If we denote $\bar{\mu}_j - \mu_\infty = \Delta\bar{\mu}_j$, and $\kappa_{j+1}(t_1, \bar{\mu}_j) = h(\kappa_j(t_1, \bar{\mu}_j), \bar{\mu}_j)$, $t_1 \in I$, we get

$$\begin{aligned}\kappa_{j+1} - \kappa^{(i+1)} &= \frac{\partial h}{\partial s}[\kappa_j - \kappa^{(i)}] + \frac{\partial h}{\partial \mu}\Delta\bar{\mu}_j \\ &= \mu_\infty[1 - 2\kappa^{(i)}][\kappa_j - \kappa^{(i)}] + \kappa^{(i)}[1 - \kappa^{(i)}]\Delta\bar{\mu}_j,\end{aligned}\tag{3.13}$$

where partial derivatives are evaluated at $s = \kappa^{(i)}(t_0, \mu_\infty)$ and $\mu = \mu_\infty$. We require $\kappa_{j+1}(t_1, \bar{\mu}_j)$ to stay in the neighborhood of $\kappa^{(i+1)}(t_0, \mu_\infty)$. Therefore, if we set

$$\kappa_{j+1}(t_1, \bar{\mu}_j) - \kappa^{(i+1)}(t_0, \mu_\infty) = 0,$$

then we obtain that

$$\Delta\bar{\mu}_j = \mu_\infty \frac{[2\kappa^{(i)} - 1][\kappa_j - \kappa^{(i)}]}{\kappa^{(i)}[1 - \kappa^{(i)}]}\tag{3.14}$$

or equivalently

$$\bar{\mu}_j = \mu_\infty \left(1 + \frac{[2\kappa^{(i)} - 1][\kappa_j - \kappa^{(i)}]}{\kappa^{(i)}[1 - \kappa^{(i)}]} \right).\tag{3.15}$$

This equation holds only when the trajectory κ_j enters a small neighborhood of the period- p orbit, hence the required parameter perturbation $\Delta\bar{\mu}_j$ is small. When the trajectory is outside the neighborhood of the target periodic orbit, we do not apply any parameter perturbation, so the system evolves at its nominal parameter value μ_∞ . Hence, we set $\bar{\mu}_j = \mu_\infty$, when $|\Delta\bar{\mu}_j| > \delta$.

Suppose that $t_0 \in I$ is fixed such that the sequence $\{\kappa_i(t_0, \mu_\infty)\}$ is p -periodic. Thus, for given $\delta > 0$, there exist $\varepsilon > 0$ and $i_0, j_0 \in \mathbb{N}$ such that for all $i, i_0 \leq i \leq i_0 + j_0$, we have $|\Delta\bar{\mu}_i| \leq \delta$ and $|\kappa_i(t_1, \bar{\mu}_i) - \kappa_i(t_0, \mu_\infty)| < \varepsilon$ [82, 163, 195, 196], where $\kappa_{i+1}(t_1, \bar{\mu}_i) = h(\kappa_i(t_1, \bar{\mu}_i), \bar{\mu}_i)$. The number j_0 is, in general, finite, since the nonlinearity is not included in (3.13). We will use the numbers ε, i_0 and j_0 for Theorem 3.3.1.

We note that the control of chaos is not achieved immediately after switching on the control mechanism, rather, there is a transient time before the logistic map is controlled. The transient time increases if the δ decreases [82, 195].

Now, we consider a simulation for the stabilization of the logistic map. Namely, of the sequence $\{\kappa_i\}$, where $\kappa_{i+1} = 3.8\kappa_i(1 - \kappa_i)$, $i \geq 0$ and $\kappa_0 = t_1 = 0.5$. If the OGY control method is applied around the fixed point $2.8/3.8$, that is the period-1 orbit of the logistic equation $h(s, 3.8) = 3.8s(1 - s)$, we obtain the result that is shown in Figure 3.4. We used the value $\delta = 0.19$. The control starts at the iteration number $i = 25$ and ends at $i = 60$. Despite the control was switched off at 60^{th} iteration, the stabilization prolongs till the 110^{th} iteration.

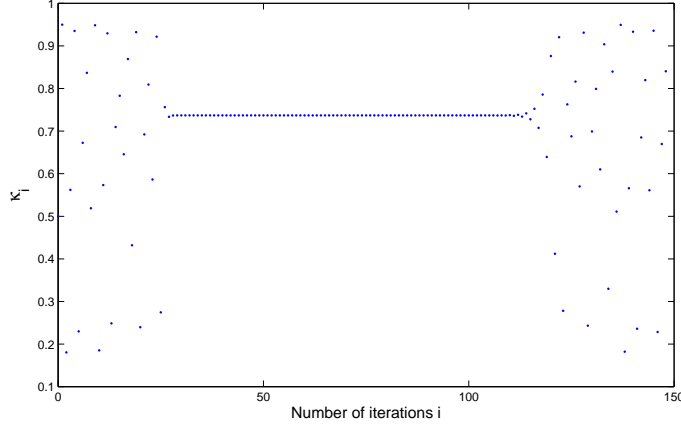


Figure 3.4: The OGY control method applied to the sequence $\{\kappa_i\}$, where $\kappa_{i+1} = 3.8\kappa_i(1 - \kappa_i)$, $\kappa_0 = 0.5$, around the fixed point $2.8/3.8$ of the logistic map with $\delta = 0.19$. The control is switched on at the iteration number $i = 25$ and switched off at $i = 60$.

3.3.2 The general system control

From the description made above, it is seen that the control by OGY method means construction of a sequence of the parameter's value μ near a chaotic value of the parameter, μ_∞ , to generate a solution, which is close to the chosen periodic one. It is obvious that similar control problem can be formulated for the system (3.3), and consequently, for equation (3.2).

To control system (3.3), we replace the parameter μ by the control sequence $\{\mu^i\}$ and define

$$v(t, t_1, \mu^i) = \begin{cases} m_0, & \text{if } \zeta_{2i}(t_1, \mu^i) < t \leq \zeta_{2i+1}(t_1, \mu^i) \\ m_1, & \text{if } \zeta_{2i+1}(t_1, \mu^i) < t \leq \zeta_{2i+2}(t_1, \mu^i), \end{cases} \quad (3.16)$$

where $i \geq 0$ is an integer, $m_0, m_1 \in \mathbb{R}^n$, the same as for the function $v(t, t_0, \mu)$ in (3.5). The sequence $\zeta(t_1, \mu^i) = \{\zeta_i(t_1, \mu^i)\}$, $i \geq 0$, is defined through the equation $\zeta_i(t_1, \mu^i) = i + \kappa_i(t_1, \mu^i)$, with $\kappa_{i+1}(t_1, \mu^i) = h(\kappa_i(t_1, \mu^i), \mu^i)$, $\kappa_0(t_1, \mu^i) = t_1$.

Consider, now, the system,

$$\begin{aligned} z'(t) &= Az(t) + f(t, z) + v(t, t_1, \mu^i) \\ z(t_1) &= z_1, (t_1, z_1) \in I \times \mathbb{R}^n, \end{aligned} \quad (3.17)$$

which is the control system conjugate to the system (3.4).

Our aim is to determine the sequence $\{\mu^i\}$ which stabilizes the periodic solutions of (3.4) and in the next theorem a convenient choice for this sequence is indicated.

By $\phi(t, \bar{t}, \bar{z})$, $\bar{t} \in I$, $\bar{z} \in \mathbb{R}^n$, we denote a solution of (3.17) with $t_1 = \bar{t}$ and $z_1 = \bar{z}$.

In the following theorem we shall use the numbers ε , i_0 , and j_0 , which were mentioned above for the stabilization of the logistic map.

Suppose that $z_p(t)$, $p \in \mathbb{N}$, denotes the periodic solution of (3.4) with $z_p(t_0) = z_0$ and $\mu = \mu_\infty$. Take $z_1 \in \mathbb{R}^n$ and consider the solution $z(t) = \phi(t, t_1, z_1)$ of system (3.17). If $z(\zeta_{i_0}(t_0, \mu_\infty))$ is not equal to $z_p(\zeta_{i_0}(t_0, \mu_\infty))$, then suppose that the number $T(\varepsilon, z_1)$ is the maximum of the numbers $\zeta_{i_0}(t_0, \mu_\infty) + \frac{1}{NL+\alpha} \ln \left(\frac{1-e^{\alpha\varepsilon}}{N\|z(\zeta_{i_0}(t_0, \mu_\infty)) - z_p(\zeta_{i_0}(t_0, \mu_\infty))\|} \right)$ and $\zeta_{i_0}(t_0, \mu_\infty)$. In the case that $z(\zeta_{i_0}(t_0, \mu_\infty))$ and $z_p(\zeta_{i_0}(t_0, \mu_\infty))$ are equal to each other, take $T(\varepsilon, z_1) = \zeta_{i_0}(t_0, \mu_\infty)$. The number $T(\varepsilon, z_1)$ will be needed in the following theorem, which is one of the main results of this chapter.

In the proof of the following theorem, we assume without loss of generality that $i_0 = 0$. In this case, $\zeta_{i_0}(t_0, \mu_\infty) = t_0$ and $\zeta_{i_0}(t_1, \bar{\mu}_i) = t_1$. It is worth saying that since $\frac{-NL}{\alpha} < \frac{-KNL}{\alpha} < 1$, we have $NL + \alpha < 0$.

Theorem 3.3.1 *Assume that $T(\varepsilon, z_1) < i_0 + j_0$. Then the sequence $\{\bar{\mu}_i\}$ stabilizes the periodic solution $z_p(t)$ such that*

$$\|\phi(t, t_1, z_1) - z_p(t)\| < \left(1 - \frac{Ne^{-\alpha} \|m_0 - m_1\|}{(NL + \alpha)(1 - e^{\alpha\varepsilon})} \right) (1 - e^{\alpha\varepsilon}),$$

if $t \in [T(\varepsilon, z_1), i_0 + j_0]$.

Proof. Without loss of generality, assume that $t_1 \leq t_0$. The solution $z(t) = \phi(t, t_1, z_1)$, $t_1 \in I$, $z_1 \in \mathbb{R}^n$, of (3.17) can be continued up to $t = t_0$. Let us denote $z(t_0) = \eta_1$ and $z_p(t_0) = z_0$. In this case, the integral equations

$$z(t) = e^{A(t-t_0)} \eta_1 + \int_{t_0}^t e^{A(t-s)} [f(s, z(s)) + v(s, t_1, \bar{\mu}_i)] ds$$

and

$$z_p(t) = e^{A(t-t_0)} z_0 + \int_{t_0}^t e^{A(t-s)} [f(s, z_p(s)) + v(s, t_0, \mu_\infty)] ds$$

are satisfied. Therefore, for $t \geq t_0$ we have

$$\begin{aligned} z(t) - z_p(t) &= e^{A(t-t_0)} (\eta_1 - z_0) + \int_{t_0}^t e^{A(t-s)} [f(s, z(s)) - f(s, z_p(s))] ds \\ &+ \int_{t_0}^t e^{A(t-s)} [v(s, t_1, \bar{\mu}_i) - v(s, t_0, \mu_\infty)] ds. \end{aligned} \quad (3.18)$$

Since for each i , $0 \leq i \leq j_0$, the inequality

$$|\zeta_i(t_0, \mu_\infty) - \zeta_i(t_1, \bar{\mu}_i)| = |\kappa_i(t_0, \mu_\infty) - \kappa_i(t_1, \bar{\mu}_i)| < \varepsilon$$

holds, one can verify that

$$\left| \int_{\zeta_i(t_0, \mu_\infty)}^{\zeta_i(t_1, \bar{\mu}_i)} e^{\alpha(t-s)} ds \right| < \left(\frac{-1}{\alpha} \right) (1 - e^{\alpha\varepsilon}) e^{\alpha([t]-1-i)}, \quad (3.19)$$

where $\lfloor t \rfloor$ denotes the greatest integer which is not larger than t . On the other hand, by means of the inequality (3.19) we have that

$$\begin{aligned}
& \left\| \int_{t_0}^t e^{A(t-s)} [v(s, t_1, \bar{\mu}_i) - v(s, t_0, \mu_\infty)] ds \right\| \\
& \leq \int_{t_0}^t N e^{\alpha(t-s)} \|v(s, t_1, \bar{\mu}_i) - v(s, t_0, \mu_\infty)\| ds \\
& \leq \sum_{i=1}^{\lfloor t \rfloor} \left| \int_{\zeta_i(t_0, \mu_\infty)}^{\zeta_i(t_1, \bar{\mu}_i)} N e^{\alpha(t-s)} \|m_0 - m_1\| ds \right| \\
& < \left(\frac{-N}{\alpha} \right) (1 - e^{\alpha \varepsilon}) \|m_0 - m_1\| \sum_{i=1}^{\lfloor t \rfloor} e^{\alpha(\lfloor t \rfloor - 1 - i)} \\
& < \frac{-N e^{-\alpha} \|m_0 - m_1\|}{\alpha (1 - e^\alpha)} (1 - e^{\alpha \varepsilon}).
\end{aligned}$$

Using the equation (3.18) together with the last inequality one can obtain that

$$\begin{aligned}
\|z(t) - z_p(t)\| & \leq N e^{\alpha(t-t_0)} \|\eta_1 - z_0\| + \frac{-N e^{-\alpha} \|m_0 - m_1\|}{\alpha (1 - e^\alpha)} (1 - e^{\alpha \varepsilon}) \\
& + \int_{t_0}^t N L e^{\alpha(t-s)} \|z(s) - z_p(s)\| ds.
\end{aligned}$$

Now, let $u(t) = \|z(t) - z_p(t)\| e^{-\alpha t}$. Under the circumstances we have

$$u(t) \leq N e^{-\alpha t_0} \|\eta_1 - z_0\| + \frac{-N e^{-\alpha(t+1)} \|m_0 - m_1\|}{\alpha (1 - e^\alpha)} (1 - e^{\alpha \varepsilon}) + N L \int_{t_0}^t u(s) ds.$$

Applying Lemma 2.2 [34] we attain that

$$\begin{aligned}
u(t) & \leq N e^{-\alpha t_0} \|\eta_1 - z_0\| + \frac{-N e^{-\alpha(t+1)} \|m_0 - m_1\|}{\alpha (1 - e^\alpha)} (1 - e^{\alpha \varepsilon}) \\
& + N^2 L \|\eta_1 - z_0\| e^{-\alpha t_0} \int_{t_0}^t e^{NL(t-s)} ds \\
& + \frac{-N^2 L e^{-\alpha} \|m_0 - m_1\|}{\alpha (1 - e^\alpha)} (1 - e^{\alpha \varepsilon}) \int_{t_0}^t e^{NL(t-s)} e^{-\alpha s} ds
\end{aligned}$$

Making use of the equations

$$\int_{t_0}^t e^{NL(t-s)} ds = \frac{1}{NL} \left(e^{NL(t-t_0)} - 1 \right),$$

and

$$\int_{t_0}^t e^{NL(t-s)} e^{-\alpha s} ds = \left(\frac{-1}{NL + \alpha} \right) e^{-\alpha t} \left(1 - e^{(NL + \alpha)(t-t_0)} \right)$$

it can be verified that

$$u(t) \leq N \|\eta_1 - z_0\| e^{-\alpha t_0} e^{NL(t-t_0)} - \frac{N e^{-\alpha(t+1)} \|m_0 - m_1\|}{\alpha (1 - e^\alpha)} (1 - e^{\alpha \varepsilon})$$

$$\begin{aligned}
& + \frac{N^2 L e^{-\alpha(t+1)} \|m_0 - m_1\|}{(NL + \alpha)\alpha(1 - e^\alpha)} (1 - e^{\alpha\varepsilon}) \left(1 - e^{(NL+\alpha)(t-t_0)}\right) \\
& < N \|\eta_1 - z_0\| e^{-\alpha t_0} e^{NL(t-t_0)} - \frac{N e^{-\alpha(t+1)} \|m_0 - m_1\|}{\alpha(1 - e^\alpha)} (1 - e^{\alpha\varepsilon}) \\
& + \frac{N^2 L e^{-\alpha(t+1)} \|m_0 - m_1\|}{(NL + \alpha)\alpha(1 - e^\alpha)} (1 - e^{\alpha\varepsilon}) \\
& = N \|\eta_1 - z_0\| e^{-\alpha t_0} e^{NL(t-t_0)} - \frac{N e^{-\alpha(t+1)} \|m_0 - m_1\|}{(NL + \alpha)(1 - e^\alpha)} (1 - e^{\alpha\varepsilon}).
\end{aligned}$$

Multiplication of both sides of the last inequality by $e^{\alpha t}$ implies that

$$\|z(t) - z_p(t)\| < N \|\eta_1 - z_0\| e^{(NL+\alpha)(t-t_0)} - \frac{N e^{-\alpha} \|m_0 - m_1\|}{(NL + \alpha)(1 - e^\alpha)} (1 - e^{\alpha\varepsilon}).$$

It is clear that if $\eta_1 = z_0$, then the conclusion of the theorem is true. Suppose that $\eta_1 \neq z_0$. If $t \in [T(\varepsilon, z_1), j_0]$, then one can easily verify that

$$e^{(NL+\alpha)(t-t_0)} \leq \frac{1 - e^{\alpha\varepsilon}}{N \|\eta_1 - z_0\|}.$$

Consequently, the inequality

$$\|z(t) - z_p(t)\| < \left(1 - \frac{N e^{-\alpha} \|m_0 - m_1\|}{(NL + \alpha)(1 - e^\alpha)}\right) (1 - e^{\alpha\varepsilon})$$

holds, for $t \in [T(\varepsilon, z_1), j_0]$.

The theorem is proved. \square

Implementation of Theorem 3.3.1 to the system (3.3) is mentioned in the next part.

3.3.3 The Duffing equation control

Let us, consider the main system (3.3) with $\mu_\infty = 3.8$ and $d_1 = 0.18$, $d_2 = 2$, $d_3 = 0.00004$, $D = 0.02$, $k = 2$, $m_0 = 2$, $m_1 = 1$, again. The system satisfies the conditions for existence of chaos and admits the chaos at $\mu_\infty = 3.8$. Theorem 3.3.1 is applicable to (3.3). The control system (3.17) has, in this case, the form

$$\begin{aligned}
x_1' &= x_2 \\
x_2' &= -2x_1 - 0.18x_2 - 0.00004x_1^3 + 0.02 \cos(2\pi t) + v(t, t_1, \bar{\mu}_i).
\end{aligned} \tag{3.20}$$

To simulate the result, let us take $t_1 = 0.5$, $t_0 = 2.8/3.8$ and the solution (x_1, x_2) of system (3.20) with the initial condition $x_1(t_1) = 0.01$, $x_2(t_1) = 0.025$. Its graph is seen in Figure 3.5 and it approximates the 2-periodic solution $z_1(t)$. The value $\delta = 0.19$ is used, and the control starts at time $t = \zeta_{25}$ and ends at $t = \zeta_{60}$. Here, we note that since the OGY control method is applied to the logistic map, the iteration moment \bar{i} when the control is switched on

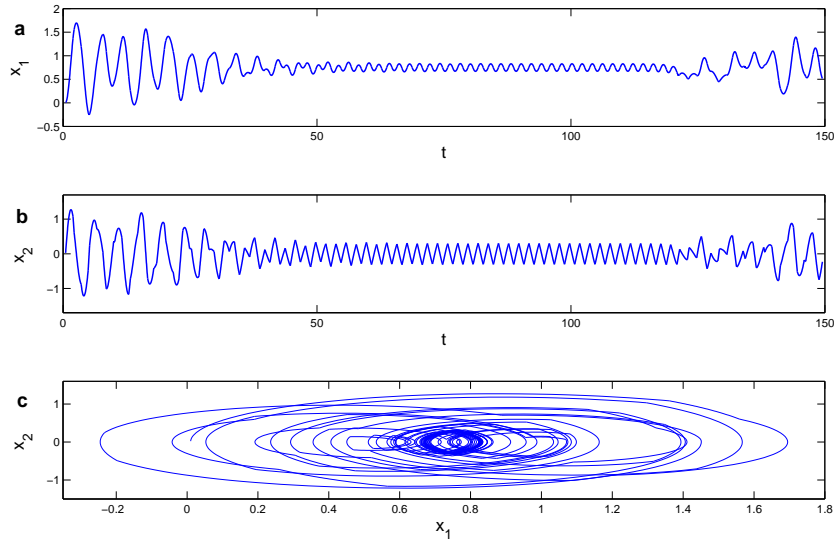


Figure 3.5: The OGY control method applied to the Duffing equation perturbed with a pulse function $x'' + 0.18x' + 2x + 0.00004x^3 - 0.02 \cos(2\pi t) = v(t, t_0, \mu_\infty)$, where $m_0 = 2, m_1 = 1$ and $\mu_\infty = 3.8$. The control starts at time $t = \zeta_{25}$ and ends at $t = \zeta_{60}$. (a) The graph of the x_1 -coordinate. (b) The graph of the x_2 -coordinate. (c) The trajectory of the solution $(x_1(t), x_2(t))$.

corresponds to the time moment $t = \zeta_{\bar{i}}$, and a similar argument is valid for the moment when the control ends.

We use the same interval of stabilization for the logistic map and the Duffing equation. But the interval of periodicity for the map is larger in the former, approximately 80 and 60 respectively. The reason is that the chaos of the equation is secondary with respect to the chaos of the logistic map. Likewise the control of the logistic map, the chaos transient time increases if the δ decreases.

To discuss our main assumptions, let us arrange the following simulations. Consider the following Duffing equation in the standard form [218]

$$x'' + 0.05x' + x^3 = 7.5 \cos t. \quad (3.21)$$

To convert this equation to a suitable form for which our theorem can be applied, we use the change of variables $u = t/\pi$ and $y(u) = x(t)$. Using these new variables and relabeling u as t , one can reduce (3.21) to the differential equation

$$y'' + 0.05\pi y' + \pi^2 y^3 = 7.5\pi^2 \cos(\pi t). \quad (3.22)$$

Defining new variables $x_1 = y$ and $x_2 = y'$ we can reduce (3.22) to the system

$$\begin{aligned} x_1' &= x_2 \\ x_2' &= -0.05\pi x_2 - \pi^2 x_1^3 + 7.5\pi^2 \cos(\pi t). \end{aligned} \quad (3.23)$$

The eigenvalues for this system are 0 and -0.05π . Since one of the eigenvalues is zero, one can expect that our results are not applicable to system (3.23). That is, the system is not controllable with our method. Take a solution of system (3.23) with $x_1(0.5) = 1, x_2(0.5) = 2$. The chaotic behavior is seen in Figure 3.6.

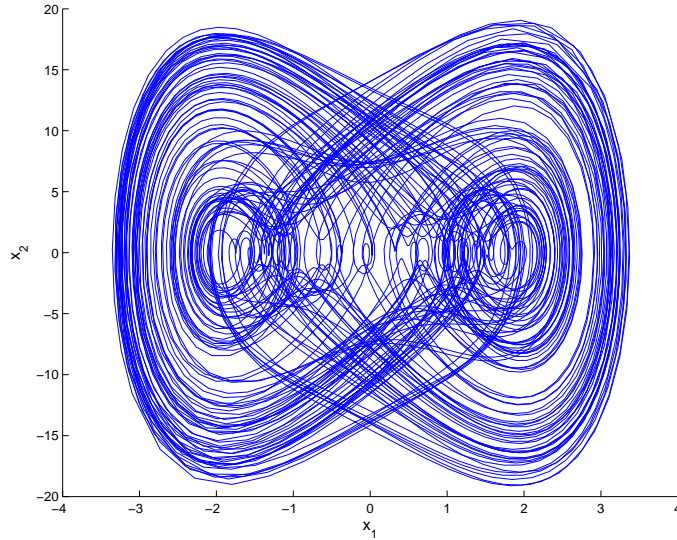


Figure 3.6: The trajectory of the solution $(x_1(t), x_2(t))$ for system (3.23).

Now, we apply the method developed in the previous part to the equation

$$y'' = -0.05\pi y' - \pi^2 y^3 + 7.5\pi^2 \cos(\pi t) + v(t, t_0, \mu_\infty). \quad (3.24)$$

The corresponding control system is

$$\begin{aligned} x_1' &= x_2 \\ x_2' &= -0.05\pi x_2 - \pi^2 x_1^3 + 7.5\pi^2 \cos(\pi t) + v(t, t_1, \bar{\mu}_i). \end{aligned} \quad (3.25)$$

Let $t_1 = 0.5, t_0 = 2.8/3.8$ and $\delta = 0.19$. We take the solution of the last system with $x_1(t_1) = 1$ and $x_2(t_1) = 2$. The control is switched on at $t = \zeta_{25}$ and switched off at $t = \zeta_{60}$. The simulation result is seen in Figure 3.7.

One can see that our way of application of the OGY method does not work for the system (3.25). The reason is that the corresponding non-perturbed Duffing equation to this system has the zero eigenvalue.

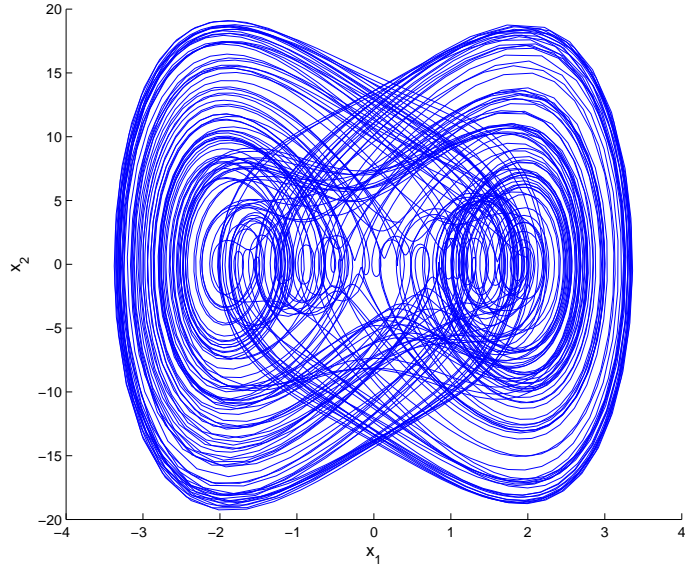


Figure 3.7: The trajectory of the solution $(x_1(t), x_2(t))$ for the control system (3.25), where $m_0 = 2$ and $m_1 = 1$.

3.4 Morphogenesis and the Logistic Map

In Subsection 3.2.2, we demonstrated that the Duffing equation perturbed with a pulse function

$$x'' + 0.18x' + 2x + 0.00004x^3 = 0.02 \cos(2\pi t) + v(t, t_0, \mu_\infty), \quad (3.26)$$

with the coefficients $m_0 = 2$, $m_1 = 1$ and $\mu_\infty = 3.8$, admits the chaos through period-doubling cascade on the time interval $[0, \infty)$ and obeys the Feigenbaum universal behavior [74].

By favour of the new variables $x_1 = x$ and $x_2 = x'$, equation (3.26) can be reduced to the system

$$\begin{aligned} x_1' &= x_2 \\ x_2' &= -0.18x_2 - 2x_1 - 0.00004x_1^3 + 0.02 \cos(2\pi t) + v(t, t_0, \mu_\infty). \end{aligned} \quad (3.27)$$

For the illustration of chaos extension, we will make use of the relay-system (3.27) as the generator, in the role of a core as displayed in Figure 2.5, and attach three replicator systems

with coordinates $x_3 - x_4$, $x_5 - x_6$ and $x_7 - x_8$ to obtain the 8–dimensional result-relay-system

$$\begin{aligned}
x_1' &= x_2 \\
x_2' &= -0.18x_2 - 2x_1 - 0.00004x_1^3 + 0.02 \cos(2\pi t) + v(t, t_0, \mu_\infty) \\
x_3' &= x_4 - 0.1x_1 \\
x_4' &= -10x_3 - 6x_4 - 0.03x_3^3 + 4x_2 \\
x_5' &= x_6 + 2x_1 \\
x_6' &= -2x_5 - 2x_6 + 0.007x_5^3 + 0.6x_2 \\
x_7' &= x_8 - 0.5x_2 \\
x_8' &= -5x_7 - 4x_8 - 0.05x_7^3 + 2.5x_1,
\end{aligned} \tag{3.28}$$

where again $m_0 = 2$, $m_1 = 1$ and $\mu_\infty = 3.8$.

Our theoretical results mentioned in Chapter 2 reveal that system (3.28), as well as the replicators, admit the chaos through period-doubling cascade and obey the universal behavior of Feigenbaum. Figure 3.8 shows the 2–dimensional projections on the $x_1 - x_2$, $x_3 - x_4$, $x_5 - x_6$ and $x_7 - x_8$ planes of the trajectory of the result-relay-system (3.28) with initial data $x_1(0) = 1.37$, $x_2(0) = -0.05$, $x_3(0) = 0.05$, $x_4(0) = -0.1$, $x_5(0) = 1.09$, $x_6(0) = -0.81$, $x_7(0) = 0.08$ and $x_8(0) = 0.21$. The picture seen in Figure 3.8, (a) is the attractor of the generator (3.27) and accordingly Figure 3.8, (b) – (d) represent the attractors of the first, second and the third replicator systems, respectively. It can be easily verified that all replicators used inside the system (3.28) satisfy condition (A7) of Chapter 2. The resemblance of the chaotic attractors of the generator and the replicators is a consequence of morphogenesis of chaos.

Now, let us continue with the control of morphogenesis of chaos by means of the OGY control method. In order to stabilize the unstable periodic solutions of system (3.27), we consider the system

$$\begin{aligned}
x_1' &= x_2 \\
x_2' &= -0.18x_2 - 2x_1 - 0.00004x_1^3 + 0.02 \cos(2\pi t) + v(t, t_1, \bar{\mu}_i) \\
x_3' &= x_4 - 0.1x_1 \\
x_4' &= -10x_3 - 6x_4 - 0.03x_3^3 + 4x_2 \\
x_5' &= x_6 + 2x_1 \\
x_6' &= -2x_5 - 2x_6 + 0.007x_5^3 + 0.6x_2 \\
x_7' &= x_8 - 0.5x_2 \\
x_8' &= -5x_7 - 4x_8 - 0.05x_7^3 + 2.5x_1,
\end{aligned} \tag{3.29}$$

which is the control system conjugate to the result-relay-system (3.28), where $m_0 = 2$ and $m_1 = 1$.

To simulate the control results, we make use of the values $\delta = 0.19$, $t_1 = 0.5$, $t_0 = 2.8/3.8$ and the trajectory of system (3.29) with the initial data $x_1(0) = 1.37$, $x_2(0) = -0.05$, $x_3(0) = 0.05$, $x_4(0) = -0.1$, $x_5(0) = 1.09$, $x_6(0) = -0.81$, $x_7(0) = 0.08$, $x_8(0) = 0.21$. Taking the value $t_0 = 2.8/3.8$ means that the control mechanism is applied around the fixed point of the logistic map, and consequently stabilizes the 2–periodic solutions of the generator and the existing replicators. We switch on the control mechanism at the iteration number $i = 25$ for the logistic

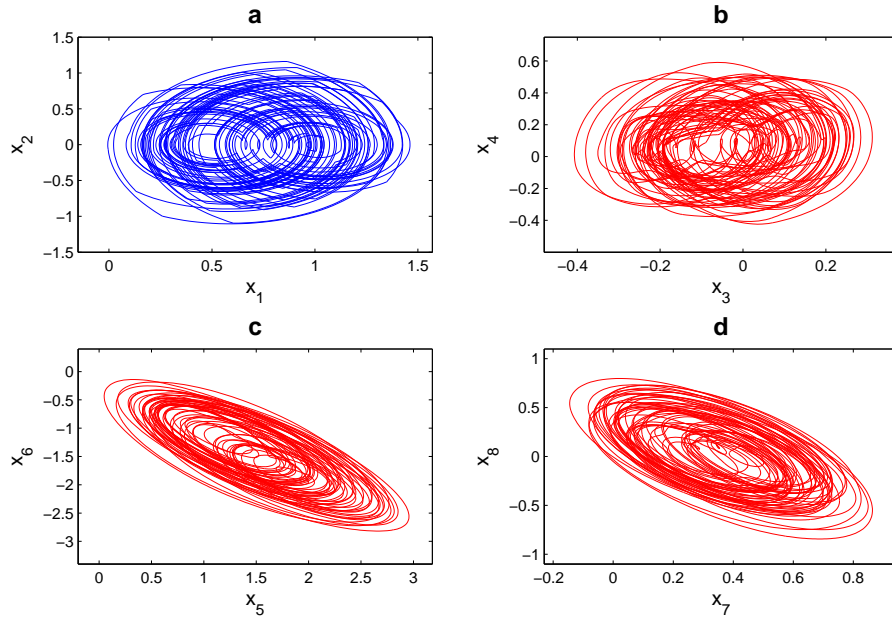


Figure 3.8: 2–dimensional projections of the chaotic attractor of the result-system (3.28). The pictures in (a), (b), (c) and (d) represent the projections on the $x_1 - x_2$, $x_3 - x_4$, $x_5 - x_6$ and $x_7 - x_8$ planes, respectively. The picture in (a) shows the attractor of the prior chaos produced by the generator (3.27), which is a relay-system, and in (b)-(d) the chaotic attractors of the replicator systems are observable. The illustrations in (b)-(d) repeated the structure of the attractor shown in (a), and the mimicry between these pictures is an indicator of the replication of chaos.

map, such that for the continuous-time system this moment corresponds to $t = \zeta_{25}$, and switch off at $i = 125$ which corresponds to the time moment $t = \zeta_{125}$. The graphs of the coordinates x_3, x_5 and x_7 are pictured in Figure 3.9, and it is possible to obtain similar illustrations for the remaining ones, which are not just simulated here. It is observable that the 2–periodic solutions of the replicators and hence of the result-relay-system (3.28) are stabilized. In other words, the extended chaos is controlled, and the result of Theorem 2.9.1 is validated one more time. One can see in Figure 3.9 that after approximately 60 iterations when the control is switched off, the chaos becomes dominant again and irregular motion reappears.

3.5 Discussion

A chaotic attractor contains an infinite number of unstable periodic orbits. The control of chaos is the stabilization of one of these orbits, by means of small perturbations applied to the system. One of the important applications of nonlinear oscillators subjected to non-smooth perturbations is the vibro-impact systems, and such systems can exhibit chaotic motions [29, 50, 101, 125, 214, 228, 245]. The pioneering paper [163] provides the famous OGY method of the control, and there have been proposed many other ideas to control chaos [2, 41, 49,

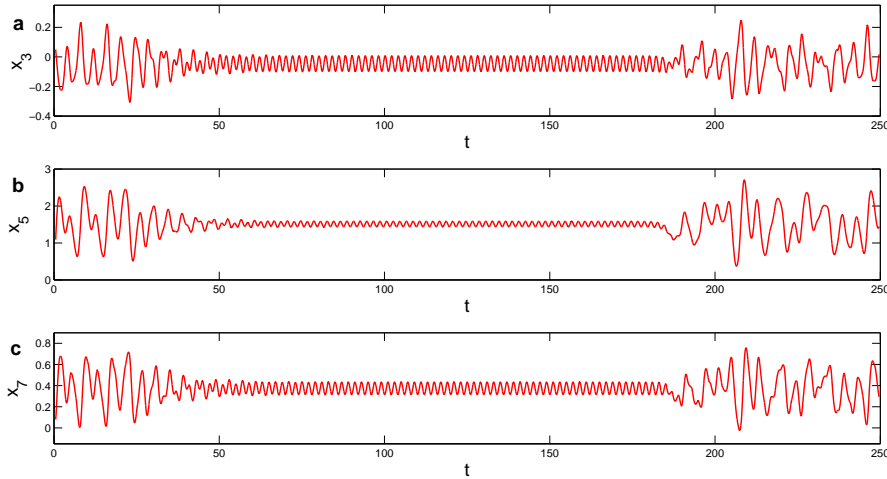


Figure 3.9: OGY control method applied to the result-relay-system (3.28). (a) The graph of the x_3 – coordinate, (b) The graph of the x_5 – coordinate, (c) The graph of the x_7 – coordinate.

63, 135, 177, 209, 237]. The parameters of the Duffing equation can be chosen such that it alternatively admits only regular motions or a chaotic attractor [82, 173, 195, 197, 218, 225, 226, 227]. In the present chapter, the Duffing equation is modified with a pulse function such that it admits the period-doubling cascade of chaos. This idea of insertion of chaotic non-smooth elements in such systems to obtain chaos has been realized in [7, 9, 10, 11, 12, 13].

We have proved that the OGY control of the logistic map stabilizes the unstable periodic solutions embedded in the attractor. The exceptional result is that an arbitrary solution of the system (3.17) approaches to the controlled periodic solution eventually, if the initial moment is chosen properly. Thus, the way is found, which extends control and chaos of low-dimensional maps to continuous systems with arbitrary large dimension. This method can be useful for construction and stabilization of mechanical systems and electric circuits with chaotic features.

One can find that to control chaos of the system (3.4), unstable periodic orbits of the logistic equation must be necessarily controlled. There are several other methods to control chaos of the logistic map such as the method proposed by Pyragas [177] and the extended time delayed auto synchronization method [243]. The main idea of the Pyragas method applied to logistic map is the usage of a perturbation in the form of a delay, that is, a perturbation of the form $\gamma(\kappa_{i-j} - \kappa_i)$. Here, the parameter γ represents the strength of the perturbation and the positive integer j is the order of the desired unstable periodic orbit [177, 243].

To show the results of Pyragas method applied to the system (3.3) with the coefficients $d_1 = 0.18$, $d_2 = 2$, $d_3 = 0.00004$, $D = 0.02$, $k = 2$, and $m_0 = 2$, $m_1 = 1$, $\mu_\infty = 3.8$, we use the method around the period-1 orbit, that is the fixed point, of the logistic map $h(s, \mu) = \mu s(1 - s)$ and

construct the following control system

$$\begin{aligned}
x_1' &= x_2 \\
x_2' &= -2x_1 - 0.18x_2 - 0.00004x_1^3 + 0.02\cos(2\pi t) + v(t, t_1, \mu_\infty) \\
\zeta_{i+1}(t_1, \mu_\infty) &= i + 1 + h(\zeta_i(t_1, \mu_\infty) - i, \mu_\infty) + \gamma(\zeta_{i-1}(t_1, \mu_\infty) \\
&\quad - \zeta_i(t_1, \mu_\infty) + 1).
\end{aligned} \tag{3.30}$$

If we simulate a solution of the last system with $t_1 = 0.5$ and $x_1(t_1) = 0.01$, $x_2(t_1) = 0.025$, the result seen in Figure 3.10 is obtained. It approximates the 2-periodic solution $z_1(t)$ of system (3.3). We use the value $\gamma = -0.5$ and the control starts at time $t = \zeta_{30}$ and ends at $t = \zeta_{100}$.

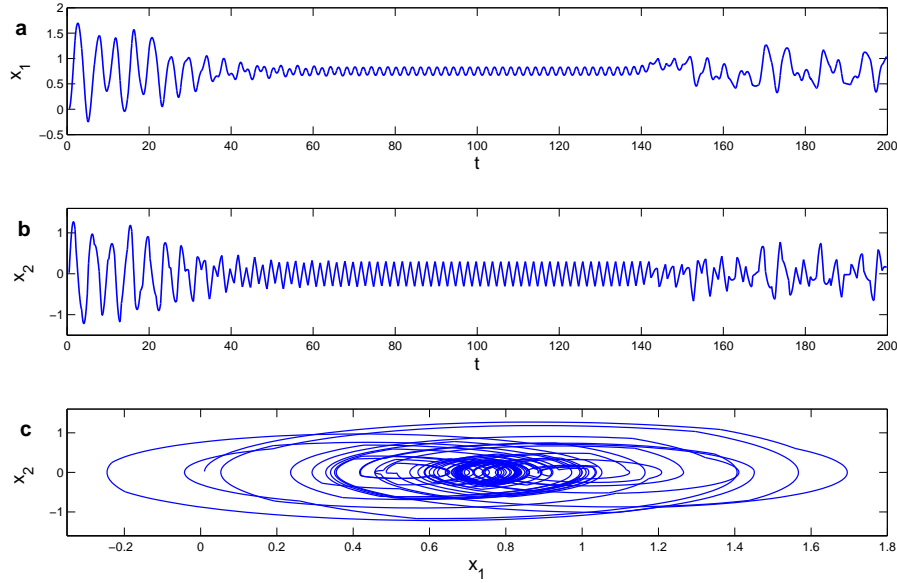


Figure 3.10: The Pyragas control method applied to the Duffing equation perturbed with a pulse function $x'' + 0.18x' + 2x + 0.00004x^3 - 0.02\cos(2\pi t) = v(t, t_0, \mu_\infty)$, where $m_0 = 2$, $m_1 = 1$ and $\mu_\infty = 3.8$. The control starts at time $t = \zeta_{30}$ and ends at $t = \zeta_{100}$. (a) The graph of the x_1 coordinate. (b) The graph of the x_2 coordinate. (c) The trajectory of the solution $(x_1(t), x_2(t))$.

Now, let us analyze through simulation an interesting question if large own frequency of unperturbed Duffing equation may suppress the chaos appearance in the perturbed system. With this aim, consider the system

$$\begin{aligned}
x_1' &= x_2 \\
x_2' &= -50x_1 - 0.18x_2 - 0.00004x_1^3 + 0.02\cos(2\pi t) + v(t, t_0, \mu_\infty),
\end{aligned} \tag{3.31}$$

which is in the form of system (3.3), where $m_0 = 2$, $m_1 = 1$ and $\mu_\infty = 3.8$. The eigenvalues for this system are $-0.09 \mp i\sqrt{50 - 0.09^2}$. Take a solution (x_1, x_2) of the system with initial data $x_1(0.5) = 0.01$ and $x_2(0.5) = 0.025$. One can see that the frequency is high, but the

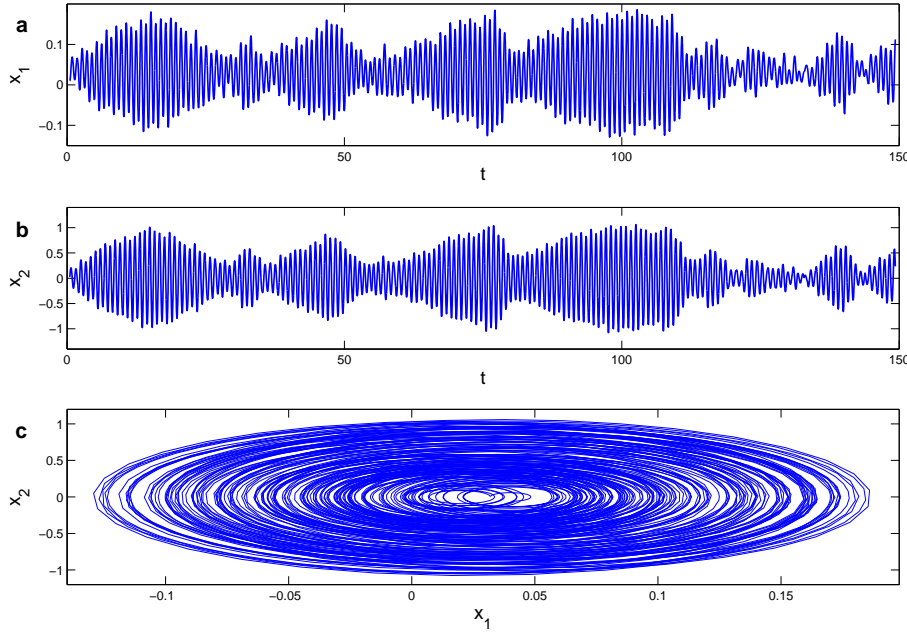


Figure 3.11: Simulation results of the perturbed Duffing equation $x'' + 0.18x' + 50x + 0.00004x^3 - 0.02\cos(2\pi t) = v(t, t_0, \mu_\infty)$, where $m_0 = 2, m_1 = 1$ and $\mu_\infty = 3.8$. (a) The graph of the x_1 coordinate. (b) The graph of the x_2 coordinate. (c) The trajectory of the solution $(x_1(t), x_2(t))$.

simulation seen in Figure 3.11 shows that the chaos appearance is persistent since conditions of our theorems are fulfilled for the system.

We have one more confirmation of our theoretical results. The control environment is sustained for the system (3.31) as seen in Figure 3.12. In this simulation, we take $t_1 = 0.5$, $t_0 = 2.8/3.8$, $\delta = 0.19$, and consider the solution (x_1, x_2) of the control system

$$\begin{aligned} x_1' &= x_2 \\ x_2' &= -50x_1 - 0.18x_2 - 0.00004x_1^3 + 0.02\cos(2\pi t) + v(t, t_1, \bar{\mu}_i), \end{aligned} \quad (3.32)$$

with the initial condition $x_1(t_1) = 0.01$, $x_2(t_1) = 0.025$. The control starts at time $t = \zeta_{25}$ and ends at $t = \zeta_{60}$.

Figure 3.12 supports our results such that the depicted solution approximates the 2-periodic solution $z_1(t)$ of system (3.31). Therefore, one can say that the chaos control results are valid even if the frequency is high. The Pyragas control method can also be used in the case of high frequency.

As the simulation results show, our proposals of generation of chaos and consequently control of it can be extended by the rich diversity of results for discrete maps. Exceptional interest is expected for development of security of communication systems [76, 82, 173, 195]. We suppose also that direct extension of the results can be done on the basis of works, which consider control of chaos generated by the logistic map [147, 148] and uses the map as an

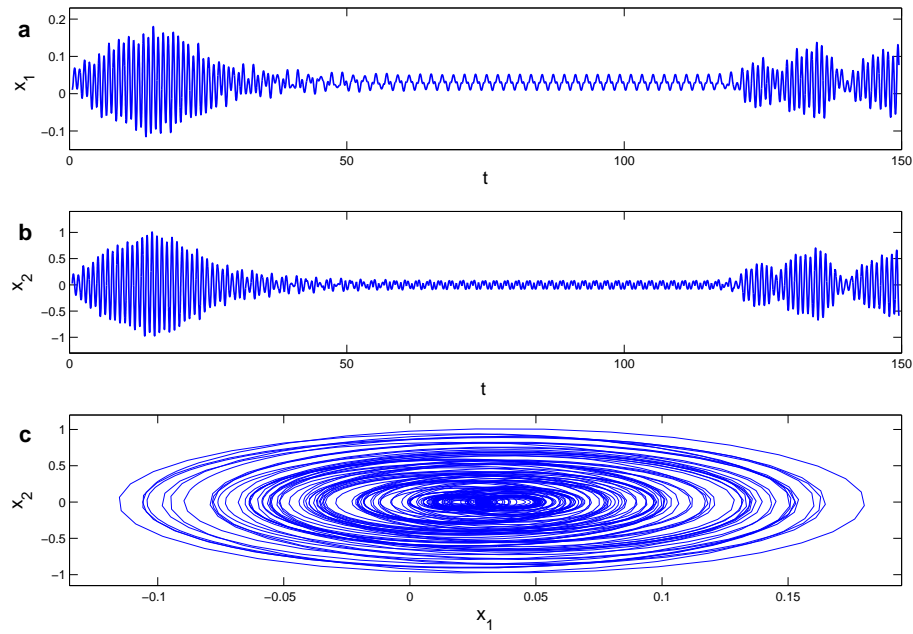


Figure 3.12: The OGY control method applied to the Duffing equation perturbed with a pulse function $x'' + 0.18x' + 50x + 0.00004x^3 - 0.02 \cos(2\pi t) = v(t, t_0, \mu_\infty)$, where $m_0 = 2, m_1 = 1$ and $\mu_\infty = 3.8$. The control starts at time $t = \zeta_{25}$ and ends at $t = \zeta_{60}$. (a) The graph of the x_1 coordinate. (b) The graph of the x_2 coordinate. (c) The trajectory of the solution $(x_1(t), x_2(t))$.

instrument of ciphering and deciphering [33]. Next extension of investigation can be done by the discussion of low dimensional discrete dynamics [57, 149].

Concerning the Lyapunov exponents, we must say that the dynamics of the system (3.4) consist of the continuous dynamics of the differential equation itself and of the discrete dynamics of the switching moments. That is, one can say that our system is a hybrid system [8, 191, 229]. The important fact is that the Lyapunov exponent of the discrete part of the system is a positive one, since it is the Lyapunov exponent of the logistic map [198].

CHAPTER 4

SICNNS WITH CHAOTIC EXTERNAL INPUTS

4.1 Introduction

A class of cellular neural networks, introduced by Bouzerdoum and Pinter [40], is the shunting inhibitory cellular neural networks (SICNNs), which have been extensively applied in psychophysics, speech, perception, robotics, adaptive pattern recognition, vision, and image processing [37, 38, 39, 47, 79, 104, 174].

The model in its most original formulation [40] is as follows. Consider a two dimensional grid of processing cells, and let C_{ij} , $i = 1, 2, \dots, m$, $j = 1, 2, \dots, n$, denote the cell at the (i, j) position of the lattice. Denote by $N_r(i, j)$ the r -neighborhood of C_{ij} , such that

$$N_r(i, j) = \{C_{kl} : \max\{|k - i|, |l - j|\} \leq r, 1 \leq k \leq m, 1 \leq l \leq n\}.$$

In SICNNs, neighboring cells exert mutual inhibitory interactions of the shunting type. The dynamics of the cell C_{ij} is described by the nonlinear ordinary differential equation

$$\frac{dx_{ij}}{dt} = -a_{ij}x_{ij} - \sum_{C_{kl} \in N_r(i, j)} C_{ij}^{kl} f(x_{kl}(t))x_{ij} + L_{ij}(t), \quad (4.1)$$

where x_{ij} is the activity of the cell C_{ij} ; $L_{ij}(t)$ is the external input to C_{ij} ; the constant a_{ij} represents the passive decay rate of the cell activity; $C_{ij}^{kl} \geq 0$ is the connection or coupling strength of postsynaptic activity of the cell C_{kl} transmitted to the cell C_{ij} ; and the activation function $f(x_{kl})$ is a positive continuous function representing the output or firing rate of the cell C_{kl} . For our theoretical discussions, we will consider continuous external inputs.

The existence and the stability of periodic, almost periodic and anti-periodic solutions of SICNNs have been published in papers [46, 66, 99, 132, 165, 171, 199, 235, 236, 244]. The main novelty of the present chapter is the verification of the chaotic behavior in SICNNs. To prove the existence of chaos, we apply the technique based on the Li-Yorke definition [134], and make use of *chaotic external inputs* in the networks. We say that the external inputs are chaotic if they belong to a collection of functions which satisfy the ingredients of chaos. That is, we consider members of a chaotic set as external input terms, and, as a result, we obtain solutions which display chaotic behavior.

Existence of a chaotic attractor in SICNNs with impulses was numerically observed in [88] without a theoretical support, as well it is the case for the paper [212]. Our results can be extended to impulsive systems [12], but they will be very specific.

4.2 Preliminaries

Throughout the chapter, \mathbb{R} will stand for the set of real numbers, and the norm

$$\|u\| = \max_{(i,j)} |u_{ij}|$$

will be used, where

$$u = \{u_{ij}\} = (u_{11}, \dots, u_{1n}, \dots, u_{m1}, \dots, u_{mn}) \in \mathbb{R}^{m \times n}$$

and m, n are natural numbers.

Suppose that \mathcal{B} is a collection of continuous functions $\psi(t) = \{\psi_{ij}(t)\}$, $i = 1, 2, \dots, m$, $j = 1, 2, \dots, n$, such that $\sup_{t \in \mathbb{R}} \|\psi(t)\| \leq M$, where M is a positive number. We start by describing the ingredients of Li-Yorke chaos for the collection \mathcal{B} .

We say that a couple $(\psi(t), \tilde{\psi}(t)) \in \mathcal{B} \times \mathcal{B}$ is proximal if for arbitrary small $\varepsilon > 0$ and arbitrary large $E > 0$, there exist infinitely many disjoint intervals of length not less than E such that $\|\psi(t) - \tilde{\psi}(t)\| < \varepsilon$, for each t from these intervals. On the other hand, a couple $(\psi(t), \tilde{\psi}(t)) \in \mathcal{B} \times \mathcal{B}$ is called frequently (ε_0, Δ) -separated if there exist positive numbers ε_0, Δ and infinitely many disjoint intervals of length not less than Δ , such that $\|\psi(t) - \tilde{\psi}(t)\| > \varepsilon_0$, for each t from these intervals. It is worth saying that the numbers ε_0 and Δ depend on the functions $\psi(t)$ and $\tilde{\psi}(t)$.

A couple $(\psi(t), \tilde{\psi}(t)) \in \mathcal{B} \times \mathcal{B}$ is a Li-Yorke pair if it is proximal and frequently (ε_0, Δ) -separated for some positive numbers ε_0 and Δ . Moreover, an uncountable set $\mathcal{C} \subset \mathcal{B}$ is called a scrambled set if \mathcal{C} does not contain any periodic functions and each couple of different functions inside $\mathcal{C} \times \mathcal{C}$ is a Li-Yorke pair.

\mathcal{B} is called a Li-Yorke chaotic set if: **(i)** There exists a positive number T_0 such that \mathcal{B} possesses a periodic function of period kT_0 , for any $k \in \mathbb{N}$; **(ii)** \mathcal{B} possesses a scrambled set \mathcal{C} ; **(iii)** For any function $\psi(t) \in \mathcal{C}$ and any periodic function $\tilde{\psi}(t) \in \mathcal{B}$, the couple $(\psi(t), \tilde{\psi}(t))$ is frequently (ε_0, Δ) -separated for some positive numbers ε_0 and Δ .

One can obtain a new Li-Yorke chaotic set from a given one as follows. Suppose that $h : \mathbb{R}^{m \times n} \rightarrow \mathbb{R}^{\bar{m} \times \bar{n}}$ is a function which satisfies for all $u_1, u_2 \in \mathbb{R}^{m \times n}$ that

$$L_1 \|u_1 - u_2\| \leq \|h(u_1) - h(u_2)\| \leq L_2 \|u_1 - u_2\|, \quad (4.2)$$

where L_1 and L_2 are positive numbers. One can verify that if the collection \mathcal{B} is Li-Yorke chaotic then the collection \mathcal{B}_h whose elements are of the form $h(\psi(t))$, $\psi(t) \in \mathcal{B}$, is also Li-Yorke chaotic.

The following conditions are needed:

(C1) $\gamma = \min_{(i,j)} a_{ij} > 0$;

(C2) There exist positive numbers M_{ij} such that $\sup_{t \in \mathbb{R}} |L_{ij}(t)| \leq M_{ij}$;

(C3) There exists a positive number M_f such that $\sup_{s \in \mathbb{R}} |f(s)| \leq M_f$;

(C4) There exists a positive number L_f such that $|f(s_1) - f(s_2)| \leq L_f |s_1 - s_2|$ for all $s_1, s_2 \in \mathbb{R}$;

(C5) $M_f \max_{(i,j)} \frac{\sum_{C_{kl} \in N_r(i,j)} C_{ij}^{kl}}{a_{ij}} < 1$;

(C6) $\frac{\bar{c}(L_f K_0 + M_f)}{\gamma} < 1$, where \bar{c} and K_0 are defined as $\bar{c} = \max_{(i,j)} \sum_{C_{kl} \in N_r(i,j)} C_{ij}^{kl}$ and $K_0 = \frac{\max_{(i,j)} \frac{M_{ij}}{a_{ij}}}{1 - M_f \max_{(i,j)} \frac{\sum_{C_{kl} \in N_r(i,j)} C_{ij}^{kl}}{a_{ij}}}$.

Using the theory of quasilinear equations [93], one can verify that a bounded on \mathbb{R} function $x(t) = \{x_{ij}(t)\}$ is a solution of the network (4.1) if and only if the following integral equation is satisfied

$$x_{ij}(t) = - \int_{-\infty}^t e^{-a_{ij}(t-s)} \left[\sum_{C_{kl} \in N_r(i,j)} C_{ij}^{kl} f(x_{kl}(s)) x_{ij}(s) - L_{ij}(s) \right] ds. \quad (4.3)$$

A result about existence of bounded on \mathbb{R} solutions is as follows.

Lemma 4.2.1 *For any $L(t) = \{L_{ij}(t)\}$, $i = 1, 2, \dots, m$, $j = 1, 2, \dots, n$, there exists a unique bounded on \mathbb{R} solution $\phi_L(t) = \{\phi_L^{ij}(t)\}$ of the network (4.1) such that $\sup_{t \in \mathbb{R}} \|\phi_L(t)\| \leq K_0$.*

Proof. Consider the set C_0 of continuous functions $u(t) = \{u_{ij}(t)\}$, $i = 1, 2, \dots, m$, $j = 1, 2, \dots, n$, such that $\|u\|_1 \leq K_0$, where $\|u\|_1 = \sup_{t \in \mathbb{R}} \|u(t)\|$. Define on C_0 the operator Π as

$$(\Pi u)_{ij}(t) \equiv - \int_{-\infty}^t e^{-a_{ij}(t-s)} \left[\sum_{C_{kl} \in N_r(i,j)} C_{ij}^{kl} f(u_{kl}(s)) u_{ij}(s) - L_{ij}(s) \right] ds,$$

where $u(t) = \{u_{ij}(t)\}$ and $\Pi u(t) = \{(\Pi u)_{ij}(t)\}$. If $u(t)$ belongs to C_0 then

$$\begin{aligned} |(\Pi u)_{ij}(t)| &\leq \int_{-\infty}^t e^{-a_{ij}(t-s)} \left[\sum_{C_{kl} \in N_r(i,j)} C_{ij}^{kl} |f(u_{kl}(s))| |u_{ij}(s)| + |L_{ij}(s)| \right] ds \\ &\leq \frac{1}{a_{ij}} \left(M_{ij} + M_f K_0 \sum_{C_{kl} \in N_r(i,j)} C_{ij}^{kl} \right). \end{aligned}$$

Accordingly, we have $\|\Pi u\|_1 \leq \max_{(i,j)} \frac{M_{ij}}{a_{ij}} + M_f K_0 \max_{(i,j)} \frac{\sum_{C_{kl} \in N_r(i,j)} C_{ij}^{kl}}{a_{ij}} = K_0$. Therefore, $\Pi(C_0) \subseteq C_0$.

On the other hand, for any $u, v \in C_0$,

$$\begin{aligned} |(\Pi u)_{ij}(t) - (\Pi v)_{ij}(t)| &\leq \int_{-\infty}^t e^{-a_{ij}(t-s)} \sum_{C_{kl} \in N_r(i,j)} C_{ij}^{kl} \left| f(u_{kl}(s)) u_{ij}(s) \right. \\ &\quad \left. - f(u_{kl}(s)) v_{ij}(s) \right| ds + \int_{-\infty}^t e^{-a_{ij}(t-s)} \sum_{C_{kl} \in N_r(i,j)} C_{ij}^{kl} \left| f(u_{kl}(s)) v_{ij}(s) \right. \\ &\quad \left. - f(v_{kl}(s)) v_{ij}(s) \right| ds \\ &\leq (L_f K_0 + M_f) \max_{(i,j)} \frac{\sum_{C_{kl} \in N_r(i,j)} C_{ij}^{kl}}{a_{ij}} \|u - v\|_1. \end{aligned}$$

Thus, $\|\Pi u - \Pi v\|_1 \leq (L_f K_0 + M_f) \max_{(i,j)} \frac{\sum_{C_{kl} \in N_r(i,j)} C_{ij}^{kl}}{a_{ij}} \|u - v\|_1$, and condition (C6) implies that the operator Π is contractive. Consequently, for any $L(t)$, there exists a unique bounded on \mathbb{R} solution $\phi_L(t)$ of the network (4.1) such that $\sup_{t \in \mathbb{R}} \|\phi_L(t)\| \leq K_0$. \square

For a given $L(t) = \{L_{ij}(t)\}$, $i = 1, 2, \dots, m$, $j = 1, 2, \dots, n$, let us denote by $x_L(t, x_0) = \{x_L^{ij}(t, x_0)\}$ the unique solution of the SICNN (4.1) with $x_L(0, x_0) = x_0$. We note that the solution $x_L(t, x_0)$ is not necessarily bounded on \mathbb{R} .

Consider the set \mathcal{L} whose elements are functions of the form $L(t) = \{L_{ij}(t)\}$, $i = 1, 2, \dots, m$, $j = 1, 2, \dots, n$, such that $\sup_{t \in \mathbb{R}} |L_{ij}(t)| \leq M_{ij}$ for each i and j . Suppose that \mathcal{A} is the collection of functions consisting of the bounded on \mathbb{R} solutions $\phi_L(t)$ of system (4.1), where $L(t) \in \mathcal{L}$. In the present chapter, we assume that \mathcal{L} is an equicontinuous family on \mathbb{R} .

The following assertion confirms the attractiveness of the set \mathcal{A} .

Lemma 4.2.2 *For any $x_0 \in \mathbb{R}^{m \times n}$ and $L(t) = \{L_{ij}(t)\}$, $i = 1, 2, \dots, m$, $j = 1, 2, \dots, n$, we have $\|x_L(t, x_0) - \phi_L(t)\| \rightarrow 0$ as $t \rightarrow \infty$.*

Proof. Making use of the relation

$$\begin{aligned} x_L^{ij}(t, x_0) - \phi_L^{ij}(t) &= e^{-a_{ij}t} \left(x_L^{ij}(0, x_0) - \phi_L^{ij}(0) \right) \\ &\quad - \int_0^t e^{-a_{ij}(t-s)} \left[\sum_{C_{kl} \in N_r(i,j)} C_{ij}^{kl} f(x_L^{kl}(s, x_0)) x_L^{ij}(s, x_0) \right. \\ &\quad \left. - \sum_{C_{kl} \in N_r(i,j)} C_{ij}^{kl} f(\phi_L^{kl}(s)) \phi_L^{ij}(s) \right] ds \end{aligned}$$

we obtain for $t \geq 0$ that

$$\left| x_L^{ij}(t, x_0) - \phi_L^{ij}(t) \right| \leq e^{-a_{ij}t} \left| x_L^{ij}(0, x_0) - \phi_L^{ij}(0) \right|$$

$$\begin{aligned}
& +M_f \sum_{C_{kl} \in N_r(i,j)} C_{ij}^{kl} \int_0^t e^{-a_{ij}(t-s)} \left| x_L^{ij}(s, x_0) - \phi_L^{ij}(s) \right| ds \\
& +L_f K_0 \int_0^t e^{-a_{ij}(t-s)} \sum_{C_{kl} \in N_r(i,j)} C_{ij}^{kl} \left| x_L^{kl}(s, x_0) - \phi_L^{kl}(s) \right| ds.
\end{aligned}$$

The last inequality implies for $t \geq 0$ that

$$e^{\gamma t} \|x_L(t, x_0) - \phi_L(t)\| \leq \|x_0 - \phi_L(0)\| + \bar{c}(L_f K_0 + M_f) \int_0^t e^{\gamma s} \|x_L(s, x_0) - \phi_L(s)\| ds.$$

Applying Gronwall-Bellman Lemma, one can attain that

$$\|x_L(t, x_0) - \phi_L(t)\| \leq \|x_0 - \phi_L(0)\| e^{[\bar{c}(L_f K_0 + M_f) - \gamma]t}, \quad t \geq 0.$$

Consequently, $\|x_L(t, x_0) - \phi_L(t)\| \rightarrow 0$ as $t \rightarrow \infty$, in accordance with condition (C6). \square

Our purpose in the next part is to prove rigorously that if the collection \mathcal{L} is chaotic in the sense of Li-Yorke then the same is true for \mathcal{A} . In other words, if the external input terms $L_{ij}(t)$ behave chaotically, then the dynamics of the SICNNs are also chaotic.

4.3 Chaotic Dynamics

The replication of the ingredients of Li-Yorke chaos from the collection \mathcal{L} to the collection \mathcal{A} will be affirmed in the following two lemmas, and the main conclusion will be stated in Theorem 4.3.1. We start with the following lemma, which indicates existence of proximality in the collection \mathcal{A} .

Lemma 4.3.1 *If a couple of functions $(L(t), \tilde{L}(t)) \in \mathcal{L} \times \mathcal{L}$ is proximal, then the same is true for the couple $(\phi_L(t), \phi_{\tilde{L}}(t)) \in \mathcal{A} \times \mathcal{A}$.*

Proof. Fix an arbitrary small positive number ε and an arbitrary large positive number E . Set

$$R = 2 \left(M_f K_0 \max_{(i,j)} \frac{\sum_{C_{kl} \in N_r(i,j)} C_{ij}^{kl}}{a_{ij}} + \max_{(i,j)} \frac{M_{ij}}{a_{ij}} \right)$$

and

$$0 < \alpha \leq \frac{\gamma - \bar{c}(L_f K_0 + M_f)}{1 + \gamma - \bar{c}(L_f K_0 + M_f)}.$$

Suppose that a given pair $(L(t), \tilde{L}(t)) \in \mathcal{L} \times \mathcal{L}$ is proximal. There exist a sequence of real numbers $\{E_q\}$ satisfying $E_q \geq E$ for each $q \in \mathbb{N}$ and a sequence $\{t_q\}$, $t_q \rightarrow \infty$ as $q \rightarrow \infty$, such that $\|L(t) - \tilde{L}(t)\| < \alpha \varepsilon$ for each t from the disjoint intervals $J_q = [t_q, t_q + E_q]$, $q \in \mathbb{N}$. Let us denote $\phi_L(t) = \{\phi_L^{ij}(t)\}$ and $\phi_{\tilde{L}}(t) = \{\phi_{\tilde{L}}^{ij}(t)\}$.

Fix $q \in \mathbb{N}$. For $t \in J_q$, using the relation (4.3), one can reach up for any i and j that

$$\begin{aligned} \phi_L^{ij}(t) - \phi_{\tilde{L}}^{ij}(t) &= - \int_{-\infty}^t e^{-a_{ij}(t-s)} \left[\sum_{C_{kl} \in N_r(i,j)} C_{ij}^{kl} f(\phi_L^{kl}(s)) \phi_L^{ij}(s) - L_{ij}(s) \right. \\ &\quad \left. - \sum_{C_{kl} \in N_r(i,j)} C_{ij}^{kl} f(\phi_{\tilde{L}}^{kl}(s)) \phi_{\tilde{L}}^{ij}(s) + \tilde{L}_{ij}(s) \right] ds. \end{aligned}$$

By means of the last equation, one can obtain that

$$\begin{aligned} \left| \phi_L^{ij}(t) - \phi_{\tilde{L}}^{ij}(t) \right| &\leq 2 \left(M_f K_0 \frac{\sum_{C_{kl} \in N_r(i,j)} C_{ij}^{kl}}{a_{ij}} + \frac{M_{ij}}{a_{ij}} \right) e^{-a_{ij}(t-t_q)} \\ &\quad + \frac{\alpha \mathcal{E}}{a_{ij}} \left(1 - e^{-a_{ij}(t-t_q)} \right) \\ &\quad + \bar{c}(L_f K_0 + M_f) \int_{t_q}^t e^{-a_{ij}(t-s)} \left\| \phi_L(s) - \phi_{\tilde{L}}(s) \right\| ds. \end{aligned}$$

Accordingly, for $t \in J_q$ we have that

$$\begin{aligned} e^{\gamma t} \left\| \phi_L(t) - \phi_{\tilde{L}}(t) \right\| &\leq R e^{\gamma t_q} + \frac{\alpha \mathcal{E}}{\gamma} (e^{\gamma t} - e^{\gamma t_q}) \\ &\quad + \bar{c}(L_f K_0 + M_f) \int_{t_q}^t e^{\gamma s} \left\| \phi_L(s) - \phi_{\tilde{L}}(s) \right\| ds. \end{aligned}$$

Application of Gronwall's Lemma to the last inequality implies for $t \in J_q$ that

$$\begin{aligned} \left\| \phi_L(t) - \phi_{\tilde{L}}(t) \right\| &\leq \frac{\alpha \mathcal{E}}{\gamma - \bar{c}(L_f K_0 + M_f)} \left(1 - e^{[\bar{c}(L_f K_0 + M_f) - \gamma](t-t_q)} \right) \\ &\quad + R e^{[\bar{c}(L_f K_0 + M_f) - \gamma](t-t_q)}. \end{aligned}$$

Suppose that the number E is sufficiently large such that

$$E > \frac{2}{\gamma - \bar{c}(L_f K_0 + M_f)} \ln \left(\frac{R}{\alpha \mathcal{E}} \right).$$

In this case, if t belongs to the interval $[t_q + E/2, t_q + E_q]$, then

$$R e^{[\bar{c}(L_f K_0 + M_f) - \gamma](t-t_q)} < \alpha \mathcal{E}.$$

Thus, for $t \in [t_q + E/2, t_q + E_q]$, the inequality

$$\left\| \phi_L(t) - \phi_{\tilde{L}}(t) \right\| < \left(1 + \frac{1}{\gamma - \bar{c}(L_f K_0 + M_f)} \right) \alpha \mathcal{E} \leq \varepsilon.$$

is valid. Consequently, since the last inequality holds for each t from the disjoint intervals $J_q^1 = [t_q + E/2, t_q + E_q]$, $q \in \mathbb{N}$, the couple $(\phi_L(t), \phi_{\tilde{L}}(t)) \in \mathcal{A} \times \mathcal{A}$ is proximal. \square

Now, let us continue with the replication the second main ingredient of Li-Yorke chaos in the next lemma.

Lemma 4.3.2 *If a couple $(L(t), \tilde{L}(t)) \in \mathcal{L} \times \mathcal{L}$ is frequently (ε_0, Δ) -separated for some positive numbers ε_0 and Δ , then there exist positive numbers ε_1 and $\bar{\Delta}$ such that the couple $(\phi_L(t), \phi_{\tilde{L}}(t)) \in \mathcal{A} \times \mathcal{A}$ is frequently $(\varepsilon_1, \bar{\Delta})$ -separated.*

Proof. Suppose that a given couple $(L(t), \tilde{L}(t)) \in \mathcal{L} \times \mathcal{L}$ is frequently (ε_0, Δ) separated, for some $\varepsilon_0 > 0$ and $\Delta > 0$. In this case, there exist infinitely many disjoint intervals $J_q, q \in \mathbb{N}$, each with length not less than Δ , such that $\|L(t) - \tilde{L}(t)\| > \varepsilon_0$ for each t from these intervals. In the proof, we will verify the existence of positive numbers $\varepsilon_1, \bar{\Delta}$ and infinitely many disjoint intervals $J_q^1 \subset J_q, q \in \mathbb{N}$, each with length $\bar{\Delta}$, such that the inequality $\|\phi_L(t) - \phi_{\tilde{L}}(t)\| > \varepsilon_1$ holds for each t from the intervals $J_q^1, q \in \mathbb{N}$.

According to the equicontinuity of \mathcal{L} , one can find a positive number $\tau < \Delta$, such that for any $t_1, t_2 \in \mathbb{R}$ with $|t_1 - t_2| < \tau$, the inequality

$$\left| \left(L_{ij}(t_1) - \tilde{L}_{ij}(t_1) \right) - \left(L_{ij}(t_2) - \tilde{L}_{ij}(t_2) \right) \right| < \frac{\varepsilon_0}{2} \quad (4.4)$$

holds for all $1 \leq i \leq m, 1 \leq j \leq n$.

Suppose that for each $q \in \mathbb{N}$, the number s_q denotes the midpoint of the interval J_q . Let us define a sequence $\{\theta_q\}$ through the equation $\theta_q = s_q - \tau/2$.

Let us fix an arbitrary $q \in \mathbb{N}$. One can find integers i_0, j_0 , such that

$$\left| L_{i_0 j_0}(s_q) - \tilde{L}_{i_0 j_0}(s_q) \right| = \left\| L(s_q) - \tilde{L}(s_q) \right\| > \varepsilon_0. \quad (4.5)$$

Making use of the inequality (4.4), for all $t \in [\theta_q, \theta_q + \tau]$ we have

$$\begin{aligned} & \left| L_{i_0 j_0}(s_q) - \tilde{L}_{i_0 j_0}(s_q) \right| - \left| L_{i_0 j_0}(t) - \tilde{L}_{i_0 j_0}(t) \right| \\ & \leq \left| \left(L_{i_0 j_0}(t) - \tilde{L}_{i_0 j_0}(t) \right) - \left(L_{i_0 j_0}(s_q) - \tilde{L}_{i_0 j_0}(s_q) \right) \right| \\ & < \frac{\varepsilon_0}{2} \end{aligned}$$

and therefore, by means of (4.5), we achieve that the inequality

$$\left| L_{i_0 j_0}(t) - \tilde{L}_{i_0 j_0}(t) \right| > \left| L_{i_0 j_0}(s_q) - \tilde{L}_{i_0 j_0}(s_q) \right| - \frac{\varepsilon_0}{2} > \frac{\varepsilon_0}{2} \quad (4.6)$$

is valid for all $t \in [\theta_q, \theta_q + \tau]$.

For each i and j , one can find numbers $\zeta_{ij}^q \in [\theta_q, \theta_q + \tau]$ such that

$$\int_{\theta_q}^{\theta_q + \tau} \left(L(s) - \tilde{L}(s) \right) ds = \tau \left(L_{11}(\zeta_{11}^q) - \tilde{L}_{11}(\zeta_{11}^q), \dots, L_{mn}(\zeta_{mn}^q) - \tilde{L}_{mn}(\zeta_{mn}^q) \right).$$

Thus, according to the inequality (4.6), we have that

$$\left\| \int_{\theta_q}^{\theta_q + \tau} \left(L(s) - \tilde{L}(s) \right) ds \right\| \geq \tau \left| L_{i_0 j_0}(\zeta_{i_0 j_0}^q) - \tilde{L}_{i_0 j_0}(\zeta_{i_0 j_0}^q) \right| > \frac{\tau \varepsilon_0}{2}. \quad (4.7)$$

For $t \in [\theta_q, \theta_q + \tau]$, using the couple of relations

$$\phi_L^{ij}(t) = \phi_L^{ij}(\theta_q) - \int_{\theta_q}^t \left[a_{ij} + \sum_{C_{kl} \in N_r(i,j)} C_{ij}^{kl} f(\phi_L^{kl}(s)) \right] \phi_L^{ij}(s) ds + \int_{\theta_q}^t L_{ij}(s) ds,$$

and

$$\phi_L^{ij}(t) = \phi_L^{ij}(\theta_q) - \int_{\theta_q}^t \left[a_{ij} + \sum_{C_{kl} \in N_r(i,j)} C_{ij}^{kl} f(\phi_L^{kl}(s)) \right] \phi_L^{ij}(s) ds + \int_{\theta_q}^t \tilde{L}_{ij}(s) ds,$$

it can be verified that

$$\begin{aligned} & \phi_L^{ij}(\theta_q + \tau) - \phi_{\tilde{L}}^{ij}(\theta_q + \tau) = \int_{\theta_q}^{\theta_q + \tau} (L_{ij}(s) - \tilde{L}_{ij}(s)) ds \\ & + (\phi_L^{ij}(\theta_q) - \phi_{\tilde{L}}^{ij}(\theta_q)) - \int_{\theta_q}^{\theta_q + \tau} a_{ij} (\phi_L^{ij}(s) - \phi_{\tilde{L}}^{ij}(s)) ds \\ & - \int_{\theta_q}^{\theta_q + \tau} \left[\sum_{C_{kl} \in N_r(i,j)} C_{ij}^{kl} f(\phi_L^{kl}(s)) \phi_L^{ij}(s) - \sum_{C_{kl} \in N_r(i,j)} C_{ij}^{kl} f(\phi_{\tilde{L}}^{kl}(s)) \phi_{\tilde{L}}^{ij}(s) \right] ds. \end{aligned}$$

Hence we achieve that

$$\begin{aligned} & \left\| \phi_L(\theta_q + \tau) - \phi_{\tilde{L}}(\theta_q + \tau) \right\| \geq \left\| \int_{\theta_q}^{\theta_q + \tau} (L(s) - \tilde{L}(s)) ds \right\| \\ & - \left\| \phi_L(\theta_q) - \phi_{\tilde{L}}(\theta_q) \right\| - \max_{(i,j)} \left| \int_{\theta_q}^{\theta_q + \tau} a_{ij} (\phi_L^{ij}(s) - \phi_{\tilde{L}}^{ij}(s)) ds \right| \\ & - \max_{(i,j)} \left| \int_{\theta_q}^{\theta_q + \tau} \left[\sum_{C_{kl} \in N_r(i,j)} C_{ij}^{kl} f(\phi_L^{kl}(s)) \phi_L^{ij}(s) - \sum_{C_{kl} \in N_r(i,j)} C_{ij}^{kl} f(\phi_{\tilde{L}}^{kl}(s)) \phi_{\tilde{L}}^{ij}(s) \right] ds \right|. \end{aligned} \quad (4.8)$$

Let us denote $\bar{\gamma} = \max_{(i,j)} a_{ij}$ and $H_0 = \max_{(i,j)} M_{ij}$. The inequalities (4.7) and (4.8) together imply that

$$\begin{aligned} & \max_{t \in [\theta_q, \theta_q + \tau]} \left\| \phi_L(t) - \phi_{\tilde{L}}(t) \right\| \geq \left\| \phi_L(\theta_q + \tau) - \phi_{\tilde{L}}(\theta_q + \tau) \right\| \\ & > \frac{\tau \varepsilon_0}{2} - [1 + \tau \bar{\gamma} + \tau \bar{c}(L_f K_0 + M_f)] \max_{t \in [\theta_q, \theta_q + \tau]} \left\| \phi_L(t) - \phi_{\tilde{L}}(t) \right\|. \end{aligned}$$

Therefore, we have $\max_{t \in [\theta_q, \theta_q + \tau]} \left\| \phi_L(t) - \phi_{\tilde{L}}(t) \right\| > \bar{\varepsilon}$, where

$$\bar{\varepsilon} = \frac{\tau \varepsilon_0}{2[2 + \tau \bar{\gamma} + \tau \bar{c}(L_f K_0 + M_f)]}.$$

Suppose that $\max_{t \in [\theta_q, \theta_q + \tau]} \left\| \phi_L(t) - \phi_{\tilde{L}}(t) \right\| = \left\| \phi_L(\xi_q) - \phi_{\tilde{L}}(\xi_q) \right\|$, for some $\xi_q \in [\theta_q, \theta_q + \tau]$. Define

$$\bar{\Delta} = \min \left\{ \frac{\tau}{2}, \frac{\bar{\varepsilon}}{4(H_0 + K_0 \bar{\gamma} + M_f K_0 \bar{c})} \right\}$$

and let

$$\theta_q^1 = \begin{cases} \xi_q, & \text{if } \xi_q \leq \theta_q + \tau/2 \\ \xi_q - \bar{\Delta}, & \text{if } \xi_q > \theta_q + \tau/2 \end{cases}.$$

For $t \in [\theta_q^1, \theta_q^1 + \bar{\Delta}]$, by favour of the integral equation

$$\phi_L^{ij}(t) - \phi_{\tilde{L}}^{ij}(t) = (\phi_L^{ij}(\xi_q) - \phi_{\tilde{L}}^{ij}(\xi_q))$$

$$\begin{aligned}
& + \int_{\xi_q}^t \left(L_{ij}(s) - \tilde{L}_{ij}(s) \right) ds - \int_{\xi_q}^t a_{ij} \left(\phi_L^{ij}(s) - \phi_{\tilde{L}}^{ij}(s) \right) ds \\
& - \int_{\xi_q}^t \left[\sum_{C_{kl} \in N_r(i,j)} C_{ij}^{kl} f(\phi_L^{kl}(s)) \phi_L^{ij}(s) - \sum_{C_{kl} \in N_r(i,j)} C_{ij}^{kl} f(\phi_{\tilde{L}}^{kl}(s)) \phi_{\tilde{L}}^{ij}(s) \right] ds,
\end{aligned}$$

we have

$$\begin{aligned}
& \|\phi_L(t) - \phi_{\tilde{L}}(t)\| \geq \|\phi_L(\xi_q) - \phi_{\tilde{L}}(\xi_q)\| \\
& - \max_{(i,j)} \left| \int_{\xi_q}^t \left(L_{ij}(s) - \tilde{L}_{ij}(s) \right) ds \right| - \max_{(i,j)} \left| \int_{\xi_q}^t a_{ij} \left(\phi_L^{ij}(s) - \phi_{\tilde{L}}^{ij}(s) \right) ds \right| \\
& - \max_{(i,j)} \left| \int_{\xi_q}^t \left[\sum_{C_{kl} \in N_r(i,j)} C_{ij}^{kl} f(\phi_L^{kl}(s)) \phi_L^{ij}(s) - \sum_{C_{kl} \in N_r(i,j)} C_{ij}^{kl} f(\phi_{\tilde{L}}^{kl}(s)) \phi_{\tilde{L}}^{ij}(s) \right] ds \right| \\
& > \bar{\varepsilon} - 2\bar{\Delta} (H_0 + K_0\bar{\gamma} + M_f K_0\bar{c}) \\
& \geq \frac{\bar{\varepsilon}}{2}.
\end{aligned}$$

Consequently, for each t from the disjoint intervals $J_q^1 = [\theta_q^1, \theta_q^1 + \bar{\Delta}]$, $q \in \mathbb{N}$, the inequality $\|\phi_L(t) - \phi_{\tilde{L}}(t)\| > \varepsilon_1$ holds, where $\varepsilon_1 = \bar{\varepsilon}/2$. \square

The following theorem, which is the main result of the present article, indicates that the network (4.1) is chaotic, provided that the external inputs are chaotic.

Theorem 4.3.1 *If \mathcal{L} is a Li-Yorke chaotic set, then the same is true for \mathcal{A} .*

Proof. Assume that the set \mathcal{L} is Li-Yorke chaotic. Under the circumstances, there exists a positive number T_0 such that for any natural number k , \mathcal{L} possesses a periodic function of period kT_0 . One can confirm that $L(t) \in \mathcal{L}$ is kT_0 -periodic if and only if $\phi_L(t) \in \mathcal{A}$ is kT_0 -periodic. Therefore, the set \mathcal{A} contains a kT_0 -periodic function for any natural number k .

Next, suppose that \mathcal{L}_S is a scrambled set inside \mathcal{L} and take into account the collection \mathcal{A}_S with elements of the form $\phi_L(t)$, where $L(t) \in \mathcal{L}_S$. Since \mathcal{L}_S is uncountable, the set \mathcal{A}_S is also uncountable. Due to the one-to-one correspondence between the periodic functions inside \mathcal{L} and \mathcal{A} , no periodic functions exist inside \mathcal{A}_S .

According to Lemmas 4.3.1 and 4.3.2, \mathcal{A}_S is a scrambled set. Moreover, Lemma 4.3.2 implies that each couple of functions inside $\mathcal{A}_S \times \mathcal{A}_P$ is frequently $(\varepsilon_1, \bar{\Delta})$ -separated for some positive numbers ε_1 and $\bar{\Delta}$, where \mathcal{A}_P denotes the set of all periodic functions inside \mathcal{A} . Consequently, the set \mathcal{A} is Li-Yorke chaotic. \square

Remark 4.3.1 *Combining the result of Theorem 4.3.1 with the one of Lemma 4.2.2, we conclude that a chaotic attractor takes place in the dynamics of system (4.1).*

4.4 Examples

To actualize the results of the chapter, one needs a source of external inputs, $L_{ij}(t)$, which are ensured to be chaotic in the Li-Yorke sense. For this reason, in the first example, we will take into account SICNNs whose external inputs are relay functions with chaotically changing switching moments. Then, to support our new theoretical results, we will make use of the solutions of this network as external inputs for another SICNNs, which is the main illustrative object for the results of the chapter. To increase the flexibility of our method for applications, we will also take advantage of nonlinear functions to build chaotic inputs.

Example 1. Let us introduce the *SICNN*

$$\frac{dz_{ij}}{dt} = -b_{ij}z_{ij} - \sum_{D_{kl} \in \mathcal{N}_1(i,j)} D_{ij}^{kl} g(z_{kl}(t)) z_{ij} + v_{ij}(t, t_0), \quad (4.9)$$

in which $i, j = 1, 2, 3$,

$$\begin{pmatrix} b_{11} & b_{12} & b_{13} \\ b_{21} & b_{22} & b_{23} \\ b_{31} & b_{32} & b_{33} \end{pmatrix} = \begin{pmatrix} 8 & 4 & 7 \\ 10 & 6 & 5 \\ 6 & 4 & 1 \end{pmatrix},$$

$$\begin{pmatrix} D_{11} & D_{12} & D_{13} \\ D_{21} & D_{22} & D_{23} \\ D_{31} & D_{32} & D_{33} \end{pmatrix} = \begin{pmatrix} 0.006 & 0 & 0.001 \\ 0.009 & 0.002 & 0.003 \\ 0 & 0.005 & 0.004 \end{pmatrix}.$$

In equation (4.9), D_{ij} denotes the cell at the (i, j) position of the lattice, and for each i, j , the relay function $v_{ij}(t, t_0)$ is defined by the equation

$$v_{ij}(t, t_0) = \begin{cases} \alpha_{ij}, & \text{if } \zeta_{2q}(t_0) < t \leq \zeta_{2q+1}(t_0), \\ \beta_{ij}, & \text{if } \zeta_{2q-1}(t_0) < t \leq \zeta_{2q}(t_0), \end{cases}$$

where $t_0 \in [0, 1]$ and the numbers $\zeta_q(t_0)$, $q \in \mathbb{Z}$, denote the switching moments, which are the same for all i, j . The switching moments are defined through the formula $\zeta_q(t_0) = q + \kappa_q(t_0)$, $q \in \mathbb{Z}$, where the sequence $\{\kappa_q(t_0)\}$, $\kappa_0(t_0) = t_0$, is generated by the logistic equation $\kappa_{q+1}(t_0) = 3.9\kappa_q(t_0)(1 - \kappa_q(t_0))$, which is chaotic in the Li-Yorke sense [134]. More information about the dynamics of relay systems and replication of chaos can be found in papers [9, 10, 14, 15, 16, 18].

In system (4.9), let $g(s) = s^2$ and $\alpha_{ij} = 1$, $\beta_{ij} = 2$ for all i, j . By results of the paper [9], the family $\{v_{ij}(t, t_0)\}$, $t_0 \in [0, 1]$, is chaotic in the sense of Li-Yorke, and the collection \mathcal{L} consisting of elements of the form $z(t) = \{z_{ij}(t)\}$, where $z(t)$ are bounded on \mathbb{R} solutions of (4.9), is a Li-Yorke chaotic set.

Next, we consider the simulations of the network (4.9). Figure 4.1 represents the chaotic solution $z(t) = \{z_{ij}(t)\}$ of (4.9) with $z_{11}(t_0) = 0.1678$, $z_{12}(t_0) = 0.3956$, $z_{13}(t_0) = 0.1987$, $z_{21}(t_0) = 0.1261$, $z_{22}(t_0) = 0.2405$, $z_{23}(t_0) = 0.3012$, $z_{31}(t_0) = 0.2412$, $z_{32}(t_0) = 0.3942$, $z_{33}(t_0) = 1.6692$, where $t_0 = 0.45$.

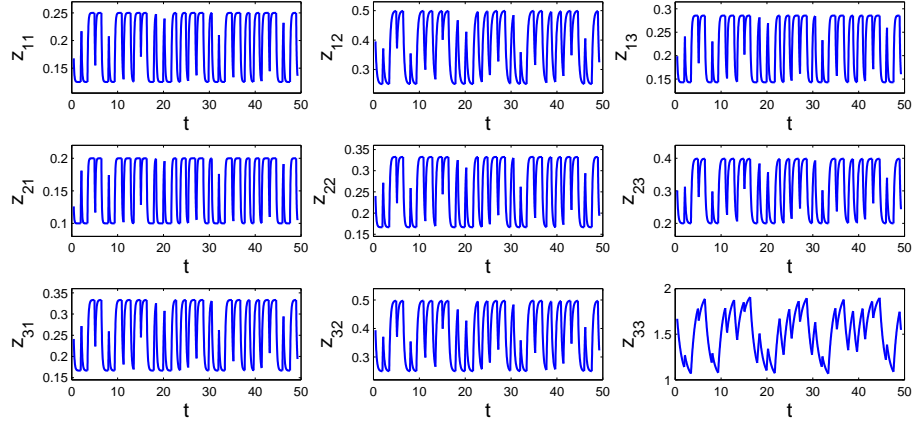


Figure 4.1: The chaotic behavior of the *SICNN* (4.9).

In Example 1, to procure a Li-Yorke chaotic set, we used an *SICNN* in the form of (4.1), where the terms $L_{ij}(t)$ are replaced by relay functions $v_{ij}(t, t_0)$, whose switching moments change chaotically. Now, to support the results of the present chapter, we will construct another *SICNN*, but this time we will use external inputs of the form $L_{ij}(t) = h_{ij}(z(t))$, where $z(t)$ are the chaotic solutions of the network (4.9) and $h(v) = \{h_{ij}(v)\}$ is a nonlinear function which satisfies the inequality (4.2).

Example 2. Consider the following *SICNN*,

$$\frac{dx_{ij}}{dt} = -a_{ij}x_{ij} - \sum_{C_{kl} \in N_1(i,j)} C_{ij}^{kl} f(x_{kl}(t))x_{ij} + L_{ij}(t), \quad (4.10)$$

in which $i, j = 1, 2, 3$,

$$\begin{pmatrix} a_{11} & a_{12} & a_{13} \\ a_{21} & a_{22} & a_{23} \\ a_{31} & a_{32} & a_{33} \end{pmatrix} = \begin{pmatrix} 5 & 12 & 2 \\ 6 & 4 & 8 \\ 2 & 9 & 3 \end{pmatrix},$$

$$\begin{pmatrix} C_{11} & C_{12} & C_{13} \\ C_{21} & C_{22} & C_{23} \\ C_{31} & C_{32} & C_{33} \end{pmatrix} = \begin{pmatrix} 0.02 & 0.04 & 0.06 \\ 0.04 & 0.07 & 0.09 \\ 0.03 & 0.04 & 0.08 \end{pmatrix},$$

and $f(s) = \frac{1}{2}s^3$. One can calculate that

$$\begin{aligned} \sum_{C_{kl} \in N_1(1,1)} C_{11}^{kl} &= 0.17, & \sum_{C_{kl} \in N_1(1,2)} C_{12}^{kl} &= 0.32, & \sum_{C_{kl} \in N_1(1,3)} C_{13}^{kl} &= 0.26, \\ \sum_{C_{kl} \in N_1(2,1)} C_{21}^{kl} &= 0.24, & \sum_{C_{kl} \in N_1(2,2)} C_{22}^{kl} &= 0.47, & \sum_{C_{kl} \in N_1(2,3)} C_{23}^{kl} &= 0.38, \\ \sum_{C_{kl} \in N_1(3,1)} C_{31}^{kl} &= 0.18, & \sum_{C_{kl} \in N_1(3,2)} C_{32}^{kl} &= 0.35, & \sum_{C_{kl} \in N_1(3,3)} C_{33}^{kl} &= 0.28. \end{aligned}$$

In the previous example, we obtained a network whose solutions behave chaotically. Now, we will make these solutions as external inputs for (4.10), with the help of a nonlinear function h .

Define a function $h(v) = \{h_{ij}(v)\}$, where $v = \{v_{ij}\}$, $i, j = 1, 2, 3$, through the equations $h_{11}(v) = 2v_{11} + \sin(v_{11})$, $h_{12}(v) = \frac{3}{2}v_{12}^2$, $h_{13}(v) = e^{v_{13}}$, $h_{21}(v) = \tan\left(\frac{v_{21}}{2}\right)$, $h_{22}(v) = v_{22} + \arctan v_{22}$, $h_{23}(v) = \frac{v_{23}^2 - v_{23} - 1}{v_{23} - 1}$, $h_{31}(v) = \frac{2}{3}(2 + v_{31})^{3/2}$, $h_{32}(v) = \tanh(v_{32})$, $h_{33}(v) = \frac{1}{4}v_{33}^3 + \frac{1}{5}v_{33}$. We note that the inequality (4.2) can be verified by using the bounded regions where each component function $z_{ij}(t)$ lies in. Accordingly, the set \mathcal{L}_h whose elements are of the form $h(z(t))$, $z(t) \in \mathcal{L}$, where \mathcal{L} is the set of bounded on \mathbb{R} solutions of (4.9), is Li-Yorke chaotic. Moreover, for each $z(t) \in \mathcal{L}$ we have $|h_{ij}(z(t))| \leq M_{ij}$, where $M_{11} = 0.78$, $M_{12} = 0.54$, $M_{13} = 1.35$, $M_{21} = 0.11$, $M_{22} = 0.69$, $M_{23} = 2.11$, $M_{31} = 2.41$, $M_{32} = 0.51$ and $M_{33} = 2.4$.

Consider the network (4.10) with $L_{ij}(t) = h_{ij}(z(t))$, where $h(z(t)) = \{h_{ij}(z(t))\} \in \mathcal{L}_h$. In this case, the condition (C6) holds for (4.10) with $M_f = 0.864$, $L_f = 2.16$, $K_0 = 1.36$, $\gamma = 2$ and $\bar{c} = 0.47$. The results of Theorem 4.3.1 ensure us to say that the collection \mathcal{A} with elements $\phi_z(t)$, $z(t) \in \mathcal{L}$, is Li-Yorke chaotic.

In the SICNN (4.10), we use the chaotically behaving solution $z(t) = \{z_{ij}(t)\}$ which is simulated in Example 1, and depict in Figure 4.2 the solution of (4.10) with $x_{11}(t_0) = 0.1341$, $x_{12}(t_0) = 0.0247$, $x_{13}(t_0) = 0.6493$, $x_{21}(t_0) = 0.0143$, $x_{22}(t_0) = 0.1503$, $x_{23}(t_0) = 0.2394$, $x_{31}(t_0) = 1.1574$, $x_{32}(t_0) = 0.0467$ and $x_{33}(t_0) = 0.5145$, where $t_0 = 0.45$. Figure 4.2 reveals that each cell C_{ij} , $i, j = 1, 2, 3$, behave chaotically, and this supports the result mentioned in Theorem 4.3.1. Moreover, Figure 4.3 shows the projection of the same trajectory on the $x_{22} - x_{31} - x_{33}$ space, and this figure also confirms the results of the present chapter.

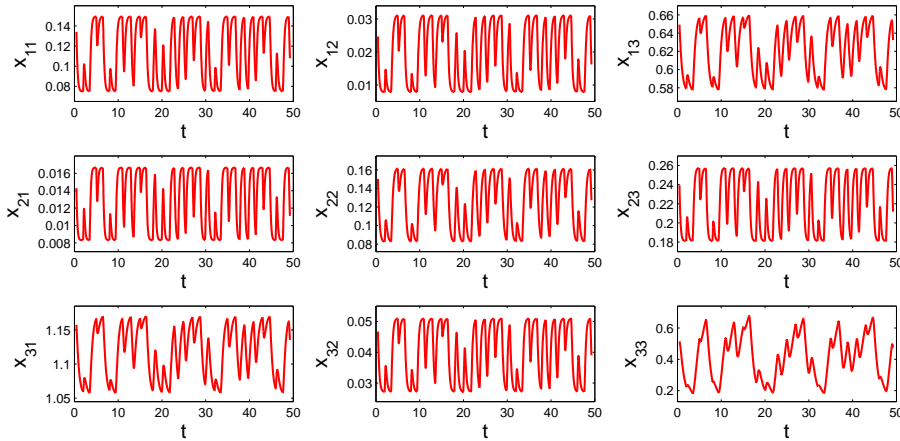


Figure 4.2: The chaotic behavior of the SICNN (4.10).

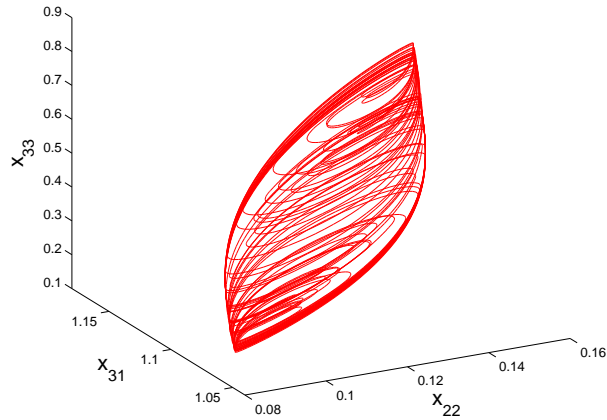


Figure 4.3: The projection of the chaotic attractor of the network (4.10) on the $x_{22} - x_{31} - x_{33}$ space.

4.5 Discussion

In this chapter, it is shown that SICNNs with chaotic external inputs admit a chaotic attractor. Considering this phenomenon with the input-output mechanism, one can say about chaos expansion among nonlinearly coupled SICNNs. The presented two examples considered together illustrate the possibility. Our method can be applied to other types of chaos, for example, that one analyzed through period-doubling cascade. The approach is suitable for the control of unstable periodic motions. Our results can be applied to the studies of chaotic communication, combinatorial optimization problems and on problems that have local minima in energy (cost) functions.

CHAPTER 5

CONCLUSIONS

Replication of different types of chaos such as the one obtained by period-doubling cascade, Devaney's and Li-Yorke chaos is recognized in the thesis. The definitions of chaotic sets as well as the hyperbolic sets of continuous functions are introduced, and the replication of the chaos is proved rigorously. The morphogenesis mechanism considered in our study is based on a chaos generating element inserted in a network of systems. Replication of intermittency as well as Shil'nikov orbits are discussed. Morphogenesis of the double-scroll Chua's attractor and quasiperiodical motions as a possible skeleton of a chaotic attractor are demonstrated numerically. We handled the problem of chaos generation in Duffing oscillators through period-doubling cascade by means of perturbations in the form of a relay function. In the thesis, it is also shown that chaotic external inputs make the dynamics of shunting inhibitory cellular neural networks behave chaotically. Moreover, control problem of the extended chaos is realized. Some of the results are illustrated through the relay system's dynamics, and appropriate simulations are presented using the indicated method successively. The results mentioned in this thesis are published in the papers [16, 18, 19], and the simulations are prepared by using MATLAB [144]. The presented methods are useful for creating chaos in systems that are encountered in mechanics, electrical systems, economic theory, meteorology, neural networks theory and communication systems.

The concept of self-replicating machines, in the abstract sense, starts with the ideas of von Neumann [160] and these ideas are supposed to be the origins of cellular automata theory [193]. Morphogenesis was deeply involved in mathematical discussions through Turing's investigations [223] as well as in the concept of structural stability [216]. In the thesis, the term "morphogenesis" is used in the meaning of "processes creating forms" where we accept the *form* not only as a type of chaos, but also accompanying concepts as the structure of the chaotic attractor, its fractal dimension, form of the bifurcation diagram, the spectra of Lyapunov exponents, inheritance of intermittency, etc. This is similar to the idea such that morphogenesis is used in fields such as urban studies [58], architecture [182], mechanics [213], computer science [36], linguistics [91] and sociology [25, 45].

According to von Neumann, it is feasible in principle to create a self-replicating machine, which he refers as an "automaton", by starting with a machine A , which has the ability to construct any other machine once it is furnished with a set of instructions, and then attaching

to A another component B that can make a copy of any instruction supplied to it. Together with a third component labeled C , it is possible to create a machine, denoted by R , with components A, B and C such that C is responsible to initiate A to construct a machine as described by the instructions, then make B to create a copy of the instructions, and supply the copy of the instructions to the entire apparatus. The component C is referred as “control mechanism”. It is the resulting machine R' , obtained by furnishing the machine R by instructions I_R , that is capable of replicating itself. Multiple usage of the set of instructions I_R is crucial in the mechanism of self-replication. First, the instructions must be fulfilled by the machine A , then they must be copied by B , and finally the copy must be attached to machine R to form the system R' once again [160, 193].

Our theory of morphogenesis of chaos relates the ideas of von Neumann about self-replicating machines in the following sense. Initially, we take into account a system of differential equations (the generator) which plays the role of machine A as in the ideas of von Neumann, and we use this system to influence in a unidirectional way, another system (the replicator) in the role of machine B , in such a manner that the replicator mimics the same ingredients of chaos furnished to the generator. In this thesis, we use such ingredients in the form of period-doubling cascade, Devaney’s and Li-Yorke chaos. In conclusion, the generator system with the replicator counterpart together, that is, the result-system, admits ingredients of the generator. In other words, a known type of chaos is replicated.

Replication of a known type of chaos in systems with arbitrary large dimension is a significant consequence of the second chapter of the thesis. More precisely, by the method presented, we show that a known type of chaos, such as obtained through period-doubling cascade and in the sense of Devaney or Li-Yorke, can be extended to systems with arbitrary large dimension. To be more precise, we provide replication of chaos between unidirectionally coupled systems such that finally to obtain a result-system admitting the same type of chaos. One can construct the morphogenesis mechanism by the formation of consecutive replications of chaos or replication of chaos from a core system. It is also possible to construct a result-system using these two mechanisms in a mixed style.

The chaotification procedure presented in the third chapter shows that not only continuous functions, but also piecewise continuous functions in the form of a relay function with chaotically changing switching moments can be used to replicate a certain type of chaos. In the third chapter, it is also shown both theoretically and numerically that the obtained chaos is controllable, and OGY and Pyragas methods are suitable to stabilize the unstable periodic solutions.

Cellular neural networks have been paid much attention in the past two decades. Exceptional role in psychophysics, speech, perception, robotics, adaptive pattern recognition, vision, and image processing has been played by shunting inhibitory cellular neural networks. Chaotic dynamics is an object of great interest in the theory neural networks. This is natural since chaotic outputs have been obtained for several types of neural networks. According to the design of neural networks, solutions of some of them can be used as an input for another

ones. Confirming one more time that the chaos phenomenon can be observed in the dynamics of neural networks, the results obtained in the fourth chapter of the present thesis make contribution to the development of neural networks theory.

The synchronization theory of chaotic systems and our method of replication of chaos are compared in the following part.

5.1 Synchronization versus Replication

According to Pecora and Carroll [168], two identical chaotic systems can be synchronized under appropriate unidirectional coupling schemes. To realize the proposal of Afraimovich et al. [4] about the synchronization of nonidentical chaotic systems that are not restricted in coupling, Rulkov et al. [184] considered the concept of generalized synchronization for unidirectionally coupled systems. Generalized synchronization [1, 3, 100, 122, 184] occurs in the dynamics of the unidirectionally coupled system (1.4) + (1.5) if the relation (1.8) holds. This relation indicates the asymptotic closeness of the solutions of the master system (1.4) and the slave system (1.5) under a transformation ψ . According to the results of Kocarev and Parlitz [122], generalized synchronization occurs in the system (1.4) + (1.5) if for all initial x_0 in a neighborhood of the chaotic attractor of the master system, the slave system is asymptotically stable [100], that is, the asymptotic stability criterion (1.9) holds.

The main disadvantage and in the same time the advantage of the synchronization of chaotic systems [1, 3, 82, 100, 122, 168, 184] is that the description of chaos is not requested. It is assumed in any form for the master system.

According to the lack of its description, chaos in the slave system is discovered through (i) asymptotic closeness, (ii) a transformation. Lyapunov's second method [239], which is first used by He and Vaidya [95] in the theory of synchronization, can be applied to indicate the asymptotic closeness.

In the studies about synchronization of chaotic systems, we suppose that the authors were forced to apply this simple method because of the absence of concrete properties of chaos. Even in the case of generalized synchronization [1, 3, 100, 122, 184] the same indicators are used. However, in the generalized synchronization, it is a difficult task to apply even the Lyapunov's second method. As well they cannot arrange the transformation theoretically. That is why other methods such as the analysis of conditional Lyapunov exponents [122], the auxiliary system approach [1] and the method of mutual false nearest neighbors [184] were proposed to detect the generalized synchronization. In other words, the theoretical support for generalized synchronization is weak.

In the replication theory, the correspondence between the chaos of the generator and replicator systems is very clear and has a definitive form. Our results are suitable for identical as well as nonidentical systems with the same or different dimensions. The correspondence

is arranged not only for identical systems but also for arbitrary nonidentical generator and replicator systems with different dimensions.

For certain type of replicator systems we can also arrange the asymptotic closeness of different type by applying linearization and Lyapunov's second method. Replication of chaos can be proved even when the asymptotical property is not definitely fulfilled. For example, the general hyperbolic case can be considered.

Further investigations about replication of chaos can be done by applying Lyapunov's second method. Moreover, in future, we will focus on chaotification of systems that possess stable limit cycles instead of equilibrium points. Such systems can occur as a result of Hopf bifurcation, and they are important for problems in biological systems, chemical reactions, neural networks, mechanics and electrical circuits.

REFERENCES

- [1] H.D.I. Abarbanel, N.F. Rulkov, and M.M. Sushchik. Generalized synchronization of chaos: The auxiliary system approach. *Phys. Rev. E*, 53(5):4528–4535, 1996.
- [2] F.H. Abed, H.O. Wang, and R.C. Chen. Stabilization of period doubling bifurcations and implications for control of chaos. *Physica D*, 70(1-2):154–164, 1994.
- [3] V. Afraimovich, J.-R. Chazottes, and A. Cordonet. Nonsmooth functions in generalized synchronization of chaos. *Phys. Lett. A*, 283(1-2):109–112, 2001.
- [4] V.S. Afraimovich, N.N. Verichev, and M.I. Rabinovich. Stochastic synchronization of oscillation in dissipative systems. *Radiophys. Quantum Electron.*, 29(9):795–803, 1986.
- [5] K. Aihara and G. Matsumoto. Chaotic oscillations and bifurcations in squid giant axons. In *A. Holden (Ed.), Chaos*, pages 257–269, Manchester, UK, 1986. Manchester University Press.
- [6] K. Aihara, T. Takabe, and M. Toyoda. Chaotic neural networks. *Phys. Lett. A*, 144(6-7):333–340, 1990.
- [7] M. Akhmet. *Principles of Discontinuous Dynamical Systems*. Springer, New York, 2010.
- [8] M. Akhmet. *Nonlinear Hybrid Continuous/Discrete-Time Models*. Atlantis Press, Paris, 2011.
- [9] M.U. Akhmet. Creating a chaos in a system with relay. *Int. J. of Qual. Theory Differ. Equat. Appl.*, 3(1-2):3–7, 2009.
- [10] M.U. Akhmet. Devaney’s chaos of a relay system. *Commun. Nonlinear Sci. Numer. Simulat.*, 14(4):1486–1493, 2009.
- [11] M.U. Akhmet. Dynamical synthesis of quasi-minimal sets. *Int. J. Bifur. Chaos*, 19(7):2423–2427, 2009.
- [12] M.U. Akhmet. Li-Yorke chaos in the impact system. *J. Math. Anal. Appl.*, 351(2):804–810, 2009.
- [13] M.U. Akhmet. Shadowing and dynamical synthesis. *Int. J. Bifur. Chaos*, 19(10):3339–3346, 2009.
- [14] M.U. Akhmet. Homoclinical structure of the chaotic attractor. *Commun. Nonlinear. Sci. Numer. Simulat.*, 15(4):819–822, 2010.
- [15] M.U. Akhmet and M.O. Fen. Chaos generation in hyperbolic systems. *Interdiscip. J. Discontinuity Nonlinearity Complexity*, 1(4):367–386, 2012.

- [16] M.U. Akhmet and M.O. Fen. Chaotic period-doubling and OGY control for the forced Duffing equation. *Commun. Nonlinear. Sci. Numer. Simulat.*, 17(4):1929–1946, 2012.
- [17] M.U. Akhmet and M.O. Fen. The period-doubling route to chaos in the relay system. In G.S. Ladde, N.G. Medhin, C. Peng, M. Sambandham (Eds.), *Proceedings of Dynamic Systems and Applications, vol. 6*, pages 22–26, Atlanta, GA, 2012. Dynamic Publisher, Inc.
- [18] M.U. Akhmet and M.O. Fen. Replication of chaos. *Commun. Nonlinear. Sci. Numer. Simulat.*, 18(10):2626–2666, 2013.
- [19] M.U. Akhmet and M.O. Fen. Shunting inhibitory cellular neural networks with chaotic external inputs. *Chaos*, 23(2):023112, 2013.
- [20] E. Akin and S. Kolyada. Li-Yorke sensitivity. *Nonlinearity*, 16(4):1421–1433, 2003.
- [21] K.T. Alligood, T.D. Sauer, and J.A. Yorke. *Chaos: An Introduction to Dynamical Systems*. Springer-Verlag, New York, 1996.
- [22] K.G. Andersson. Poincaré’s discovery of homoclinic points. *Archive for History of Exact Sciences*, 48(2):133–147, 1994.
- [23] Y.V. Andreyev, A.S. Dmitriev, and E.V. Efremova. Dynamic separation of chaotic signals in the presence of noise. *Phys. Rev. E*, 65(4):046220 1–6, 2002.
- [24] V.S. Anishchenko, T. Kapitaniak, M.A. Safonova, and O.V. Sosnovzeva. Birth of double-double scroll attractor in coupled Chua circuits. *Phys. Lett. A*, 192(2-4):207–214, 1994.
- [25] M.S. Archer. *Realistic Social Theory: The Morphogenetic Approach*. Cambridge University Press, Cambridge, 1995.
- [26] A. Arneodo, P. Coullet, and C. Tresser. Oscillators with chaotic behavior, an illustration of a theorem by Shil’nikov. *Journal of Statistical Physics*, 27(1):171–182, 1982.
- [27] K.R. Asfar and K.K. Masoud. On the period-doubling bifurcations in the Duffing’s oscillator with negative linear stiffness. *Trans. ASME, J. Vib. Acoust.*, 114(4):489–494, 1992.
- [28] J. Awrejcewicz and M.M. Holicke. *Smooth and Nonsmooth High Dimensional Chaos and the Melnikov Type Methods*. World Scientific Publishing, Singapore, 2007.
- [29] J. Awrejcewicz and C.H. Lamarque. *Bifurcation and Chaos in Nonsmooth Mechanical Systems*. World Scientific Publishing, Singapore, 2003.
- [30] A. Azevedo and S.M. Rezende. Controlling chaos in spin-wave instabilities. *Phys. Rev. Lett.*, 66(10):1342–1345, 1991.
- [31] V.I. Babitsky. *Theory of Vibro-Impact Systems and Applications*. Springer, Berlin, 1998.
- [32] G.L. Baker. Control of the chaotic driven pendulum. *Am. J. Phys.*, 63(9):832–838, 1995.
- [33] M.S. Baptista. Cryptography with chaos. *Phys. Lett. A*, 240(1-2):50–54, 1998.

- [34] E.A. Barbashin. *Introduction to the Theory of Stability*. Wolters-Noordhoff Publishing, Groningen, 1970.
- [35] S. Bielawski, D. Derozier, and P. Glorieux. Controlling unstable periodic orbits by a delayed continuous feedback. *Phys. Rev. E*, 49(2):R971–R974, 1994.
- [36] P. Bourguine and A. Lesne. *Morphogenesis: Origins of Patterns and Shapes*. Springer-Verlag, Berlin, Heidelberg, 2011.
- [37] A. Bouzerdoum, B. Nabet, and R.B. Pinter. Analysis and analog implementation of directionally sensitive shunting inhibitory cellular neural networks. In *B.P. Mathur, C. Koch (Eds.), Visual Information Processing: From Neurons to Chips (Proceedings of Spie)*, pages 29–38, Orlando, 1991. Society of Photo Optical.
- [38] A. Bouzerdoum and R.B. Pinter. A shunting inhibitory motion detector that can account for the functional characteristics of fly motion-sensitive interneurons. In *Proceedings of International Joint Conference on Neural Networks*, pages 149–153, San Diego, California, 1990. CRC Press.
- [39] A. Bouzerdoum and R.B. Pinter. Nonlinear lateral inhibition applied to motion detection in the fly visual system. In *R.B. Pinter, B. Nabet (Eds.), Nonlinear Vision*, pages 423–450, Boca Raton, FL, 1992. CRC Press.
- [40] A. Bouzerdoum and R.B. Pinter. Shunting inhibitory cellular neural networks: derivation and stability analysis. *Circuits and Systems I: Fundamental Theory and Applications, IEEE Transactions on*, 40(3):215–221, 1993.
- [41] Y. Braiman and I. Goldhirsch. Taming chaotic dynamics with weak periodic perturbations. *Phys. Rev. Lett.*, 66(20):2545–2548, 1991.
- [42] B. Branner, L. Keen, A. Douady, P. Blanchard, J.H. Hubbard, D. Schleicher, and R.L. Devaney. *Complex Dynamical Systems: The Mathematics Behind Mandelbrot and Julia Sets*. R.L. Devaney ed. American Mathematical Society, United States of America, 1994.
- [43] B. Brogliato. *Impacts in Mechanical Systems-Analysis and Modeling*. Springer, New York, 2000.
- [44] V. Brunsten, J. Cortell, and P.J. Holmes. Power spectra of chaotic vibrations of a buckled beam. *J. Sound Vib.*, 130(1):1–25, 1989.
- [45] W. Buckley. *Sociology and Modern Systems Theory*. Prentice Hall, New Jersey, 1967.
- [46] M. Cai and W. Xiong. Almost periodic solutions for shunting inhibitory cellular neural networks without global lipschitz and bounded activation functions. *Phys. Lett. A*, 362(5-6):417–423, 2007.
- [47] G.A. Carpenter and S. Grossberg. Analysis of the process of visual pattern recognition by the neocognitron. *Computer*, 21(3):77–88, 1988.
- [48] M. Cartwright and J. Littlewood. On nonlinear differential equations of the second order I: The equation $\ddot{y} - k(1 - y^2)'y + y = bk\cos(\lambda t + a)$, k large. *J. London Math. Soc.*, 20:180–189, 1945.

- [49] G. Chen and X. Yu. On time delayed feedback control of chaos. *IEEE Trans Circ Sys-I*, 46(6):767–772, 1999.
- [50] H. Cho and E.W. Bai. Convergence results for an adaptive dead zone inverse. *Int. J. Adapt. Control Signal Process*, 12(5):451–466, 1998.
- [51] L.O. Chua. Chua’s circuit: Ten years later. *IEICE Trans. Fundamentals*, E77-A(11):1811–1822, 1994.
- [52] L.O. Chua, M. Komuro, and T. Matsumoto. The double scroll family, parts I and II. *IEEE Trans. Circuit Syst.*, 33(11):1072–1118, 1986.
- [53] L.O. Chua, C.W. Wu, A. Huang, and G. Zhong. A universal circuit for studying and generating chaos-part I: Routes to chaos. *IEEE Trans. Circuit Syst.-I: Fundamental Theory and Applications*, 40(10):732–744, 1993.
- [54] C. Corduneanu. *Almost Periodic Functions*. Interscience Publishers, New-York, London, Sydney, 1968.
- [55] C. Corduneanu. *Principles of Differential and Integral Equations*. Chelsea Publishing Company, The Bronx, New York, 1977.
- [56] C. Corduneanu. *Integral Equations and Applications*. Cambridge University Press, New York, 2008.
- [57] N.J. Corron. An exactly solvable chaotic differential equation. *Dyn. Contin. Discrete Impuls. Syst. Ser. A Math. Anal.*, 16(6):777–788, 2009.
- [58] T. Courtat, C. Gloaguen, and S. Douady. Mathematics and morphogenesis of cities: A geometrical approach. *Phys. Rev. E*, 83(3):036106 1–12, 2011.
- [59] N. Crook and T. olde Scheper. A novel chaotic neural network architecture. In *Proceedings of 9th European Symposium on Artificial Neural Networks, 25-27 April 2001*, pages 295–300, Bruges, Belgium, 2001. D-Facto.
- [60] N.T. Crook, C.H. Dobbyn, and T. olde Scheper. Chaos as a desirable stable state of artificial neural networks. In *R. John, R. Birkenhead (Eds.), Advances in Soft Computing: Soft Computing Techniques and Applications*, pages 52–60, New York, 2000. Physica-Verlag.
- [61] K.M. Cuomo and A.V. Oppenheim. Circuit implementation of synchronized chaos with applications to communications. *Phys. Rev. Lett.*, 71(1):65–68, 1993.
- [62] J.A. Davies. *Mechanisms of Morphogenesis: The Creation of Biological Form*. Elsevier Academic Press, United States of America, 2005.
- [63] M. de Sousa Vieira and A.J. Lichtenberg. Controlling chaos using nonlinear feedback with delay. *Phys. Rev. E*, 54(2):1200–1207, 1996.
- [64] R.L. Devaney. *An Introduction to Chaotic Dynamical Systems*. Addison-Wesley, United States of America, 1989.
- [65] M. di Bernardo, C.J. Budd, A.R. Champneys, and P. Kowalczyk. *Piecewise-Smooth Dynamical Systems*. Springer, London, 2008.

- [66] H-S. Ding, J. Liang, and T-J. Xiao. Existence of almost periodic solutions for SICNNs with time-varying delays. *Phys. Lett. A*, 372(33):5411–5416, 2008.
- [67] M. Ding and E. Ott. Enhancing synchronism of chaotic systems. *Phys. Rev. E*, 49(2):R945–R948, 1994.
- [68] W.L. Ditto, S. N. Tauseo, and M.L. Spano. Experimental control of chaos. *Phys. Rev. Lett.*, 65(26):3211–3214, 1990.
- [69] E.H. Dowell and C. Pazeshki. On the understanding of chaos in Duffing’s equation including a comparison with experiment. *J. Appl. Mech.*, 53(1):5–9, 1986.
- [70] U. Dressler and G. Nitsche. Controlling chaos using time delay coordinates. *Phys. Rev. Lett.*, 68(1):1–4, 1992.
- [71] F. Drubi, S. Ibáñez, and J.A. Rodriguez. Coupling leads to chaos. *J. Differential Equations*, 239(2):371–385, 2007.
- [72] F. Drubi, S. Ibáñez, and J.A. Rodriguez. Singularities and chaos in coupled systems. *Bull. Belg. Math. Soc. Simon Stevin*, 15(5):797–808, 2008.
- [73] F. Drubi, S. Ibáñez, and J.A. Rodriguez. Hopf-pitchfork singularities in coupled systems. *Physica D*, 240(9-10):825–840, 2011.
- [74] M.J. Feigenbaum. Universal behavior in nonlinear systems. *Los Alamos Science*, 1(1):4–27, 1980.
- [75] A.M. Fink. *Almost Periodic Differential Equations*. Lecture Notes in Mathematics, Springer-Verlag, Berlin, Heidelberg, New York, 1974.
- [76] A.L. Fradkov. *Cybernetical Physics*. Springer-Verlag, Berlin, Heidelberg, 2007.
- [77] W.J. Freeman. Tutorial on neurobiology: from single neurons to brain chaos. *Int. J. Bifurcation Chaos*, 2(3):451–482, 1992.
- [78] W.J. Freeman and J.M. Barrie. Chaotic oscillations and the genesis of meaning in cerebral cortex. In *G. Buzsaki, Y. Christen (Eds.), Temporal Coding in the Brain*, pages 13–37, Berlin, 1994. Springer-Verlag.
- [79] K. Fukushima. Analysis of the process of visual pattern recognition by the neocognitron. *Neural Networks*, 2(6):413–420, 1989.
- [80] A. Garfinkel, M.L. Spano, W.L. Ditto, and J.N. Weiss. Controlling cardiac chaos. *Science*, 257:1230–1233, 1992.
- [81] S.V. Gonchenko, L.P. Shil’nikov, and D.V. Turaev. Dynamical phenomena in systems with structurally unstable Poincaré homoclinic orbits. *Chaos*, 6(1):15–31, 1996.
- [82] J.M. Gonzales-Miranda. *Synchronization and Control of Chaos*. Imperial College Press, London, 2004.
- [83] J.A. Gottwald, L.N. Virgin, and E. Dowell. Experimental mimicry of Duffing’s equation. *J. Sound Vib.*, 158(3):447–467, 1992.
- [84] C. Grebogi and J.A. Yorke. *The Impact of Chaos on Science and Society*. United Nations University Press, Tokyo, 1997.

- [85] J. Guckenheimer and P.J. Holmes. *Nonlinear Oscillations, Dynamical Systems and Bifurcations of Vector Fields*. Springer, New York, 1997.
- [86] J. Guckenheimer and R.A. Oliva. Chaos in the Hodgkin-Huxley model. *Siam J. Applied Dynamical Systems*, 1(1):105–114, 2002.
- [87] J. Guckenheimer and R.F. Williams. Structural stability of Lorenz attractors. *Publ. Math.*, 50(1):59–72, 1979.
- [88] Z. Gui and W. Ge. Periodic solution and chaotic strange attractor for shunting inhibitory cellular neural networks with impulses. *Chaos*, 16(3):033116, 2006.
- [89] D. Gulick. *Encounters With Chaos*. University of Maryland, College Park, 1992.
- [90] J. Hadamard. Les surfaces à courbures opposées et leurs lignes géodésiques. *J. Math. Pures et Appl.*, 4:27–74, 1898.
- [91] C. Hagège. *The Language Builder: An Essay on the Human Signature in Linguistic Morphogenesis*. John Benjamins Publishing Co., Amsterdam, Netherlands, 1993.
- [92] J. Hale and H. Koçak. *Dynamics and Bifurcations*. Springer-Verlag, New York, 1991.
- [93] J.K. Hale. *Ordinary Differential Equations*. Krieger Publishing Company, Malabar, Florida, 1980.
- [94] S. Hayes, C. Grebogi, and E. Ott. Communicating with chaos. *Phys. Rev. Lett.*, 70(20):3031–3034, 1993.
- [95] R. He and P.G. Vaidya. Analysis and synthesis of synchronous periodic and chaotic systems. *Phys. Rev. A*, 46(12):7387–7392, 1992.
- [96] M. Hénon. A two-dimensional mapping with a strange attractor. *Comm. Math. Phys.*, 50(1):69–77, 1976.
- [97] G. Herrmann. A robust delay adaptation scheme for Pyragas’ chaos control method. *Phys. Lett. A*, 287(3-4):245–256, 2001.
- [98] R.A. Horn and C.R. Johnson. *Matrix Analysis*. Cambridge University Press, United States of America, 1992.
- [99] X. Huang and J. Cao. Almost periodic solution of shunting inhibitory cellular neural networks with time-varying delay. *Phys. Lett. A*, 314(3):222–231, 2003.
- [100] B.R. Hunt, E. Ott, and J.A. Yorke. Differentiable generalized synchronization of chaos. *Phys. Rev. E*, 55(4):4029–4034, 1997.
- [101] R.A. Ibrahim. *Vibro-Impact Dynamics*. Springer-Verlag, Berlin, Heidelberg, 2009.
- [102] K. Ikeda, K. Matsumoto, and K. Otsuka. Maxwell-Bloch turbulence. *Prog. Theor. Phys.*, Suppl. 99(3):295–324, 1989.
- [103] M.V. Jacobson. Absolutely continuous invariant measures for one-parameter families of one-dimensional maps. *Comm. Math. Phys.*, 81(30):39–88, 1981.
- [104] M.E. Jernigen and G.F. McLean. Lateral inhibition and image processing. In *R.B. Pinter and B. Nabet (Eds.), Non-linear vision: Determination of neural receptive fields, function, and networks*, pages 451–462, Boca Raton, FL, 1992. CRC Press.

- [105] M.R. Joglekar, E. Sander, and J.A. Yorke. Fixed points indices and period-doubling cascades. *J. Fixed Point Theory Appl.*, 8(1):151–176, 2010.
- [106] J.R. Kalagnanam. Controlling chaos, the example of an impact oscillator. *ASME J. Dyn. Syst. Measur. Control*, 116(3):557–564, 1994.
- [107] K. Kaneko. Clustering, coding, switching, hierarchical ordering, and control in network of chaotic elements. *Physica D*, 41(2):137–172, 1990.
- [108] K. Kaneko. Globally coupled circle maps. *Physica D*, 54(1-2):5–19, 1991.
- [109] K. Kaneko and I. Tsuda. *Complex Systems: Chaos and Beyond, A Constructive Approach with Applications in Life Sciences*. Springer-Verlag, Berlin, Heidelberg, New York, 2000.
- [110] K. Kaneko and I. Tsuda. Chaotic itinerancy. *Publ. Math.*, 13(3):926–936, 2003.
- [111] T. Kapitaniak. Controlling chaotic oscillators without feedback. *Chaos, Solitons and Fractals*, 2(5):519–530, 1992.
- [112] T. Kapitaniak. Transition to hyperchaos in chaotically forced coupled oscillators. *Phys. Rev. E*, 47(5):R2975–R2978, 1993.
- [113] T. Kapitaniak. Synchronization of chaos using continuous control. *Phys. Rev. E*, 50(2):1642–1644, 1994.
- [114] T. Kapitaniak. *Controlling Chaos: Theoretical and Practical Methods in Non-linear Dynamics*. Academic Press, San Diego, 1996.
- [115] T. Kapitaniak, L. O. Chua, and G. Zhong. Experimental hyperchaos in coupled Chua’s circuits. *IEEE Transactions on Circuits and Systems-I: Fundamental Theory and Applications*, 41(7):499–503, 1994.
- [116] T. Kapitaniak and L.O. Chua. Hyperchaotic attractors of unidirectionally-coupled Chua’s circuits. *Int. J. Bifurcation Chaos*, 4(2):477–482, 1994.
- [117] J. Kennedy and J.A. Yorke. Topological horseshoes. *Transactions of the American Mathematical Society*, 353:2513–2530, 2001.
- [118] A. Khadra, X. Liu, and X. Shen. Application of impulsive synchronization to communication security. *IEEE Trans. Circuit Syst.*, 50(3):341–351, 2003.
- [119] P. Kim, T. Ko, H. Jeong, K.J. Lee, and S.K. Han. Emergence of chaotic itinerancy in simple ecological systems. *Phys. Rev. E*, 76(6):065201(R) 1–4, 2007.
- [120] P. Kloeden and Z. Li. Li-Yorke chaos in higher dimensions: a review. *J. Differ. Equ. Appl.*, 12(3-4):247–269, 2006.
- [121] A.E. Kobrinskii and A.A. Kobrinskii. *Vibro-Shock Systems (Russian)*. Nauka, Moscow, 1971.
- [122] L. Kocarev and U. Parlitz. Generalized synchronization, predictability, and equivalence of unidirectionally coupled dynamical systems. *Phys. Rev. Lett.*, 76(11):1816–1819, 1996.

- [123] G. Kolumban, P. Kennedy, and L.O. Chua. The role of synchronization in digital communications using chaos-part II: chaotic modulation and chaotic synchronization. *IEEE Trans. Circuit Syst.*, 45(11):1129–1140, 1998.
- [124] T. Kousaka, T. Ueta, and H. Kawakami. Controlling chaos in a state-dependent nonlinear system. *Int. J. Bifur. Chaos*, 12(5):1111–1119, 2002.
- [125] A.J. Kurdila and G. Webb. Compensation for distributed hysteresis operators in active structural systems. *J. Guid. Control. Dyn.*, 20(6):1133–1140, 1997.
- [126] J. Kuroiwa, N. Masutani, S. Nara, and K. Aihara. Chaotic wandering and its sensitivity to external input in a chaotic neural network. In L. Wang, J.C. Rajapakse, K. Fukushima, S.Y. Lee and X. Yao (Eds.), *Proceedings of the 9th International Conference on Neural Information Processing (ICONIP'02)*, pages 353–357, Singapore, 2002. Orchid Country Club.
- [127] J.Y. Lee and J.J. Yan. Control of impact oscillator. *Chaos, Solitons and Fractals*, 28(1):136–142, 2006.
- [128] J.Y. Lee and J.J. Yan. Position control of double-side impact oscillator. *Mechanical Systems and Signal Processing*, 21(2):1076–1083, 2007.
- [129] L.M. Lerman and L.P. Shil'nikov. Homoclinical structures in nonautonomous systems: nonautonomous chaos. *Chaos*, 2(3):447–454, 1992.
- [130] M. Levi. *Qualitative Analysis of the Periodically Forced Relaxation Oscillations*. Memoirs of the American Mathematical Society, United States of America, 1981.
- [131] N. Levinson. A second order differential equation with singular solutions. *Ann. of Math.*, 50(1):127–153, 1949.
- [132] L. Li, Z. Fang, and Y. Yang. A shunting inhibitory cellular neural network with continuously distributed delays of neutral type. *Nonlinear Analysis: Real World Applications*, 13(3):1186–1196, 2012.
- [133] P. Li, Z. Li, W.A. Halang, and G. Chen. Li-Yorke chaos in a spatiotemporal chaotic system. *Chaos, Solitons and Fractals*, 33(2):335–341, 2007.
- [134] T.Y. Li and J.A. Yorke. Period three implies chaos. *The American Mathematical Monthly*, 82(10):985–992, 1975.
- [135] R. Lima and M. Pettini. Suppression of chaos by resonant parametric perturbations. *Phys. Rev. A*, 41(2):726–733, 1990.
- [136] Q. Liu and S. Zhang. Adaptive lag synchronization of chaotic Cohen-Grossberg neural networks with discrete delays. *Chaos*, 22(3):033123, 2012.
- [137] E.N. Lorenz. Deterministic nonperiodic flow. *J. Atmos. Sci.*, 20(2):130–141, 1963.
- [138] H.W. Lorenz. *Nonlinear Dynamical Economics and Chaotic Motion*. Springer-Verlag, Berlin, New York, 1989.
- [139] C. Lourenco and A. Babloyantz. Control of spatiotemporal chaos in neural networks. *Int. J. Neural Syst.*, 7(4):507–517, 1996.

- [140] W. Lu and T. Chen. Synchronization of coupled connected neural networks with delays. *IEEE Transactions on Circuits and Systems-I: Regular Papers*, 51(12):2491–2503, 2004.
- [141] B.M. Mandelbrot. *Fractals: Form, Chance and Dimension*. Freeman, San Fransisco, 1977.
- [142] B.M. Mandelbrot. *The Fractal Geometry of Nature*. Freeman, San Fransisco, 1982.
- [143] F.R. Marotto. Snap-back repellers imply chaos in R^n . *J. Math. Anal. Appl.*, 63(1):199–223, 1978.
- [144] MATLAB. *Version 7.12.0 (R2011a)*. The MathWorks Inc., Natick, Massachusetts, 2011.
- [145] T. Matsumoto, L.O. Chua, and M. Komuro. The double scroll. *IEEE Trans. Circuit Syst.*, 32(8):797–818, 1985.
- [146] R.M. May. Simple mathematical models with very complicated dynamics. *Nature*, 261:459–467, 1976.
- [147] J. McGuire, M.T. Batchelor, and B. Davies. Linear and optimal non-linear control of one-dimensional maps. *Phys. Lett. A*, 233(4-6):361–364, 1997.
- [148] P. Melby, J. Kaidel, N. Weber, and A. Hübler. Adaptation to the edge of chaos in the self-adjusting logistic map. *Phys. Rev. Lett.*, 84(26):5991–5993, 2000.
- [149] W. Melo and S. Strien. *One-Dimensional Dynamics*. Springer-Verlag, Berlin, Heidelberg, 1993.
- [150] R. Meucci, W. Gadowski, M. Ciofini, and F.T. Arecchi. Experimental control of chaos by means of weak parametric perturbations. *Phys. Rev. E*, 49(4):R2528–R2531, 1994.
- [151] K.R. Meyer and G.R. Sell. Homoclinic orbits and bernoulli bundles in almost periodic systems. In *Oscillations, bifurcation and chaos, CMS Conf. Proc.*, vol. 8, pages 527–544, Toronto, Ont., 1987. Amer. Math. Soc.
- [152] J. Milnor. *Dynamics in One Complex Variable*. Princeton University Press, United States of America, 2006.
- [153] F.C. Moon. Experiments on chaotic motions of a forced nonlinear oscillator: strange attractors. *J. Appl. Mech.*, 47(3):638–644, 1980.
- [154] F.C. Moon. *Chaotic Vibrations: An Introduction For Applied Scientists and Engineers*. John Wiley & Sons, Hoboken, New Jersey, 2004.
- [155] F.C. Moon and P.J. Holmes. A magnetoelastic strange attractor. *J. Sound Vib.*, 65(2):275–296, 1979.
- [156] M. Morse and G.A. Hedlund. Symbolic dynamics. *Amer. J. Math.*, 60(4):815–866, 1938.
- [157] R.F. Nagaev. *Mechanical Processes with Repeated and Decaying Impacts (Russian)*. Nauka, Moscow, 1985.

- [158] S. Nara and P. Davis. Chaotic wandering and search in a cycle-memory neural network. *Prog. Theor. Phys.*, 88(5):845–855, 1992.
- [159] S. Nara, P. Davis, M. Kawachi, and H. Totsuji. Chaotic memory dynamics in a recurrent neural network with cycle memories embedded by pseudo-inverse method. *Int. J. Bifurcation and Chaos*, 5(4):1205–1212, 1995.
- [160] J. Von Neumann and A.W. Burks. *The Theory of Self-Reproducing Automata*. University of Illinois Press, Urbana and London, 1966.
- [161] A.B. Nordmark. Existence of periodic orbits in grazing bifurcations of impacting mechanical oscillators. *Nonlinearity*, 14(6):1517–1542, 2001.
- [162] H.E. Nusse, E. Ott, and J.A. Yorke. Border-collision bifurcations: an explanation for observed bifurcation phenomena. *Phys. Rev. E*, 49(2):1073–1076, 1994.
- [163] E. Ott, C. Grebogi, and J.A. Yorke. Controlling chaos. *Phys. Rev. Lett.*, 64(11):1196–1199, 1990.
- [164] E. Ott, T. Sauer, and J.A. Yorke. *Coping With Chaos: Analysis of Chaotic Data and the Exploitation of Chaotic Systems*. Wiley, New York, 1994.
- [165] C. Ou. Almost periodic solutions for shunting inhibitory cellular neural networks. *Nonlinear Analysis: Real World Applications*, 10(5):2652–2658, 2009.
- [166] K. Palmer. *Shadowing in Dynamical Systems*. Kluwer Academic Publishers, Dordrecht, The Netherlands, 2000.
- [167] K.R. Palmer and D. Stoffer. Chaos in almost periodic systems. *J. Appl. Math. Phys. (ZAMP)*, 40(4):592–602, 1989.
- [168] L.M. Pecora and T.L. Carroll. Synchronization in chaotic systems. *Phys. Rev. Lett.*, 64(8):821–825, 1990.
- [169] L.M. Pecora and T.L. Carroll. Driving systems with chaotic signals. *Phys. Rev. A*, 44(4):2374–2383, 1991.
- [170] H.O. Peitgen, H. Jürgens, and D. Saupe. *Chaos and Fractals: New Frontiers of Science*. Springer-Verlag, New York, 2004.
- [171] G. Peng and L. Huang. Anti-periodic solutions for shunting inhibitory cellular neural networks with continuously distributed delays. *Nonlinear Analysis: Real World Applications*, 10(4):2434–2440, 2009.
- [172] F. Peterka. Part I: Theoretical analysis of n-multiple $(1/n)$ -impact solutions. *CSAV Acta Technica*, 26(2):462–473, 1974.
- [173] A. Pikovsky, M. Rosenblum, and J. Kurths. *Synchronization: A Universal Concept in Nonlinear Sciences*. Cambridge University Press, New York, 2001.
- [174] R.B. Pinter, R.M. Olberg, and E. Warrant. Luminance adaptation of preferred object size in identified dragonfly movement detectors. In *Proceedings of IEEE International Conference on Systems, Man and Cybernetics*, pages 682–686, Cambridge, MA, 1989.
- [175] Y. Pomeau and P. Manneville. Intermittent transition to turbulence in dissipative dynamical systems. *Commun. Math. Phys.*, 74(2):189–197, 1980.

- [176] A. Potapov and M.K. Ali. Robust chaos in neural networks. *Phys. Lett. A*, 277(6):310–322, 2000.
- [177] K. Pyragas. Continuous control of chaos by self-controlling feedback. *Phys. Rev. A*, 170(6):421–428, 1992.
- [178] K. Ramasubramanian and M.S. Sriram. A comparative study of computation of Lyapunov spectra with different algorithms. *Physica D*, 139(1-2):72–86, 2000.
- [179] C. Robinson. *Dynamical Systems: Stability, Symbolic Dynamics, and Chaos*. CRC Press, Boca Raton/Ann Arbor/London/Tokyo, 1995.
- [180] O.E. Rössler. An equation for continuous chaos. *Phys. Lett. A*, 57(5):397–398, 1976.
- [181] O.E. Rössler. An equation for hyperchaos. *Phys. Lett. A*, 71(2-3):155–157, 1979.
- [182] S. Roudavski. Towards morphogenesis in architecture. *International Journal of Architectural Computing*, 7(3):345–374, 2009.
- [183] D. Ruelle and F. Takens. On the nature of turbulence. *Commun. Math. Phys.*, 20(3):167–192, 1971.
- [184] N.F. Rulkov, M.M. Sushchik, L.S. Tsimring, and H.D.I. Abarbanel. Generalized synchronization of chaos in directionally coupled chaotic systems. *Phys. Rev. E*, 51(2):980–994, 1995.
- [185] A.M. Samoilenko and N.A. Perestyuk. *Impulsive Differential Equations*. World Scientific, Singapore, 1995.
- [186] E. Sander and J.A. Yorke. Period-doubling cascades for large perturbations of Hénon families. *J. Fixed Point Theory Appl.*, 6(1):153–163, 2009.
- [187] E. Sander and J.A. Yorke. Period-doubling cascades galore. *Ergod. Th. & Dynam. Sys.*, 31:1249–1267, 2011.
- [188] E. Sander and J.A. Yorke. Connecting period-doubling cascades to chaos. *Int. J. Bifur. Chaos*, 22(2):1250022, 2012.
- [189] S. Sato, M. Sano, and Y. Sawada. Universal scaling property in bifurcation structure of Duffing’s and of generalized Duffing’s equations. *Phys. Rev. A*, 28(3):1654–1658, 1983.
- [190] T. Sauer. Chaotic itinerancy based on attractors of one-dimensional maps. *Chaos*, 13(3):947–952, 2003.
- [191] A.V. Savkin and R.J. Evans. *Hybrid Dynamical Systems: Controller and Sensor Switching Problems*. Birkhäuser, Boston, Basel, Berlin, 2002.
- [192] J. Scheurle. Chaotic solutions of systems with almost periodic forcing. *J. Appl. Math. Phys. (ZAMP)*, 37(1):12–26, 1986.
- [193] J.L. Schiff. *Cellular Automata: A Discrete View of the World*. John Wiley & Sons, Inc., Hoboken, New Jersey, 2008.
- [194] S.J. Schiff, K. Jerger, D.H. Duong, T. Chang, M.L. Spano, and W.L. Ditto. Controlling chaos in the brain. *Nature*, 370:615–620, 1994.

- [195] E. Schöll and H.G. Schuster. *Handbook of Chaos Control*. Wiley-Vch, Weinheim, 2008.
- [196] H.G. Schuster. *Handbook of Chaos Control*. Wiley-Vch, Weinheim, 1999.
- [197] H.G. Schuster and W. Just. *Chaos in Dynamical Systems*. Cambridge University Press, New York, 1993.
- [198] H.G. Schuster and W. Just. *Deterministic Chaos: An Introduction*. Wiley-Vch, Weinheim, 2005.
- [199] J. Shao. Anti-periodic solutions for shunting inhibitory cellular neural networks with time-varying delays. *Phys. Lett. A*, 372(30):5011–5016, 2008.
- [200] S.W. Shaw, A.G. Haddow, and S.R. Hsieh. Properties of cross-well chaos in an impacting systems. *Phil. Trans. R. Soc. Lond. A*, 347(1683):391–410, 1994.
- [201] M. Shibasaki and M. Adachi. Response to external input of chaotic neural networks based on Newman-Watts model. In *J. Liu, C. Alippi, B. Bouchon-Meunier, G.W. Greenwood, H.A. Abbass (Eds.), The 2012 International Joint Conference on Neural Networks*, pages 1–7, Brisbane, Australia, 2012.
- [202] L. Shilnikov. Bifurcations and strange attractors. In *Proceedings of the International Congress of Mathematicians, Vol. III*, pages 349–372, Beijing, 2002. Higher Ed. Press.
- [203] L.P. Shilnikov. A case of the existence of a denumerable set of periodic motions. *Sov. Math. Dokl.*, 6:163–166, 1965.
- [204] L.P. Shil'nikov. On a Poincaré-Birkhoff problem. *Math. USSR-Sbornik*, 3(3):353–371, 1967.
- [205] C.A. Skarda and W.J. Freeman. How brains make chaos in order to make sense of the world. *Behavioral and Brain Sci.*, 10(2):161–173, 1987.
- [206] S. Smale. Diffeomorphisms with many periodic points. In *Differential and Combinatorial Topology: A Symposium in Honor of Marston Morse*, pages 63–70, Princeton, NJ, 1965. Princeton University Press.
- [207] S. Smale. Differentiable dynamical systems. *Bull. Amer. Math. Soc.*, 73:747–817, 1967.
- [208] S. Smale. A mathematical model of two cells via Turing's equation. In *Some Mathematical Questions in Biology, V, Proc. Seventh Sympos., Mathematical Biology, Math. Life Sci., vol. 6*, pages 15–26, Mexico City, 1973. Amer. Math. Soc.
- [209] J.E.S. Socolar, D.W. Sukow, and D.J. Gauthier. Stabilizing unstable periodic orbits in fast dynamical systems. *Phys. Rev. E*, 50(4):3245–3248, 1994.
- [210] J.C. Sprott. *Chaos and Time-Series Analysis*. Oxford University Press, New York, 2003.
- [211] J.C. Sprott. *Elegant Chaos: Algebraically Simple Chaotic Flows*. World Scientific Publishing, Singapore, 2010.
- [212] J. Sun. Stationary oscillation for chaotic shunting inhibitory cellular neural networks with impulses. *Chaos*, 17(4):043123, 2007.

- [213] L.A. Taber. Towards a unified theory for morphomechanics. *Phil. Trans. R. Soc. A*, 367:3555–3583, 2009.
- [214] G. Tao and F.L. Lewis. *Adaptive Control of Nonsmooth Dynamic Systems*. Springer-Verlag, London, 2001.
- [215] K. Thamilmaran and M. Lakshmanan. Rich variety of bifurcations and chaos in a variant of Murali-Lakshmanan-Chua circuit. *Int. J. Bifur. Chaos*, 10(7):1781–1785, 2000.
- [216] R. Thom. *Stabilité Structurelle et Morphogénèse*. W.A. Benjamin, New York, 1972.
- [217] R. Thom. *Mathematical Models of Morphogenesis*. Ellis Horwood Limited, Chichester, England, 1983.
- [218] J.M.T. Thompson and H.B. Stewart. *Nonlinear Dynamics And Chaos*. John Wiley, England, 2002.
- [219] C. Tresser, P.A. Worfolk, and H. Bass. Master-slave synchronization from the point of view of global dynamics. *Chaos*, 5(4):693–699, 1995.
- [220] I. Tsuda. Chaotic itinerancy as a dynamical basis of hermeneutics in brain and mind. *World Futures*, 32(2-3):167–184, 1991.
- [221] I. Tsuda. Dynamic link of memory-chaotic memory map in nonequilibrium neural networks. *Neural Networks*, 5(2):313–326, 1992.
- [222] I. Tsuda. A new type of self-organization associated with chaotic dynamics in neural networks. *Int. J. Neural Syst.*, 7(4):451–459, 1996.
- [223] A.M. Turing. The chemical basis of morphogenesis. *Philosophical Transactions of the Royal Society of London, Series B, Biological Sciences*, 237(641):37–72, 1952.
- [224] M. Čiklová. Li-Yorke sensitive minimal maps. *Nonlinearity*, 19(2):517–529, 2006.
- [225] Y. Ueda. Randomly transitional phenomena in the system governed by Duffing’s equation. *J. Stat. Phys.*, 20(2):181–196, 1979.
- [226] Y. Ueda. Explosion of strange attractors exhibited by Duffing’s equation. *Ann. NY Acad. Sci.*, 357:422–434, 1980.
- [227] Y. Ueda. Steady motions exhibited by Duffing’s equation: a picture book of regular and chaotic motions. In *New Approaches to Nonlinear Problems in Dynamics, Holmes P.J. (Ed.)*, pages 311–322, Philadelphia, 1980. SIAM.
- [228] A.F. Vakakis, L.I. Manevitch, Y.V. Mikhlin, V.N. Plipchuk, and A.A. Zevin. *Normal Modes and Localization in Nonlinear Systems*. John Wiley and Sons, New York, 1996.
- [229] A.J. van der Schaft and J.M. Schumacher. *An Introduction to Hybrid Dynamical Systems*. Springer, London, 2000.
- [230] A. Venkatesan, S. Parthasarathy, and M. Lakshmanan. Occurrence of multiple period-doubling bifurcation route to chaos in periodically pulsed chaotic dynamical systems. *Chaos, Solitons and Fractals*, 18(4):891–898, 2003.

- [231] X. Wang. Period-doublings to chaos in a simple neural network: an analytical proof. *Complex Systems*, 5:425–441, 1991.
- [232] S. Wiggins. *Global Bifurcations and Chaos: Analytical Methods*. Springer-Verlag, New York, 1988.
- [233] S. Wiggins. *Introduction to Applied Nonlinear Dynamical Systems and Chaos*. Springer-Verlag, New York, 2003.
- [234] L.A. Wood and K.P. Byrne. Analysis of a random repeated impact process. *J. Sound Vib.*, 78(3):329–345, 1981.
- [235] Y. Xia, J. Cao, and Z. Huang. Existence and exponential stability of almost periodic solution for shunting inhibitory cellular neural networks with impulses. *Chaos, Solitons and Fractals*, 34(5):1599–1607, 2007.
- [236] C. Liu Y. Li and L. Zhu. Global exponential stability of periodic solution for shunting inhibitory CNNs with delays. *Phys. Lett. A*, 337(1-2):46–54, 2005.
- [237] L. Yang, Z. Liu, and J. Mao. Controlling hyperchaos. *Phys. Rev. Lett.*, 84(1):67–70, 2000.
- [238] T. Yang and L.O. Chua. Impulsive control and synchronization of nonlinear dynamical systems and application to secure communication. *Int. J. Bifur. Chaos*, 7(3):645–664, 1997.
- [239] T. Yoshizawa. *Stability Theory and the Existence of Periodic Solutions and Almost Periodic Solutions*. Springer-Verlag, New-York, Heidelberg, Berlin, 1975.
- [240] W. Yu, J. Cao, and W. Lu. Synchronization control of switched linearly coupled neural networks with delay. *Neurocomputing*, 73(4-6):858–866, 2010.
- [241] W-J. Yuan, X-S. Luo, P-Q. Jiang, B-H. Wang, and J-Q. Fang. Transition to chaos in small-world dynamical network. *Chaos, Solitons and Fractals*, 37(3):799–806, 2008.
- [242] K.V. Zadiraka. Investigation of irregularly perturbed differential equations. In *Questions of the theory and history of differential equations (in Russian)*, pages 81–108, Kiev, 1986. Nauk. Dumka.
- [243] I. Zelinka, S. Celikovsky, H. Richter, and G. Chen. *Evolutionary Algorithms and Chaotic Systems*. Springer-Verlag, Berlin, Heidelberg, 2010.
- [244] W. Zhao and H. Zhang. On almost periodic solution of shunting inhibitory cellular neural networks with variable coefficients and time-varying delays. *Nonlinear Analysis: Real World Applications*, 9(5):2326–2336, 2008.
- [245] J. Zhou and C. Wen. *Adaptive Backstepping Control of Uncertain Systems, Nonsmooth Nonlinearities, Interactions or Time-Variations*. Springer-Verlag, Berlin, Heidelberg, 2008.
- [246] V.F. Zhuravlev. A method for analyzing vibration-impact systems by means of special functions. *Mech. Solids*, 11:23–27, 1976.

CURRICULUM VITAE

PERSONAL INFORMATION

Surname, Name: Fen, Mehmet Onur
Nationality: Turkish (TC)
Date and Place of Birth: 29.06.1985, Ankara
Marital Status: Single
E-mail: monur.fen@gmail.com

EDUCATION

Degree	Institution	Year of Graduation
B.S. (Double Major)	METU Physics	2008
B.S.	METU Mathematics	2007
High School	Çağrıbey Anatolian High School	2002

PROFESSIONAL EXPERIENCE

Year	Place	Enrollment
2007-2013	METU Mathematics	Research Assistant

FOREIGN LANGUAGES

Advanced English

PUBLICATIONS

Publications in Refereed Journals

1. M.U. Akhmet and M.O. Fen, Shunting inhibitory cellular neural networks with chaotic external inputs, Chaos 23(2):023112, 2013.

2. M.U. Akhmet and M.O. Fen, Replication of chaos, *Commun. Nonlinear Sci. Numer. Simulat.* 18(10):2626-2666, 2013.
3. M.U. Akhmet and M.O. Fen, Chaos generation in hyperbolic systems, *Interdiscip. J. Discontinuity Nonlinearity Complexity* 1(4):367-386, 2012.
4. M.U. Akhmet and M.O. Fen, Chaotic period-doubling and OGY control of forced Duffing equation, *Commun. Nonlinear Sci. Numer. Simulat.* 17(4):1929-1946, 2012.
5. M.O. Fen and Ş. Erkoç, Distributions of circles on a circle and correlation between vortex rings of superfluids, *Turk. J. Phys.* 31(3):151-159, 2007.

International Conference Publications

1. M.U. Akhmet and M.O. Fen, The period-doubling route to chaos in a relay system. In G.S. Ladde, N.G. Medhin, C. Peng, M. Sambandham (Eds.), *Proceedings of Dynamics Systems and Applications*, vol. 6, pages 22-26, Atlanta, GA, 2012. Dynamic Publisher, Inc.

CONFERENCE PRESENTATIONS

1. *Replication of Discrete Chaos*, 6th Chaotic Modeling and Simulation International Conference, 11-14 June 2013, Yeditepe University, İstanbul, Turkey (a joint work with Prof. Dr. Marat Akhmet).
2. *Kaosun Kenetlenmesi*, 1. Ulusal Karmaşık Dinamik Sistemler ve Uygulamaları Çalıştayı, 12-13 Ekim 2012, TOBB Ekonomi ve Teknoloji Üniversitesi, Ankara (a joint work with Prof. Dr. Marat Akhmet).
3. *OGY Control of the Forced Duffing Equation*, Sixth International Conference on Dynamic Systems and Applications, 25-28 May 2011, Atlanta, GA USA (a joint work with Prof. Dr. Marat Akhmet).